Contributions to Information and Energy Systems

Samir M. Perlaza

N° d'ordre NNT : 2021 HDR 009

Accreditation to Supervise Research

presented to:

l'Institut National des Sciences Appliquées de Lyon and
l'Université Claude Bernard LYON I

Specialization: Electrical Engineering

defended on the 29th of June 2021 by:

Samir M. Perlaza

Contributions to Information and Energy Systems

Members of the Jury:

Reviewers:			
Michèle Wigger	Professor	Télécom ParisTech	France
Sheng Yang	Professor	CentraleSupélec	France
Aylin Yener	Professor	The Ohio State University	USA
Examiners:			
Jean-Marie Gorce	Professor	INSA de Lyon	France
Alain Jean-Marie	Director of Research	INRIA	France
Hervé Liebgott	Professor	Université Lyon I	France
H. Vincent Poor	Professor	Princeton University	USA

N° d'ordre NNT : 2021 HDR 009

Habilitation à Diriger des Recherches

présentée devant

l'Institut National des Sciences Appliquées de Lyon et
l'Université Claude Bernard LYON I

Spécialité : Génie Électrique

Soutenue publiquement le 29 juin 2021, par :

Samir M. Perlaza

Contributions aux Systèmes d'Information et d'Énergie

Devant le jury composé de :

Rapporteurs :			
Michèle Wigger	Professeur	Télécom ParisTech	France
Sheng Yang	Professeur	CentraleSupélec	France
Aylin Yener	Professeur	The Ohio State University	USA
Examinateurs :			
Jean-Marie Gorce	Professeur	INSA de Lyon	France
Alain Jean-Marie	Directeur de Recherche	INRIA	France
Hervé Liebgott	Professeur	Université Lyon I	France
H. Vincent Poor	Professeur	Princeton University	USA

Contents

Chapter 1

Liminary

The purpose of this document is to report part of the research works to which I have contributed over the period 2014–2020 as a permanent member of the scientific staff (chargé de recherche) at INRIA. The aim is not to provide an exhaustive summary of all results and contributions. Instead, my choice is to highlight those results that are the most complete, at least in my opinion. Research results previous to my appointment at INRIA, that is, those obtained during my PhD at Télécom ParisTech and my postdoctoral appointments at Supélec and Princeton University, are excluded. This is independent of whether their publication dates fall within the period 2014–2020.

Following the reasoning above, I have selected three areas in which I believe some of my research results might be of general interest:

- Feedback in Wireless Communications;
- Simultaneous Information and Energy Transmission; and
- Data Integrity in Power Systems.

The first part of this document reports the contributions in the area of *Feedback in Wireless Communications*. The problem of feedback in multi-user channels was introduced to me by Ravi Tandon (University of Arizona) during our postdocs under the guidance of H. Vincent (Vince) Poor at Princeton University. Therein, we studied the problem of perfect output feedback in the Gaussian interference channel (G-IC) using tools from both information theory and game theory [1, 2]. This problem was my tiny door for entering the magical realm of information theory. Once at INRIA, together with Ravi and Vince, the study of this problem continued by considering a more realistic model: noisy channel output feedback instead of perfect channel output feedback. Initially, a symmetry assumption was made to simplify the analysis [3, 4]. Later, this condition was dropped and the problem was studied in full generality leveraging these first exploratory works. The main contributions presented in the first part of this document were obtained during the PhD of Victor Quintero (Universidad del Cauca), who was supervised together with my colleague

Jean-Marie Gorce (INSA de Lyon). During this PhD, Iñaki Esnaola (The University of Sheffield) and Vince were regular contributors. These results appear in the following publications [5–11].

The methodology used to obtain these results consisted in approximating the capacity region of the G-IC in terms of six parameters: (*a*) Four signal to noise ratios (SNRs), one for each of the forward links and another one for each of the feedback links; and (*b*) Two signal to interference ratios (INRs), one for each receiver with respect to the interference of the non-intended transmitter. The analysis under the assumption that both transmitter-receiver pairs act in a coordinated manner, i.e., due to a central controller, is presented in Chapter 3. Therein, an approximation to the capacity region within a constant gap is presented. Today, this result remains being the most precise approximation to the capacity region of the G-IC with noisy channel output feedback. Alternatively, the analysis under the assumption that both transmitter-receiver pairs are competing selfish entities aiming to maximize their individual information rates is presented in Chapter 4. Therein, the main result is an approximation to the Nash equilibrium region. That is, the subset of the capacity region that is achievable under the assumption that transmissions are decentralized. This result is the first description of the fundamental limits on the information rates that can be achieved in the decentralized G-IC with noisy channel output feedback. The relevance of this result is that communications networks arising in the context of the internet of things are decentralized networks and thus, subject to the fundamental limits described by the Nash region.

The second part of the manuscript describes my contributions in the area of *Simultaneous Information and Energy Transmission*. This topic was presented to me by Ioannis Krikidis (University of Cyprus) in 2015. By then, the study of the fundamental limits of this technology was in its infancy. These limits were well understood in the point-to-point case, but very little was known about multi-user channels. The results presented in this part were obtained during the postdoctoral appointment of Selma Belhadj Amor (DataRobot at Singapore) and the PhD of Nizar Khalfet (University of Cyprus), who were jointly supervised with Jean-Marie Gorce.

Chapter 6 presents the main results in the Gaussian multiple access channel (MAC) in which two transmitters aim to send information to an information receiver; and energy to one external energy harvester (EH). The main result is the exact characterization of the set of information and energy rates that can be simultaneously achieved, i.e., the information-energy capacity region. This characterization is presented in both the case in which perfect channel output feedback is available; and the case in which feedback is not present. Chapter 7 presents similar results in the case of the G-IC. In this case, two transmitter-receiver pairs are engaged with a dual objective: First, transmitting information from the transmitter to the intended receiver; and second, transmitting energy to an external EH. The main result consists in an approximation of the information-energy capacity region within a constant gap. These results appeared in the following publications [12–22]

The third part of the document presents the results in the area of *Data Integrity in Power Systems* and the focus is on data injection attacks. The problem of data injection attacks was presented to me by Iñaki Esnaola (The University of Sheffield) in 2014 during a visit to his group in Sheffield. Since then, we have kept a continuous collaboration around this topic. At the beginning, our work focused on injection of deterministic data attacks in order to tamper with the state estimation of smart grids [23]. Later, during the PhD of Sun Ke (The University of Sheffield), this study evolved to the case of random attacks. Chapter 9 describes the contributions in the design of deterministic attacks. Two types of data injection attacks are characterized: (a) Data injection vectors that maximize the excess distortion subject to the fact that the probability of attack detection is smaller than a given threshold; and (b) Data injection vectors that minimize the probability of attack detection subject to the fact that the excess distortion is not smaller than a given threshold. Chapter 10 describes data injection attacks that achieve a trade-off between two competing objectives: First, minimizing the mutual information between the observations collected by the network operator and the state of the network; and second, minimizing the probability of attack detection. These results appeared in the following publications [23–32]

The methodology used to obtain these results relies on constructing a hypothesis test to accept or reject the hypothesis: The data observations contain a data injection attack. This statistical formulation provides an explicit expression for the probability of attack detection. This expression together with the expression for the distortion induced by the attack on the state estimation provides the ingredients to formulate the design of data injection attacks as an optimization problem. In such optimization problem the objective function is a weighted sum of the expression that accounts for the disruption in the information; and the expression that accounts for the probability of attack detection.

The bibliography of this document is the same used when the results were presented the first time. Hence, contributions that appear later than the date of publications of the above mentioned results are not referenced. From this perspective, this document must be considered only for the purposes of the evaluation of my *Habilitation à Diriger des Recherches* (HDR) and not as a reference on the state of the art of these research topics.

The document is completed with a series of appendices that provide information on my career development in the context of the evaluation for obtaining the HDR. Appendix A presents my extended curriculum vitae. Appendix B presents a brief description of my teaching at ENS de Lyon. The complete list of publications after my PhD is included in Appendix C.

Samir M. Perlaza
Punaauia, French Polynesia
May 1, 2021

Part I

Feedback in Wireless Communications

Chapter 2

Introduction

The interference channel (IC) is one of the simplest yet more interesting multi-user channels in communications theory. An example of an IC is the two-user Gaussian interference channel (GIC) that consists in two point-to-point links subject to mutual interference; and additive white Gaussian noise (AWGN). More specifically, in the two-user GIC, each channel output is the sum of the three signals: The signals sent by both transmitters and a source of AWGN. From this perspective, the interest on this model stems from the fact that it simultaneously captures the effect of the additive noise and the effect of interference.

The calculation of the capacity region of a two-user GIC, i.e, the set of information transmission rates that can be simultaneously achieved by both point-to-point links, remains as a long standing open problem. This region is known only in two particular cases: The very strong interference regime [33]; and the strong interference regime [34, 35]. In both cases, each receiver must decode the non-intended message in order to eliminate the interference. The best known achievable region for the two-user GIC in the other regimes is given in [34, 36]. The achievability strategy used in [34] uses rate-splitting [37], whereas the strategy in [36] uses both rate-splitting [34, 37] and block-Markov superposition coding [38]. These strategies split each user's message into two parts: (1) a common part that is decoded by both receivers; and (2) a private part that is decoded at the intended receiver. From this perspective, message splitting and partial decoding provide the means of controlling, at least partially, the interference. The achievable region described in [36] is proved to be at most one bit away from the capacity region of the two-user GIC. That is, the capacity region is approximated to within one bit [39].

Using transmission schemes that allow partial decoding of the transmitted messages implies some sort of cooperation between both transmitter-receiver pairs. More specifically, it requires each receiver to know the transmission schemes used by both transmitters. This is often not possible in practice, e.g., small devices in the internet of things, and thus, in such cases interference must be treated as noise [40–43]. This observation leads to the question whether further cooperation might enlarge the

capacity region of the GIC, which is the central question in the following chapters. One way to achieve cooperation is through channel-output feedback, which consists in letting a transmitter to observe the channel-output at its intended receiver. This observation can also be subject to additive noise or other impairments. Perfect observation of the channel-output at the intended receiver by each one of the corresponding transmitters is studied in [44]. Therein, perfect feedback (PF) has been shown to bring an unprecedented gain on the generalized degree of freedom (GDoF) with respect to the case without feedback in the GIC [44].

In order to define the GDoF, for all $i \in \{1,2\}$ and $j \in \{1,2\} \setminus \{i\}$, let $\overrightarrow{h}_{ii} \geqslant 0$ and $h_{ji} \geqslant 0$ be the channel coefficients from transmitter i to receivers i and j, respectively. Let also x_i be the symbol transmitted by transmitter i; and let the random variable $\overrightarrow{Y}_i = \overrightarrow{h}_{ii}x_i + h_{ij}x_j + \overrightarrow{Z}_i$ be the signal observed by receiver i, where $\overrightarrow{Z}_i$ is a Gaussian random variable with zero mean and unit variance. Subject to a unitary average power constraint at each transmitter, the signal to noise ratio at receiver i is denoted by $\overrightarrow{\text{SNR}}_i = \overrightarrow{h}_{ii}^2$; and the interference to noise ratio at receiver i is denoted by $\text{INR}_{ij} = h_{ij}^2$. For two positive reals $\overrightarrow{\text{SNR}}$ and INR, assume that $\overrightarrow{\text{SNR}}_1 = \overrightarrow{\text{SNR}}_2 = \overrightarrow{\text{SNR}}$ and $\text{INR}_{12} = \text{INR}_{21} = \text{INR}$. Hence, let $\mathcal{C}(\overrightarrow{\text{SNR}}, \text{INR})$ denote a set containing all achievable rates of a symmetric GIC with parameters $\overrightarrow{\text{SNR}}$ and INR. In this context, the GDoF [45] is defined as follows:

$$\text{GDoF}(\alpha) = \lim_{\overrightarrow{\text{SNR}} \to \infty} \frac{\sup\left\{R : (R,R) \in \mathcal{C}(\overrightarrow{\text{SNR}}, \overrightarrow{\text{SNR}}^{\alpha})\right\}}{\log\left(\overrightarrow{\text{SNR}}\right)}, \tag{2.1}$$

where $\alpha = \frac{\log(\text{INR})}{\log(\overrightarrow{\text{SNR}})}$. In Figure 2.1, the GDoF is plotted as a function of α when $\mathcal{C}(\overrightarrow{\text{SNR}}, \text{INR})$ is calculated without feedback [39]; and with PF from each receiver to their corresponding transmitters [44]. Note that with PF, $\text{GDoF}(\alpha) \to \infty$ when $\alpha \to \infty$, which implies an arbitrarily large increment. Surprisingly, using only one PF link from one of the receivers to the corresponding transmitter provides the same sum-capacity as having four PF links from both receivers to both transmitters [8,46,47] in certain interference regimes. These benefits rely on the fact that feedback provides relevant information about the interference. Hence, such information can be retransmitted to: (a) perform interference cancellation at the intended receiver or (b) provide an alternative communication path between the other transmitter-receiver pair.

The capacity region of the GIC with PF has been approximated to within two bits in [44]. The achievability scheme presented therein is based on three well-known techniques: rate splitting [34, 37], block-Markov superposition coding [38], and backward decoding [48, 49]. The converse in [44] is obtained following classical tools among cut-set bounds and genie-aided models. Other achievability schemes have been presented in [50] and [51] using rate-splitting, block-Markov superposition coding, backward decoding, and binning/dirty paper coding in the context of a more general channel, i.e., GIC with generalized feedback (IC-GF).

From a system analysis perspective, PF might be an exceptionally optimistic model to study the benefits of feedback in the GIC. Denote by $\overrightarrow{\boldsymbol{y}} = (\overrightarrow{y}_1, \overrightarrow{y}_2, \ldots, \overrightarrow{y}_N)$ a given sequence of N channel outputs at a given receiver. A realistic model of channel-output feedback is to consider that the feedback signal, denoted by $\overleftarrow{\boldsymbol{Y}}$, satisfies $\overleftarrow{\boldsymbol{Y}} = g\left(\overrightarrow{\boldsymbol{y}}\right)$, with g being a random transformation in $\mathbb{R}^N$. Hence, a relevant question is: what is a realistic assumption on g? This question has been solved aiming to highlight different impairments that feedback signals might go through. Some of these answers are discussed in the following sections.

2.1 Rate-Limited Feedback

Consider that the receiver produces the feedback signal using a deterministic transformation g, such that for a large N, a positive finite $C_F \in \mathbb{R}$ and for all $\overrightarrow{\boldsymbol{y}} \in \mathbb{R}^N$:

$$\overleftarrow{\boldsymbol{y}} = g(\overrightarrow{\boldsymbol{y}}) \in \mathcal{D}, \tag{2.2}$$

such that for all $\delta > 0$, the set $\mathcal{D} \subseteq \mathbb{R}^N$ satisfies

$$|\mathcal{D}| < 2^{N(C_F+\delta)}. \tag{2.3}$$

This model is known in literature as *rate limited feedback* (RLF) [52–54], where C_F is the capacity of the feedback link. The choice of the deterministic transformation g subject to (2.3) is part of the coding scheme, i.e., the transformation g takes the N channel outputs observed during block $t > 0$ and chooses a codeword in the codebook $\mathcal{D}$. Such a codeword is sent back to the transmitter during block $t + 1$. From this standpoint, this model highlights the signal impairments derived from transmitting a signal with continuous support via a channel with finite-capacity. Note that if $C_F = \infty$, then g can be the identity function and thus,

$$\overleftarrow{\boldsymbol{y}} = g(\overrightarrow{\boldsymbol{y}}) = \overrightarrow{\boldsymbol{y}}, \tag{2.4}$$

which is the case of PF [44]. When $C_F = 0$, then $|\mathcal{D}| = 1$ and thus, no information can be conveyed through the feedback links, which is the case studied in [34,36,39]. The main result in [52] is twofold: first, given a fixed C_F, the authors provide a deterministic transformation g using lattice coding [55] and a particular power assignment such that partial or complete decoding of the interference is possible at the transmitter. An achievable region is presented using random coding arguments with rate splitting, block-Markov superposition coding, and backward decoding. Second, the authors provide outer bounds that hold for any deterministic g in (2.2). This result induces a converse region whose sum-rate is shown to be at a constant gap of the achievable sum-rate, at least in the symmetric case. These results are generalized for the K-user GIC with RLF in the symmetric case in [53,54], where the analysis focuses on the fundamental limit of the symmetric rate. The main novelty on the extension to $K > 2$ users lies in the joint use of interference alignment and lattice codes for the proof of the achievability. The proof of converse remains an open problem when $K > 2$, even for the symmetric case.

2.2 Intermittent Feedback

Assume that for all $n \in \{1, 2 \ldots, N\}$, the random transformation g is such that given a channel output $\overrightarrow{y}_n$,

$$\overleftarrow{Y}_n = \begin{cases} \star & \text{with probability} \quad 1-p \\ \overrightarrow{y}_n & \text{with probability} \quad p, \end{cases} \tag{2.5}$$

where $\star$ represents an erasure and $p \in [0, 1]$. That is, the feedback channel is an erasure channel. Note that the random transformation g is fully determined by the parameters of the channels, e.g., the probability p. Thus, as opposed to the RLF, the transformation g cannot be optimized as part of the receiver design. This model emphasizes the fact that the usage of the feedback link might be available only during certain channel uses, not necessarily known by the receivers with anticipation. This model is referred to as *intermittent feedback* (IF) [56]. The main result in [56] is an approximation of the capacity region to within a constant gap. The achievability scheme relies upon random coding arguments with forward decoding and a quantize-map-and-foward strategy to retransmit the information obtained through feedback. This is because erasures might constrain either partial or complete decoding of the interference at the transmitter. Nonetheless, even a quantized version of the interference might be useful for interference cancellation or for providing an alternative path.

2.3 Noisy Feedback

Assume that for all $n \in \{1, 2 \ldots, N\}$, the random transformation g is such that given a channel output $\overrightarrow{y}_n$,

$$\overleftarrow{Y}_n = g(\overrightarrow{y}_n) = \overleftarrow{h}\,\overrightarrow{y}_n + Z_n, \tag{2.6}$$

where $\overrightarrow{h} \in \mathbb{R}_+$ is a parameter of the channel and Z_n is a real Gaussian random variable with zero mean and unit variance. This model is known in literature as *noisy feedback* (NF) or *partial feedback* [57–59]. Note that no processing is applied to the channel output observed by the intended receiver and thus, the transmitter observes a re-scaled and noisy copy of the channel output. From this point of view, as opposed to RLF, this model does not focus on the constraint on the number of codewords that can be used to perform feedback, but rather on the fact that the feedback channel might be of finite capacity due to noise. In [58], the capacity of the GIC with NF has been approximated to within a constant gap for the symmetric case. The achievable scheme in [58] is a particular case of a more general achievability scheme presented in [50,51]. An outer bound using the Hekstra-Willems dependence-balance arguments [60] has been introduced in [57]. In the GIC, these results suggest that feedback loses its efficacy on increasing the capacity region roughly when the noise variance on the feedback link is larger than on the forward link. Inner and

outer bounds on the sum-capacity of the GIC with NF using the existing connections between channel-output feedback and conferencing transmitters have been presented in [61]. More general channel models, for instance when channel-outputs are fed back to both receivers, have been studied in [47, 62–64].

2.4 A Comparison Between Feedback Models

In both IF and NF, the feedback signal is obtained via a random transformation. In particular, IF models the feedback link as an erasure-channel, whereas NF models the feedback link as an additive white Gaussian noise (AWGN) channel. Alternatively in RLF, the feedback signal is obtained via a deterministic transformation. Let $\overleftarrow{\mathrm{SNR}}$ be the SNR in each of the feedback links from the receiver to the corresponding transmitters in the symmetric GIC with NF (G-IC-NF) mentioned above. Let also β and β' be

$$\beta = \frac{\log\left(\overleftarrow{\mathrm{SNR}}\right)}{\log\left(\overrightarrow{\mathrm{SNR}}\right)} \tag{2.7a}$$

and

$$\beta' = \frac{C_F}{\log\left(\overrightarrow{\mathrm{SNR}}\right)}. \tag{2.7b}$$

These parameters approximate the ratio between the capacity of the feedback link and the capacity of the forward link in the NF and RLF case, respectively. Hence, a fair comparison of RLF and NF must be made with $\beta = \beta'$. The GDoF is plotted as a function of α when $\mathcal{C}(\overrightarrow{\mathrm{SNR}}, \mathrm{INR})$ is calculated with NF for several values of β in Figure 2.1(a); with RLF for different values of β' in Figure 2.1(b); and with IF for several values of p in Figure 2.1(c).

The most pessimistic channel-output feedback model between NF and RLF, in terms of the GDoF when $\beta = \beta'$, is NF. When $\alpha \in (0, \frac{2}{3})$ or $\alpha \in (2, \infty)$, RLF increases the GDoF for all $\beta' > 0$. Note that RLF with $\beta' = \frac{1}{2}$ achieves the same performance as PF, for all $\alpha \in [0, 3]$. In the case of NF, there does not exist any benefit in terms of the GDoF for all $0 < \beta < \frac{1}{2}$. A noticeable effect of NF occurs when $\alpha \in (0, \frac{2}{3})$, for all $\beta > \frac{1}{2}$; and when $\alpha \in (2, \infty)$, for all $\beta > 1$. This observation can be explained from the fact that in RLF, receivers extract relevant information about interference and send it via a noiseless channel. Alternatively, NF requires sending to the transmitter an exact copy of the channel output via an AWGN channel. Hence with $\beta = \beta' > 0$, the transmitters are always able to obtain information about the interference in RLF, whereas the same is not always true for NF. Finally, note that in both NF and RLF, the GDoF is not monotonically increasing with α in the interval $[2, \infty)$. Instead, it is upper-bounded by $\min\left(\frac{\alpha}{2}, \beta\right)$ in NF and by $\min\left(\frac{\alpha}{2}, 1 + \beta\right)$ in RLF.

The most optimistic model in terms of the GDoF, aside from PF, is IF. In particular because for any value of $p > 0$, there always exists an improvement of the GDoF for

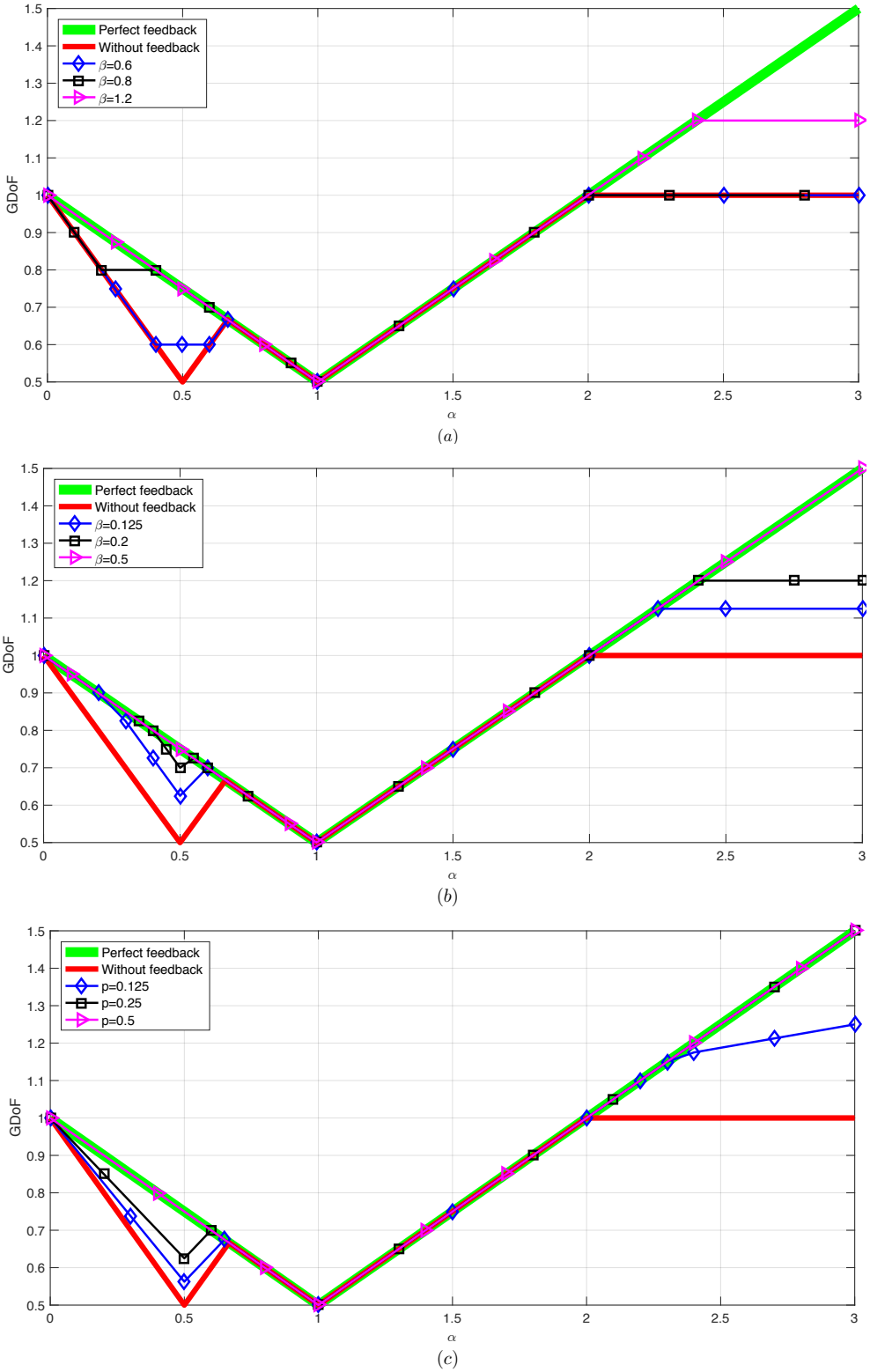

Figure 2.1: Generalized degree of freedom (GDoF) of a symmetric two-user GIC; (a) case with NF with $\beta \in \{0.6, 0.8, 1.2\}$; (b) case with RLF with $\beta \in \{0.125, 0.2, 0.5\}$; and (c) case with IF with $p \in \{0.125, 0.25, 0.5\}$.

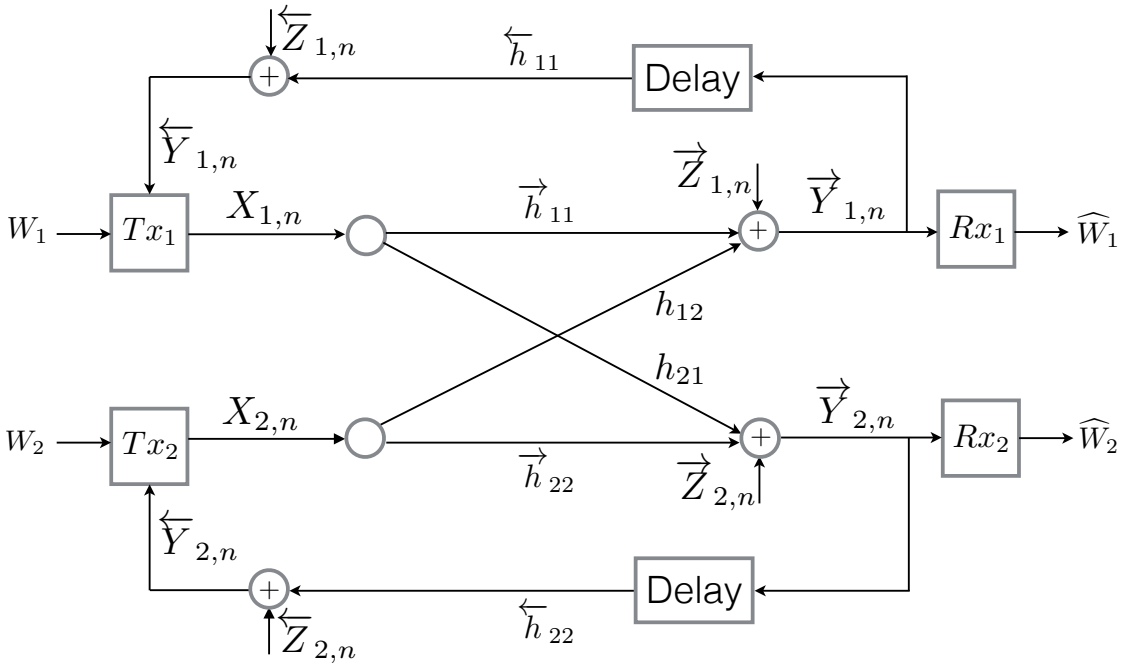

Figure 2.2: Gaussian interference channel with noisy channel-output feedback at channel use n.

all $\alpha \in (0, \frac{2}{3})$ and $\alpha \in (2, \infty)$. Note that, with $p \geqslant \frac{1}{2}$, IF provides the same GDoF as PF. Note also that the GDoF remains being monotonically increasing with α in the interval $[2, \infty)$ for any positive value of p in (2.5), which implies an arbitrarily large increment in the GDoF.

The following chapters focus on NF within two general scenarios: (1) centralized GICs, in which the entire network is controlled by a central entity that configures both transmitter-receiver pairs; and (2) decentralized GICs, in which each transmitter-receiver pair autonomously configures its transmission-reception parameters. The analysis in these two scenarios provides the characterization of the approximate capacity region and the approximate η-Nash equilibrium (η-NE) region of the two-user GIC-NOF.

2.5 Mathematical Models

Consider the two-user GIC-NOF depicted in Figure 2.2. Transmitter i, with $i \in \{1, 2\}$, communicates with receiver i subject to the interference produced by transmitter j, with $j \in \{1, 2\} \backslash \{i\}$. There are two independent and uniformly distributed messages, $W_i \in \mathcal{W}_i$, with $\mathcal{W}_i = \{1, 2, \ldots, \lfloor 2^{N_i R_i} \rfloor\}$, where N_i denotes the fixed block-length in channel uses and R_i the information transmission rate in bits per channel use. At each block, transmitter i sends the codeword $\boldsymbol{X}_i = (X_{i,1}, X_{i,2}, \ldots, X_{i,N_i})^{\mathsf{T}} \in$

$\mathcal{C}_i \subseteq \mathbb{R}_i^{N_i}$, where $\mathcal{C}_i$ is the codebook of transmitter i.

All channel coefficients are assumed to be non-negative real numbers. This contrasts with the case of multi-antenna channels in which channel coefficients are assumed to be vectors. The channel coefficient from transmitter j to receiver i is denoted by h_{ij}; the channel coefficient from transmitter i to receiver i is denoted by $\overrightarrow{h}_{ii}$; and the channel coefficient from channel output i to transmitter i is denoted by $\overleftarrow{h}_{ii}$. All channel coefficients are assumed to be non-negative real numbers. At a given channel use $n \in \{1, 2, \ldots, N\}$, with

$$N = \max(N_1, N_2), \tag{2.8}$$

the channel output at receiver i is denoted by $\overrightarrow{Y}_{i,n}$. During channel use n, the input-output relation of the channel model is given by

$$\overrightarrow{Y}_{i,n} = \overrightarrow{h}_{ii} X_{i,n} + h_{ij} X_{j,n} + \overrightarrow{Z}_{i,n}, \tag{2.9}$$

where $X_{i,n} = 0$ for all $n > N_i$ and $\overrightarrow{Z}_{i,n}$ is a real Gaussian random variable with zero mean and unit variance that represents the noise at the input of receiver i. At a given channel use n, the feedback signal at the input of transmitter i is denoted by $\overleftarrow{Y}_{i,n}$. Let $d > 0$ be the finite feedback delay measured in channel uses. At the end of channel use n, transmitter i observes $\overleftarrow{Y}_{i,n}$, which consists of a scaled and noisy version of $\overrightarrow{Y}_{i,n-d}$. More specifically,

$$\overleftarrow{Y}_{i,n} = \begin{cases} \overleftarrow{Z}_{i,n} & \text{for } n \in \{1,2,\ldots,d\} \\ \overleftarrow{h}_{ii} \overrightarrow{Y}_{i,n-d} + \overleftarrow{Z}_{i,n}, & \text{for } n \in \{d+1,d+2,\ldots,N\}, \end{cases} \tag{2.10}$$

where $\overleftarrow{Z}_{i,n}$ is a real Gaussian random variable with zero mean and unit variance that represents the noise in the feedback link of transmitter-receiver pair i. The random variables $\overrightarrow{Z}_{i,n}$ and $\overleftarrow{Z}_{i,n}$ are assumed to be independent. In the following, without loss of generality, the feedback delay is assumed to be one channel use, i.e., $d = 1$ and known by all receivers. The encoder of transmitter i is defined by a set of deterministic functions $f_{i,1}^{(N)}, f_{i,2}^{(N)}, \ldots, f_{i,N_i}^{(N)}$, with $f_{i,1}^{(N)} : \mathcal{W}_i \times \mathbb{N} \to \mathcal{C}_i$ and for all $n \in \{2, 3, \ldots, N_i\}$, $f_{i,n}^{(N)} : \mathcal{W}_i \times \mathbb{N} \times \mathbb{R}^{n-1} \to \mathcal{C}_i$, such that

$$X_{i,1} = f_{i,1}^{(N)}(W_i, \Omega_i), \text{ and} \tag{2.11a}$$

$$X_{i,n} = f_{i,n}^{(N)}\left(W_i, \Omega_i, \overleftarrow{Y}_{i,1}, \overleftarrow{Y}_{i,2}, \ldots, \overleftarrow{Y}_{i,n-1}\right), \tag{2.11b}$$

where $\Omega_i \in \mathbb{N}$ is an additional index randomly generated. The index Ω_i is assumed to be known by both transmitter i and receiver i, while unknown by transmitter j and receiver j. These indices play a central role in the analysis of the decentralized G-IC in Chapter 4.

The components of the input vector $\boldsymbol{X}_i$ are real numbers subject to an average power constraint

$$\frac{1}{N_i} \sum_{n=1}^{N_i} \mathbb{E}\left[X_{i,n}^2\right] \leq 1. \tag{2.12}$$

where the expectation is taken over the joint distribution of the message indexes W_1, W_2, the random indices Ω_1 and Ω_2, and the noise terms, i.e., $\overrightarrow{Z}_1$, $\overrightarrow{Z}_2$, $\overleftarrow{Z}_1$, and $\overleftarrow{Z}_2$. The dependence of $X_{i,n}$ on W_1, W_2, Ω_1, Ω_2 and the previously observed noise realizations is due to the effect of feedback as shown in (2.10) and (2.11).

The decoder of receiver i is defined by a deterministic function $\psi_i^{(N)} : \mathbb{R}^N \times \mathbb{N} \to \mathcal{W}_i$. At the end of the communication, receiver i uses the vector $\left(\overrightarrow{Y}_{i,1}, \overrightarrow{Y}_{i,2}, \ldots, \overrightarrow{Y}_{i,N}\right)$ and the index Ω_i to obtain an estimate of the message index:

$$\widehat{W}_i = \psi_i^{(N)}\left(\overrightarrow{Y}_{i,1}, \overrightarrow{Y}_{i,2}, \ldots, \overrightarrow{Y}_{i,N}, \Omega_i\right), \tag{2.13}$$

where $\widehat{W}_i \in \mathcal{W}_i$ is an estimate of the message index W_i.

A transmit-receive configuration for transmitter-receiver pair i is described in terms of the block-length N_i, the codebook $\mathcal{C}_i$, the encoding functions $f_{i,1}^{(N)}, f_{i,2}^{(N)}, \ldots, f_{i,N_i}^{(N)}$, and the decoding function $\psi_i^{(N)}$, etc.

The decoding bit error probability in the two-user D-GIC-NOF, denoted by P_i for transmitter-receiver pair i, is given by

$$P_i(N) = \Pr\left[\widehat{W}_i \neq W_i\right]. \tag{2.14}$$

The maximum decoding error probability, denoted by P_e, is given by

$$P_e(N) = \max\left(\Pr\left[\widehat{W}_1 \neq W_1\right], \Pr\left[\widehat{W}_2 \neq W_2\right]\right). \tag{2.15}$$

The definition of an achievable rate pair $(R_1, R_2) \in \mathbb{R}_+^2$ si

Definition 1 (Achievable Rate Pairs)**.** A rate pair $(R_1, R_2) \in \mathbb{R}_+^2$ is achievable if there exists encoding functions $f_{1,1}^{(N)}, f_{1,2}^{(N)}, \ldots, f_{1,N_1}^{(N)}$ and $f_{2,1}^{(N)}, f_{2,2}^{(N)}, \ldots, f_{2,N_2}^{(N)}$ and decoding functions $\psi_1^{(N)}$ and $\psi_2^{(N)}$ such that the decoding error probability P_e can be made arbitrarily small by letting the block-lengths N_1 and N_2 grow to infinity.

The set of all achievable rates on the two-user GIC-NOF in Figure 2.2 can be described by six parameters: $\overrightarrow{\mathrm{SNR}}_i$, $\overleftarrow{\mathrm{SNR}}_i$, and INR_{ij}, with $i \in \{1,2\}$ and $j \in \{1,2\}\backslash\{i\}$, which are defined as follows:

$$\overrightarrow{\mathrm{SNR}}_i = \overrightarrow{h}_{ii}^2, \tag{2.16}$$

$$\mathrm{INR}_{ij} = h_{ij}^2, \text{ and} \tag{2.17}$$

$$\overleftarrow{\mathrm{SNR}}_i = \overleftarrow{h}_{ii}^2 \left(\overrightarrow{h}_{ii}^2 + 2\overrightarrow{h}_{ii} h_{ij} + h_{ij}^2 + 1\right). \tag{2.18}$$

The analysis presented in this section focuses exclusively on the case in which $\mathrm{INR}_{ij} > 1$ for all $i \in \{1,2\}$ and $j \in \{1,2\} \setminus \{i\}$. The reason for exclusively considering this case follows from the fact that when $\mathrm{INR}_{ij} \leqslant 1$, transmitter-receiver pair i is impaired mainly by noise instead of interference. In this case, feedback does not bring a significant rate improvement.

2.5.1 Centralized Interference Channels

The two-user GIC-NF depicted in Figure 2.2 is said to be centralized if there exists an entity that jointly determines the transmission parameters of both transmitter-receiver pairs. More specifically, a GIC-NF is centralized when the block lengths N_1 and N_2, the encoding functions $f_{1,1}^{(N)}, f_{1,2}^{(N)}, \ldots, f_{1,N_1}^{(N)}$ and $f_{2,1}^{(N)}, f_{2,2}^{(N)}, \ldots, f_{2,N_2}^{(N)}$ and the decoding functions $\psi_1^{(N)}$ and $\psi_2^{(N)}$ are determined by the same entity in order to optimize a global metric parameter, e.g., sum rate, minimum individual rate, minimum individual decoding error probability, decoding error probability. In this case a typical choice is

$$N = N_1 = N_2. \tag{2.19}$$

Moreover, the additional randomness due to Ω_1 and Ω_2 in (2.11) is not used.

The fundamental limits of a C-GIC are characterized by the capacity region.

Definition 2 (Capacity region of a two-user GIC)**.** *The capacity region of a two-user GIC is the closure of the set of all possible achievable rate pairs* $(R_1, R_2) \in \mathbb{R}_+^2$.

2.5.2 Decentralized Interference Channels

In a decentralized GIC (D-GIC), each transmitter-receiver pair acts autonomously and tunes its individual transmit-receive configuration aiming to optimize a given performance metric. More specifically, in a D-GIC, the transmitter-receiver pair i, with $i \in \{1, 2\}$, chooses the block length N_i, the encoding functions $f_i^{(1)}, f_i^{(2)}, \ldots, f_i^{(N)}$ and the decoding function $\psi_i^{(N)}$ aiming to optimize an individual metric parameter, e.g., individual rate, or individual decoding error probability.

In D-GICs, a competitive scenario arises in which the individual improvement of one transmitter-receiver pair's individual metric often implies the detriment of its counterpart's individual metric due to mutual interference. From this point of view, in D-GICs, the notion of capacity region is shifted to the notion of equilibrium region. Such a region varies depending on the associated notion of equilibrium, e.g., Nash equilibrium (NE) [65], η-Nash equilibrium (η-NE) [66], correlated equilibrium [67], satisfaction equilibrium [68], etc. In particular, when each individual transmitter-receiver pair aims to selfishly optimize its individual transmission rate by tuning its transmit-receive configuration, the equilibrium region is a subregion of the capacity region and it must be understood in terms of the η-NE. Once an η-NE is achieved, none of the transmitter-receiver pairs has a particular interest in unilaterally deviating from the actual transmit-receive configuration as any deviation would bring an improvement of at most η bits/s/Hz. When, $\eta = 0$, an η-NE corresponds to an NE. Essentially, any deviation from an NE implies no gain or even a loss in the individual rate of the deviating transmitter. Therefore, any rate tuple outside the NE-region is not stable as there always exists at least one transmitter-receiver pair that is able to increase its own transmission rate by updating its own transmit-receive configuration.

An approximate characterization of the η-NE region of the decentralized Gaussian IC without feedback is presented in [69], with $\eta > 0$ arbitrarily small. This characterization implies two important points. First, in all the interference regimes, the η-NE region is non-empty, which verifies some of the existing results in [70, 71] and [72]. Second, the individual rates achievable at an η-NE are both lower and upper bounded. The lower bound corresponds to the rate achieved by treating interference as noise, whereas the upper bound requires partial decoding of the interference. Interestingly, in some cases of the strong and very strong interference regimes, it is shown that the η-NE region equals the capacity region. Conversely, in all the other cases, the η-NE region is a subregion of the capacity region and often, it does not contain all the strictly Pareto optimal rate pairs, e.g., the rate pairs on the boundary of the sum-capacity.

In the case of the D-GIC with feedback, conventional wisdom leads to the idea that the η-NE region must not be different from the η-NE region of the IC without feedback. This follows from the fact that feedback can be seen as an altruistic action in which the benefit is not for the transmitter-receiver pair that implements feedback but rather for the other pair [1]. Note for instance that, the alternative path from transmitter i to receiver i mentioned above appears thanks to the feedback from receiver j to transmitter j. Therefore, intuitively, feedback should not be useful in decentralized channels given that transmitter-receiver pairs whose individual interest is their own transmission rate might not have a particular interest in using it. However, the following chapters shows the opposite. Even in the strictly competitive scenario in which both transmitter-receiver pairs are selfish, the use of feedback can be shown to be individually advantageous and thus, transmitter-receiver pairs might opt to use it in some cases. This is basically because, when one transmitter-receiver pair uses feedback, it induces the others to use it, which leads to a mutually beneficial situation and thus, to an equilibrium. This observation leads to two of the most important conclusions of this work: (i) The η-NE region achieved with feedback is larger than or equal to the η-NE region without feedback. More importantly, for each rate pair achievable at an η-NE without feedback, there exists at least one rate pair achievable at an η-NE with feedback that is, at least, weakly Pareto superior; and (ii) There always exists an η-NE transmit-receive configuration pair that achieves a rate pair that is at most 1 bit/s/Hz per user away from the outer bound of the capacity region even when the network is fully decentralized.

Chapter 3

Centralized Interference Channels with Feedback

This chapter introduces an achievable region (see Theorem 1) and a converse region (see Theorem 2), denoted by $\underline{\mathcal{C}}_{\mathrm{GIC-NF}}$ and $\overline{\mathcal{C}}_{\mathrm{GIC-NF}}$ respectively, for a two-user GIC-NF with fixed parameters $\overrightarrow{\mathrm{SNR}}_1$, $\overrightarrow{\mathrm{SNR}}_2$, INR_{12}, INR_{21}, $\overleftarrow{\mathrm{SNR}}_1$, and $\overleftarrow{\mathrm{SNR}}_2$. In general, the capacity region of a given multi-user channel is said to be approximated to within a constant gap according to the following definition.

Definition 3 (Approximation to within ξ units)**.** A closed and convex set $\mathcal{T} \subset \mathbb{R}_+^m$ is approximated to within ξ units by the sets $\underline{\mathcal{T}}$ and $\overline{\mathcal{T}}$ if $\underline{\mathcal{T}} \subseteq \mathcal{T} \subseteq \overline{\mathcal{T}}$ and for all $\boldsymbol{t} = (t_1, t_2, \ldots, t_m) \in \overline{\mathcal{T}}$, $\left((t_1 - \xi)^+, (t_2 - \xi)^+, \ldots, (t_m - \xi)^+ \right) \in \underline{\mathcal{T}}$.

Denote by $\mathcal{C}_{\mathrm{GIC-NF}}$ the capacity region of the 2-user GIC-NF. The achievable region $\underline{\mathcal{C}}_{\mathrm{GIC-NF}}$ (Theorem 1) and the converse region $\overline{\mathcal{C}}_{\mathrm{GIC-NF}}$ (Theorem 2) approximate the capacity region $\mathcal{C}_{\mathrm{GIC-NF}}$ to within 4.4 bits (Theorem 3).

These results generalize the approximate capacity region of the GIC-NF presented in [58, 59] for the symmetric case. The gap between the new achievable region and the new converse region is slightly improved with respect to the one obtained in [58].

The methodology is similar to the one used in [2, 39, 44, 56, 58], i.e., a linear deterministic (LD) approximation [73] to the GIC, referred to as LD-IC, is studied to gain insight on the construction of both inner and outer bounds.

The achievability scheme presented in this chapter as well as the one in [58] use a four-layer block-Markov superposition coding and backward decoding. Note that the achievability scheme used in [58] is obtained as a special case of the one presented in [50, 51]. The achievability scheme presented in this chapter is developed independently. The main difference between these achievability schemes lies on the choice of the random variables used to generate the codewords of each of the layers of the codebook. Another difference is the power optimization made to obtain the corresponding achievable regions.

The converse region presented in this chapter uses existing bounds from the case of PF in [44] and new bounds that generalize those in [58]. The proof of converse presented in [58] uses standard techniques including cut-set bounds and genie-aided channels, which are the same techniques used in this chapter. Nonetheless, such generalization is far from trivial, as suggested in [58, Section IV-D].

3.1 An Achievable Region with Noisy Feedback

The description of the achievable region $\underline{\mathcal{C}}_{\mathrm{GIC-NF}}$ is presented using the constants $a_{1,i}$; the functions $a_{2,i} : [0,1] \to \mathbb{R}_+$, $a_{l,i} : [0,1]^2 \to \mathbb{R}_+$, with $l \in \{3,\ldots,6\}$; and $a_{7,i} : [0,1]^3 \to \mathbb{R}_+$, which are defined as follows, for all $i \in \{1,2\}$, with $j \in \{1,2\} \setminus \{i\}$:

$$a_{1,i}=\frac{1}{2}\log\left(2+\frac{\overrightarrow{\mathrm{SNR}_i}}{\mathrm{INR}_{ji}}\right)-\frac{1}{2}, \tag{3.1a}$$

$$a_{2,i}(\rho)=\frac{1}{2}\log\Big(b_{1,i}(\rho)+1\Big)-\frac{1}{2}, \tag{3.1b}$$

$$a_{3,i}(\rho,\mu)=\frac{1}{2}\log\left(\frac{\overleftarrow{\mathrm{SNR}_i}\Big(b_{2,i}(\rho)+2\Big)+b_{1,i}(1)+1}{\overleftarrow{\mathrm{SNR}_i}\Big((1-\mu)b_{2,i}(\rho)+2\Big)+b_{1,i}(1)+1}\right), \tag{3.1c}$$

$$a_{4,i}(\rho,\mu)=\frac{1}{2}\log\Big(\Big(1-\mu\Big)b_{2,i}(\rho)+2\Big)-\frac{1}{2}, \tag{3.1d}$$

$$a_{5,i}(\rho,\mu)=\frac{1}{2}\log\left(2+\frac{\overrightarrow{\mathrm{SNR}_i}}{\mathrm{INR}_{ji}}+\Big(1-\mu\Big)b_{2,i}(\rho)\right)-\frac{1}{2}, \tag{3.1e}$$

$$a_{6,i}(\rho,\mu)=\frac{1}{2}\log\left(\frac{\overrightarrow{\mathrm{SNR}_i}}{\mathrm{INR}_{ji}}\Big(\Big(1-\mu\Big)b_{2,j}(\rho)+1\Big)+2\right)-\frac{1}{2}, \tag{3.1f}$$

and

$$a_{7,i}(\rho,\mu_1,\mu_2)=\frac{1}{2}\log\left(\frac{\overrightarrow{\mathrm{SNR}_i}}{\mathrm{INR}_{ji}}\Big(\Big(1-\mu_i\Big)b_{2,j}(\rho)+1\Big)+\Big(1-\mu_j\Big)b_{2,i}(\rho)+2\right)-\frac{1}{2}, \tag{3.1g}$$

where the functions $b_{l,i} : [0,1] \to \mathbb{R}_+$, with $(l,i) \in \{1,2\}^2$ are defined as follows:

$$b_{1,i}(\rho)=\overrightarrow{\mathrm{SNR}_i}+2\rho\sqrt{\overrightarrow{\mathrm{SNR}_i}\mathrm{INR}_{ij}}+\mathrm{INR}_{ij} \text{ and} \tag{3.2a}$$

$$b_{2,i}(\rho)=\Big(1-\rho\Big)\mathrm{INR}_{ij}-1, \tag{3.2b}$$

with $j \in \{1,2\} \setminus \{i\}$.

Note that the functions in (3.1) and (3.2) depend on $\overrightarrow{\text{SNR}}_1$, $\overrightarrow{\text{SNR}}_2$, INR_{12}, INR_{21}, $\overleftarrow{\text{SNR}}_1$, and $\overleftarrow{\text{SNR}}_2$, however as these parameters are fixed in this analysis, this dependence is not emphasized in the definition of these functions. Finally, using this notation, the following theorem presents an achievable region for the GIC-NOF.

Theorem 1. The capacity region $\mathcal{C}_{\text{GIC}-\text{NF}}$ contains the region given by the closure of all non-negative rate pairs (R_1, R_2) that satisfy

$$R_1 \leqslant \min\Big(a_{2,1}(\rho), a_{6,1}(\rho,\mu_1) + a_{3,2}(\rho,\mu_1), a_{1,1} + a_{3,2}(\rho,\mu_1) + a_{4,2}(\rho,\mu_1)\Big), \tag{3.3a}$$

$$R_2 \leqslant \min\Big(a_{2,2}(\rho), a_{3,1}(\rho,\mu_2) + a_{6,2}(\rho,\mu_2), a_{3,1}(\rho,\mu_2) + a_{4,1}(\rho,\mu_2) + a_{1,2}\Big), \tag{3.3b}$$

$$\begin{aligned} R_1 + R_2 \leqslant \min\Big(&a_{2,1}(\rho) + a_{1,2}, a_{1,1} + a_{2,2}(\rho), a_{3,1}(\rho,\mu_2) + a_{1,1} + a_{3,2}(\rho,\mu_1) \\ &+ a_{7,2}(\rho,\mu_1,\mu_2), a_{3,1}(\rho,\mu_2) + a_{5,1}(\rho,\mu_2) + a_{3,2}(\rho,\mu_1) + a_{5,2}(\rho,\mu_1), a_{3,1}(\rho,\mu_2) \\ &+ a_{7,1}(\rho,\mu_1,\mu_2) + a_{3,2}(\rho,\mu_1) + a_{1,2}\Big), \end{aligned} \tag{3.3c}$$

$$\begin{aligned} 2R_1 + R_2 \leqslant \min\Big(&a_{2,1}(\rho) + a_{1,1} + a_{3,2}(\rho,\mu_1) + a_{7,2}(\rho,\mu_1,\mu_2), \\ &a_{3,1}(\rho,\mu_2) + a_{1,1} + a_{7,1}(\rho,\mu_1,\mu_2) + 2a_{3,2}(\rho,\mu_1) + a_{5,2}(\rho,\mu_1), a_{2,1}(\rho) + a_{1,1} \\ &+ a_{3,2}(\rho,\mu_1) + a_{5,2}(\rho,\mu_1)\Big), \end{aligned} \tag{3.3d}$$

$$\begin{aligned} R_1 + 2R_2 \leqslant \min\Big(&a_{3,1}(\rho,\mu_2) + a_{5,1}(\rho,\mu_2) + a_{2,2}(\rho) + a_{1,2}, a_{3,1}(\rho,\mu_2) + a_{7,1}(\rho,\mu_1,\mu_2) \\ &+ a_{2,2}(\rho) + a_{1,2}, 2a_{3,1}(\rho,\mu_2) + a_{5,1}(\rho,\mu_2) + a_{3,2}(\rho,\mu_1) + a_{1,2} + a_{7,2}(\rho,\mu_1,\mu_2)\Big) \end{aligned} \tag{3.3e}$$

with $(\rho,\mu_1,\mu_2) \in \left[0, \left(1 - \max\left(\frac{1}{\text{INR}_{12}}, \frac{1}{\text{INR}_{21}}\right)\right)^+\right] \times [0,1] \times [0,1]$.

The proof of the achievability is based on random coding arguments. The techniques are rate splitting, block-Markov superposition coding, and backward decoding. The complete proof is described in [11]. However, a brief description of the ideas leading to the construction of an achievability scheme are discussed hereunder.

One of the central observations is that thanks to feedback transmitters can correlated their channel inputs. This stems from the fact that some messages indices sent by transmitter i can be decoded by receiver j, e.g., common message indices; fed back to transmitter j and finally, retransmitted by transmitter j. See for instance [2, 44, 51, 58], and [63]. This observation is the driving idea in the construction of the achievability schemes presented in previous works and it is central in the proof of Theorem 1.

Let the message index sent by transmitter i during the t-th block be denoted by $W_i^{(t)} \in \{1, 2, \ldots, 2^{NR_i}\}$. Following a rate-splitting argument, assume that $W_i^{(t)}$ is represented by three subindices $(W_{i,C1}^{(t)}, W_{i,C2}^{(t)}, W_{i,P}^{(t)}) \in \{1, 2, \ldots, 2^{NR_{i,C1}}\} \times \{1, 2, \ldots, 2^{NR_{i,C2}}\} \times \{1, 2, \ldots, 2^{NR_{i,P}}\}$, where $R_{i,C1} + R_{i,C2} + R_{i,P} = R_i$. The message index $(W_{i,C1}^{(t)}$ must be decoded by both receivers and transmitter j; message index $(W_{i,C2}^{(t)}$

must be decoded by both receivers and but not by transmitter j; and message index ($W_{i,P}^{(t)}$ must be only decoded by receiver i.

The codeword generation follows a four-level superposition coding scheme. The number of layers is the number of rate splits plus an additional common layer that accounts for the correlation between codewords. This correlation is induced as follows. The index $W_{i,C1}^{(t-1)}$ is assumed to be decoded at transmitter j via the feedback link of transmitter-receiver pair j at the end of the transmission of block $t-1$. Therefore, at the beginning of block t, each transmitter possesses the knowledge of the indices $W_{1,C1}^{(t-1)}$ and $W_{2,C1}^{(t-1)}$. Using these indices both transmitters are able to identify the same codeword in the first code-layer. In the case of the first block $t=1$ and the last block $t=T$, the indices $W_{1,C1}^{(0)}$, $W_{2,C1}^{(0)}$, $W_{1,C1}^{(T)}$, and $W_{2,C1}^{(T)}$ correspond to indices assumed to be known by all transmitters and receivers.

The first code-layer is a sub-codebook of $2^{N(R_{1,C1}+R_{2,C1})}$ codewords (see Figure 3.1). Denote by $\boldsymbol{u}\left(W_{1,C1}^{(t-1)},\, W_{2,C1}^{(t-1)}\right)$ the corresponding codeword in the first code-layer. The second codeword used by transmitter i is selected using $W_{i,C1}^{(t)}$ from the second code-layer, which is a sub-codebook of $2^{N\,R_{i,C1}}$ codewords specific to $\boldsymbol{u}\left(W_{1,C1}^{(t-1)}, W_{2,C1}^{(t-1)}\right)$ as shown in Figure 3.1. Denote by $\boldsymbol{u}_i\left(W_{1,C1}^{(t-1)}, W_{2,C1}^{(t-1)}, W_{i,C1}^{(t)}\right)$ the corresponding codeword in the second code-layer. The third codeword used by transmitter i is selected using $W_{i,C2}^{(t)}$ from the third code-layer, which is a sub-codebook of $2^{N\,R_{i,C2}}$ codewords specific to $\boldsymbol{u}_i\left(W_{1,C1}^{(t-1)}, W_{2,C1}^{(t-1)}, W_{t,C1}^{(t)}\right)$ as shown in Figure 3.1. Denote by $\boldsymbol{v}_i\left(W_{1,C1}^{(t-1)}, W_{2,C1}^{(t-1)}, W_{i,C1}^{(t)}, W_{i,C2}^{(t)}\right)$ the corresponding codeword in the third code-layer. The fourth codeword used by transmitter i is selected using $W_{i,P}^{(t)}$ from the fourth code-layer, which is a sub-codebook of $2^{N\,R_{i,P}}$ codewords specific to $\boldsymbol{v}_i\left(W_{1,C1}^{(t-1)}, W_{2,C1}^{(t-1)}, W_{i,C1}^{(t)}, W_{i,C2}^{(t)}\right)$ as shown in Figure 3.1. Denote by $\boldsymbol{x}_{i,P}\Big(W_{1,C1}^{(t-1)}$, $W_{2,C1}^{(t-1)}$, $W_{i,C1}^{(t)}$, $W_{i,C2}^{(t)}$, $W_{i,P}^{(t)}\Big)$ the corresponding codeword in the fourth code-layer. Finally, the channel input sequence at transmitter i during block t is denoted by $\boldsymbol{x}_{i,t} = (x_{i,t,1}, x_{i,t,2}, \ldots, x_{i,t,N})$, with $t \in \{1, 2, \ldots, T\}$, and it is a weighted sum of the codewords $\boldsymbol{u}\Big(W_{1,C1}^{(t-1)}, W_{2,C1}^{(t-1)}\Big)$, $\boldsymbol{u}_i\Big(W_{1,C1}^{(t-1)}, W_{2,C1}^{(t-1)}, W_{i,C1}^{(t)}\Big)$, $\boldsymbol{v}_i\Big(W_{1,C1}^{(t-1)}, W_{2,C1}^{(t-1)}, W_{i,C1}^{(t)}, W_{i,C2}^{(t)}\Big)$ and $\boldsymbol{x}_{i,P}\Big(W_{1,C1}^{(t-1)}$, $W_{2,C1}^{(t-1)}$, $W_{i,C1}^{(t)}$, $W_{i,C2}^{(t)}$, $W_{i,P}^{(t)}\Big)$.

The decoders follow a classical backward decoding scheme, as suggested in [2,44,58]. This achievability scheme is thoroughly described in [11].

Other achievable schemes, as reported in [58], can also be obtained as special cases of the more general scheme presented in [50]. However, in this more general case, the resulting code for the IC-NOF counts with a handful of unnecessary superposing code-layers, which demands further optimization.

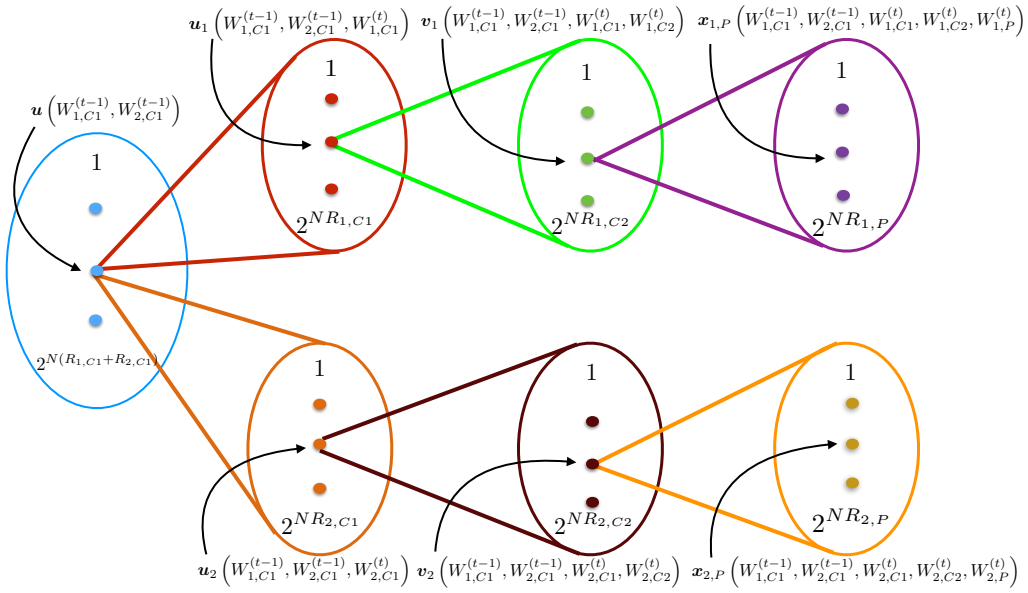

Figure 3.1: Structure of the superposition code. The codewords corresponding to the message indices $W_{1,C1}^{(t-1)}, W_{2,C1}^{(t-1)}, W_{i,C1}^{(t)}, W_{i,C2}^{(t)}, W_{i,P}^{(t)}$ with $i \in \{1,2\}$ as well as the block index t are both highlighted. The (approximate) number of codewords for each code layer is also highlighted.

3.2 A Converse Region with Noisy Feedback

This section describes a converse region for the GIC-NF, which is described in terms of eight inequalities. Three of such inequalities, in particular two on the individual rates and another on the sum rate, are the same as in the perfect channel-output feedback GIC [44]. The five remaining inequalities are new and are obtained using Fano's inequality [74] and by considering several scenarios in which the receivers are assumed to have access to additional information. These scenarios are described in Figure 3.2.

In the scenario described in Figure 3.2(a), receiver 1 is granted with the knowledge of the message index of transmitter 2, i.e., W_2; and the feedback signal observed by transmitter 2. That is, at the end of the communication, receiver 1 observes $\overleftarrow{Y}_{2,1}$, $\overleftarrow{Y}_{2,2}$, …, $\overleftarrow{Y}_{2,N}$. Under this scenario, an upper bound on R_1 is obtained. Using the same arguments, an upper-bound on R_2 is obtained.

In the scenario described in Figure 3.2(b), both receivers are granted with the knowledge of the feedback signal observed by their corresponding transmitter. That is, at the end of the communication, receiver i, with $i \in \{1,2\}$, observes $\overleftarrow{Y}_{i,1}$, $\overleftarrow{Y}_{i,2}$, …, $\overleftarrow{Y}_{i,N}$. Under this scenario, an upper bound on $R_1 + R_2$ is obtained.

In the scenario described in Figure 3.2(c), both receivers are granted with the knowledge of the feedback signal observed by their corresponding transmitter. That is, at the end of the communication, receiver i, with $i \in \{1,2\}$, observes $\overleftarrow{Y}_{i,1}$, $\overleftarrow{Y}_{i,2}$, …, $\overleftarrow{Y}_{i,N}$. An additional receiver is also considered. Such a receiver observes the channel

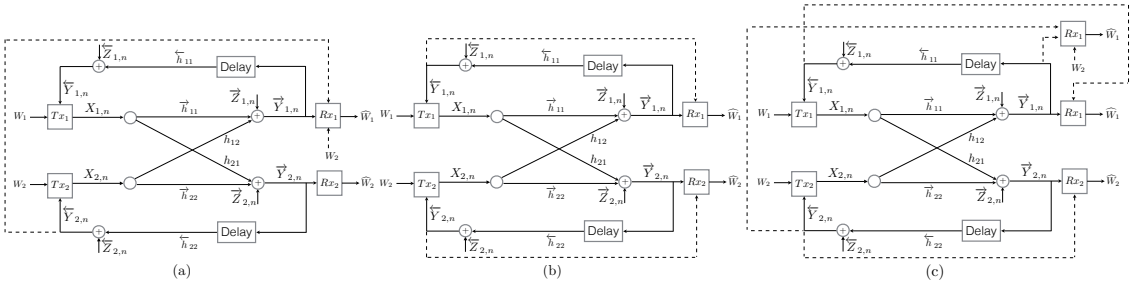

Figure 3.2: Genie-Aided G-IC-NOF models for channel use n. (a) Model used to calculate the outer-bound on R_1; (b) Model used to calculate the outer-bound on $R_1 + R_2$; and (c) Model used to calculate the outer-bound on $2R_1 + R_2$.

output observed by receiver 1 and the feedback signal observed by transmitter 2. That is, at the end of the communication, the new receiver observes $\overrightarrow{Y}_{1,1}$, $\overrightarrow{Y}_{1,2}$, …, $\overrightarrow{Y}_{1,N}$ and $\overleftarrow{Y}_{2,1}$, $\overleftarrow{Y}_{2,2}$, …, $\overleftarrow{Y}_{2,N}$. Under this scenario, an upper bound on $2R_1+R_2$ is obtained. Using a similar argument, an upper bound on R_1+2R_2 is obtained.

The description of the converse region $\overline{\mathcal{C}}_{\mathrm{GIC-NF}}$ is determined by two events denoted by $S_{l_1,1}$ and $S_{l_2,2}$, where $(l_1, l_2) \in \{1, \ldots, 5\}^2$. The events are defined as follows:

$$S_{1,i}\colon \quad \overrightarrow{\mathrm{SNR}}_j < \min\left(\mathrm{INR}_{ij}, \mathrm{INR}_{ji}\right), \tag{3.4a}$$

$$S_{2,i}\colon \quad \mathrm{INR}_{ji} \leqslant \overrightarrow{\mathrm{SNR}}_j < \mathrm{INR}_{ij}, \tag{3.4b}$$

$$S_{3,i}\colon \quad \mathrm{INR}_{ij} \leqslant \overrightarrow{\mathrm{SNR}}_j < \mathrm{INR}_{ji}, \tag{3.4c}$$

$$S_{4,i}\colon \quad \max\left(\mathrm{INR}_{ij}, \mathrm{INR}_{ji}\right) \leqslant \overrightarrow{\mathrm{SNR}}_j < \mathrm{INR}_{ij}\mathrm{INR}_{ji}, \tag{3.4d}$$

$$S_{5,i}\colon \quad \overrightarrow{\mathrm{SNR}}_j \geqslant \mathrm{INR}_{ij}\mathrm{INR}_{ji}. \tag{3.4e}$$

Note that for all $i \in \{1, 2\}$, the events $S_{1,i}$, $S_{2,i}$, $S_{3,i}$, $S_{4,i}$, and $S_{5,i}$ are mutually exclusive. This observation shows that given any 4-tuple $(\overrightarrow{\mathrm{SNR}}_1, \overrightarrow{\mathrm{SNR}}_2, \mathrm{INR}_{12}, \mathrm{INR}_{21})$, there always exists one and only one pair of events $(S_{l_1,1}, S_{l_2,2})$, with $(l_1, l_2) \in \{1, \ldots, 5\}^2$, which determines a unique scenario. Note also that the pairs of events $(S_{2,1}, S_{2,2})$ and $(S_{3,1}, S_{3,2})$ are not feasible. In view of this, twenty-three different scenarios can be identified using the events in (3.4). Once the exact scenario is identified, the converse region is described using the functions $\kappa_{l,i} : [0, 1] \to \mathbb{R}_+$, with $l \in \{1, \ldots, 3\}$; $\kappa_l : [0, 1] \to \mathbb{R}_+$, with $l \in \{4, 5\}$; $\kappa_{6,l} : [0, 1] \to \mathbb{R}_+$, with $l \in \{1, \ldots, 4\}$; and $\kappa_{7,i,l} : [0, 1] \to \mathbb{R}_+$, with $l \in \{1, 2\}$. These functions are defined

as follows, for all $i \in \{1,2\}$, with $j \in \{1,2\} \setminus \{i\}$:

$$\kappa_{1,i}(\rho)=\frac{1}{2}\log\Big(b_{1,i}(\rho)+1\Big), \tag{3.5a}$$

$$\kappa_{2,i}(\rho)=\frac{1}{2}\log\Big(1+b_{5,j}(\rho)\Big)+\frac{1}{2}\log\left(1+\frac{b_{4,i}(\rho)}{1+b_{5,j}(\rho)}\right), \tag{3.5b}$$

$$\kappa_{3,i}(\rho)=\frac{1}{2}\log\left(\frac{\Big(b_{4,i}(\rho)+b_{5,j}(\rho)+1\Big)\overleftarrow{\mathrm{SNR}}_j}{\Big(b_{1,j}(1)+1\Big)\Big(b_{4,i}(\rho)+1\Big)}+1\right) +\frac{1}{2}\log\Big(b_{4,i}(\rho)+1\Big), \tag{3.5c}$$

$$\kappa_{4}(\rho)=\frac{1}{2}\log\left(1+\frac{b_{4,1}(\rho)}{1+b_{5,2}(\rho)}\right)+\frac{1}{2}\log\Big(b_{1,2}(\rho)+1\Big), \tag{3.5d}$$

$$\kappa_{5}(\rho)=\frac{1}{2}\log\left(1+\frac{b_{4,2}(\rho)}{1+b_{5,1}(\rho)}\right)+\frac{1}{2}\log\Big(b_{1,1}(\rho)+1\Big), \tag{3.5e}$$

$$\kappa_6(\rho)=\begin{cases}\kappa_{6,1}(\rho) & \text{if } (S_{1,2}\vee S_{2,2}\vee S_{5,2})\\ & \quad\wedge(S_{1,1}\vee S_{2,1}\vee S_{5,1})\\ \kappa_{6,2}(\rho) & \text{if } (S_{1,2}\vee S_{2,2}\vee S_{5,2})\\ & \quad\wedge(S_{3,1}\vee S_{4,1})\\ \kappa_{6,3}(\rho) & \text{if } (S_{3,2}\vee S_{4,2})\\ & \quad\wedge(S_{1,1}\vee S_{2,1}\vee S_{5,1})\\ \kappa_{6,4}(\rho) & \text{if } (S_{3,2}\vee S_{4,2})\\ & \quad\wedge(S_{3,1}\vee S_{4,1}),\end{cases} \tag{3.5f}$$

$$\kappa_{7,i}(\rho)=\begin{cases}\kappa_{7,i,1}(\rho) & \text{if } (S_{1,i}\vee S_{2,i}\vee S_{5,i})\\ \kappa_{7,i,2}(\rho) & \text{if } (S_{3,i}\vee S_{4,i}),\end{cases} \tag{3.5g}$$

where,

$$\kappa_{6,1}(\rho)=\frac{1}{2}\log\Big(b_{1,1}(\rho)+b_{5,1}(\rho)\mathrm{INR}_{21}\Big)-\frac{1}{2}\log\Big(1+\mathrm{INR}_{12}\Big)$$

$$
\begin{aligned}
&+\frac{1}{2}\log\left(1+\frac{b_{5,2}(\rho)\overleftarrow{\mathrm{SNR}_2}}{b_{1,2}(1)+1}\right)\\
&+\frac{1}{2}\log\left(b_{1,2}(\rho)+b_{5,1}(\rho)\mathrm{INR}_{21}\right)-\frac{1}{2}\log\left(1+\mathrm{INR}_{21}\right)\\
&+\frac{1}{2}\log\left(1+\frac{b_{5,1}(\rho)\overleftarrow{\mathrm{SNR}_1}}{b_{1,1}(1)+1}\right)+\log(2\pi e), \qquad (3.6a)\\
\kappa_{6,2}(\rho)&=\frac{1}{2}\log\left(b_{6,2}(\rho)+\frac{b_{5,1}(\rho)\mathrm{INR}_{21}}{\overrightarrow{\mathrm{SNR}_2}}\left(\overrightarrow{\mathrm{SNR}_2}+b_{3,2}\right)\right)\\
&-\frac{1}{2}\log\left(1+\mathrm{INR}_{12}\right)+\frac{1}{2}\log\left(1+\frac{b_{5,1}(\rho)\overleftarrow{\mathrm{SNR}_1}}{b_{1,1}(1)+1}\right)\\
&+\frac{1}{2}\log\left(b_{1,1}(\rho)+b_{5,1}(\rho)\mathrm{INR}_{21}\right)-\frac{1}{2}\log\left(1+\mathrm{INR}_{21}\right)\\
&+\frac{1}{2}\log\left(1+\frac{b_{5,2}(\rho)}{\overrightarrow{\mathrm{SNR}_2}}\left(\mathrm{INR}_{12}+\frac{b_{3,2}\overleftarrow{\mathrm{SNR}_2}}{b_{1,2}(1)+1}\right)\right)\\
&-\frac{1}{2}\log\left(1+\frac{b_{5,1}(\rho)\mathrm{INR}_{21}}{\overrightarrow{\mathrm{SNR}_2}}\right)+\log(2\pi e), \qquad (3.6b)\\
\kappa_{6,3}(\rho)&=\frac{1}{2}\log\left(b_{6,1}(\rho)+\frac{b_{5,1}(\rho)\mathrm{INR}_{21}}{\overrightarrow{\mathrm{SNR}_1}}\left(\overrightarrow{\mathrm{SNR}_1}+b_{3,1}\right)\right)\\
&-\frac{1}{2}\log\left(1+\mathrm{INR}_{12}\right)+\frac{1}{2}\log\left(1+\frac{b_{5,2}(\rho)\overleftarrow{\mathrm{SNR}_2}}{b_{1,2}(1)+1}\right)\\
&+\frac{1}{2}\log\left(b_{1,2}(\rho)+b_{5,1}(\rho)\mathrm{INR}_{21}\right)-\frac{1}{2}\log\left(1+\mathrm{INR}_{21}\right)\\
&+\frac{1}{2}\log\left(1+\frac{b_{5,1}(\rho)}{\overrightarrow{\mathrm{SNR}_1}}\left(\mathrm{INR}_{21}+\frac{b_{3,1}\overleftarrow{\mathrm{SNR}_1}}{b_{1,1}(1)+1}\right)\right)\\
&-\frac{1}{2}\log\left(1+\frac{b_{5,1}(\rho)\mathrm{INR}_{21}}{\overrightarrow{\mathrm{SNR}_1}}\right)+\log(2\pi e), \qquad (3.6c)\\
\kappa_{6,4}(\rho)&=\frac{1}{2}\log\left(b_{6,1}(\rho)+\frac{b_{5,1}(\rho)\mathrm{INR}_{21}}{\overrightarrow{\mathrm{SNR}_1}}\left(\overrightarrow{\mathrm{SNR}_1}+b_{3,1}\right)\right)\\
&-\frac{1}{2}\log\left(1+\mathrm{INR}_{12}\right)-\frac{1}{2}\log\left(1+\mathrm{INR}_{21}\right)\\
&+\frac{1}{2}\log\left(1+\frac{b_{5,2}(\rho)}{\overrightarrow{\mathrm{SNR}_2}}\left(\mathrm{INR}_{12}+\frac{b_{3,2}\overleftarrow{\mathrm{SNR}_2}}{b_{1,2}(1)+1}\right)\right)\\
&-\frac{1}{2}\log\left(1+\frac{b_{5,1}(\rho)\mathrm{INR}_{21}}{\overrightarrow{\mathrm{SNR}_2}}\right)\\
&-\frac{1}{2}\log\left(1+\frac{b_{5,1}(\rho)\mathrm{INR}_{21}}{\overrightarrow{\mathrm{SNR}_1}}\right)\\
&+\frac{1}{2}\log\left(b_{6,2}(\rho)+\frac{b_{5,1}(\rho)\mathrm{INR}_{21}}{\overrightarrow{\mathrm{SNR}_2}}\left(\overrightarrow{\mathrm{SNR}_2}+b_{3,2}\right)\right)\\
&+\frac{1}{2}\log\left(1+\frac{b_{5,1}(\rho)}{\overrightarrow{\mathrm{SNR}_1}}\left(\mathrm{INR}_{21}+\frac{b_{3,1}\overleftarrow{\mathrm{SNR}_1}}{b_{1,1}(1)+1}\right)\right)\\
&+\log(2\pi e), \qquad (3.6d)
\end{aligned}
$$

and

$$\begin{aligned}\kappa_{7,i,1}(\rho) = &\frac{1}{2}\log\Big(b_{1,i}(\rho)+1\Big) - \frac{1}{2}\log\Big(1+\mathrm{INR}_{ij}\Big)\\ &+\frac{1}{2}\log\left(1+\frac{b_{5,j}(\rho)\overleftarrow{\mathrm{SNR}}_j}{b_{1,j}(1)+1}\right)+2\log(2\pi e)\\ &+\frac{1}{2}\log\Big(b_{1,j}(\rho)+b_{5,i}(\rho)\mathrm{INR}_{ji}\Big)\end{aligned}$$

$$+\frac{1}{2}\log\Big(1+b_{4,i}(\rho)+b_{5,j}(\rho)\Big)-\frac{1}{2}\log\Big(1+b_{5,j}(\rho)\Big) \tag{3.7a}$$

$$\begin{aligned}\kappa_{7,i,2}(\rho) = &\frac{1}{2}\log\Big(b_{1,i}(\rho)+1\Big) - \frac{1}{2}\log\Big(1+\mathrm{INR}_{ij}\Big)\\ &-\frac{1}{2}\log\Big(1+b_{5,j}(\rho)\Big)+\frac{1}{2}\log\Big(1+b_{4,i}(\rho)+b_{5,j}(\rho)\Big)\\ &+\frac{1}{2}\log\left(1+\Big(1-\rho^2\Big)\frac{\mathrm{INR}_{ji}}{\overrightarrow{\mathrm{SNR}}_j}\left(\mathrm{INR}_{ij}+\frac{b_{3,j}\overleftarrow{\mathrm{SNR}}_j}{b_{1,j}(1)+1}\right)\right)\\ &-\frac{1}{2}\log\left(1+\frac{b_{5,i}(\rho)\mathrm{INR}_{ji}}{\overrightarrow{\mathrm{SNR}}_j}\right)\\ &+\frac{1}{2}\log\left(b_{6,j}(\rho)+\frac{b_{5,i}(\rho)\mathrm{INR}_{ji}}{\overrightarrow{\mathrm{SNR}}_j}\Big(\overrightarrow{\mathrm{SNR}}_j+b_{3,j}\Big)\right)\\ &+2\log(2\pi e).\end{aligned} \tag{3.7b}$$

The functions $b_{l,i}$, with $(l,i)\in\{1,2\}^2$ are defined in (3.2); $b_{3,i}$ are constants; and the functions $b_{l,i}:[0,1]\to\mathbb{R}_+$, with $(l,i)\in\{4,5,6\}\times\{1,2\}$ are defined as follows, with $j\in\{1,2\}\setminus\{i\}$:

$$b_{3,i}=\overrightarrow{\mathrm{SNR}}_i-2\sqrt{\overrightarrow{\mathrm{SNR}}_i\mathrm{INR}_{ji}}+\mathrm{INR}_{ji}, \tag{3.8a}$$

$$b_{4,i}(\rho)=\Big(1-\rho^2\Big)\overrightarrow{\mathrm{SNR}}_i, \tag{3.8b}$$

$$b_{5,i}(\rho)=\Big(1-\rho^2\Big)\mathrm{INR}_{ij}, \tag{3.8c}$$

$$\begin{aligned}b_{6,i}(\rho)=&\overrightarrow{\mathrm{SNR}}_i+\mathrm{INR}_{ij}+2\rho\sqrt{\mathrm{INR}_{ij}}\left(\sqrt{\overrightarrow{\mathrm{SNR}}_i}-\sqrt{\mathrm{INR}_{ji}}\right)\\ &+\frac{\mathrm{INR}_{ij}\sqrt{\mathrm{INR}_{ji}}}{\overrightarrow{\mathrm{SNR}}_i}\left(\sqrt{\mathrm{INR}_{ji}}-2\sqrt{\overrightarrow{\mathrm{SNR}}_i}\right).\end{aligned} \tag{3.8d}$$

Finally, using this notation, Theorem 2 is presented below.

Theorem 2. The capacity region $\mathcal{C}_{\mathrm{GIC-NF}}$ is contained within the region $\overline{\mathcal{C}}_{\mathrm{GIC-NF}}$ given by the closure of the set of non-negative rate pairs (R_1,R_2) that for all $i\in$

$\{1,2\}$, with $j \in \{1,2\} \setminus \{i\}$ satisfy:

$$R_i \leqslant \min\Big(\kappa_{1,i}(\rho), \kappa_{2,i}(\rho)\Big), \tag{3.9a}$$

$$R_i \leqslant \kappa_{3,i}(\rho), \tag{3.9b}$$

$$R_1 + R_2 \leqslant \min\Big(\kappa_4(\rho), \kappa_5(\rho)\Big), \tag{3.9c}$$

$$R_1 + R_2 \leqslant \kappa_6(\rho), \tag{3.9d}$$

$$2R_i + R_j \leqslant \kappa_{7,i}(\rho), \tag{3.9e}$$

with $\rho \in [0,1]$.

The outer bounds (3.9a) and (3.9c) correspond to the outer bounds for the case of perfect channel-output feedback [44]. The bounds (3.9b), (3.9d) and (3.9e) correspond to new outer bounds that generalize those presented in [58] for the two-user symmetric G-IC-NF. These new outer-bounds were obtained using the genie-aided models shown in Figure 3.2.

3.3 The Gap Between the Achievable Region and the Converse Region

The following theorem describes the gap between the achievable region $\underline{\mathcal{C}}_{\mathrm{GIC-NF}}$ and the converse region $\overline{\mathcal{C}}_{\mathrm{GIC-NF}}$ (Definition 3).

Theorem 3. The capacity region of the two-user GIC-NF is approximated to within 4.4 bits by the achievable region $\underline{\mathcal{C}}_{\mathrm{GIC-NF}}$ and the converse region $\overline{\mathcal{C}}_{\mathrm{GIC-NF}}$.

This approximation to the capacity region of the GIC-NF is the most general with respect to existing literature and the one that guarantees the smallest gap between the achievable and converse regions when feedback links are subject to Gaussian additive noise. Figure 3.3 presents the exact gap existing between the achievable region $\underline{\mathcal{C}}_{\mathrm{GIC-NF}}$ and the converse region $\overline{\mathcal{C}}_{\mathrm{GIC-NF}}$ for the case in which $\overrightarrow{\mathrm{SNR}}_1 = \overrightarrow{\mathrm{SNR}}_2 = \overrightarrow{\mathrm{SNR}}$, $\mathrm{INR}_{12} = \mathrm{INR}_{21} = \mathrm{INR}$, and $\overleftarrow{\mathrm{SNR}}_1 = \overleftarrow{\mathrm{SNR}}_2 = \overleftarrow{\mathrm{SNR}}$ as a function of $\alpha = \frac{\log \mathrm{INR}}{\log \overrightarrow{\mathrm{SNR}}}$ and $\beta = \frac{\log \overleftarrow{\mathrm{SNR}}}{\log \overrightarrow{\mathrm{SNR}}}$. Note that in this case, the maximum gap is 1.1 bits and occurs when $\alpha = 1.05$ and $\beta = 1.2$.

3.4 Concluding Remarks

In this chapter, an achievability region (Theorem 1) and a converse region (Theorem 2) have been presented for the two-user GIC-NF. These two regions approximate the capacity region of the GIC-NF to within 4.4 bits (Theorem 3).

Despite the contributions made in this chapter, several questions remain unsolved in the understanding of the benefits of channel-output feedback in the GIC-NF. For instance, the case in which the channel-output feedback is observed by both transmitters is still an open problem. Only the case of symmetric channels has

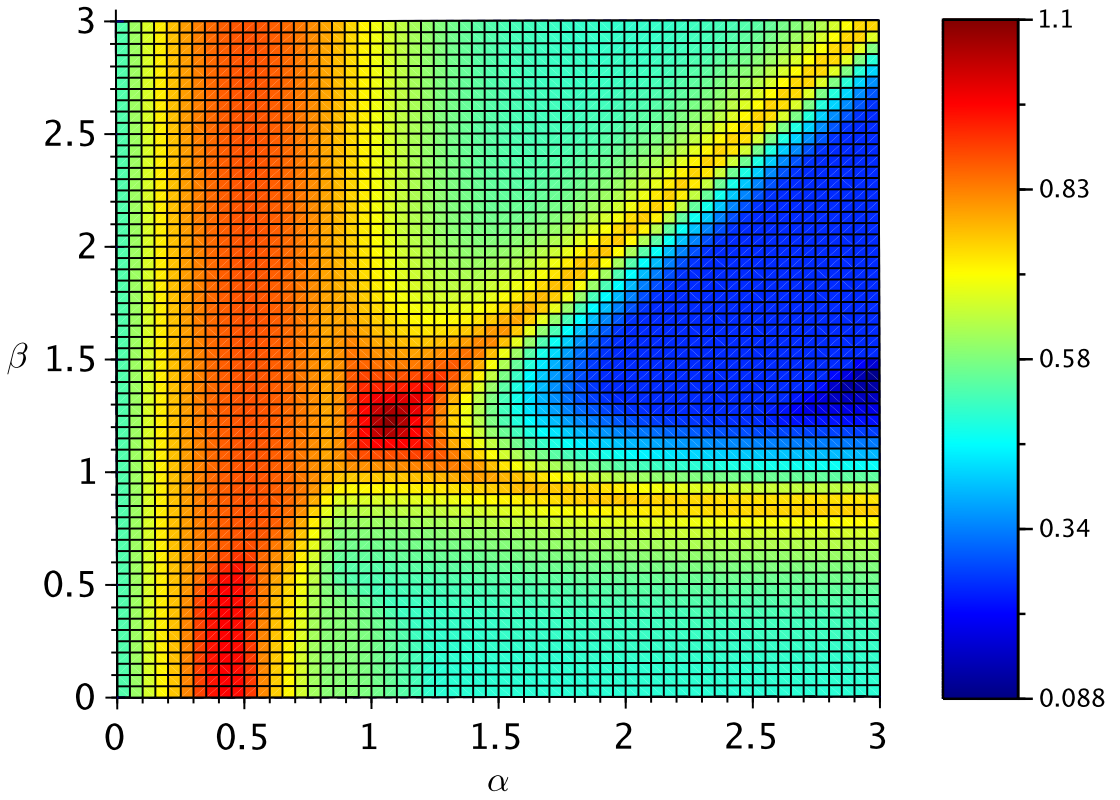

Figure 3.3: Gap between the converse region $\overline{\mathcal{C}}_{\mathrm{GIC-NF}}$ and the achievable region $\underline{\mathcal{C}}_{\mathrm{GIC-NF}}$ of the two-user GIC-NF, under symmetric channel conditions, i.e., $\overrightarrow{\mathrm{SNR}}_1 = \overrightarrow{\mathrm{SNR}}_2 = \overrightarrow{\mathrm{SNR}}$, $\mathrm{INR}_{12} = \mathrm{INR}_{21} = \mathrm{INR}$, and $\overleftarrow{\mathrm{SNR}}_1 = \overleftarrow{\mathrm{SNR}}_2 = \overleftarrow{\mathrm{SNR}}$, as a function of $\alpha = \frac{\log \mathrm{INR}}{\log \overrightarrow{\mathrm{SNR}}}$ and $\beta = \frac{\log \overleftarrow{\mathrm{SNR}}}{\log \overrightarrow{\mathrm{SNR}}}$.

been fully studied. Another case in which very little is known about the benefits of channel-output feedback is that of a large number of users (more than two) and large number of antennas (more than one) at each network component.

Theorem 1 generalizes previous results on the achievable region of the two-user GIC with channel-output feedback. For instance, when $\overleftarrow{\mathrm{SNR}}_1 = 0$, $\overleftarrow{\mathrm{SNR}}_2 = 0$, and $\rho = 0$, Theorem 1 describes the achievable region of the GIC without feedback [34, 36, 75]; when $\overleftarrow{\mathrm{SNR}}_1 \to \infty$ and $\overleftarrow{\mathrm{SNR}}_2 \to \infty$, Theorem 1 describes the achievable region of the GIC-PF (Theorem 2 in [44]); when $\overrightarrow{\mathrm{SNR}}_1 = \overrightarrow{\mathrm{SNR}}_2$, $\mathrm{INR}_{12} = \mathrm{INR}_{21}$ and $\overleftarrow{\mathrm{SNR}}_1 = \overleftarrow{\mathrm{SNR}}_2$, Theorem 1 describes the achievable region of the symmetric GIC-NF (Theorem 3 in [58]). Theorem 2 generalizes previous results on the converse region of the two-user GIC with channel-output feedback. For instance, when $\overleftarrow{\mathrm{SNR}}_1 = 0$, $\overleftarrow{\mathrm{SNR}}_2 = 0$, and $\rho = 0$, Theorem 2 describes the converse region of the GIC without feedback [39]; when $\overleftarrow{\mathrm{SNR}}_1 \to \infty$ and $\overleftarrow{\mathrm{SNR}}_2 \to \infty$, Theorem 2 describes the converse region of the GIC-PF (Theorem 3 in [44]); when $\overrightarrow{\mathrm{SNR}}_1 = \overrightarrow{\mathrm{SNR}}_2$, $\mathrm{INR}_{12} = \mathrm{INR}_{21}$ and $\overleftarrow{\mathrm{SNR}}_1 = \overleftarrow{\mathrm{SNR}}_2$, Theorem 2 describes the converse region of the symmetric GIC-NF (Theorem 2 in [58]).

Chapter 4

Contributions to Decentralized Interference Channels with Feedback

In this chapter, an achievable η-Nash equilibrium (η-NE) region for the two-user Gaussian interference channel with noisy channel-output feedback is presented for all $\eta \geqslant 1$. This result is obtained in a scenario in which each transmitter-receiver pair chooses its own transmit-receive configuration in order to maximize its own individual information transmission rate. At an η-NE, any unilateral deviation by either of the pairs does not increase the corresponding individual rate by more than η bits per channel use.

4.1 Game Formulation

The competitive interaction between the two transmitter-receiver pairs in the interference channel can be modeled by the following game in normal-form:

$$\mathcal{G} = \left(\mathcal{K}, \{\mathcal{A}_k\}_{k\in\mathcal{K}}, \{u_k\}_{k\in\mathcal{K}}\right). \tag{4.1}$$

The set $\mathcal{K} = \{1, 2\}$ is the set of players, that is, the set of transmitter-receiver pairs. The sets $\mathcal{A}_1$ and $\mathcal{A}_2$ are the sets of actions of player 1 and 2, respectively. An action of a player $i \in \mathcal{K}$, which is denoted by $s_i \in \mathcal{A}_i$, is basically its transmit-receive configuration as described in Section 2.5.2. The utility function of player i is $u_i : \mathcal{A}_1 \times \mathcal{A}_2 \to \mathbb{R}_+$ and it is defined as the achieved rate of transmitter i,

$$u_i(s_1, s_2) = \begin{cases} R_i, & \text{if } P_i(N) < \epsilon \\ 0, & \text{otherwise,} \end{cases} \tag{4.2}$$

where $\epsilon > 0$ is an arbitrarily small number and R_i denotes a transmission rate achievable with the configurations s_1 and s_2. This game formulation was first proposed in [76] and [77].

A class of transmit-receive configurations $\boldsymbol{s}^* = (s_1^*, s_2^*) \in \mathcal{A}_1 \times \mathcal{A}_2$ that are particularly important in the analysis of this game is referred to as the set of η-Nash equilibria (η-NE), with $\eta > 0$. This type of configuration satisfies the following definition.

Definition 4 (η-Nash equilibrium [66])**.** In the game $\mathcal{G} = \left(\mathcal{K}, \{\mathcal{A}_k\}_{k\in\mathcal{K}}, \{u_k\}_{k\in\mathcal{K}}\right)$, an action profile (s_1^*, s_2^*) is an η-Nash equilibrium if for all $s_1 \in \mathcal{A}_1$ and $s_2 \in \mathcal{A}_2$, there exits an $\eta > 0$ such that

$$u_1(s_1, s_2^*) \leqslant u_1(s_1^*, s_2^*) + \eta \text{ and} \tag{4.3a}$$

$$u_2(s_1^*, s_2) \leqslant u_2(s_1^*, s_2^*) + \eta. \tag{4.3b}$$

Let (s_1^*, s_2^*) be an η-Nash equilibrium action profile of the game in (9.18). Then, none of the transmitters can increase its own information transmission rate more than η bits per channel use by changing its own transmit-receive configuration and keeping the individual decoding error probability arbitrarily close to zero. Note that for η sufficiently large, from Definition 4, any pair of configurations can be an η-NE. Alternatively, for $\eta = 0$, the classical definition of Nash equilibrium is obtained [65]. In this case, if a pair of configurations is a Nash equilibrium ($\eta = 0$), then each individual configuration is optimal with respect to each other. Hence, the interest is to describe the set of all possible η-NE rate pairs (R_1, R_2) of the game in (9.18) with the smallest η for which there exists at least one equilibrium configuration pair.

The set of rate pairs that can be achieved at an η-NE is known as the η-Nash equilibrium region.

Definition 5 (η-NE Region)**.** Let $\eta > 0$ be fixed. An achievable rate pair (R_1, R_2) is said to be in the η-NE region of the game $\mathcal{G} = \left(\mathcal{K}, \{\mathcal{A}_k\}_{k\in\mathcal{K}}, \{u_k\}_{k\in\mathcal{K}}\right)$ if there exists a pair $(s_1^*, s_2^*) \in \mathcal{A}_1 \times \mathcal{A}_2$ that is an η-NE and the following holds:

$$u_1(s_1^*, s_2^*) = R_1 \quad \text{and} \quad u_2(s_1^*, s_2^*) = R_2. \tag{4.4}$$

4.2 An Achievable η-Nash Equilibrium Region

Let the η-NE region (Definition 5) of the two-user D-GIC-NF be denoted by $\mathcal{N}_\eta$. This section introduces a region $\underline{\mathcal{N}}_\eta \subseteq \mathcal{N}_\eta$ that is achievable using the randomized Han-Kobayashi scheme with noisy channel output feedback (RHK-NF), presented in [10]. The RHK-NF is proved to be an η-NE action profile with $\eta \geqslant 1$. That is, any unilateral deviation from the RHK-NF by any of the transmitter-receiver pairs might lead to an individual rate improvement that is at most one bit per channel use. The description of the achievable η-NE region $\underline{\mathcal{N}}_\eta$ is presented using the constants $a_{1,i}$; the functions $a_{2,i} : [0,1] \to \mathbb{R}_+$, $a_{l,i} : [0,1]^2 \to \mathbb{R}_+$, with $l \in \{3, \ldots, 6\}$; and $a_{7,i} : [0,1]^3 \to \mathbb{R}_+$, which are defined for all $i \in \{1,2\}$, with $j \in \{1,2\} \setminus \{i\}$ in (3.1) and (3.2). Using this notation, the main result is presented in the following theorem.

Theorem 4. *Let $\eta \geqslant 1$. The achievable η-NE region $\underline{\mathcal{N}}_\eta$ is given by the closure of all possible achievable rate pairs $(R_1, R_2) \in \underline{\mathcal{C}}_{\mathrm{GIC-NF}}$ that satisfy, for all $i \in \{1,2\}$ and $j \in \{1,2\} \setminus \{i\}$, the following conditions:*

$$R_i \geqslant \Big(a_{2,i}(\rho) - a_{3,i}(\rho,\mu_j) - a_{4,i}(\rho,\mu_j) - \eta\Big)^+, \tag{4.5a}$$

$$\begin{aligned} R_i \leqslant \min\Big(& a_{2,i}(\rho) + a_{3,j}(\rho,\mu_i) + a_{5,j}(\rho,\mu_i) - a_{2,j}(\rho) + \eta, \\ & a_{3,i}(\rho,\mu_j) + a_{7,i}(\rho,\mu_1,\mu_2) + 2a_{3,j}(\rho,\mu_i) + a_{5,j}(\rho,\mu_i) - a_{2,j}(\rho) + \eta, \\ & a_{2,i}(\rho) + a_{3,i}(\rho,\mu_j) + 2a_{3,j}(\rho,\mu_i) + a_{5,j}(\rho,\mu_i) + a_{7,j}(\rho,\mu_1,\mu_2) - 2a_{2,j}(\rho) + 2\eta\Big), \end{aligned} \tag{4.5b}$$

$$R_1 + R_2 \leqslant a_{1,i} + a_{3,i}(\rho,\mu_j) + a_{7,i}(\rho,\mu_1,\mu_2) + a_{2,j}(\rho) + a_{3,j}(\rho,\mu_1) - a_{2,i}(\rho) + \eta, \tag{4.5c}$$

for all $(\rho,\mu_1,\mu_2) \in \left[0, \left(1 - \max\left(\frac{1}{\mathrm{INR}_{12}}, \frac{1}{\mathrm{INR}_{21}}\right)\right)^+\right] \times [0,1] \times [0,1]$.

The proof of Theorem 4 consists in proving the existence of an achievability scheme for each of the rate pairs in $\underline{\mathcal{N}}_\eta$. The achievability scheme used for this proof is essentially a modification of the coding scheme with noisy feedback presented in Section 3.1. The novelty consists in allowing users to introduce common randomness as suggested in [2, 69].

Consider without any loss of generality that $N = N_1 = N_2$. Let $W_i^{(t)} \in \{1,2,\ldots,2^{NR_i}\}$ and $\Omega_i^{(t)} \in \{1,2,\ldots,2^{NR_{i,R}}\}$ denote the message index and the random message index sent by transmitter i during the t-th block, with $t \in \{1,2,\ldots,T\}$, respectively. Following a rate-splitting argument, assume that $\left(W_i^{(t)}, \Omega_i^{(t)}\right)$ is represented by the indices $\left(W_{i,C1}^{(t)}, \Omega_{i,R1}^{(t)}, W_{i,C2}^{(t)}, \Omega_{i,R2}^{(t)}, W_{i,P}^{(t)}\right) \in \{1,2,\ldots,2^{NR_{i,C1}}\} \times \{1,2,\ldots,2^{NR_{i,R1}}\} \times \{1,2,\ldots,2^{NR_{i,C2}}\} \times \{1,2,\ldots,2^{NR_{i,R2}}\} \times \{1,2,\ldots,2^{NR_{i,P}}\}$, where $R_i = R_{i,C1} + R_{i,C2} + R_{i,P}$ and $R_{i,R} = R_{i,R1} + R_{i,R2}$. The rate $R_{i,R}$ is the number of transmitted bits that are known by both transmitter i and receiver i per channel use, and thus it does not have an impact on the information rate R_i.

The codeword generation follows a four-level superposition coding scheme as shown in Figure 4.1. The indices $W_{i,C1}^{(t-1)}$ and $\Omega_{i,R1}^{(t-1)}$ are assumed to be decoded at transmitter j via the feedback link of transmitter-receiver pair j at the end of the transmission of block $t-1$. Therefore, at the beginning of block t, each transmitter possesses the knowledge of the indices $W_{1,C1}^{(t-1)}$, $\Omega_{1,R1}^{(t-1)}$, $W_{2,C1}^{(t-1)}$ and $\Omega_{2,R1}^{(t-1)}$. In the case of the first block $t = 1$, the indices $W_{1,C1}^{(0)}$, $\Omega_{1,R1}^{(0)}$, $W_{2,C1}^{(0)}$ and $\Omega_{1,R2}^{(0)}$ are assumed to be known by all transmitters and receivers. Using these indices, both transmitters are able to identify the same codeword in the first code-layer. This first code-layer, which is common for both transmitter-receiver pairs, is a sub-codebook of $2^{N\left(R_{1,C1}+R_{2,C1}+R_{1,R1}+R_{2,R1}\right)}$ codewords. Denote by $\vec{u}\left(W_{1,C1}^{(t-1)}, \Omega_{1,R1}^{(t-1)}, W_{2,C1}^{(t-1)}, \Omega_{2,R1}^{(t-1)}\right)$ the corresponding codeword in the first code-layer. The second codeword used by transmitter i is selected using $\left(W_{i,C1}^{(t)}, \Omega_{i,R1}^{(t)}\right)$ from the second code-layer, which is a sub-codebook of $2^{N\left(R_{i,C1}+R_{i,R1}\right)}$ codewords corresponding to the codeword $\vec{u}\left(W_{1,C1}^{(t-1)}, \Omega_{1,R1}^{(t-1)}, W_{2,C1}^{(t-1)}, \Omega_{2,R1}^{(t-1)}\right)$. Denote by $\vec{u}_i\left(W_{1,C1}^{(t-1)}, \Omega_{1,R1}^{(t-1)}, W_{2,C1}^{(t-1)}, \Omega_{2,R1}^{(t-1)}, W_{i,C1}^{(t)}, \Omega_{i,R1}^{(t)}\right)$ the corresponding codeword in the second code-layer. The third codeword used by transmitter i is selected using

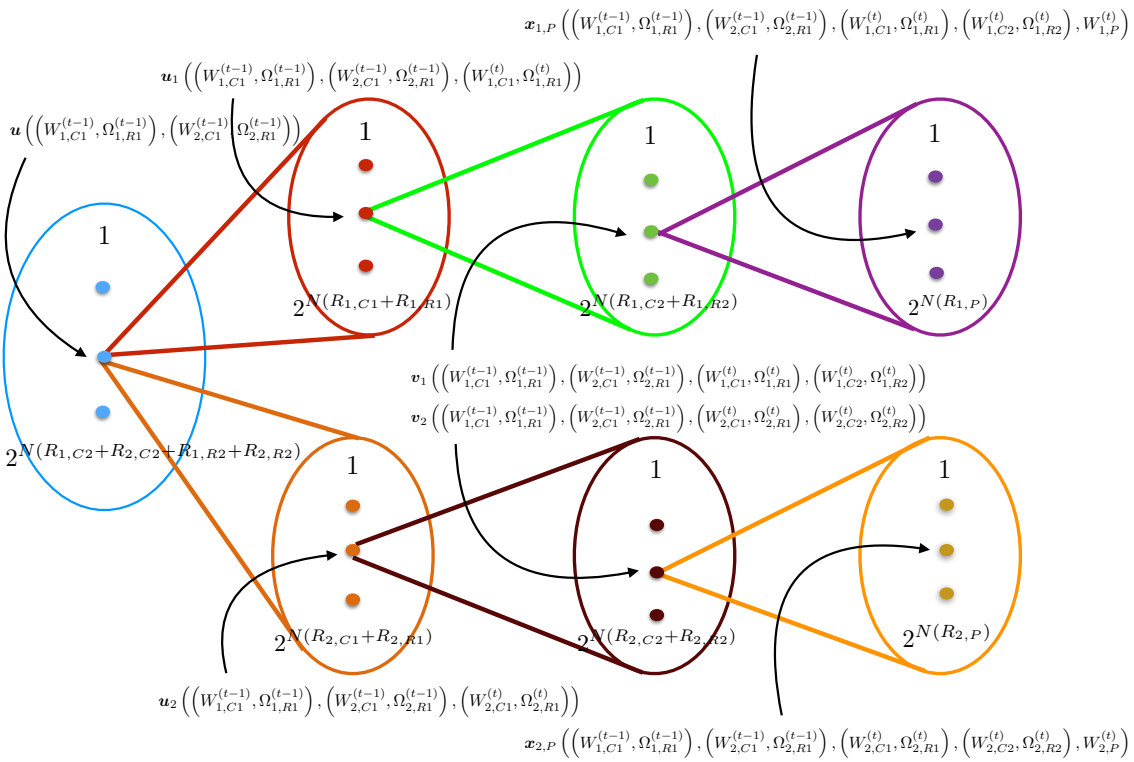

Figure 4.1: Structure of the superposition code. The codewords corresponding to the message indices $W_{1,C1}^{(t-1)}, W_{2,C1}^{(t-1)}, W_{i,C1}^{(t)}, W_{i,C2}^{(t)}, W_{i,P}^{(t)}$ with $i \in \{1,2\}$ as well as the block index t are both highlighted. The (approximate) number of codewords for each code layer is also highlighted.

$\left(W_{i,C2}^{(t)}, \Omega_{i,R2}^{(t)}\right)$ from the third code-layer, which is a sub-codebook of $2^{N\left(R_{i,C2}+R_{i,R2}\right)}$ codewords corresponding to the codeword $\vec{u}_i\left(W_{1,C1}^{(t-1)}, \Omega_{1,R1}^{(t-1)}, W_{2,C1}^{(t-1)}, \Omega_{2,R1}^{(t-1)}, W_{i,C1}^{(t)}, \Omega_{i,R1}^{(t)}\right)$. Denote by $\vec{v}_i\left(W_{1,C1}^{(t-1)}, \Omega_{1,R1}^{(t-1)}, W_{2,C1}^{(t-1)}, \Omega_{2,R1}^{(t-1)}, W_{i,C1}^{(t)}, \Omega_{i,R1}^{(t)}, W_{i,C2}^{(t)}, \Omega_{i,R2}^{(t)}\right)$ the corresponding codeword in the third code-layer. The fourth codeword used by transmitter i is selected using $W_{i,P}^{(t)}$ from the fourth code-layer, which is a sub-codebook of $2^{N\,R_{i,P}}$ codewords corresponding to the codeword $\vec{v}_i\left(W_{1,C1}^{(t-1)}, \Omega_{1,R1}^{(t-1)}, W_{2,C1}^{(t-1)}, \Omega_{2,R1}^{(t-1)}, W_{i,C1}^{(t)}, \Omega_{i,R1}^{(t)}, W_{i,C2}^{(t)}, \Omega_{i,R2}^{(t)}\right)$. Denote by $\vec{x}_{i,P}\left(W_{1,C1}^{(t-1)}, \Omega_{1,R1}^{(t-1)}, W_{2,C1}^{(t-1)}, \Omega_{2,R1}^{(t-1)}, W_{i,C1}^{(t)}, \Omega_{i,R1}^{(t)}, W_{i,C2}^{(t)}, \Omega_{i,R2}^{(t)}, W_{i,P}^{(t)}\right)$ the corresponding codeword in the fourth code-layer. Finally, the codeword $\vec{x}_i\left(W_{1,C1}^{(t-1)}, \Omega_{1,R1}^{(t-1)}, W_{2,C1}^{(t-1)}, \Omega_{2,R1}^{(t-1)}, W_{i,C1}^{(t)}, \Omega_{i,R1}^{(t)}, W_{i,C2}^{(t)}, \Omega_{i,R2}^{(t)}, W_{i,P}^{(t)}\right)$ to be sent during block $t \in \{1, 2, \ldots, T\}$ is a simple arithmetic sum of all previous codewords, *i.e.*$\vec{x}_i = \vec{u}^{\mathsf{T}} + \vec{u}_i^{\mathsf{T}} + \vec{v}_i^{\mathsf{T}} + \vec{x}_{i,P}^{\mathsf{T}}$, where the message indices have been dropped for ease of notation.

The role of the random variables $\Omega_{1,R1}^{(t)}$, $\Omega_{1,R2}^{(t)}$, $\Omega_{2,R1}^{(t)}$ and $\Omega_{2,R2}^{(t)}$ is to allow both transmitter-receiver pairs to limit the rate improvement of each other when either of them deviates from an equilibrium rate pair. This follows from the fact that $\Omega_{i,R1}^{(t)}$, $\Omega_{i,R2}^{(t)}$ are both known at transmitter-receiver pair i and known at transmitter-

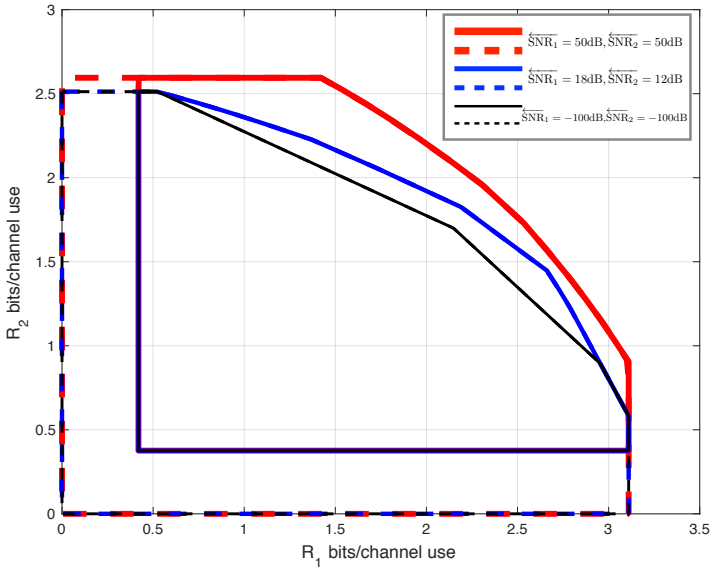

Figure 4.2: Achievable regions (dashed-lines) $\underline{\mathcal{C}}_{\mathrm{GIC-NF}}$ in Theorem 1 and achievable η-NE regions (solid lines) in Theorem 4 of the two-user GIC-NF with parameters $\overrightarrow{\mathrm{SNR}}_1 = 24$ dB, $\overrightarrow{\mathrm{SNR}}_2 = 18$ dB, $\mathrm{INR}_{12} = 16$ dB, $\mathrm{INR}_{21} = 10$ dB, $\overleftarrow{\mathrm{SNR}}_1 \in \{-100, 18, 50\}$ dB, $\overleftarrow{\mathrm{SNR}}_2 \in \{-100, 12, 50\}$ dB, and $\eta = 1$.

receiver pair j. That is, they represent extra message indices to be decoded by transmitter-receiver pair j, which do not need to be decoded by transmitter-receiver pair i, in order to implement the backward decoding. In the following, this coding scheme is referred to as a randomized Han-Kobayashi coding scheme with noisy feedback (RHK-NOF).

The RHK-NOF possesses the following property. When $\eta \geqslant 1$ and $R_{1,C1}$, $R_{1,R1}$, $R_{1,C2}$, $R_{1,R2}$, $R_{1,P}$, $R_{2,C1}$, $R_{2,R1}$, $R_{2,C2}$, $R_{2,R2}$, and $R_{2,P}$ are chosen such that for all $i \in \{1,2\}$ and $j \in \{1,2\} \setminus \{i\}$,

$$R_{i,C} + R_{i,P} + R_{j,C} + R_{j,R} = \frac{1}{2}\log\left(\overrightarrow{\mathrm{SNR}}_i + 2\rho\sqrt{\overrightarrow{\mathrm{SNR}}_i \mathrm{INR}_{ij}} + \mathrm{INR}_{ij} + 1\right) - \frac{1}{2}, \quad (4.6)$$

with $\rho \in [0,1]$, it follows that the rate pair $(R_1, R_2) \in \mathbb{R}_+^2$, with $R_{i,C} = R_{i,C1} + R_{i,C2}$ and $R_i = R_{i,P} + R_{i,C}$ is achievable at an η-NE. This leads to the additional inequalities in (4.5), which together with to those defining the achievable region $\underline{\mathcal{C}}_{\mathrm{GIC-NF}}$ in Theorem 1 form the achievable η-NE denoted by $\underline{\mathcal{N}}_\eta$ described in Theorem 4.

The following examples describe some interesting observations from Theorem 4. Figure 4.2 shows the achievable region $\underline{\mathcal{C}}_{\mathrm{GIC-NF}}$ in Theorem 1 and the achievable η-NE region in Theorem 4 for a two-user GIC-NF channel with parameters $\overrightarrow{\mathrm{SNR}}_1 = 24$ dB, $\overrightarrow{\mathrm{SNR}}_2 = 18$ dB, $\mathrm{INR}_{12} = 16$ dB, $\mathrm{INR}_{21} = 10$ dB, $\overleftarrow{\mathrm{SNR}}_1 \in \{-100, 18, 50\}$ dB, $\overleftarrow{\mathrm{SNR}}_2 \in \{-100, 12, 50\}$ dB, and $\eta = 1$. At low values of $\overleftarrow{\mathrm{SNR}}_1$ and $\overleftarrow{\mathrm{SNR}}_2$, the achievable η-NE region approaches the region reported in [69] for the case of the two-user GIC without feedback. Alternatively, for high values of $\overleftarrow{\mathrm{SNR}}_1$ and $\overleftarrow{\mathrm{SNR}}_2$,

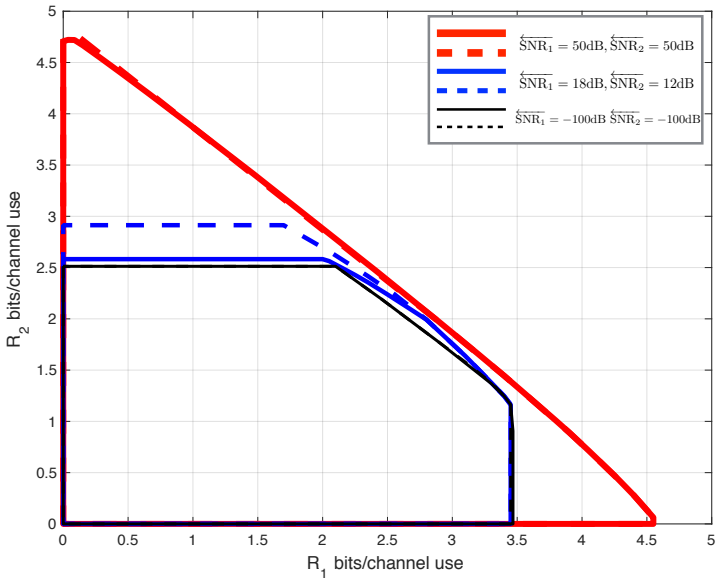

Figure 4.3: Achievable regions (dashed-lines) $\underline{\mathcal{C}}_{\mathrm{GIC-NF}}$ in Theorem 1 and achievable η-NE regions (solid lines) in Theorem 4 of the two-user GIC-NF with parameters $\overrightarrow{\mathrm{SNR}}_1 = 24$ dB, $\overrightarrow{\mathrm{SNR}}_2 = 18$ dB, $\mathrm{INR}_{12} = 48$ dB, $\mathrm{INR}_{21} = 30$ dB, $\overleftarrow{\mathrm{SNR}}_1 \in \{-100, 18, 50\}$ dB, $\overleftarrow{\mathrm{SNR}}_2 \in \{-100, 12, 50\}$ dB, and $\eta = 1$.

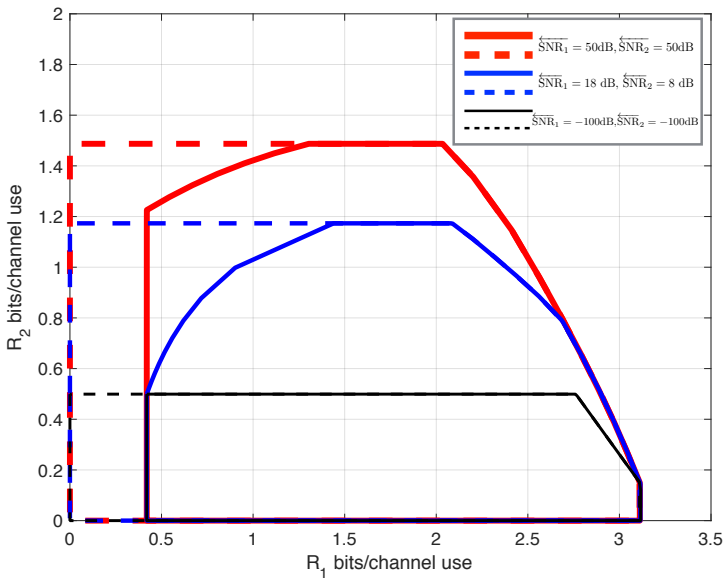

Figure 4.4: Achievable regions (dashed-lines) $\underline{\mathcal{C}}_{\mathrm{GIC-NF}}$ in Theorem 1 and achievable η-NE regions (solid lines) in Theorem 4 of the two-user GIC-NF with parameters $\overrightarrow{\mathrm{SNR}}_1 = 24$ dB, $\overrightarrow{\mathrm{SNR}}_2 = 3$ dB, $\mathrm{INR}_{12} = 16$ dB, $\mathrm{INR}_{21} = 9$ dB, $\overleftarrow{\mathrm{SNR}}_1 \in \{-100, 18, 50\}$ dB, $\overleftarrow{\mathrm{SNR}}_2 \in \{-100, 8, 50\}$ dB, and $\eta = 1$.

the achievable η-NE region approaches the region reported in [2] for the case of the two-user GIC with perfect channel output feedback.

Figure 4.3 shows the achievable region $\underline{\mathcal{C}}_{\mathrm{GIC-NF}}$ in Theorem 1 and the achievable η-

NE region in Theorem 4 for a two-user GIC-NF channel with parameters $\overrightarrow{\mathrm{SNR}}_1 = 24$ dB, $\overrightarrow{\mathrm{SNR}}_2 = 18$ dB, $\mathrm{INR}_{12} = 48$ dB, $\mathrm{INR}_{21} = 30$ dB, $\overleftarrow{\mathrm{SNR}}_1 \in \{-100, 18, 50\}$ dB, $\overleftarrow{\mathrm{SNR}}_2 \in \{-100, 12, 50\}$ dB, and $\eta = 1$. In this case, the achievable η-NE region and the the achievable region$\underline{\mathcal{C}}_{\mathrm{GIC-NF}}$ in Theorem 1 are almost identical, which implies that in the cases in which $\overrightarrow{\mathrm{SNR}}_i < \mathrm{INR}_{ij}$, for all $i \in \{1, 2\}$, with $j \in \{1, 2\} \setminus \{i\}$, the η-NE region is almost the same as the achievable region in the centralized case [11].

Figure 4.4 shows the achievable region $\underline{\mathcal{C}}_{\mathrm{GIC-NF}}$ in Theorem 1 and the achievable η-NE region in Theorem 4 for a two-user GIC-NF channel with parameters $\overrightarrow{\mathrm{SNR}}_1 = 24$ dB, $\overrightarrow{\mathrm{SNR}}_2 = 3$ dB, $\mathrm{INR}_{12} = 16$ dB, $\mathrm{INR}_{21} = 9$ dB, $\overleftarrow{\mathrm{SNR}}_1 \in \{-100, 18, 50\}$ dB, $\overleftarrow{\mathrm{SNR}}_2 \in \{-100, 8, 50\}$ dB, and $\eta = 1$. Note that in this case, the feedback parameter $\overleftarrow{\mathrm{SNR}}_2$ does not have an effect on the achievable η-NE region and the achievable region $\underline{\mathcal{C}}_{\mathrm{GIC-NF}}$ in Theorem 1. This is due to the fact that when one transmitter-receiver pair is in low interference regime (LIR) and the other transmitter-receiver pair is in high interference regime (HIR), feedback is useless on the transmitter-receiver pair in HIR, c.f., [8]

4.3 A Non-Equilibrium Region

This section introduces a non-equilibrium region, denoted by $\overline{\mathcal{N}}_\eta$. That is, $\overline{\mathcal{N}}_\eta \supseteq \mathcal{N}_\eta$. More specifically, any rate pair $(R_1, R_2) \in \overline{\mathcal{N}}_\eta^{\,\mathsf{c}}$ is not an η-NE. This region is described in terms of the convex region $\overline{\mathcal{B}}_\eta$. Here, for the case of the two-user D-GIC-NOF, the region $\overline{\mathcal{B}}_\eta$ is given by the closure of the rate pairs $(R_1, R_2) \in \mathbb{R}_+^2$ that satisfy for all $i \in \{1, 2\}$, with $j \in \{1, 2\} \setminus \{i\}$:

$$\overline{\mathcal{B}}_\eta = \Big\{(R_1, R_2) \in \mathbb{R}_+^2 : R_i \geqslant L_i, \text{ for all } i \in \mathcal{K} = \{1, 2\}\Big\}, \tag{4.7}$$

where,

$$L_i \triangleq \left(\frac{1}{2}\log\left(1 + \frac{\overrightarrow{\mathrm{SNR}}_i}{1 + \mathrm{INR}_{ij}}\right) - \eta\right)^+. \tag{4.8}$$

Note that L_i is the rate achieved by the transmitter-receiver pair i when it saturates the power constraint in (2.12) and treats interference as noise. Following this notation, the imposibility region of the two-user GIC-NOF, i.e., $\overline{\mathcal{N}}_\eta$, can be described as follows.

Theorem 5. Let $\eta \geqslant 1$ be fixed. The imposibility region $\overline{\mathcal{N}}_\eta$ of the two-user D-GIC-NOF is given by the closure of all possible non-negative rate pairs $(R_1, R_2) \in \overline{\mathcal{C}}_{\mathrm{GIC-NF}} \cap \overline{\mathcal{B}}_\eta$ for all $\rho \in [0, 1]$.

Note that L_i is the rate achieved by the transmitter-receiver pair i when it saturates the power constraint in (2.12) and treats interference as noise. This rate is always

achievable by transmitter-receiver pair i as it does not depend on the configuration used by transmitter-receiver pair j.

The relevance of Theorem 5 relies on the implication that if the pair of configurations (s_1, s_2) is an η-NE, then transmitter-receiver pair 1 and transmitter-receiver pair 2 always achieve a rate equal to or larger than L_1 and L_2, with L_1 and L_2 in (4.8), respectively.

Figure 4.5 - Figure 4.8 show the achievable region $\underline{\mathcal{C}}_{\mathrm{GIC-NF}}$ in Theorem 1, the converse region $\overline{\mathcal{C}}_{\mathrm{GIC-NF}}$ in Theorem 2, the achievable η-NE region $\underline{\mathcal{N}}_{\eta}$ in Theorem 4, the non-equilibrium region $\overline{\mathcal{N}}_{\eta}$ in Theorem 5 for a two-user GIC-NF with different values for the parameters $\overrightarrow{\mathrm{SNR}}_1$, $\overrightarrow{\mathrm{SNR}}_2$, INR_{12}, INR_{21}, $\overleftarrow{\mathrm{SNR}}_1$, $\overleftarrow{\mathrm{SNR}}_2$ and $\eta = 1$.

4.4 Concluding Remarks

An achievable η-NE region for the two-user GIC-NF have been built using common randomness in the coding schemes, i.e., the random variables Ω_1 and Ω_2 in (2.11). This technique was first introduced in [69] for studying the G-IC without feedback and plays a central role in this work. This common randomness allows both transmitter-receiver pairs to limit the rate improvement of each other when either of them deviates from an equilibrium rate pair. A non-equilibrium region has also been presented for the two-user GIC-NOF. This led to a definition of an η-NE region for the two-user GIC-NOF with $\eta \geqslant 1$. Future works in this area must consider the cost of feedback. This implies the definition of metrics to analyze if the improvements on the individual rates justify using feedback. One of these metrics is the energy consumption due to the use of feedback, which is not taken into account in this work. Another path of research is that of equilibrium selection. In this work, the η-NE region has been characterized in the sense that the existence of an achievability scheme for each rate pair therein is proved. Nonetheless, an exact achievability for a given rate pair achievable at an equilibrium is still unknown.

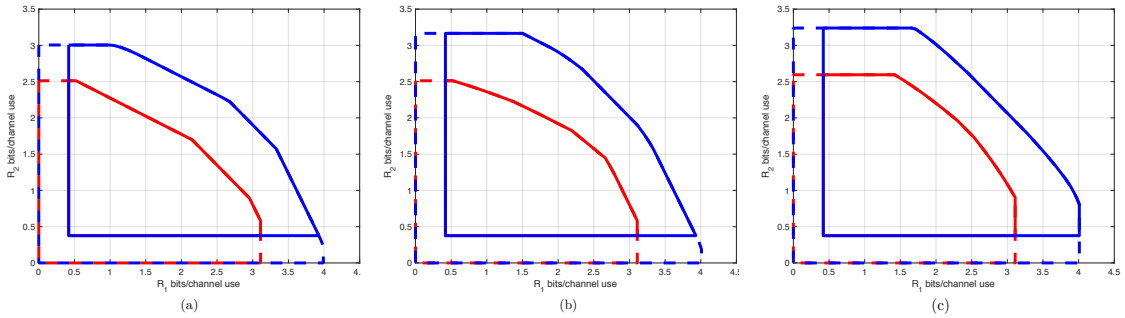

Figure 4.5: Converse region (blue dashed-line) $\overline{\mathcal{C}}_{\mathrm{GIC-NF}}$ in Theorem 2, non-equilibrium region (blue solid line) in Theorem 5 with $\eta = 1$, achievable capacity region $\underline{\mathcal{C}}_{\mathrm{GIC-NF}}$ in Theorem 1, and achievable η-NE region (red solid line) in Theorem 4 with $\eta = 1$ of the two-user GIC-NF with parameters $\overrightarrow{\mathrm{SNR}}_1 = 24$ dB, $\overrightarrow{\mathrm{SNR}}_2 = 18$ dB, $\mathrm{INR}_{12} = 16$ dB, $\mathrm{INR}_{21} = 10$ dB, (a) $\overleftarrow{\mathrm{SNR}}_1 = -100$ dB and $\overleftarrow{\mathrm{SNR}}_2 = -100$ dB; (b) $\overleftarrow{\mathrm{SNR}}_1 = 18$ dB and $\overleftarrow{\mathrm{SNR}}_2 = 12$dB; and (c) $\overleftarrow{\mathrm{SNR}}_1 = 50$ dB and $\overleftarrow{\mathrm{SNR}}_2 = 50$dB.

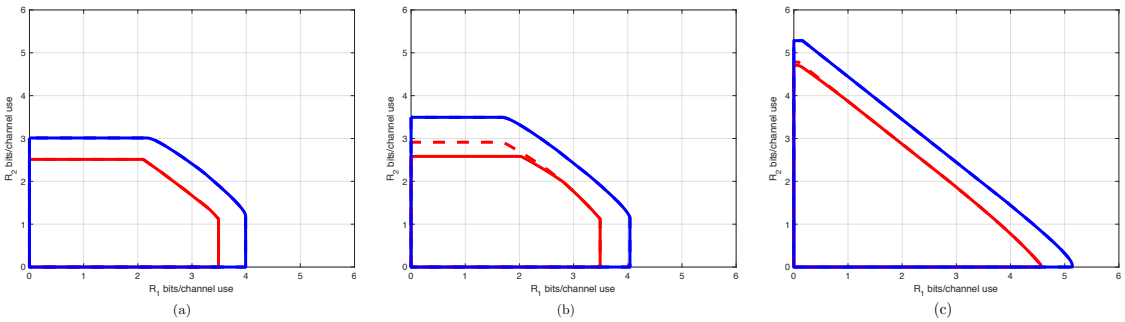

Figure 4.6: Converse region (blue dashed-line) $\overline{\mathcal{C}}_{\mathrm{GIC-NF}}$ in Theorem 2, non-equilibrium region (blue solid line) in Theorem 5 with $\eta = 1$, achievable capacity region $\underline{\mathcal{C}}_{\mathrm{GIC-NF}}$ in Theorem 1, and achievable η-NE region (red solid line) in Theorem 4 with $\eta = 1$ of the two-user GIC-NF with parameters $\overrightarrow{\mathrm{SNR}}_1 = 24$ dB, $\overrightarrow{\mathrm{SNR}}_2 = 18$ dB, $\mathrm{INR}_{12} = 48$ dB, $\mathrm{INR}_{21} = 30$ dB, (a) $\overleftarrow{\mathrm{SNR}}_1 = -100$ dB and $\overleftarrow{\mathrm{SNR}}_2 = -100$ dB; (b) $\overleftarrow{\mathrm{SNR}}_1 = 18$ dB and $\overleftarrow{\mathrm{SNR}}_2 = 12$dB; and (c) $\overleftarrow{\mathrm{SNR}}_1 = 50$ dB and $\overleftarrow{\mathrm{SNR}}_2 = 50$dB.

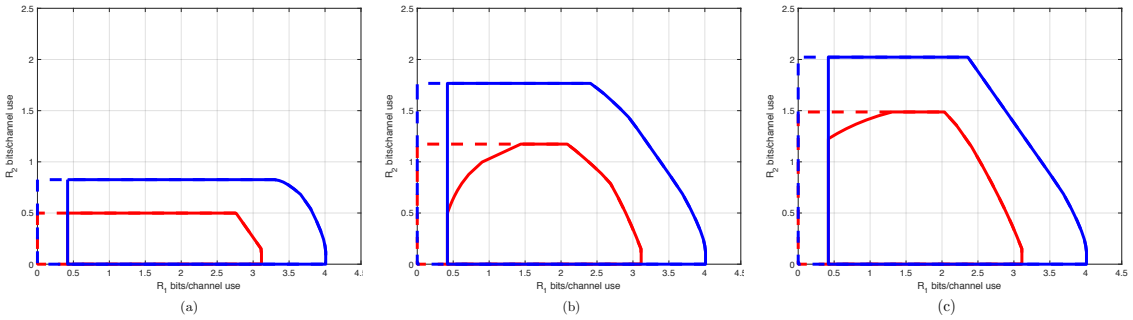

Figure 4.7: Converse region (blue dashed-line) $\overline{\mathcal{C}}_{\mathrm{GIC-NF}}$ in Theorem 2, non-equilibrium region (blue solid line) in Theorem 5 with $\eta = 1$, achievable capacity region $\underline{\mathcal{C}}_{\mathrm{GIC-NF}}$ in Theorem 1, and achievable η-NE region (red solid line) in Theorem 4 with $\eta = 1$ of the two-user GIC-NF with parameters $\overrightarrow{\mathrm{SNR}}_1 = 24$ dB, $\overrightarrow{\mathrm{SNR}}_2 = 3$ dB, $\mathrm{INR}_{12} = 16$ dB, $\mathrm{INR}_{21} = 9$ dB, (a) $\overleftarrow{\mathrm{SNR}}_1 = -100$ dB and $\overleftarrow{\mathrm{SNR}}_2 = -100$ dB; (b) $\overleftarrow{\mathrm{SNR}}_1 = 18$ dB and $\overleftarrow{\mathrm{SNR}}_2 = 8$dB; and (c) $\overleftarrow{\mathrm{SNR}}_1 = 50$ dB and $\overleftarrow{\mathrm{SNR}}_2 = 50$dB.

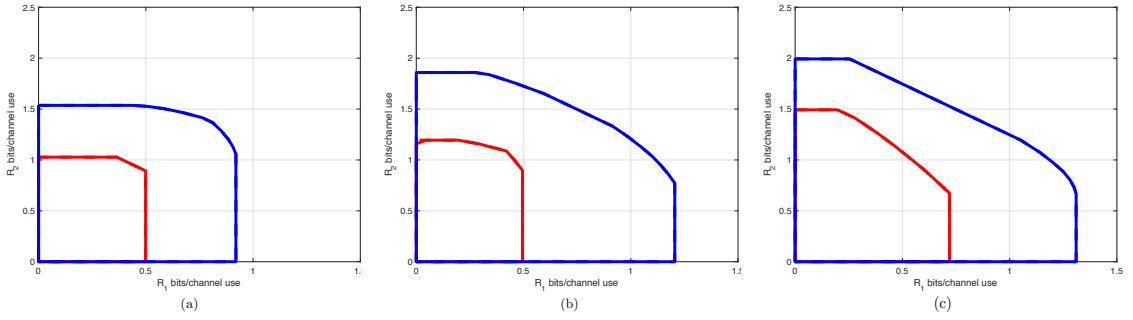

Figure 4.8: Converse region (blue dashed-line) $\overline{\mathcal{C}}_{\mathrm{GIC-NF}}$ in Theorem 2, non-equilibrium region (blue solid line) in Theorem 5 with $\eta = 1$, achievable capacity region $\underline{\mathcal{C}}_{\mathrm{GIC-NF}}$ in Theorem 1, and achievable η-NE region (red solid line) in Theorem 4 with $\eta = 1$ of the two-user GIC-NF with parameters $\overrightarrow{\mathrm{SNR}}_1 = 3$ dB, $\overrightarrow{\mathrm{SNR}}_2 = 8$ dB, $\mathrm{INR}_{12} = 16$ dB, $\mathrm{INR}_{21} = 5$ dB, (a) $\overleftarrow{\mathrm{SNR}}_1 = -100$ dB and $\overleftarrow{\mathrm{SNR}}_2 = -100$ dB; (b) $\overleftarrow{\mathrm{SNR}}_1 = 9$ dB and $\overleftarrow{\mathrm{SNR}}_2 = 6$dB; and (c) $\overleftarrow{\mathrm{SNR}}_1 = 50$ dB and $\overleftarrow{\mathrm{SNR}}_2 = 50$dB.

Part II

Simultaneous Information and Energy Transmission

Chapter 5

Introduction

Battery dependence is a critical issue when communications systems are deployed in hard-to-reach locations, e.g., remote geographical areas, concrete structures, human bodies, disaster/war zones, or simply, require constant mobility. In this case, the lifetime of electronic devices, their availability and reliability, are strongly constrained by the performance of the batteries involved. An effective remedy is using energy harvesting technologies. Specifically, energy can be harvested from different ambient sources such as light, vibrations, heat, chemical reactions, physiological processes, among other sources. Yet, another interesting source of energy are radio frequency (RF) signals. From this perspective, any communications system independently of the purpose of the transmission becomes an energy source. For instance, energy can be recovered from TV broadcast systems and cellular systems by energy harvesters put in open spaces at no additional cost or modification of the information transmission system.

The idea of wireless energy transmission traces back to Tesla during the twentieth century [78]. Nonetheless, for decades, the traditional engineering perspective was to exclusively use RF signals for information transmission. Only recently, the idea of simultaneous information and energy transmission (SIET) has been properly formalized, c.f., [79–83] and [84]. This implies, of course, re-thinking modulation schemes, coding, transmission durations, etc., to meet two goals: (i) To reliably transmit information to a receiver at a given rate with a sufficiently small decoding error probability; and (ii) To transmit energy to an energy harvester (EH) at a given rate with a sufficiently small energy outage probability.

Within this context, RF signals might be used by other information transmission systems for obtaining energy to power up or enhance their own RF transmissions. In this case, scientists evoke a cooperation of the transmitters at the energy level, as often the goal of these energy exchanges is increasing the reliability of the information transmission task, see for instance [85–88] and [89]. Energy can also be harvested from RF signals by ultra-low power peripheral devices such as data acquisition systems or information storage devices, which are not involved with the information

transmission system, as an alternative for battery recharging. This is the application on which the following chapters focus, which includes powering up low-power data acquisition systems, sensors, IoT devices, or simply, battery recharging.

In the following chapters, the scenario under study is that in which transmitters belonging to a given communication system cooperate to guarantee an energy rate at a given external energy harvesting system at some tolerable energy outage probability. More precisely, the EH system might not necessarily be co-located with an information receiver. More specifically, the EH might possess a set of antennas (rectennas) exclusively dedicated to the energy harvesting task, which are independent of those dedicated to the information receiving task, if they exist. In the special case in which an information receiver is co-located with the EH system, that is, they share the same antenna, a signal division via time-sharing or power-splitting is implemented. In the former, a fraction of time the antenna is connected to the information receiver, whereas the remaining time it is connected to the EH. The latter implies a signal division in which part of the signal is sent to the information receiver and the remaining part is sent to the EH, c.f., [90].

Through the lenses of information theory, the problem of point-to-point SIET with a co-located EH is cast into a problem of information transmission subject to minimum energy constraints at the channel output [81, 91], and this is the methodology used in the following chapters. One of the main conclusion presented in this part of the manuscript is that information and energy transmission are often conflicting tasks, and thus subject to a trade-off between the information transmission rate (bits per channel use) and the energy transmission rate (energy-units per channel use). This trade-off is easily evidenced in finite constellation schemes. Consider the noiseless transmission of a 4-PAM signal over a point-to-point channel with input alphabet $\{-2, -1, 1, 2\}$ and with a co-located EH. Assume that the symbols -2 and 2 (resp. -1 and 1) deliver 4 (resp. 1) energy-units/ch.use. Hence, without any energy rate constraint, the system conveys a maximum of 2 bits/ch.use and $\frac{5}{2}$ energy-units/ch.use by choosing all available symbols with equal probability. However, if the received energy rate must be for instance at least 4 energy-units/ch.use, the maximum information rate is 1 bit/ch.use. This is mainly because the transmitter is forced to communicate using only the symbols capable of delivering the maximum energy rate. From this simple example, it is easy to see how additional energy rate constraints may hinder information transmission in a point-to-point scenario.

The following chapters present the mathematical models for which the trade-off between the information transmission rate (bits per channel use) and the energy transmission rate (energy-units per channel use) is studied, i.e., the Gaussian multiple access channel (GMAC) and the Gaussian interference channel (GIC). In the former, the information-energy capacity region, i.e., the set of all information rates and energy rates that can be simultaneously achieved, is fully characterized. In the latter, only an approximation within a constant gap (Definition 3) is provided.

Chapter 6

Gaussian Multiple Access Channels with Energy Transmission

More specifically, the chapter provides the first full characterization of the information-energy capacity region for the GMAC with and without feedback, i.e., all the achievable information and energy transmission rates in bits per channel use and energy-units per channel use, respectively. Furthermore, the fundamental limits on the individual information rates and the information sum-rates given a minimum energy rate ensured at the EH are also provided. In the case without feedback, an achievability scheme based on power-splitting and successive interference cancellation is shown to be optimal. Alternatively, in the case with feedback (GMAC-F), a simple yet optimal achievability scheme that is based on power-splitting and Ozarow's capacity achieving scheme is presented. Although the proofs of achievability and converse build upon standard information-theoretic techniques, extending these techniques to account for the energy constraint involves many challenges. For instance, to derive upper bounds on the achievable information-energy rate triplets, there are two parts to consider: one that is related to the information transmission for which Fano's inequality is used, and another that is related to the energy transmission for which concentration inequalities are used to derive an upper bound on the energy rate. Finally, the enhancement of the energy transmission rate induced by the use of feedback is quantified. It is shown that feedback can at most double the energy transmission rate at high SNRs when the information transmission sum-rate is kept fixed at the sum-capacity of the GMAC, but it has no effect at very low SNRs.

6.1 Mathematical Model

Consider the two-user memoryless GMAC with an EH with perfect channel-output-feedback (GMAC-F) in Fig. 6.1 and without feedback in Fig. 6.2. In both channels, at each channel use $t \in \mathbb{N}$, $X_{1,t}$ and $X_{2,t}$ denote the real symbols sent by transmit-

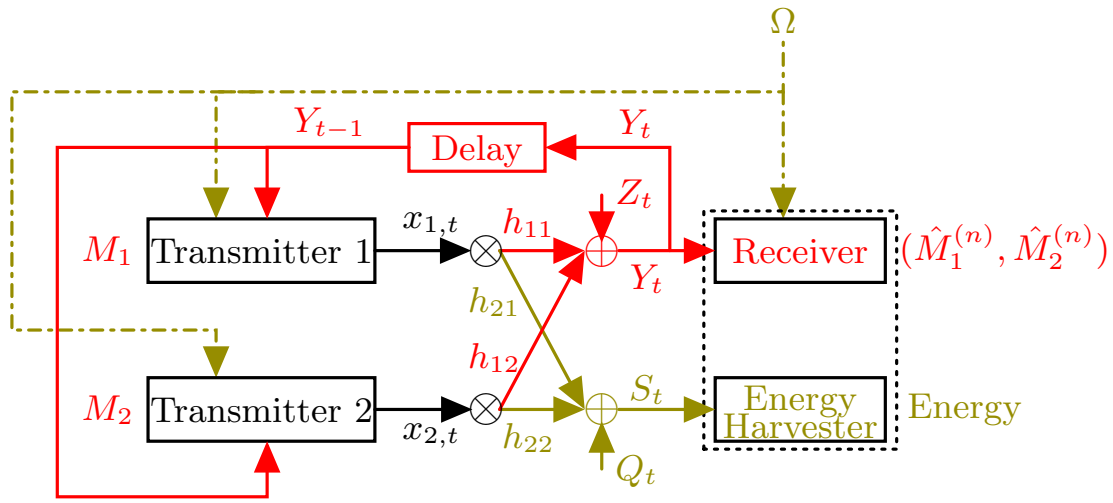

Figure 6.1: Two-user memoryless GMAC-F with an EH.

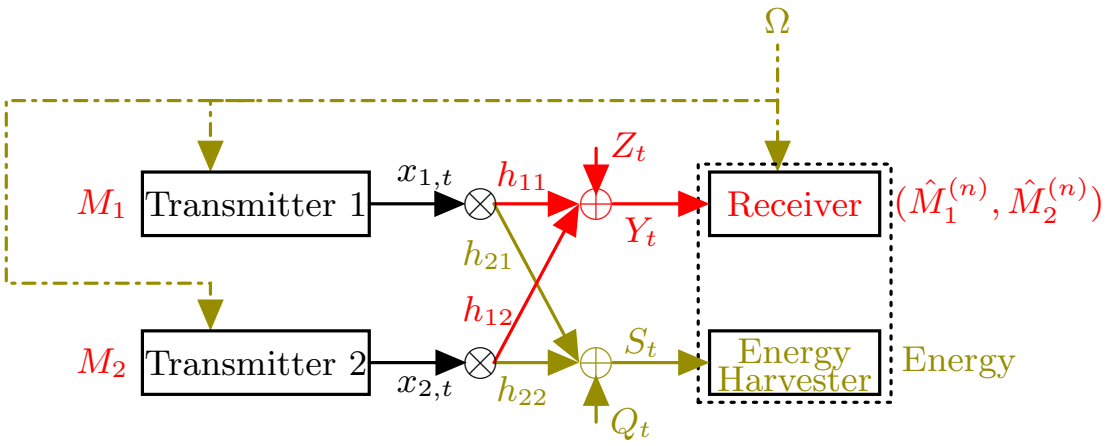

Figure 6.2: Two-user memoryless GMAC with an EH.

ters 1 and 2, respectively. Let $n \in \mathbb{N}$ denote the blocklength. The receiver observes the real channel output

$$Y_{1,t} = h_{11}X_{1,t} + h_{12}X_{2,t} + Z_t, \tag{6.1}$$

and the EH observes

$$Y_{2,t} = h_{21}X_{1,t} + h_{22}X_{2,t} + Q_t, \tag{6.2}$$

where h_{1i} and h_{2i} are the corresponding constant non-negative real channel coefficients from transmitter i to the receiver and the EH, respectively. The channel coefficients are assumed to satisfy the following $\mathcal{L}_2$-norm condition:

$$\forall j \in \{1, 2\}, \quad \|\boldsymbol{h}_j\|^2 \leqslant 1, \tag{6.3}$$

with $\boldsymbol{h}_j \triangleq (h_{j1}, h_{j2})^{\mathsf{T}}$ to satisfy the principle of conservation of energy.

The noise terms Z_t and Q_t are realizations of two identically distributed zero-mean real Gaussian random variables with variances σ_1^2 and σ_2^2, respectively. In the following, there is no particular assumption on the joint distribution of Q_t and Z_t.

In the G-MAG-F with an EH, a perfect feedback link from the receiver to transmitter i allows at the end of each channel use t, the observation of the channel output Y_{t-d} at transmitter i, with $d \in \mathbb{N}$ the delay of the feedback channel. Without any loss of generality, the delay is assumed to be the same from the receiver to both transmitters and equivalent to one channel use, i.e., $d = 1$.

Within this context, two main tasks are to be simultaneously accomplished: information transmission and energy transmission.

6.1.1 Information Transmission

The goal of the communication is to convey the independent messages M_1 and M_2 from transmitters 1 and 2 to the common receiver. The messages M_1 and M_2 are independent of the noise terms $Z_1, \ldots, Z_n$, $Q_1, \ldots, Q_n$ and uniformly distributed over the sets $\mathcal{M}_1 \triangleq \{1, \ldots, \lfloor 2^{nR_1} \rfloor\}$ and $\mathcal{M}_2 \triangleq \{1, \ldots, \lfloor 2^{nR_2} \rfloor\}$, where R_1 and R_2 denote the information transmission rates and $n \in \mathbb{N}$ the blocklength.

In the GMAC-F with an EH, at each time t, the existence of feedback links allows the t-th symbol of transmitter i to be dependent on all previous channel outputs $Y_1, \ldots, Y_{t-1}$ as well as its message index M_i and a randomly generated index $\Omega \in \{1, \ldots, \lfloor 2^{nR_r} \rfloor\}$, with $R_r \geqslant 0$. The index Ω is independent of both M_1 and M_2 and assumed to be known by all transmitters and the receiver. More specifically,

$$X_{i,1} = f_{i,1}^{(n)}(M_i, \Omega) \quad \text{and} \tag{6.4a}$$

$$X_{i,t} = f_{i,t}^{(n)}(M_i, \Omega, Y_{1,1}, \ldots, Y_{1,t-1}), \quad t \in \{2, \ldots, n\}, \tag{6.4b}$$

for some encoding functions

$$f_{i,1}^{(n)} \colon \mathcal{M}_i \times \mathbb{N} \to \mathbb{R} \quad \text{and} \tag{6.5}$$

$$f_{i,t}^{(n)} \colon \mathcal{M}_i \times \mathbb{N} \times \mathbb{R}^{t-1} \to \mathbb{R}. \tag{6.6}$$

In the GMAC with an EH, at each time t, the t-th symbol of transmitter i is

$$X_{i,t} = g_{i,t}^{(n)}(M_i, \Omega), \quad t \in \{1, \ldots, n\}, \tag{6.7a}$$

where $g_{i,t}^{(n)} \colon \mathcal{M}_i \times \mathbb{N} \to \mathbb{R}$ is the encoding function.

In the GMAC-F and in the GMAC with an EH, for all $i \in \{1, 2\}$, transmitter i's channel inputs $X_{i,1}, \ldots, X_{i,n}$ satisfy an expected average *input power constraint*

$$\frac{1}{n} \sum_{t=1}^{n} \mathbb{E}\left[X_{i,t}^2\right] \leqslant P_i, \tag{6.8}$$

where P_i denotes the average transmit power of transmitter i in energy-units per channel use and where the expectation is over the message indices, the random index, and the noise realizations prior to channel use t. The dependence of $X_{i,t}$ on $Y_{1,1}, \ldots, Y_{1,t-1}$ (and thus on $Z_1, \ldots, Z_{t-1}$) is shown by (6.4).

The GMAC-F and GMAC with an EH are fully described by the signal to noise ratios (SNRs): SNR_{ji}, with $\forall (i,j) \in \{1,2\}^2$. These SNRs are defined as follows

$$\mathrm{SNR}_{ji} \triangleq \frac{|h_{ji}|^2 P_i}{\sigma_j^2}. \tag{6.9}$$

The receiver produces an estimate $(\hat{M}_1^{(n)}, \hat{M}_2^{(n)}) = \Phi^{(n)}(Y_{1,1}, \ldots, Y_{1,n}, \Omega)$ of the message-pair (M_1, M_2) via a decoding function $\Phi^{(n)} \colon \mathbb{R}^n \times \mathbb{N} \to \mathcal{M}_1 \times \mathcal{M}_2$, and the average decoding error probability is

$$P_{\mathrm{DE}}^{(n)}(R_1, R_2) \triangleq \Pr\left[(\hat{M}_1^{(n)}, \hat{M}_2^{(n)}) \neq (M_1, M_2)\right]. \tag{6.10}$$

6.1.2 Energy Transmission

The empirical energy transmission rate (in energy-units per channel use) induced by the sequence $(Y_{2,1}, \ldots, Y_{2,n})$ at the input of the EH is

$$B^{(n)} \triangleq \frac{1}{n} \sum_{t=1}^{n} Y_{2,t}^2. \tag{6.11}$$

This rate $B^{(n)}$ (in energy-units per channel use) must satisfy

$$0 \leqslant B^{(n)} \leqslant \sigma_2^2 \left(1 + \mathrm{SNR}_{21} + \mathrm{SNR}_{22} + 2\sqrt{\mathrm{SNR}_{21}\mathrm{SNR}_{22}}\right), \tag{6.12}$$

for the problem to be feasible. In fact, $\sigma_2^2 \left(1 + \mathrm{SNR}_{21} + \mathrm{SNR}_{22} + 2\sqrt{\mathrm{SNR}_{21}\mathrm{SNR}_{22}}\right)$ is the maximum energy rate that can be achieved at the input of the EH given the input power constraints in (6.8). This rate can be achieved when the transmitters use all their power budgets to send fully correlated channel inputs.

The goal of the energy transmission is to guarantee that the empirical energy rate $B^{(n)}$ is not less than a given operational energy transmission rate B that must satisfy

$$B \leqslant \sigma_2^2 \left(1 + \mathrm{SNR}_{21} + \mathrm{SNR}_{22} + 2\sqrt{\mathrm{SNR}_{21}\mathrm{SNR}_{22}}\right). \tag{6.13}$$

Hence, the probability of energy outage is defined as follows:

$$P_{\mathrm{EO}}^{(n)}(B) \triangleq \Pr\left[B^{(n)} < B - \epsilon\right], \tag{6.14}$$

for some $\epsilon > 0$ arbitrarily small.

In the sequel, for ease of notation, the acronyms GMAC-F-E and GMAC-E refer to the GMAC-F and the GMAC with an EH as depicted in Fig. 6.1 and Fig. 6.2, respectively, with fixed SNRs: SNR_{11}, SNR_{12}, SNR_{21}, and SNR_{22}; and fixed noise variance at the EH: σ_2^2.

6.1.3 Simultaneous Information and Energy Transmission

The GMAC-F-E (and GMAC-E, respectively) is said to operate at the information-energy rate triplet $(R_1, R_2, B) \in [0, \infty)^3$ when both transmitters and the receiver use a transmit-receive configuration such that: (i) reliable communication at information rates R_1 and R_2 is ensured; and (ii) the empirical energy transmission rate in (7.9) at the input of the EH during the entire blocklength is not lower than B. A formal definition is given below.

Definition 6 (Achievable Rates)**.** *The triplet $(R_1, R_2, B) \in [0, \infty)^3$ is achievable in the* GMAC-F-E *(and* GMAC-E*, resp.) if there exists a sequence of encoding and decoding functions $\left\{\{f_{1,t}^{(n)}\}_{t=1}^{n}, \{f_{2,t}^{(n)}\}_{t=1}^{n}, \Phi^{(n)}\right\}_{n=1}^{\infty}$ (and $\left\{\{g_{1,t}^{(n)}\}_{t=1}^{n}, \{g_{2,t}^{(n)}\}_{t=1}^{n}, \Phi^{(n)}\right\}_{n=1}^{\infty}$, resp.) such that both the average error probability and the energy-outage probability tend to zero as the blocklength n tends to infinity. That is, for all $\epsilon > 0$,*

$$\limsup_{n\to\infty} \; P_{\mathrm{DE}}^{(n)}(R_1, R_2) = 0, \tag{6.15}$$

$$\limsup_{n\to\infty} \; P_{\mathrm{EO}}^{(n)}(B) \qquad = 0. \tag{6.16}$$

Often, increasing the energy transmission rate implies decreasing the information transmission rates and *vice-versa*. This trade-off is accurately captured by the notion of *information-energy capacity region*.

Definition 7 (Information-Energy Capacity Region)**.** *The information-energy capacity region of the* GMAC-F-E *(and* GMAC-E*, resp.), denoted by $\mathcal{E}_b^{\mathrm{FB}}$ ($\mathcal{E}_b$, resp.) is the closure of all achievable information-energy rate triplets (R_1, R_2, B).*

In Chapter 6, the information-energy capacity regions of the GMAC-E and GMAC-F-E are characterized.

6.2 The Information-Energy Capacity Region

For any non-negative SNRs: SNR_{11}, SNR_{12}, SNR_{21}, SNR_{22}; and noise variance at the EH: σ_2^2, the main results presented in this chapter are provided in terms of the information-energy capacity region (Definition 7). The information-energy capacity region of the GMAC-F-E is fully characterized by the following theorem.

Theorem 6 (Information-Energy Capacity Region)**.** *The information-energy capacity region $\mathcal{E}^{\mathrm{FB}}$ of the* GMAC-F-E *is the set of information-energy rate triplets*

(R_1, R_2, B) that satisfy

$$R_1 \leqslant \frac{1}{2}\log_2\left(1+\beta_1\ \mathrm{SNR}_{11}\left(1-\rho^2\right)\right), \tag{6.17a}$$

$$R_2 \leqslant \frac{1}{2}\log_2\left(1+\beta_2\ \mathrm{SNR}_{12}\left(1-\rho^2\right)\right), \tag{6.17b}$$

$$\begin{aligned} R_1+R_2 \leqslant \frac{1}{2}\log_2\big(1+\beta_1\ \mathrm{SNR}_{11}+\beta_2\ \mathrm{SNR}_{12} \\ +2\rho\sqrt{\beta_1\mathrm{SNR}_{11}\beta_2\mathrm{SNR}_{12}}\big), \end{aligned} \tag{6.17c}$$

$$\begin{aligned} B \leqslant 1+\mathrm{SNR}_{21}+\mathrm{SNR}_{22}+2\rho\sqrt{\beta_1\mathrm{SNR}_{21}\beta_2\mathrm{SNR}_{22}} \\ +2\sqrt{(1-\beta_1)\mathrm{SNR}_{21}\ (1-\beta_2)\mathrm{SNR}_{22}}, \end{aligned} \tag{6.17d}$$

with $(\rho, \beta_1, \beta_2) \in [0,1]^3$.

From an achievability perspective, the parameter ρ can be interpreted as the Pearson correlation factor between the signals sent by both transmitters. This interpretation will become clearer later in this chapter. For the moment, the key conclusion of this interpretation is that given the fact that correlation between the signal is achieved thanks to feedback, setting $\rho = 0$ in (6.17) would lead to the information-energy capacity region of the GMAC-E. The following theorem confirms this intuition.

Theorem 7 (Information-Energy Capacity Region)**.** *The information-energy capacity region $\mathcal{E}$ of the* GMAC-E *is the set of all information-energy rate triplets (R_1, R_2, B) that satisfy*

$$R_1 \leqslant \frac{1}{2}\log_2\left(1+\beta_1\ \mathrm{SNR}_{11}\right), \tag{6.18a}$$

$$R_2 \leqslant \frac{1}{2}\log_2\left(1+\beta_2\ \mathrm{SNR}_{12}\right), \tag{6.18b}$$

$$R_1+R_2 \leqslant \frac{1}{2}\log_2\big(1+\beta_1\ \mathrm{SNR}_{11}+\beta_2\ \mathrm{SNR}_{12}\big), \tag{6.18c}$$

$$B \leqslant 1+\mathrm{SNR}_{21}+\mathrm{SNR}_{22}+2\sqrt{(1-\beta_1)\mathrm{SNR}_{21}(1-\beta_2)\mathrm{SNR}_{22}}, \tag{6.18d}$$

with $(\beta_1, \beta_2) \in [0,1]^2$.

Note that the information-energy capacity region of the GMAC is included in the information-energy capacity region of the GMAC-F, i.e.,

$$\mathcal{E} \subseteq \mathcal{E}^{\mathrm{FB}}. \tag{6.19}$$

Note that this inclusion can be strict. For instance, any rate triplet (R_1, R_2, B) that is achievable in the GMAC-F, and for which $R_1 + R_2$ equals the perfect feedback sum-capacity cannot be achieved in the GMAC.

The remainder of this section highlights some important observations on the achievability and converse proofs of Theorem 6 and Theorem 7.

6.2.1 Comments on the Achievability

The achievability scheme in the proof of Theorem 6 is based on power-splitting and Ozarow's capacity-achieving scheme [92]. From an achievability standpoint, the parameters β_1 and β_2 in Theorem 6 might be interpreted as the fractions of average power that transmitters 1 and 2 allocate for information transmission. More specifically, transmitter i generates two signals: an information-carrying (IC) signal with average power $\beta_i P_i$ energy-units per channel use; and a no-information-carrying (NIC) signal with power $(1-\beta_i)P_i$ energy-units per channel use. The IC signal is constructed using Ozarow's scheme [92]. The role of the NIC signal is to exclusively transmit energy from the transmitter to the EH. Conversely, the role of the IC signal is twofold: information transmission from the transmitter to the receiver and energy transmission from the transmitter to the EH.

The parameter ρ is the average Pearson correlation coefficient between the IC signals sent by both transmitters. This parameter plays a fundamental role in both information transmission and energy transmission. Note for instance that the upper-bounds on the information sum-rate (6.17c) and on the energy harvested per unit-time (6.17d) monotonically increase with ρ, whereas the upper-bounds on the individual rates (6.17a) and (6.17b) monotonically decrease with ρ. If $\beta_1 \neq 0$ and $\beta_2 \neq 0$, let $\rho^\star(\beta_1,\beta_2)$ be the unique solution in $(0,1)$ to the following equation in ρ:

$$\begin{aligned}&1+\beta_1\,\mathrm{SNR}_{11}+\beta_2\,\mathrm{SNR}_{12}+2\rho\sqrt{\beta_1\mathrm{SNR}_{11}\beta_2\mathrm{SNR}_{12}}\\&=\left(1+\beta_1\,\mathrm{SNR}_{11}(1-\rho^2)\right)\left(1+\beta_2\,\mathrm{SNR}_{12}(1-\rho^2)\right),\end{aligned}\tag{6.20}$$

otherwise, let $\rho^\star(\beta_1,\beta_2)=0$. When $\rho=\rho^\star(\beta_1,\beta_2)$, the sum of (6.17a) and (6.17b) is equal to (6.17c) giving the maximum information sum-rate which can be achieved when the transmitters are using powers $\beta_1 P_1$ and $\beta_2 P_2$ for transmitting information, i.e., $\rho^\star(\beta_1,\beta_2)$ is the information sum-rate optimal correlation coefficient.

Existence and Uniqueness of $\rho^\star(\beta_1,\beta_2)$: For a fixed power-splitting $(\beta_1,\beta_2)\in(0,1]^2$, let the function $\varphi_{\beta_1,\beta_2}:[0,1]\to\mathbb{R}$ denote the difference between the right-hand-side and the left-hand-side of (6.20), i.e.,

$$\begin{aligned}&\varphi_{\beta_1,\beta_2}(\rho)\triangleq\\&1+\beta_1\,\mathrm{SNR}_{11}+\beta_2\,\mathrm{SNR}_{12}+2\rho\sqrt{\beta_1\mathrm{SNR}_{11}\beta_2\mathrm{SNR}_{12}}\\&-\left(1+\beta_1\,\mathrm{SNR}_{11}(1-\rho^2)\right)\left(1+\beta_2\,\mathrm{SNR}_{12}(1-\rho^2)\right).\end{aligned}\tag{6.21}$$

The function $\varphi_{\beta_1,\beta_2}(\rho)$ is continuous in ρ on the closed interval $[0,1]$ and is such that $\varphi_{\beta_1,\beta_2}(0)<0$ and $\varphi_{\beta_1,\beta_2}(1)>0$, and thus there exists at least one $\rho_0\in(0,1)$ such that $\varphi_{\beta_1,\beta_2}(\rho_0)=0$ (Bolzano's Intermediate Value Theorem). Furthermore, this solution ρ_0 is unique because $\varphi_{\beta_1,\beta_2}(\rho)$ is strictly monotonic on $[0,1]$. This unique solution is $\rho^\star(\beta_1,\beta_2)$.

Note also that the Pearson correlation factor between the NIC signals of both transmitters does not appear in Theorem 6. This is mainly because maximum energy

transmission occurs using NIC signals that are fully correlated, and thus the corresponding Pearson correlation coefficient is one. Similarly, the Pearson correlation factor between the NIC signal of transmitter i and the IC signal of transmitter j, with $j \in \{1,2\}$ and $j \neq i$, does not appear in Theorem 6 either. This observation stems from the fact that, without loss of optimality, NIC signals can be chosen to be independent of the message indices and the noise terms. NIC signals can also be assumed to be known by both the receiver and the transmitters. Hence, the interference they create at the receiver can easily be eliminated using successive decoding. Under this assumption, a power-splitting $(\beta_1, \beta_2) \in [0,1]^2$ guarantees the achievability of non-negative rate pairs (R_1, R_2) satisfying (6.17a)-(6.17c) by simply using Ozarow's capacity achieving scheme. At the EH, both the IC and NIC signals contribute to the total harvested energy (7.9). The IC signal is able to convey at most $\beta_1 \mathrm{SNR}_{21} + \beta_2 \mathrm{SNR}_{22} + 2\rho\sqrt{\beta_1 \mathrm{SNR}_{21} \beta_2 \mathrm{SNR}_{22}}$ energy-units per channel use, while the NIC signal is able to convey at most $(1-\beta_1)\mathrm{SNR}_{21} + (1-\beta_2)\mathrm{SNR}_{22} + 2\sqrt{(1-\beta_1)\mathrm{SNR}_{21}(1-\beta_2)\mathrm{SNR}_{22}}$ energy-units per channel use. The sum of these two contributions as well as the contribution of the noise at the EH justifies the upper-bound on the energy transmission rate in (6.17d).

The information-energy capacity region without feedback described by Theorem 7 is identical to the information-energy capacity region described by Theorem 6 in the case in which channel inputs are chosen to be mutually independent, i.e., $\rho = 0$. To prove the achievability of the region presented in Theorem 7, Ozarow's scheme is replaced by the scheme proposed independently by Cover [93] and Wyner [94], in which the channel inputs are independent Gaussian variables.

6.2.2 Comments on the Converse

The proof of the converse to Theorem 6 is in two steps. First, it is shown that any information-energy rate triplet $(R_1, R_2, B) \in \mathcal{E}^{\mathrm{FB}}$ must satisfy

$$nR_1 \leqslant \sum_{t=1}^{n} I(X_{1,t}; Y_{1,t}|X_{2,t}) + \epsilon_1^{(n)}, \tag{6.22a}$$

$$nR_2 \leqslant \sum_{t=1}^{n} I(X_{2,t}; Y_{1,t}|X_{1,t}) + \epsilon_2^{(n)}, \tag{6.22b}$$

$$n(R_1+R_2) \leqslant \sum_{t=1}^{n} I(X_{1,t}X_{2,t}; Y_{1,t}) + \epsilon_{12}^{(n)}, \tag{6.22c}$$

$$B \leqslant \mathbb{E}\left[B^{(n)}\right] + \delta^{(n)}, \tag{6.22d}$$

where $\frac{\epsilon_1^{(n)}}{n}$, $\frac{\epsilon_2^{(n)}}{n}$, $\frac{\epsilon_1^{(n)}}{n}$, and $\delta^{(n)}$ tend to zero as n tends to infinity. Second, these bounds are evaluated for a general choice of jointly distributed pair of inputs $(X_{1,t}, X_{2,t})$ such that $\mathbb{E}[X_{i,t}] = \mu_{i,t}$, $\mathbb{V}_{X_{i,t}}[=]\sigma_{i,t}^2$, and $\mathrm{Cov}[X_{1,t}, X_{2,t}] = \lambda_t$, $\forall i \in \{1,2\}$ and $\forall t \in \{1,\ldots,n\}$.

The converse to Theorem 7 follows the same lines as in the case with feedback,

with the assumption that $X_{1,t}$ and $X_{2,t}$ are independent (i.e., $\forall t \in \{1,\dots,n\}$, $\lambda_t = 0$).

6.3 Maximum Individual Rates Given a Minimum Energy Rate Constraint

In this section, for any fixed non-negative SNRs: SNR_{11}, SNR_{12}, SNR_{21}, and SNR_{22}, and for any energy rate constraint B at the input of the EH satisfying (6.13), the maximum individual information rates of transmitters 1 and 2 in the GMAC-F-E and GMAC-E are identified.

Let $\xi : \mathbb{R}_+ \to [0,1]$ be defined as follows:

$$\xi(B) \triangleq \frac{\left(\frac{B}{\sigma_2^2} - (1 + \mathrm{SNR}_{21} + \mathrm{SNR}_{22})\right)^+}{2\sqrt{\mathrm{SNR}_{21}\mathrm{SNR}_{22}}}. \tag{6.23}$$

Note that $\xi(B)$ is the minimum correlation of the channel inputs that is required to achieve the target energy rate B. That is, $\xi(B)$ is the solution in $x \in [0,1]$ to

$$B = \sigma_2^2 \left(1 + \mathrm{SNR}_{21} + \mathrm{SNR}_{22} + 2x\sqrt{\mathrm{SNR}_{21}\mathrm{SNR}_{22}}\right). \tag{6.24}$$

6.3.1 Case with Feedback

The maximum individual information rate of transmitter i, with $i \in \{1,2\}$, subject to an energy rate constraint B at the input of the EH, denoted by $R_i^{\mathrm{FB}}(B)$, in the GMAC-F-E is the solution to an optimization problem of the form

$$R_i^{\mathrm{FB}}(B) = \max_{(R_1,R_2,B)\in\mathcal{E}^{\mathrm{FB}}} R_i. \tag{6.25}$$

The solution to (6.25) is given by the following proposition.

Proposition 1. *The maximum individual information rate of transmitter i in a* GMAC-F-E *subject to an energy rate constraint B at the input of the EH, is given by*

$$R_i^{\mathrm{FB}}(B) = \frac{1}{2}\log_2\left(1 + \left(1 - \xi(B)^2\right)\mathrm{SNR}_{1i}\right), \quad i \in \{1,2\}, \tag{6.26}$$

with $\xi(B) \in [0,1]$ defined in (6.23).

6.3.2 Case without Feedback

The maximum individual information rate of transmitter i in the GMAC-E, with $i \in \{1,2\}$, subject to an energy rate constraint B at the input of the EH, denoted by $R_i^{\mathrm{NF}}(B)$, is the solution to an optimization problem of the form

$$R_i^{\mathrm{NF}}(B) = \max_{(R_1,R_2,B)\in\mathcal{E}} R_i. \tag{6.27}$$

The solution to (6.27) is given by the following proposition.

Proposition 2. *The maximum individual information rate of transmitter i in a* GMAC-E*, subject to an energy rate constraint B at the input of the EH, is given by*

$$R_i^{\mathrm{NF}}(B)=R_i^{\mathrm{FB}}(B), \quad i \in \{1,2\}. \tag{6.28}$$

That is, the maximum individual information rates, subject to an energy rate constraint B at the input of the EH, in the GMAC-F-E and in the GMAC-E, coincide.

6.4 Maximum Information Sum-Rate Given a Minimum Energy Rate Constraint

In this section, the maximum information sum-rate, subject to an energy rate constraint B at the input of the EH, is identified in the GMAC-F-E and in the GMAC-E.

6.4.1 Case with Feedback

The maximum information sum rate in the GMAC-F-E, subject to an energy rate constraint B at the input of the EH, denoted by $R_{\mathrm{sum}}^{\mathrm{FB}}(B)$ is the solution to an optimization problem of the form

$$R_{\mathrm{sum}}^{\mathrm{FB}}(B) = \max_{(R_1,R_2,B)\in\mathcal{E}^{\mathrm{FB}}} R_1+R_2. \tag{6.29}$$

The solution to (6.29) is given by the following proposition.

Proposition 3. *The maximum information sum rate in the* GMAC-F-E*, subject to an energy rate constraint B at the input of the EH, denoted by $R_{\mathrm{sum}}^{\mathrm{FB}}(B)$, is*

1. *For all $B \in \left[0, \sigma_2^2\left(1+\mathrm{SNR}_{21}+\mathrm{SNR}_{22}+2\rho^\star(1,1)\sqrt{\mathrm{SNR}_{21}\mathrm{SNR}_{22}}\right)\right]$,*

$$R_{\mathrm{sum}}^{\mathrm{FB}}(B) = \frac{1}{2}\log_2(1+\mathrm{SNR}_{11}+\mathrm{SNR}_{12}+2\rho^\star(1,1)\sqrt{\mathrm{SNR}_{11}\mathrm{SNR}_{12}}); \tag{6.30}$$

2. *For all $B \in \mathbb{R}$ such that*

$$B \geqslant \sigma_2^2\left(1+\mathrm{SNR}_{21}+\mathrm{SNR}_{22}+2\rho^\star(1,1)\sqrt{\mathrm{SNR}_{21}\mathrm{SNR}_{22}},\right) \text{ and } \tag{6.31}$$

$$B \leqslant \sigma_2^2\left(1+\mathrm{SNR}_{21}+\mathrm{SNR}_{22}+2\sqrt{\mathrm{SNR}_{21}\mathrm{SNR}_{22}}\right), \tag{6.32}$$

$$\begin{aligned} R_{\mathrm{sum}}^{\mathrm{FB}}(B)=&\frac{1}{2}\log_2(1+(1-\xi(B)^2)\mathrm{SNR}_{11}) \\ &+\frac{1}{2}\log_2(1+(1-\xi(B)^2)\mathrm{SNR}_{12}); \end{aligned} \tag{6.33}$$

3. *For all $B \in \left[\sigma_2^2\left(1+\mathrm{SNR}_{21}+\mathrm{SNR}_{22}+2\sqrt{\mathrm{SNR}_{21}\mathrm{SNR}_{22}}\right), \infty\right)$,*

$$R_{\mathrm{sum}}^{\mathrm{FB}}(B) = 0, \tag{6.34}$$

where $\rho^\star(1,1)$ denotes the unique solution in $(0,1)$ to (6.20) *with $\beta_1=\beta_2=1$ and the function ξ is defined in* (6.23).

6.4.2 Case without Feedback

The maximum information sum-rate in the GMAC-E, subject to an energy rate constraint B at the input of the EH, denoted by $R_{\text{sum}}^{\text{NF}}(B)$, is the solution to an optimization problem of the form

$$R_{\text{sum}}^{\text{NF}}(B) = \max_{(R_1,R_2,B)\in\mathcal{E}} R_1 + R_2. \tag{6.35}$$

The solution to (6.35) is given by the following proposition.

Proposition 4. *The maximum information sum-rate in the* GMAC-E*, subject to an energy rate constraint B at the input of the EH, denoted by $R_{\text{sum}}^{\text{NF}}(B)$, is*

1. *For all $B \geqslant 0$ such that*

$$B \leqslant \sigma^2\left(1+\text{SNR}_{21}+\text{SNR}_{22}+2\sqrt{\text{SNR}_{21}\text{SNR}_{22}}\min\left\{\sqrt{\frac{\text{SNR}_{12}}{\text{SNR}_{11}}},\sqrt{\frac{\text{SNR}_{11}}{\text{SNR}_{12}}}\right\}\right),$$

$$R_{\text{sum}}^{\text{NF}}(B) = \frac{1}{2}\log_2\left(1+\text{SNR}_{11}+\text{SNR}_{12}-2\xi(b)\sqrt{\text{SNR}_{11}\text{SNR}_{12}}\right), \tag{6.36}$$

2. *For all $B \in \mathbb{R}$ such that*

$$B \leqslant \sigma_2^2\Big(1+\text{SNR}_{21}+\text{SNR}_{22}+2\sqrt{\text{SNR}_{21}\text{SNR}_{22}}\min\left\{\sqrt{\frac{\text{SNR}_{12}}{\text{SNR}_{11}}},\sqrt{\frac{\text{SNR}_{11}}{\text{SNR}_{12}}}\right\}\Big) \text{ and}$$

$$B \geqslant \sigma_2^2\Big(1+\text{SNR}_{21}+\text{SNR}_{22}+2\sqrt{\text{SNR}_{21}\text{SNR}_{22}}\Big),$$

$$R_{\text{sum}}^{\text{NF}}(b) = \frac{1}{2}\log_2\left(1+\left(1-\xi(b)^2\right)\text{SNR}_{1i}\right), \tag{6.37}$$

with $i = \underset{k\in\{1,2\}}{\text{argmax}}\ \text{SNR}_{1k}$,

3. *For all $B \in \Big[\sigma_2^2\Big(1+\text{SNR}_{21}+\text{SNR}_{22}+2\sqrt{\text{SNR}_{21}\text{SNR}_{22}}\Big),\infty\Big)$,*

$$R_{\text{sum}}^{\text{NF}}(B) = 0, \tag{6.38}$$

with the function ξ defined in (6.23)*.*

From Propositions 3 and 4, it can be seen that in the case with feedback, both users might transmit information and energy simultaneously as feedback creates signal correlation, which allows the system to meet the minimum energy rate. That is, the correlation induced by the use of the feedback is beneficial to both information transmission and energy transmission. Alternatively, in the case without feedback, artificial correlation via common randomness is required to meet the energy rate constraint. Such a correlation only benefits the energy transmission task and comes at the expense of the information transmission task as the information sum-rate is necessarily reduced. For instance, one way of achieving (6.37) is when the transmitter with the lowest SNR uses common randomness at its maximum power (transmits only energy), while the other transmitter transmits both energy and information.

6.5 Examples

Figure 6.3 shows the information-energy capacity region of the GMAC-F-E and the GMAC-E, respectively, with $\sigma_2^2 = 1$, and $\mathrm{SNR}_{11} = \mathrm{SNR}_{12} = \mathrm{SNR}_{21} = \mathrm{SNR}_{22} = 10$.

Therein, in each case, the figure in the center is a 3-D representation of the information-energy capacity region, whereas left and right figures represent a bi-dimensional view in the R_1-R_2 and B-R_2 planes, respectively. The triplet Q_1 with the highest energy transmission rate is

$$Q_1 = \left(0, 0, \sigma_2^2 \left(1 + \mathrm{SNR}_{21} + \mathrm{SNR}_{22} + 2\sqrt{\mathrm{SNR}_{21}\mathrm{SNR}_{22}}\right)\right).$$

The triplets Q_2, Q_2', Q_4 and Q_5 are coplanar and they satisfy $B = \sigma_2^2 (1 + \mathrm{SNR}_{21} + \mathrm{SNR}_{22})$. More specifically,

$$Q_4 = \left(\frac{1}{2}\log_2 (1 + \mathrm{SNR}_{11}), 0, \sigma_2^2 (1 + \mathrm{SNR}_{21} + \mathrm{SNR}_{22})\right)$$

and

$$Q_5 = \left(\frac{1}{2}\log_2 (1 + \mathrm{SNR}_{11}), \frac{1}{2}\log_2 \left(1 + \frac{\mathrm{SNR}_{11}}{1 + \mathrm{SNR}_{12}}\right), \sigma_2^2 (1 + \mathrm{SNR}_{21} + \mathrm{SNR}_{22})\right)$$

are achievable with and without feedback.

In Figure 6.3, the triplets Q_2, Q_3 and Q_6 guarantee information transmission at the perfect feedback maximum information sum-rate, i.e.,

$$R_1 + R_2 = \frac{1}{2}\log_2 \left(1 + \mathrm{SNR}_{11} + \mathrm{SNR}_{12} + 2\rho^\star(1,1)\sqrt{\mathrm{SNR}_{11}\mathrm{SNR}_{12}}\right).$$

In the GMAC-E, the triplets Q_2, Q_3, and Q_5 guarantee information transmission at the maximum information sum rate without feedback, i.e., $R_1 + R_2 = \frac{1}{2}\log_2 (1 + \mathrm{SNR}_{11} + \mathrm{SNR}_{12})$.

For a given $k \in \mathbb{N}$, let $\mathcal{B}(b_k) \subset \mathbb{R}_+^2$ be a two-dimensional set of the form

$$\mathcal{B}(b_k) = \left\{(R_1, R_2) \in \mathbb{R}_+^2 : R_i \leqslant \frac{1}{2}\log_2 \left(1 + \left(1 - \xi(b_k)^2\right)\mathrm{SNR}_{1i}\right), i \in \{1, 2\}\right\}. \quad (6.39)$$

Using this notation, the case with and without feedback are studied separately in the following sections.

6.5.1 Case with Feedback

Figure 6.4 shows a general example of the intersection of the volume $\mathcal{E}_0^{\mathrm{FB}}$, in the Cartesian coordinates (R_1, R_2, B), with the planes $B = b_k \geqslant 0$, with $k \in \{0, 1, 2, 3\}$,

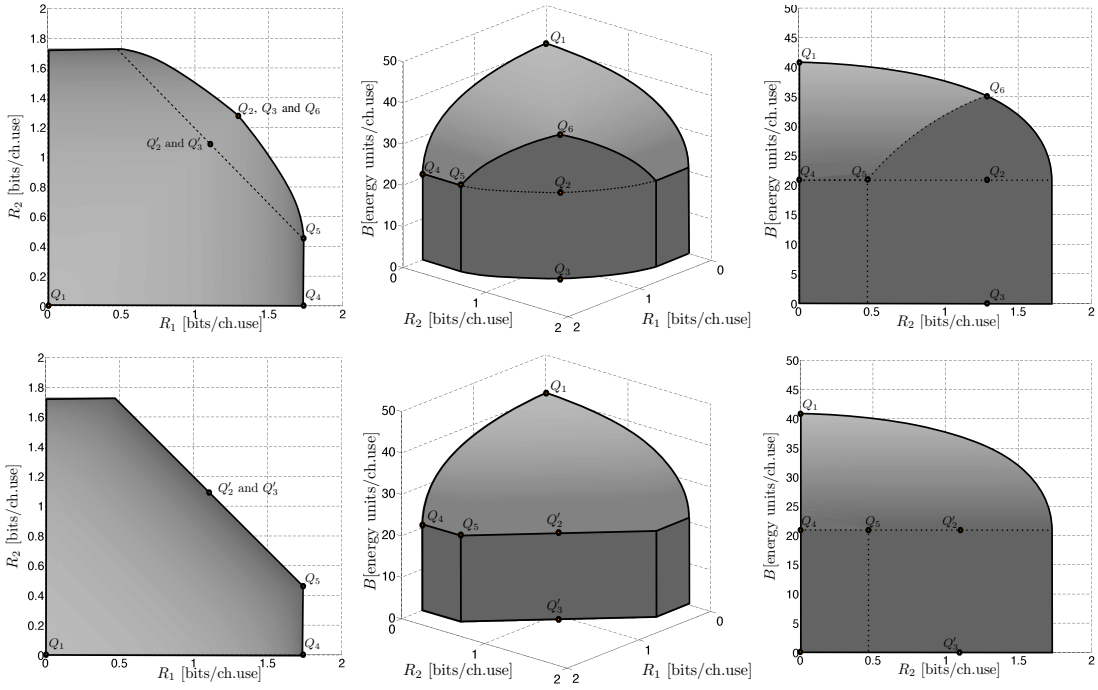

Figure 6.3: 3-D representation of the information-energy capacity region of the GMAC-F-E (top figures) and GMAC-E (bottom figures), $\mathcal{E}^{\mathrm{FB}}$ and $\mathcal{E}$, respectively, in the coordinate system (R_1, R_2, B). In each case, the figure in the center is a 3-D representation of the information-energy capacity region, whereas left and right figures represent a bi-dimensional view in the R_1-R_2 and B-R_2 planes, respectively.

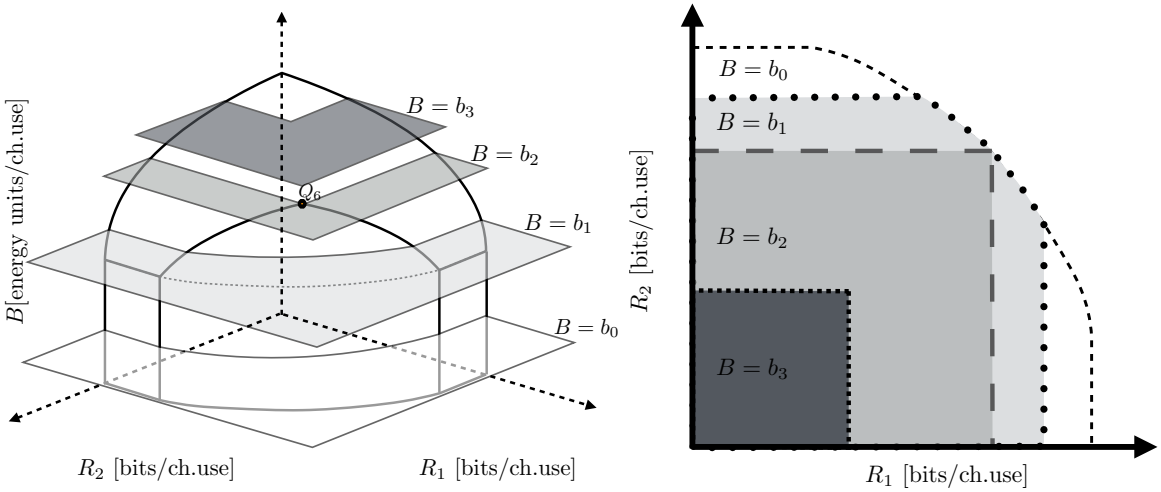

Figure 6.4: Intersection of the the information-energy capacity region of the GMAC-F-E, $\mathcal{E}$, with the planes $B = b_0$, $B = b_1$, $B = b_2$ and $B = b_3$, where for all $k \in \{1, 2, 3\}$ b_k is defined in (6.40).

such that

$$
\begin{aligned}
b_0 &\leqslant \sigma_2^2 \left(1 + \mathrm{SNR}_{21} + \mathrm{SNR}_{22}\right), && \text{(6.40a)}\\
b_1 &\leqslant \sigma_2^2 \left(1 + \mathrm{SNR}_{21} + \mathrm{SNR}_{22} + 2\rho^\star(1,1)\sqrt{\mathrm{SNR}_{21}\mathrm{SNR}_{22}}\right), && \text{(6.40b)}\\
b_1 &\geqslant \sigma_2^2 \left(1 + \mathrm{SNR}_{21} + \mathrm{SNR}_{22}\right), && \text{(6.40c)}\\
b_2 &= \sigma_2^2 \left(1 + \mathrm{SNR}_{21} + \mathrm{SNR}_{22} + 2\rho^\star(1,1)\sqrt{\mathrm{SNR}_{21}\mathrm{SNR}_{22}}\right), && \text{(6.40d)}\\
b_3 &\leqslant \sigma_2^2 \left(1 + \mathrm{SNR}_{21} + \mathrm{SNR}_{22} + 2\sqrt{\mathrm{SNR}_{21}\mathrm{SNR}_{22}}\right), \text{ and} && \text{(6.40e)}\\
b_3 &\geqslant \sigma_2^2 \left(1 + \mathrm{SNR}_{21} + \mathrm{SNR}_{22} + 2\rho^\star(1,1)\sqrt{\mathrm{SNR}_{21}\mathrm{SNR}_{22}}\right). && \text{(6.40f)}
\end{aligned}
$$

Case 1: $\mathbf{B = b_0}$. In this case, any intersection of the volume $\mathcal{E}^{\mathrm{FB}}$ with a plane $B = b_0$ corresponds to the set of triplets (R_1, R_2, b_0), in which the corresponding pairs (R_1, R_2) form a set that is identical to the information capacity region of the GMAC-F (without EH), denoted by $\mathcal{C}_{\mathrm{FB}}$. In this case, $\xi(b_0) = 0$, and thus from Proposition 1 and Proposition 3, the energy constraint does not add any additional bound on the individual rates and sum-rate other than (6.17a), (6.17b), and (6.17c). That is, the minimum energy transmission rate requirement can always be met by exclusively transmitting information.

Case 2: $\mathbf{B = b_1}$. In this case, any intersection of the volume $\mathcal{E}^{\mathrm{FB}}$ with a plane $B = b_1$ is a set of triplets (R_1, R_2, b_1) for which the corresponding pairs (R_1, R_2) satisfy $(R_1, R_2) \in \mathcal{B}(b_1) \cap \mathcal{C}_{\mathrm{FB}}$, which forms a strict subset of $\mathcal{C}_{\mathrm{FB}}$. Note that $\xi(b_1) > 0$, and thus from Proposition 1, the energy constraint limits the individual rates. That is, transmitter i's individual information rate is bounded away from $\frac{1}{2}\log_2\left(1 + \mathrm{SNR}_{1i}\right)$. Nevertheless, it is important to highlight that in this case, $\xi(b_1) \leqslant \rho^\star(1,1)$, and thus the individual rates

$$
R_1 = \frac{1}{2}\log_2\left(1 + \left(1 - \left(\rho^\star(1,1)\right)^2\right)\mathrm{SNR}_{11}\right)
$$

and

$$R_2 = \frac{1}{2}\log_2\left(1 + \left(1 - (\rho^\star(1,1))^2\right)\mathrm{SNR}_{12}\right)$$

are always achievable. Hence, this intersection always includes the triplet (R_1, R_2, b_1), with $R_1 + R_2 = \frac{1}{2}\log_2\left(1 + \mathrm{SNR}_{11} + \mathrm{SNR}_{12} + 2\rho^\star(1,1)\sqrt{\mathrm{SNR}_{11}\mathrm{SNR}_{12}}\right) = R_{\mathrm{sum}}^{\mathrm{FB}}(b_1) = R_{\mathrm{sum}}^{\mathrm{FB}}(0)$. That is, the power-split $\beta_1 = \beta_2 = 1$ is always feasible. Note that the intersection of the volume $\mathcal{E}^{\mathrm{FB}}$ with the plane $B = b_2$ is a particular case of this regime.

Case 3: $\mathbf{B = b_3}$. In this case, any intersection of the volume $\mathcal{E}^{\mathrm{FB}}$ with a plane $B = b_3$ is a set of triplets (R_1, R_2, b_3) for which the corresponding pairs (R_1, R_2) satisfy $(R_1, R_2) \in \mathcal{B}(b_3) = \mathcal{B}(b_3) \cap \mathcal{C}_{\mathrm{FB}}$, which is a strict subset of $\mathcal{C}_{\mathrm{FB}}$. Note that $\rho^\star(1,1) < \xi(b_3) \leqslant 1$, and thus from Proposition 1, the individual information rates are limited by $R_i \leqslant \frac{1}{2}\log_2\left(1 + (1 - \xi(b_3)^2)\,\mathrm{SNR}_{1i}\right) < \frac{1}{2}\log_2\left(1 + \left(1 - (\rho^\star(1,1))^2\right)\mathrm{SNR}_{1i}\right)$. For any $b_3 > 1 + \mathrm{SNR}_{21} + \mathrm{SNR}_{22} + 2\rho^\star(1,1)\sqrt{\mathrm{SNR}_{21}\mathrm{SNR}_{22}}$, the set $\mathcal{B}(b_3)$ monotonically shrinks with b_3. Consequently, for these values of b_3, there exists a loss of sum-rate and $R_{\mathrm{sum}}^{\mathrm{FB}}(0)$ is not achievable. Nonetheless, note that $R_{\mathrm{sum}}^{\mathrm{FB}}(b_3)$ is a continuous function in b_3. When $b_3 = \sigma_2^2\big(1 + \mathrm{SNR}_{21} + \mathrm{SNR}_{22} + 2(\rho^\star(1,1) + \epsilon)\sqrt{\mathrm{SNR}_{21}\mathrm{SNR}_{22}}\big)$, for some $\epsilon > 0$, it holds that $\xi(b_3) = \rho^\star(1,1) + \epsilon$. Substituting this into (6.33) and taking the limit when ϵ tends to 0, by the definition of $\rho^\star(1,1)$, the resulting value is given by (6.30). Clearly, the maximum energy rate is achieved when $\beta_1 = \beta_2 = 0$, which implies that no information is conveyed from the transmitters to the receiver.

6.5.2 Case without Feedback

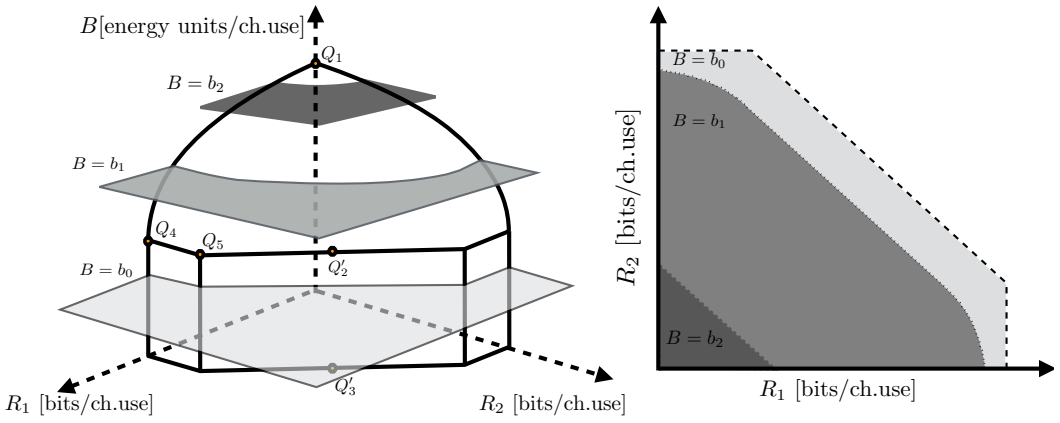

Figure 6.5: Intersection of the information-energy capacity region of the GMAC-E, $\mathcal{E}$, with the planes $B = b_0$, $B = b_1$, and $B = b_2$, where for all $k \in \{1, 2, 3\}$ b_k is defined in (6.41)..

Figure 6.5 shows a general example of the intersection of the volume $\mathcal{E}$, in the Cartesian coordinates (R_1, R_2, B), with the planes $B = b_k$, with $k \in \{0, 1, 2\}$, such

that

$$b_0 \leqslant \sigma_2^2 \left(1 + \mathrm{SNR}_{21} + \mathrm{SNR}_{22}\right), \tag{6.41a}$$

$$b_1 \geqslant \sigma_2^2 \left(1 + \mathrm{SNR}_{21} + \mathrm{SNR}_{22}\right), \tag{6.41b}$$

$$b_1 \leqslant \sigma_2^2 \left(1 + \mathrm{SNR}_{21} + \mathrm{SNR}_{22} + 2\sqrt{\mathrm{SNR}_{21}\mathrm{SNR}_{22}} \min\left\{\sqrt{\frac{\mathrm{SNR}_{12}}{\mathrm{SNR}_{11}}}, \sqrt{\frac{\mathrm{SNR}_{11}}{\mathrm{SNR}_{12}}}\right\}\right), \tag{6.41c}$$

$$b_2 \geqslant \sigma_2^2 \left(1 + \mathrm{SNR}_{21} + \mathrm{SNR}_{22} + 2\sqrt{\mathrm{SNR}_{21}\mathrm{SNR}_{22}} \min\left\{\sqrt{\frac{\mathrm{SNR}_{12}}{\mathrm{SNR}_{11}}}, \sqrt{\frac{\mathrm{SNR}_{11}}{\mathrm{SNR}_{12}}}\right\}\right), \tag{6.41d}$$

$$b_2 \leqslant \sigma_2^2 \left(1 + \mathrm{SNR}_{21} + \mathrm{SNR}_{22} + 2\sqrt{\mathrm{SNR}_{21}\mathrm{SNR}_{22}}\right). \tag{6.41e}$$

Case 1: $\mathbf{B = b_0}$. In this case, any intersection of the volume $\mathcal{E}$, in the Cartesian coordinates (R_1, R_2, B), with a plane $B = b_0$ corresponds to the set of triplets (R_1, R_2, b_0), in which the corresponding pairs (R_1, R_2) form a set that is identical to the information capacity region of the GMAC (without EH), denoted by $\mathcal{C}$. Note that $\xi(b_0) = 0$, and thus from Proposition 2 and Proposition 4, it holds that $R_i^{\mathrm{NF}}(b_0) = \frac{1}{2}\log_2\left(1 + \mathrm{SNR}_{1i}\right)$, for $i \in \{1, 2\}$, and $R_{\mathrm{sum}}^{\mathrm{NF}}(b_0) = \frac{1}{2}\log_2\left(1 + \mathrm{SNR}_{11} + \mathrm{SNR}_{12}\right)$. Hence, exclusively transmitting information is enough for satisfying the energy rate constraint $B = b_0$.

Case 2: $\mathbf{B = b_1}$. In this case, any intersection of the volume $\mathcal{E}$, in the Cartesian coordinates (R_1, R_2, B), with a plane $B = b_1$ corresponds to the set of triplets (R_1, R_2, b_1) in which the corresponding pairs (R_1, R_2) form a set that is equivalent to a proper subset of the information capacity region of the GMAC $\mathcal{C}$. Note that $\xi(b_1) > 0$, and thus from Proposition 2 and Proposition 4, $R_i^{\mathrm{NF}}(b_1)$ and $R_{\mathrm{sum}}^{\mathrm{NF}}(b_1)$ decrease with b_1. This is mainly due to the fact that part of each transmitter's power budget is dedicated to the transmission of energy. Furthermore, the information sum-rate optimal strategy involves information transmission at both users since the sum-capacity is strictly larger than the maximum individual rate of the user with the highest SNR.

Case 3: $\mathbf{B = b_2}$. In this case, any intersection of the volume $\mathcal{E}$, in the Cartesian coordinates (R_1, R_2, B), with a plane $B = b_2$ corresponds to the set of triplets (R_1, R_2, b_2) in which the corresponding pairs (R_1, R_2) form a set that is equivalent to a proper subset of the information capacity region of the GMAC, $\mathcal{C}$. The maximum information sum-rate corresponds to the maximum individual rate (Proposition 2) of the transmitter with the highest SNR. That is, in order to maximize the information sum-rate, it is optimal to have information transmission exclusively at the stronger user with the highest SNR. The transmitter with the weakest SNR uses all its power budget to exclusively transmit energy.

6.6 Energy Transmission Enhancement with Feedback

In this section, the enhancement on the energy transmission rate due to the use of feedback is quantified when the information sum-rate is $R_{\text{sum}}^{\text{NF}}(0)$ (see the blue triangles and orange squares in Figure 6.6).

Denote by $B_{\text{NF}} = \sigma_2^2\left(1+\text{SNR}_{21}+\text{SNR}_{22}\right)$ the maximum energy rate that can be guaranteed at the EH in the GMAC-E when the information sum-rate is $R_{\text{sum}}^{\text{NF}}(0)$. Denote also by B_{FB} the maximum energy rate that can be guaranteed at the EH in the GMAC-F-E when the information sum-rate is $R_{\text{sum}}^{\text{NF}}(0)$. The exact value of B_{FB} is the solution to an optimization problem of the form

$$\begin{aligned} B_{\text{FB}} \quad &= \max \quad B \\ \text{subject to:} \quad & R_{\text{sum}}^{\text{FB}}(B) = R_{\text{sum}}^{\text{NF}}(0). \end{aligned} \tag{6.42}$$

The solution to (6.42) is given by the following theorem.

Theorem 8. *The maximum energy rate B_{FB} that can be guaranteed at the EH in the* GMAC-F-E *when the information sum-rate is $R_{\text{sum}}^{\text{NF}}(0)$ is*

$$B_{\text{FB}} = \sigma_2^2\left(1+\text{SNR}_{21}+\text{SNR}_{22}+2\sqrt{(1-\gamma)\text{SNR}_{21}\text{SNR}_{22}}\right), \tag{6.43}$$

with $\gamma \in (0,1)$ defined as follows:

$$\gamma \triangleq \frac{\text{SNR}_{11}+\text{SNR}_{12}}{2\text{SNR}_{11}\text{SNR}_{12}}\left[\sqrt{1+\frac{4\text{SNR}_{11}\text{SNR}_{12}}{\text{SNR}_{11}+\text{SNR}_{12}}}-1\right]. \tag{6.44}$$

To quantify the energy rate enhancement induced by feedback, it is of interest to consider the ratio $\frac{B_{\text{FB}}}{B_{\text{NF}}}$ given by

$$\frac{B_{\text{FB}}}{B_{\text{NF}}} = 1+\frac{2\sqrt{(1-\gamma)\text{SNR}_{21}\text{SNR}_{22}}}{1+\text{SNR}_{21}+\text{SNR}_{22}}. \tag{6.45}$$

Note that the impact of the SNRs in the information transmission branch (SNR_{11} and SNR_{12}) are captured by γ.

Let $\nu_i \triangleq \frac{\text{SNR}_{1i}}{\text{SNR}_{1j}} \in \mathbb{R}_+$ and $\eta_i \triangleq \frac{\text{SNR}_{2i}}{\text{SNR}_{2j}} \in \mathbb{R}_+$, with $(i,j) \in \{1,2\}^2$ and $i \neq j$ measure the asymmetry in the channel from the transmitters to the receiver and to the EH, respectively. Let also $\psi_i \triangleq \frac{\text{SNR}_{2i}}{\text{SNR}_{1i}} \in \mathbb{R}_+$ capture the strength ratio between the information and the energy channels of transmitter i.

With these parameters, γ in (6.44) can be rewritten as

$$\gamma = \frac{1+\nu_i}{2\nu_i\text{SNR}_{1j}}\left[\sqrt{1+\frac{4\nu_i\text{SNR}_{1j}}{1+\nu_i}}-1\right], \tag{6.46}$$

with $(i,j) \in \{1,2\}^2$ and $i \neq j$.

Note that, for all $(i,j) \in \{1,2\}^2$ with $i \neq j$, when $\mathrm{SNR}_{1j} \to 0$ while the ratio ν_i remains constant, from (6.46), it follows that

$$\lim_{\mathrm{SNR}_{1j}\to 0} \gamma = 1. \tag{6.47}$$

Thus, when the SNRs in the information branch (SNR_{11} and SNR_{12}) are very low, the improvement on the energy transmission rate due to feedback is inexistent. This observation is independent of the SNRs in the EH branch (SNR_{21} and SNR_{22}).

Alternatively, when $\mathrm{SNR}_{1j} \to \infty$ while the ratio ν_i remains constant, it follows that

$$\lim_{\mathrm{SNR}_{1j}\to \infty} \gamma = 0. \tag{6.48}$$

Thus, when the SNRs in the information branch (SNR_{11} and SNR_{12}) are very high, the improvement on the energy transmission rate due to feedback is given by

$$\lim_{\mathrm{SNR}_{1j}\to \infty} \frac{B_{\mathrm{FB}}}{B_{\mathrm{NF}}} = 1 + \frac{2\sqrt{\mathrm{SNR}_{21}\mathrm{SNR}_{22}}}{1+\mathrm{SNR}_{21}+\mathrm{SNR}_{22}}. \tag{6.49}$$

More generally, using the above parameters, the ratio $\frac{B_{\mathrm{FB}}}{B_{\mathrm{NF}}}$ in (6.45) can be written as

$$\frac{B_{\mathrm{FB}}}{B_{\mathrm{NF}}} = 1 + \frac{2\psi_j \mathrm{SNR}_{1j}\sqrt{\eta_i\left(1-\left(\frac{1+\nu_i}{2\nu_i\mathrm{SNR}_{1j}}\left(\sqrt{1+\frac{4\nu_i\mathrm{SNR}_{1j}}{1+\nu_i}}-1\right)\right)\right)}}{1+(1+\eta_i)\psi_j\mathrm{SNR}_{1j}}. \tag{6.50}$$

Based on (6.50), the following corollary evaluates the very low SNR asymptotic energy enhancement with feedback.

Corollary 1. *For all $(i,j) \in \{1,2\}^2$ with $i \neq j$, when $\mathrm{SNR}_{1j} \to 0$ while the ratios ν_i, η_i, and ψ_i remain constant, it holds that*

$$\lim_{\mathrm{SNR}_{1j}\to 0} \frac{B_{\mathrm{FB}}}{B_{\mathrm{NF}}} = 1, \tag{6.51}$$

and thus feedback does not enhance energy transmission at very low SNR.

In the very high SNR regime, the asymptotic energy enhancement with feedback is given by the following corollary that is also based on (6.50).

Corollary 2. *For all $(i,j) \in \{1,2\}^2$ with $i \neq j$, when $\mathrm{SNR}_{1j} \to \infty$ while the ratios ν_i, η_i, and ψ_i remain constant, the maximum energy rate improvement with feedback is given by*

$$\lim_{\mathrm{SNR}_{1j}\to \infty} \frac{B_{\mathrm{FB}}}{B_{\mathrm{NF}}} = 1 + \frac{2\sqrt{\eta_i}}{1+\eta_i}. \tag{6.52}$$

From Corollary 1 and Corollary 2, it holds that:

Corollary 3. *Feedback can at most double the energy transmission rate:*

$$1 \leqslant \frac{B_{\mathrm{FB}}}{B_{\mathrm{NF}}} \leqslant 2, \tag{6.53}$$

where the upper-bound holds with equality when $\eta_i = 1$*, i.e.,* $\mathrm{SNR}_{21} = \mathrm{SNR}_{22}$*.*

Figure 6.7 compares the exact value of the ratio $\frac{B_{\mathrm{FB}}}{B_{\mathrm{NF}}}$ in (6.50) to the high-SNR limit in (6.52) as a function of the SNRs. This implies that the channel coefficients between the transmitters and the receiver are identical to those between the transmitters and the EH., i.e., $\mathrm{SNR}_{11} = \mathrm{SNR}_{21} = \mathrm{SNR}_1$ and $\mathrm{SNR}_{12} = \mathrm{SNR}_{22} = \mathrm{SNR}_2$. Note that in the symmetric case, i.e., $\mathrm{SNR}_1 = \mathrm{SNR}_2 = \mathrm{SNR}$, the upper-bound in (6.52) is tight since the ratio $\frac{B_{\mathrm{FB}}}{B_{\mathrm{NF}}}$ becomes arbitrarily close to two as SNR tends to infinity. In the non-symmetric cases $\mathrm{SNR}_1 \neq \mathrm{SNR}_2$, this bound is loose.

6.7 Conclusion and Further Work

This chapter has characterized the information-energy capacity region of the two-user GMAC with an EH, with and without feedback, and has determined the energy transmission enhancement induced by the use of feedback. An important conclusion of this work is that SIET requires additional transmitter cooperation/coordination. From this viewpoint, any technique that allows transmitter cooperation (i.e., feedback, conferencing, etc.) is likely to provide performance gains in SIET in general multi-user networks. The results on the energy transmission enhancement induced by feedback in the two-user GMAC-F can be extended to the K-user GMAC-F with EH for arbitrary $K \geqslant 3$.

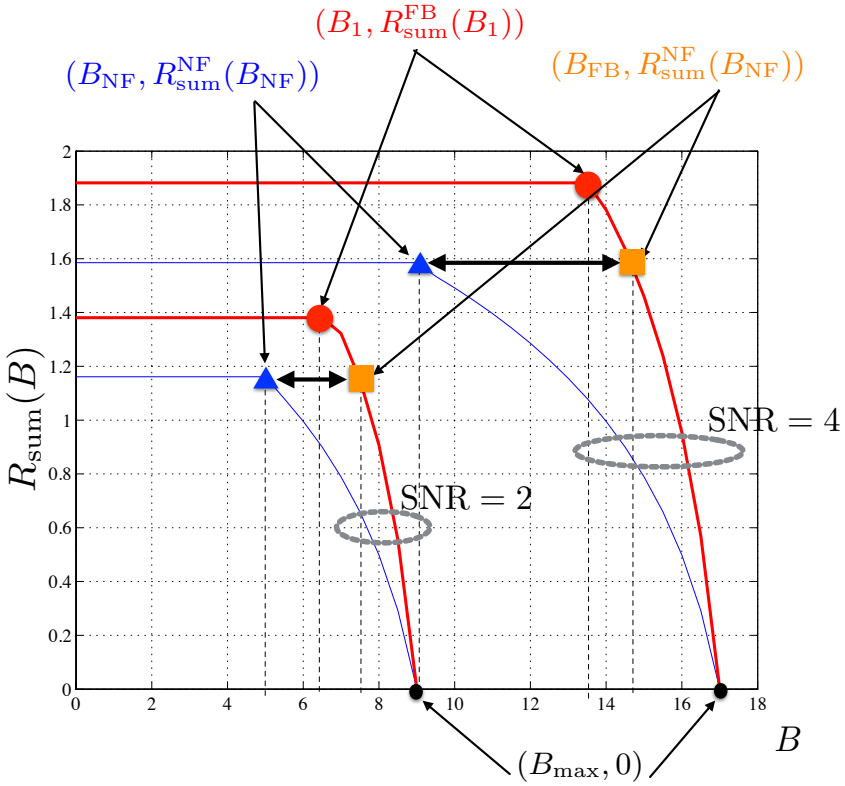

Figure 6.6: Maximum information sum-rate of the symmetric two-user memoryless GMAC-F-E (thick red line) and GMAC-E (thin blue line), with $\sigma_2^2 = 1$ and $\text{SNR}_{11} = \text{SNR}_{12} = \text{SNR}_{21} = \text{SNR}_{22} = \text{SNR}$, as a function of B. Red (big) circles represent the pairs $(B_1, R_{\text{sum}}^{\text{FB}}(B_1))$ in which $R_{\text{sum}}^{\text{FB}}(B_1)$ is the maximum information sum-rate with feedback when only information transmission is performed and $B_1 \triangleq \sigma_2^2\,(1 + 2(1 + \rho^\star(1,1))\text{SNR})$ represents the corresponding maximum energy rate that can be guaranteed at the EH. Blue triangles represent the pairs $(B_{\text{NF}}, R_{\text{sum}}^{\text{NF}}(B_{\text{NF}}))$ in which $R_{\text{sum}}^{\text{NF}}(B_{\text{NF}})$ is the maximum information sum-rate without feedback and $B_{\text{NF}} \triangleq \sigma_2^2\,(1 + 2\text{SNR})$ is the corresponding maximum energy rate that can be guaranteed at the EH without feedback. Orange squares represent the pairs $(B_{\text{FB}}, R_{\text{sum}}^{\text{NF}}(B_{\text{F}}))$ in which B_{FB} is the corresponding maximum energy rate that can be guaranteed at the EH with feedback. Black (small) circles represent the pairs $(B_{\max}, 0)$ in which $B_{\max} \triangleq \sigma_2^2\,(1 + 4\text{SNR})$ is the maximum energy rate at the EH.

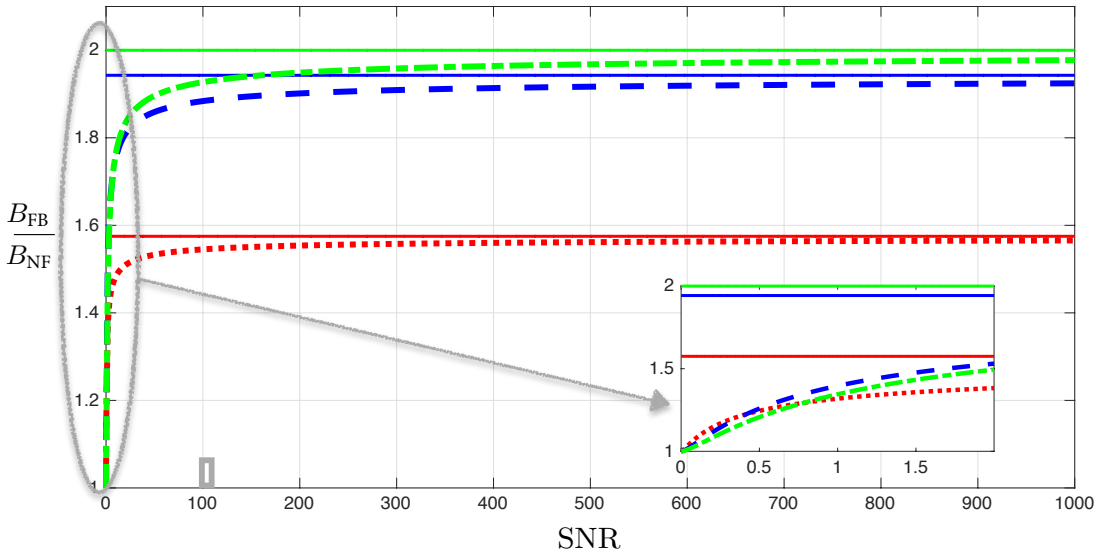

Figure 6.7: The ratio $\frac{B_{\mathrm{FB}}}{B_{\mathrm{NF}}}$ and its high-SNR limit as a function of SNR and $\mathrm{SNR}_{11} = \mathrm{SNR}_{21} = \mathrm{SNR}_1$ and $\mathrm{SNR}_{12} = \mathrm{SNR}_{22} = \mathrm{SNR}_2$. The solid line is the high-SNR limit in (6.52); the dash-dotted line, the dashed line and the dotted line are the exact values of the ratio $\frac{B_{\mathrm{FB}}}{B_{\mathrm{NF}}}$ in (6.50) when $\mathrm{SNR}_1 = \mathrm{SNR}_2 = \mathrm{SNR}$; $\frac{\mathrm{SNR}_1}{2} = \mathrm{SNR}_2 = \mathrm{SNR}$; and $\frac{\mathrm{SNR}_1}{10} = \mathrm{SNR}_2 = \mathrm{SNR}$, respectively.

Chapter 7

Gaussian Interference Channels with Energy Transmission

This chapter characterizes the fundamental limits of simultaneous information and energy transmission in the two-user GIC with and without feedback. More specifically, all the achievable information and energy transmission rates (in bits per channel use and energy-units per channel use, respectively) are approximated within a constant gap, in the sense of Definition 3.

7.1 Mathematical Model

Consider a two-user GIC with a non-colocated energy harvester (EH) with and without point-to-point perfect channel-output feedback (PF) from each receiver to its corresponding transmitter. These two scenarios are depicted in Figure 7.1(a) and Figure 7.1(b), respectively. Note that there is no feedback from the EH to any of the transmitters. Within this context, transmitter i, with $i \in \{1, 2\}$, aims to simultaneously execute two tasks: (a) information transmission to its intended receiver; and (b) energy transmission to the EH.

7.1.1 Information Transmission

From the information transmission standpoint, the goal of transmitter i, with $i \in \{1, 2\}$, is to convey a message index $W_i \in \mathcal{W}_i = \{1, 2, \ldots, \lfloor 2^{NR_i} \rfloor\}$ to receiver i using N channel input symbols $X_{i,1}, X_{i,2}, \ldots, X_{i,N}$. That is, information is transmitted at rate $R_i > 0$ bits per channel use. The channel coefficient from transmitter k to receiver i, with $k \in \{1, 2\}$, is denoted by $h_{i,k} \in \mathbb{R}_+$, where $\mathbb{R}_+$ denotes the positive reals. At receiver i, during channel use n, input symbol $X_{i,n}$ is observed at receiver i subject to the interference produced by the symbol $X_{j,n}$ sent by transmitter j, with $j \in \{1, 2\} \setminus \{i\}$, and a real additive Gaussian noise $Z_{i,n}$ with zero mean and variance σ_i^2. Hence, the channel output at receiver i during channel use n, denoted by $Y_{i,n}$,

is:

$$Y_{i,n} = h_{i,i}X_{i,n} + h_{i,j}X_{j,n} + Z_{i,n}. \tag{7.1}$$

In the case without feedback, at each channel use n, the symbol $X_{i,n}$ sent by transmitter i depends upon the message index W_i and a randomly generated index $\Omega \in \mathbb{N}$. Let $f_{i,n}^{(N)} : \mathcal{W}_i \times \mathbb{N} \to \mathbb{R}$ be the encoding function at channel use n, such that for all $n \in \{1, 2, \ldots, N\}$, the following holds:

$$X_{i,n}{=}f_{i,n}^{(N)}(W_i, \Omega). \tag{7.2}$$

In the case with feedback, the symbol $X_{i,n}$ sent by transmitter i depends upon the indices W_i and Ω, but also upon all previous channel-outputs $Y_{i,1}, Y_{i,2}, \ldots, Y_{i,n-d}$, with $d \in \mathbb{N}$ the feedback delay. In the following, it is assumed that d is equal to one channel use, without any loss of generality. Thus, the first channel input symbol $X_{i,1}$ depends only on the message index W_i and Ω. More specifically, $f_{i,1}^{(N)} : \mathcal{W}_i \times \mathbb{N} \to \mathbb{R}$. Alternatively, for all $n \in \{2, 3, \ldots, N\}$, the encoding functions are $f_{i,n}^{(N)} : \mathcal{W}_i \times \mathbb{N} \times \mathbb{R}^{n-1} \to \mathbb{R}$. Essentially,

$$X_{i,1}{=}f_{i,1}^{(N)}(W_i, \Omega), \tag{7.3a}$$

and for all $n > 1$,

$$X_{i,n}{=}f_{i,n}^{(N)}(W_i, \Omega, Y_{i,1}, Y_{i,2}, \ldots, Y_{i,n-1}). \tag{7.3b}$$

In both cases, with and without feedback, the random index Ω is assumed to be known by all transmitters and receivers. Moreover, channel input symbols $X_{i,1}, X_{i,2}, \ldots, X_{i,N}$ are subject to an average power constraint of the form

$$\frac{1}{N}\sum_{n=1}^{N} \mathbb{E}_{X_{i,n}}\left[X_{i,n}^2\right] \leq P_i, \tag{7.4}$$

where P_i denotes the average transmit power of transmitter i in energy units per channel use. The decoder of receiver i observes the channel outputs $Y_{i,1}, Y_{i,2}, \ldots, Y_{i,N}$ and uses a decoding function $\phi_i^{(N)} \colon \mathbb{N} \times \mathbb{R}^N \to \mathcal{W}_i$, to get an estimate of the message indices:

$$\widehat{W_i} = \phi_i^{(N)}\left(\Omega, Y_{i,1}, Y_{i,2}, \ldots, Y_{i,N}\right), \tag{7.5}$$

where $\widehat{W_i}$ is an estimate of the message index W_i. The decoding error probability of a codebook of block-length N, denoted by $P_{\text{DE}}^{(N)}$, is given by

$$P_{\text{DE}}^{(N)} = \max\left[\Pr\left[\widehat{W_1} \neq W_1\right], \Pr\left[\widehat{W_2} \neq W_2\right]\right]. \tag{7.6}$$

The signal to noise ratio (SNR) at receiver i is denoted by

$$\text{SNR}_i = \frac{|h_{i,i}|^2 P_i}{\sigma_i^2}. \tag{7.7a}$$

The interference to noise ratio (INR) at receiver i is denoted by

$$\text{INR}_i = \frac{|h_{i,j}|^2 P_j}{\sigma_i^2}, \text{ with } j \neq i. \tag{7.7b}$$

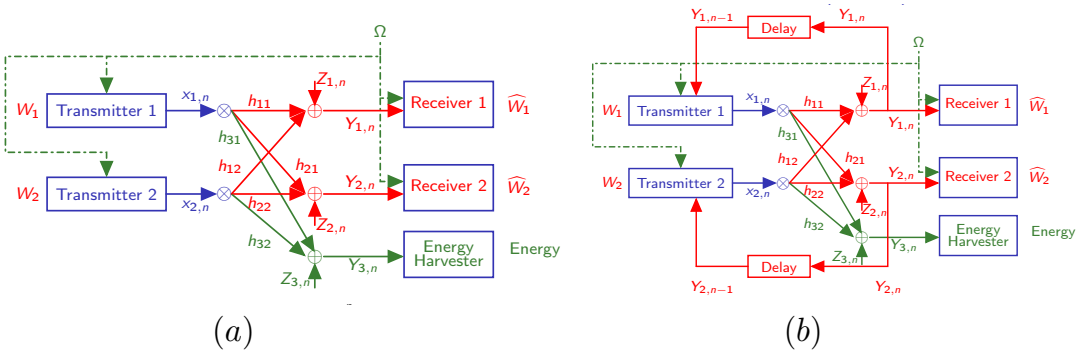

Figure 7.1: Two-user Gaussian interference channels with a non-colocated energy harvester at channel use n. (a) Case without feedback; and (b) Case with perfect channel output feedback.

7.1.2 Energy Transmission

Let $h_{3,i} \in \mathbb{R}_+$ be the channel coefficient from transmitter i to the EH. The symbols sent by the transmitters during channel use n are observed by the EH subject to an additive Gaussian noise $Z_{3,n}$ with zero mean and variance σ_3^2. More specifically, the channel output at the EH during channel use n, denoted by $Y_{3,n}$, is:

$$Y_{3,n} = h_{3,1}X_{1,n} + h_{3,2}X_{2,n} + Z_{3,n}. \tag{7.8}$$

From the energy transmission standpoint, the goal of both transmitters is to jointly guarantee an average energy rate at the EH.

Let $B^{(N)} : \mathbb{R}^N \to \mathbb{R}_+$ be a function that determines the energy obtained from the channel outputs $Y_{3,1}, Y_{3,2}, \ldots, Y_{3,N}$. In the following, this function is chosen to be the average energy rate (in energy-units per channel use) at the end of N channel uses. That is,

$$B^{(N)}(Y_{3,1}, Y_{3,2}, \ldots, Y_{3,N}) \triangleq \frac{1}{N}\sum_{n=1}^{N} Y_{3,n}^2, \tag{7.9}$$

which implies that the energy carried by a given channel output $Y_{3,t}$, with $t \in \{1, 2, \ldots, N\}$, is $Y_{3,t}^2$. This assumption is very optimistic given the dependency of the delivered DC power on higher order statistics of the channel input distribution [80, 95]. Nonetheless, from the fundamental limits point of view, any more realistic model would induce fundamental limits that are more pessimistic than the results presented in the following sections.

The SNR of transmitter i at the EH is denoted by

$$\mathrm{SNR}_{3i} = \frac{|h_{3,i}|^2 P_i}{\sigma_3^2}. \tag{7.10}$$

Note that the maximum average energy rate, denoted by $B_{\max}$, is:

$$B_{\max} = \sigma_3^2\left(1 + \mathrm{SNR}_{31} + \mathrm{SNR}_{32} + 2\sqrt{\mathrm{SNR}_{31}\mathrm{SNR}_{32}}\right), \tag{7.11}$$

which can be achieved in the asymptotic block-length regime when both channel inputs exhibit a correlation coefficient equal to one. Hence, given an energy rate $B \in [0, B_{\max}]$, the energy outage probability, denoted by $P_{\text{EO}}^{(N)}(B)$, is:

$$P_{\text{EO}}^{(N)} \triangleq \Pr\left[B^{(N)}(\boldsymbol{Y}_3) < B\right]. \tag{7.12}$$

7.1.3 Simultaneous Information and Energy Transmission

The system is said to operate at the information-energy rate triplet $(R_1, R_2, B) \in \mathbb{R}_+^3$ when both transmitter-receiver pairs use a transmit-receive configuration such that: (i) reliable communication at information rates R_1 and R_2 is ensured; and (ii) reliable energy transmission at energy rate B is ensured. A formal definition is given below.

Definition 8 (Achievable Rates)**.** The triplet $(R_1, R_2, B) \in \mathbb{R}_+^3$ is achievable if for all $i \in \{1, 2\}$, there exists a sequence of encoding functions $f_{i,1}^{(N)}, f_{i,2}^{(N)}, \ldots, f_{i,N}^{(N)}$ and two decoding functions $\phi_1^{(N)}$ and $\phi_2^{(N)}$ such that both the average decoding error probability $P_{\text{DE}}^{(N)}$ and the energy-outage probability $P_{\text{EO}}^{(N)}$ tend to zero as the block-length N tends to infinity. That is,

$$\limsup_{N\to\infty} P_{\text{DE}}^{(N)} = 0 \text{ and} \tag{7.13a}$$

$$\limsup_{N\to\infty} P_{\text{EO}}^{(N)} = 0. \tag{7.13b}$$

Using Definition 8, the fundamental limits of simultaneous information and energy transmission in the Gaussian interference channel can be described by the information-energy capacity region [16], defined as follows.

Definition 9 (Information-Energy Capacity Region)**.** The information-energy capacity region, denoted by $\mathcal{E}^{\text{F}}$ in the case with feedback and $\mathcal{E}$ in the case without feedback, corresponds to the closure of all achievable information-energy rate triplets (R_1, R_2, B).

In Chapter 7, the information-energy capacity region of the GIC with and without feedback is approximate within a constant gap (Definition 3).

7.2 The Information-Energy Capacity Region

7.2.1 Case without Feedback

The information-energy capacity region of the GIC with an EH and without feedback, denoted by $\mathcal{E}$, is approximated by the regions $\underline{\mathcal{E}} \subset \mathbb{R}_+^3$, which represents an information-energy achievable region (Theorem 12); and $\overline{\mathcal{E}} \subset \mathbb{R}_+^3$, which represents an information-energy converse region (Theorem 13). Regions $\underline{\mathcal{E}}$ and $\overline{\mathcal{E}}$ satisfy $\underline{\mathcal{E}} \subseteq \mathcal{E} \subseteq \overline{\mathcal{E}}$ and approximate the information-energy region $\mathcal{E}$ to within a given gap (Definition 3).

An Achievable Information-Energy Region

The following theorem introduces an achievable information-energy region.

Theorem 9. *The information-energy capacity region $\mathcal{E}$ contains the set $\underline{\mathcal{E}} \subseteq \mathbb{R}_+^3$ of all rate tuples (R_1, R_2, B) that satisfy:*

$$R_1 \leq \frac{1}{2}\log\left(1+\frac{(1-\lambda_{1e})\mathrm{SNR}_1}{1+\lambda_{2p}\mathrm{INR}_1}\right), \tag{7.14a}$$

$$R_2 \leq \frac{1}{2}\log\left(1+\frac{(1-\lambda_{2e})\mathrm{SNR}_2}{1+\lambda_{1p}\mathrm{INR}_2}\right), \tag{7.14b}$$

$$R_1+R_2 \leq \frac{1}{2}\log\left(\frac{1+(1-\lambda_{1e})\mathrm{SNR}_1+(1-\lambda_{2e})\mathrm{INR}_1}{1+\lambda_{2p}\mathrm{INR}_1}\right)+\frac{1}{2}\log\left(1+\frac{\lambda_{2p}\mathrm{SNR}_2}{1+\lambda_{1p}\mathrm{INR}_2}\right), \tag{7.14c}$$

$$R_1+R_2 \leq \frac{1}{2}\log\left(\frac{1+(1-\lambda_{2e})\mathrm{SNR}_2+(1-\lambda_{1e})\mathrm{INR}_2}{1+\lambda_{1p}\mathrm{INR}_2}\right)+\frac{1}{2}\log\left(1+\frac{\lambda_{1p}\mathrm{SNR}_1}{1+\lambda_{2p}\mathrm{INR}_1}\right), \tag{7.14d}$$

$$\begin{aligned} R_1+R_2 \leq & \frac{1}{2}\log\left(\frac{1+\lambda_{1p}\mathrm{SNR}_1+(1-\lambda_{2e})\mathrm{INR}_1}{1+\lambda_{2p}\mathrm{INR}_1}\right) \\ & +\frac{1}{2}\log\left(\frac{1+\lambda_{2p}\mathrm{SNR}_2+(1-\lambda_{1e})\mathrm{INR}_2}{1+\lambda_{1p}\mathrm{INR}_2}\right), \end{aligned} \tag{7.14e}$$

$$\begin{aligned} 2R_1+R_2 \leq & \frac{1}{2}\log\left(\frac{1+(1-\lambda_{1e})\mathrm{SNR}_1+(1-\lambda_{2e})\mathrm{INR}_1}{1+\lambda_{2p}\mathrm{INR}_1}\right) \\ & +\frac{1}{2}\log\left(\frac{1+\lambda_{2p}\mathrm{SNR}_2+(1-\lambda_{1e})\mathrm{INR}_2}{1+\lambda_{1p}\mathrm{INR}_2}\right) \\ & +\frac{1}{2}\log\left(1+\frac{\lambda_{1p}\mathrm{SNR}_1}{1+\lambda_{2p}\mathrm{INR}_1}\right) \end{aligned} \tag{7.14f}$$

$$\begin{aligned} R_1+2R_2 \leq & \frac{1}{2}\log\left(\frac{1+(1-\lambda_{2e})\mathrm{SNR}_2+(1-\lambda_{1e})\mathrm{INR}_2}{1+\lambda_{1p}\mathrm{INR}_2}\right) \\ & +\frac{1}{2}\log\left(\frac{1+\lambda_{1p}\mathrm{SNR}_1+(1-\lambda_{2e})\mathrm{INR}_1}{1+\lambda_{2p}\mathrm{INR}_1}\right) \\ & +\frac{1}{2}\log\left(1+\frac{\lambda_{2p}\mathrm{SNR}_2}{1+\lambda_{1p}\mathrm{INR}_2}\right), \end{aligned} \tag{7.14g}$$

$$B \leq \sigma_3^2\left(1+\mathrm{SNR}_{31}+\mathrm{SNR}_{32}+2\sqrt{\mathrm{SNR}_{31}\mathrm{SNR}_{32}}\sqrt{\lambda_{1e}\lambda_{2e}}\right), \tag{7.14h}$$

for some $(\lambda_{ip}, \lambda_{ie}) \in [0,1]^2$ such that $\lambda_{ip}+\lambda_{ie} \leq 1$, for all $i \in \{1,2\}$.

The proof of Theorem 9 is presented in [96]. Essentially, the achievability scheme used to obtain the region $\underline{\mathcal{E}}$ described in Theorem 9 is built upon random coding arguments using four key ingredients: (a) superposition coding [36]; (b) rate-splitting [34]; (c) common randomness [2, 69]; and (d) power-spliting [17].

The codebook of transmitter i, with $i \in \{1,2\}$, is generated by superposing three different code layers. The first code layer is a sub-codebook generated for the exclusive purpose of energy transmission. Note that this code layer can be chosen to

be the same for both transmitters. The key point is to ensure that codewords in the first code layer of transmitter 1 and 2 exhibit a correlation factor equal to one. For each codeword in the first layer, a new sub-codebook is generated. This set of sub-codebooks is referred to as the second code layer and it is designed to broadcast information to both receivers. However, even if it is not the primary goal, these codewords naturally carry energy to the EH, as well. Finally, for each codeword in the second layer, a new sub-codebook is generated. This set of sub-codebooks is referred to as the third layer of the codebook and it is designed for the exclusive purpose of transmitting information to receiver i. Nonetheless, as for the codewords in the first and second layer, these codewords also carry energy to the EH.

In a nutshell, codewords from all layers of the codebook are capable of carrying energy to the EH but only those in the second and third layer carry both information and energy. The size of the first layer of the codebook determines the number of different codewords that can be used to transmit energy to the EH. However, the size of this layer does not have any impact on the information or energy rate of the transmitters. Alternatively, the size of the second and third layer determine the information rate of the corresponding transmitter. The exact size of each of these layers lies upon a decoding error probability analysis that is presented in [96].

Rate splitting is the ingredient that allows the convenient exploitation of the codebooks with the form described above. Note that at the beginning of each transmission, transmitter i possesses two indices to transmit: common random index Ω and message index W_i. The message index W_i is divided into two subindices: $W_{i,C}$ and $W_{i,P}$. The index Ω is used to choose a codeword in the first layer and the indices $W_{i,C}$ and $W_{i,P}$ are used to choose a codeword in the second and third layer, respectively. This justifies the name of the technique as the information rate of transmitter i is *split* into two streams: *common* and *private*. Note that the second layers contain codewords that are decoded at both receivers (common messages) whereas the third layers contain codewords that are decoded only at the intended receiver (private messages). Intuitively, the codewords from the second layer of the code of transmitter i can be decoded at receiver j, with $j \in \{1,2\} \setminus \{i\}$, which allows some interference cancellation. On the other hand, the codewords from the third layer of transmitter i are treated as interference at receiver j. The interference produced by the codewords from the first layer on both transmitters can be fully eliminated, as by assumption, the index Ω is known by all transmitters and receivers.

Finally, to prove the existence of at least one code that achieves the rates described by Theorem 9, it suffices to average the information and energy rates that are achievable by all possible codebooks that can be generated using the structure described above. If the average of such rates satisfies the inequalities in Theorem 9, then for each rate tuple in $\underline{\mathcal{E}}$, there exists at least one code that achieves such a rate tuple. Assume for instance that the codewords of the first, second and third layers of transmitter i are N-length sequences of realizations of the following three independent random variables respectively: $V \sim \mathcal{N}(0,1)$; $U_i \sim \mathcal{N}(0,\lambda_{ic})$; and $S_i \sim \mathcal{N}(0,\lambda_{ip})$, where $\lambda_{ic} + \lambda_{ip} + \lambda_{ie} \leqslant 1$. Let also the channel input of transmitter i, during any

given channel use be:

$$X_i = \sqrt{P_i}S_i + \sqrt{P_i}U_i + \sqrt{\lambda_{ie}P_i}V. \tag{7.15}$$

At channel use n and given any possible codebook with the structure described above, the n-th channel input of transmitter i is a weighted sum of the n-th symbols of the corresponding codewords in the three layers of such codebook. The weighting is referred to as *power splitting* to highlight that a fraction λ_{ie} of the total average power P_i is used to transmit a codeword whose role is to exclusively transmit energy to the EH. The information-carrying component, which is the sum of the codewords from the second and third layers of the codebook, is transmitted using an average power $\lambda_{ic} + \lambda_{ip} \leqslant 1 - \lambda_{ie}$.

The role of the first layer of the codebook becomes clearer after the following remarks.

Remark 1: *When $\lambda_{1e} = \lambda_{2e} = 1$, the left-hand sides of inequalities* (7.14a)-(7.14g) *become zero, whereas the left-hand side of inequality* (7.14h) *is maximized. That is, a zero information rate is achieved at the same time that the highest energy rate $B_{\max}$ in* (7.11) *is achieved. This is essentially because the transmitted codewords belong to the first layers of the codebooks of both transmitters. Note also that the choice is made such that the correlation coefficient of both channel inputs is one.*

Remark 2: *When $\lambda_{1e} = \lambda_{2e} = 0$, the codewords of the first layers of the code are not transmitted. From this perspective, both channel input signal are independent of each other and thus, the energy rate is at most $\sigma_3^2\left(1 + \mathrm{SNR}_{31} + \mathrm{SNR}_{32}\right)$ energy units per channel use.*

Note that Remark 1 and Remark 2 highlight the fact that the no-information component is needed to transmit energy beyond the energy rate $\sigma_3^2\left(1 + \mathrm{SNR}_{31} + \mathrm{SNR}_{32}\right)$. Thanks to this no-information component, the signals of both transmitters can be correlated, which results into higher energy rates than those achieved by independent signals.

Remark 3: *A consequence of Remark* 2 *is that for all rate tuples $(R_1, R_2, B) \in \underline{\mathcal{E}}$, with*

$$B \leqslant \sigma_3^2\left(1 + \mathrm{SNR}_{31} + \mathrm{SNR}_{32}\right),$$

it follows that the rate pairs (R_1, R_2) form respectively the achievable region of the information capacity region described in [34]. Alternatively, for all rate tuples $(R_1, R_2, B) \in \underline{\mathcal{E}}$, with $B > \sigma_3^2\left(1 + \mathrm{SNR}_{31} + \mathrm{SNR}_{32}\right)$, it follows that the rate pairs (R_1, R_2) form a proper set of the achievable region described in [34]. This observation implies that a trade-off between energy and information rates is observed when $B > \sigma_3^2\left(1 + \mathrm{SNR}_{31} + \mathrm{SNR}_{32}\right)$. This is compliant with previous observations in the Gaussian multiple access channel in Chapter 6.

Remark 4: *Note that the first layer of the code does not contribute to the information rate. Hence, there is no constraint on reducing the size of the first layer to*

one codeword. That is, the assumption of common randomness can be soften to the knowledge of a sufficiently large codeword whose purpose is exclusively transmitting energy to the EH, e.g., a pseudo-random sequence.

In Section 7.4, Remark 1 - Remark 3 are highlighted in particular numerical examples.

A Converse Information-Energy Region

The following Theorem introduces an information-energy converse region.

Theorem 10. *The information-energy capacity region $\mathcal{E}$ is contained into the set $\overline{\mathcal{E}} \in \mathbb{R}_+^3$, which contains all rate tuples (R_1, R_2, B) that satisfy:*

$$R_1 \leq \frac{1}{2}\log(1+\beta_1 \mathrm{SNR}_1), \tag{7.16a}$$

$$R_2 \leq \frac{1}{2}\log(1+\beta_2 \mathrm{SNR}_2), \tag{7.16b}$$

$$R_1 + R_2 \leq \frac{1}{2}\log(1+\beta_1 \mathrm{SNR}_1 + \beta_2 \mathrm{INR}_1) + \frac{1}{2}\log\left(1+\frac{\beta_2 \mathrm{SNR}_2}{1+\beta_2 \mathrm{INR}_1}\right), \tag{7.16c}$$

$$R_1 + R_2 \leq \frac{1}{2}\log(1+\beta_2 \mathrm{SNR}_2 + \beta_1 \mathrm{INR}_2) + \frac{1}{2}\log\left(1+\frac{\beta_1 \mathrm{SNR}_1}{1+\beta_1 \mathrm{INR}_2}\right), \tag{7.16d}$$

$$\begin{aligned} R_1 + R_2 \leq & \frac{1}{2}\log\left(1+\frac{\beta_1 \mathrm{SNR}_1 + \beta_2 \mathrm{INR}_1 + \beta_1\beta_2 \mathrm{INR}_1 \mathrm{INR}_2}{1+\beta_1 \mathrm{INR}_2}\right) \\ & + \frac{1}{2}\log\left(1+\frac{\beta_2 \mathrm{SNR}_2 + \beta_1 \mathrm{INR}_2 + \beta_1\beta_2 \mathrm{INR}_1 \mathrm{INR}_2}{1+\beta_2 \mathrm{INR}_1}\right), \end{aligned} \tag{7.16e}$$

$$\begin{aligned} 2R_1 + R_2 \leq & \frac{1}{2}\log\left(1+\frac{\beta_1 \mathrm{SNR}_1}{1+\beta_1 \mathrm{INR}_2}\right) + \frac{1}{2}\log(1+\beta_1 \mathrm{SNR}_1 + \beta_2 \mathrm{INR}_1) \\ & + \frac{1}{2}\log\left(1+\frac{\beta_2 \mathrm{SNR}_2 + \beta_1 \mathrm{INR}_2 + \beta_1\beta_2 \mathrm{INR}_1 \mathrm{INR}_2}{1+\beta_2 \mathrm{INR}_1}\right), \end{aligned} \tag{7.16f}$$

$$\begin{aligned} R_1 + 2R_2 \leq & \frac{1}{2}\log\left(1+\frac{\beta_2 \mathrm{SNR}_2}{1+\beta_2 \mathrm{INR}_1}\right) + \frac{1}{2}\log(1+\beta_2 \mathrm{SNR}_2 + \beta_1 \mathrm{INR}_2) \\ & + \frac{1}{2}\log\left(1+\frac{\beta_1 \mathrm{SNR}_1 + \beta_2 \mathrm{INR}_1 + \beta_1\beta_2 \mathrm{INR}_1 \mathrm{INR}_2}{1+\beta_1 \mathrm{INR}_2}\right), \end{aligned} \tag{7.16g}$$

$$B \leq \sigma_3^2\left(1+\mathrm{SNR}_{31}+\mathrm{SNR}_{32}+2\sqrt{\mathrm{SNR}_{31}\mathrm{SNR}_{32}}\sqrt{(1-\beta_1)(1-\beta_2)}\right), \tag{7.16h}$$

for some $(\beta_1, \beta_2) \in [0,1]^2$.

From the information transmission perspective, the proof of the upper bounds on the information rates is identical to the proof presented in [97]. That is, (7.16a) and (7.16b) are simple cut-set bounds. The bounds (7.16c) - (7.16g) are obtained considering genie-aided channels and Fano's inequality [74]. For completness, the proof of the upper-bounds (7.16a)-(7.16g) is presented in [96]. The upper-bound on the energy transmission rate (7.16h) is new.

An Approximation to the Information-Energy Capacity Region

Using the inner region $\underline{\mathcal{E}}$ and the outer region $\overline{\mathcal{E}}$, described respectively by Theorem 9 and Theorem 10, the information-energy capacity region $\mathcal{E}$ can be approximated in the sense of Definition 3. The following theorem presents this result.

Theorem 11. *Let $\underline{\mathcal{E}} \subset \mathbb{R}_+^3$ and $\overline{\mathcal{E}} \subset \mathbb{R}_+^3$ be the sets of tuples (R_1, R_2, B) described by Theorem 9 and Theorem 10, respectively. Then,*

$$\underline{\mathcal{E}} \subset \mathcal{E} \subset \overline{\mathcal{E}}, \tag{7.17}$$

and for all $(R_1, R_2, B) \in \overline{\mathcal{E}}$ it follows that $\left((R_1-1/2)^+, (R_2-1/2)^+, \left(B-\frac{B_{\max}}{2}\right)^+\right) \in \underline{\mathcal{E}}$.

The proof of Theorem 11 is presented in [96]. It is essentially algebraic and thus, no further comment is made about this proof. Note that the approximation in Theorem 11 is not an approximation within a constant gap. This is because the gap in the energy component is at most $\frac{B_{\max}}{2}$ energy units per channel use, with $B_{\max}$ in (7.11). Thus, it depends on σ_3^2, SNR_{31} and SNR_{32}. A constant gap approximation is obtained only when considering the set of tuples formed by the information rates R_1 and R_2 in bits per channel use and the normalized rate $\frac{B}{B_{\max}}$. That is, the set $\mathcal{E}' = \left\{\left(R_1, R_2, \frac{B}{B_{\max}}\right) : (R_1, R_2, B) \in \mathcal{E}\right\}$ is approximated to within $\frac{1}{2}$ units by the sets

$$\underline{\mathcal{E}}' = \left\{\left(R_1, R_2, \frac{B}{B_{\max}}\right) : (R_1, R_2, B) \in \underline{\mathcal{E}}\right\} \text{ and} \tag{7.18}$$

$$\overline{\mathcal{E}}' = \left\{\left(R_1, R_2, \frac{B}{B_{\max}}\right) : (R_1, R_2, B) \in \overline{\mathcal{E}}\right\}. \tag{7.19}$$

That is, $\underline{\mathcal{E}}' \subset \mathcal{E}' \subset \overline{\mathcal{E}}'$, and for all $(R_1, R_2, b) \in \overline{\mathcal{E}}'$, it follows that $\Big((R_1-1/2)^+, (R_2-1/2)^+, (b-1/2)^+\Big) \in \underline{\mathcal{E}}'$.

7.2.2 Case with Feedback

The information-energy capacity region of the GIC with an EH and with feedback, denoted by $\mathcal{E}^{\mathrm{F}}$, is approximated by the regions $\underline{\mathcal{E}}^{\mathrm{F}} \subset \mathbb{R}_+^3$, which represents an information-energy achievable region (Theorem 12); and $\overline{\mathcal{E}}^{\mathrm{F}} \subset \mathbb{R}_+^3$, which represents an information-energy converse region (Theorem 13). Regions $\underline{\mathcal{E}}^{\mathrm{F}}$ and $\overline{\mathcal{E}}^{\mathrm{F}}$ satisfy $\underline{\mathcal{E}}^{\mathrm{F}} \subseteq \mathcal{E}^{\mathrm{F}} \subseteq \overline{\mathcal{E}}^{\mathrm{F}}$ and approximate the information-energy region $\mathcal{E}$ to within a given gap (Definition 3).

An Achievable Region

The following theorem introduces an achievable information-energy region.

Theorem 12. *The information-energy capacity region $\mathcal{E}^{\mathrm{F}}$ contains the set $\underline{\mathcal{E}}^{\mathrm{F}} \subseteq \mathbb{R}_+^3$ of all rate tuples (R_1, R_2, B) that satisfy:*

$$R_1 \leq \frac{1}{2}\log\left(\frac{1+(1-\lambda_{1e})\mathrm{SNR}_1+(1-\lambda_{2e})\mathrm{INR}_1+2\rho\sqrt{\mathrm{SNR}_1\mathrm{INR}_1}}{1+\lambda_{2p}\mathrm{INR}_1}\right), \tag{7.20a}$$

$$R_1 \leq \frac{1}{2}\log\left(\frac{1+(1-(\rho+\lambda_{1e}))\mathrm{INR}_2}{1+\lambda_{1p}\mathrm{INR}_2}\right) \tag{7.20b}$$

$$+\frac{1}{2}\log\left(\frac{1+\lambda_{1p}\mathrm{SNR}_1+\lambda_{2p}\mathrm{INR}_1}{1+\lambda_{2p}\mathrm{INR}_1}\right), \tag{7.20c}$$

$$R_2 \leq \frac{1}{2}\log\left(\frac{1+(1-\lambda_{2e})\mathrm{SNR}_2+(1-\lambda_{1e})\mathrm{INR}_2+2\rho\sqrt{\mathrm{SNR}_2\mathrm{INR}_2}}{1+\lambda_{1p}\mathrm{INR}_2}\right), \tag{7.20d}$$

$$R_2 \leq \frac{1}{2}\log\left(\frac{1+(1-(\rho+\lambda_{2e}))\mathrm{INR}_1}{1+\lambda_{2p}\mathrm{INR}_1}\right) \tag{7.20e}$$

$$+\frac{1}{2}\log\left(\frac{1+\lambda_{2p}\mathrm{SNR}_1+\lambda_{1p}\mathrm{INR}_1}{1+\lambda_{1p}\mathrm{INR}_1}\right), \tag{7.20f}$$

$$R_1+R_2 \leq \frac{1}{2}\log\left(\frac{1+\lambda_{1p}\mathrm{SNR}_1+\lambda_{2p}\mathrm{INR}_1}{1+\lambda_{2p}\mathrm{INR}_1}\right)$$

$$+\frac{1}{2}\log\left(\frac{1+(1-\lambda_{2e})\mathrm{SNR}_2+(1-\lambda_{1e})\mathrm{INR}_2+2\rho\sqrt{\mathrm{SNR}_2\mathrm{INR}_2}}{1+\lambda_{1p}\mathrm{INR}_2}\right), \tag{7.20g}$$

$$R_1+R_2 \leq \frac{1}{2}\log\left(\frac{1+\lambda_{2p}\mathrm{SNR}_1+\lambda_{1p}\mathrm{INR}_1}{1+\lambda_{1p}\mathrm{INR}_1}\right)$$

$$+\frac{1}{2}\log\left(\frac{1+(1-\lambda_{1e})\mathrm{SNR}_1+(1-\lambda_{2e})\mathrm{INR}_1+2\rho\sqrt{\mathrm{SNR}_1\mathrm{INR}_1}}{1+\lambda_{2p}\mathrm{INR}_1}\right), \tag{7.20h}$$

$$B \leq \sigma_3^2\left(1+\mathrm{SNR}_{31}+\mathrm{SNR}_{32}+2\sqrt{\mathrm{SNR}_{31}\mathrm{SNR}_{32}}(\rho+\sqrt{\lambda_{1e}\lambda_{2e}})\right), \tag{7.20i}$$

for some $(\rho, \lambda_{ip}, \lambda_{ie}) \in [0,1]^3$ such that $\rho+\lambda_{ip}+\lambda_{ie} \leq 1$, for all $i \in \{1,2\}$.

The proof of Theorem 12 is based on random coding arguments using rate-splitting [34, 37]; block Markov superposition coding [38, 98]; backward decoding [48, 49]; and power splitting [17].

The codebook of transmitter i, with $i \in \{1,2\}$, is generated by superposing four different sub-codebooks. This contrasts with the three-layer codebook used in the case without feedback. However, both codebooks share profound similarities. The first layer in the case with and without feedback are identical and play the same role. The second layer of the codebook with feedback is obtained by the union of the second layers of both transmitters in the case without feedback. The third and fourth layers of the codebook with feedback are identical to the second and third layers of the codebook without feedback. The roles of these two layers are identical in the case with and without feedback.

The convenient exploitation of this four-layer codebook is possible thanks to a rate splitting argument similar to the one used in the case without feedback. Assume

that T blocks are transmitted and each block is a sequence of N channel uses. In each block a message index is transmitted. The message index of transmitter i is split into a common and a private component with message indices $W_{ic}^{(t)}$ and $W_{ip}^{(t)}$, where $t \in \{1, 2, \ldots, T\}$ is an index that denotes the block. At the beginning of block t, each transmitter possesses five indices: the random index $\Omega^{(t)}$; the common and private message indices $W_{ic}^{(t)}$ and $W_{ip}^{(t)}$; and the common messages $W_{1c}^{(t-1)}$ and $W_{2c}^{(t-1)}$. Transmitter i obtains the message index $W_{jc}^{(t-1)}$ of transmitter j, with $j \in \{1, 2\} \setminus \{i\}$, via feedback at the end of block $t-1$. For the first block $t = 1$, the previous common message indices are chosen arbitrarily as $W_{1c}^{(0)} = W_{2c}^{(0)} = 1$ and are assumed to be known by all transmitters and receivers. Similarly, the last common message indices are chosen arbitrarily as $W_{1c}^{(T)} = W_{2c}^{(T)} = 1$ and are also assumed to be known by all transmitters and receivers. Under this assumption, the random index $\Omega^{(t)}$ is used to choose a codeword from the first layer; the pair $(W_{1c}^{(t-1)}, W_{2c}^{(t-1)})$ are jointly used to choose a common codeword from the second layer. Note that the second layer of transmitter 1 is identical to the second layer of transmitter 2 by construction of the code. Moreover, thanks to feedback both transmitters are able to choose the same codeword from their second layers at each block t. The message indices $W_{ic}^{(t)}$ and $W_{ip}^{(t)}$ are used at transmitter i to choose codewords from the third and fourth layers respectively.

The channel input of transmitter i at channel use n is, as in the case without feedback, a weighted sum of the n-th symbols of the corresponding codewords in each of the four layers. A power splitting argument is also used as in the case without feedback.

At the receivers backward decoding is used. More specifically, given that the last common indices $W_{1c}^{(T)}$ and $W_{2c}^{(T)}$ are known at the transmitters, receiver i is capable of decoding $W_{1c}^{(T-1)}$ and $W_{2c}^{(T-1)}$ and $W_{ip}^{(T)}$ at the first decoding stage by using joint-typicality arguments. At the second decoding stage, $W_{1c}^{(T-1)}$ and $W_{2c}^{(T-1)}$ are used to decode $W_{1c}^{(T-2)}$, $W_{2c}^{(T-2)}$ and $W_{ip}^{(T-1)}$. The decoding goes on until decoding stage T at which only $W_{ip}^{(1)}$ is decoded as $W_{1c}^{(0)}$ and $W_{2c}^{(0)}$ are both known.

Note that Remark 1 - Remark 3 also hold for the case with feedback taking into account the differences on the structure of the codes with and without feedback. The role of the second layer of the codebook with feedback becomes clearer after the following remark.

Remark 5**:** The second layer of the codebooks of both transmitters are identical and thus, given the common message indices $W_{1c}^{(t-1)}$ and $W_{2c}^{(t-1)}$ at the beginning of block t, both transmitters are able to choose the same codeword to generate their corresponding channel inputs. This creates a correlation between the channel input symbols $X_{1,n}$ and $X_{2,n}$, for all $n \in \{1, 2, \ldots, N\}$, which is advantageous to increase the information transmission sum-rate and the energy transmission rate. This implies that feedback is beneficial for both information and energy transmission.

The additional correlation highlighted in Remark 5 is captured by the term ρ in (7.20). Note that the left hand side of inequalities (7.20g) and (7.20h) (infor-

mation transmission sum-rate) are monotonically increasing with ρ and so is the left hand side of (7.20i) (energy transmission rate). The benefits of feedback in SIET are studied in Section 7.4.

A Converse Region

The following theorem describes a converse region denoted by $\overline{\mathcal{E}}^{\mathrm{F}}$.

Theorem 13. *The information-energy capacity region $\mathcal{E}^{\mathrm{F}}$ is contained into the set $\overline{\mathcal{E}}^{\mathrm{F}} \in \mathbb{R}_+^3$ of all rate tuples (R_1, R_2, B) that satisfy:*

$$R_1 \leq \frac{1}{2}\log\left(1+\beta_1\mathrm{SNR}_1+\beta_2\mathrm{INR}_1+2\rho\sqrt{\beta_1\mathrm{SNR}_1\beta_2\mathrm{INR}_1}\right), \tag{7.21a}$$

$$R_1 \leq \frac{1}{2}\log\left(1+\frac{\beta_1(1-\rho^2)\mathrm{SNR}_1}{1+\beta_1(1-\rho^2)\mathrm{INR}_2}\right)+\frac{1}{2}\log\left(1+\beta_1(1-\rho^2)\mathrm{INR}_2\right), \tag{7.21b}$$

$$R_2 \leq \frac{1}{2}\log\left(1+\beta_2\mathrm{SNR}_2+\beta_1\mathrm{INR}_2+2\rho\sqrt{\beta_2\mathrm{SNR}_2\beta_1\mathrm{INR}_2}\right), \tag{7.21c}$$

$$R_2 \leq \frac{1}{2}\log\left(1+\frac{\beta_2(1-\rho^2)\mathrm{SNR}_2}{1+\beta_2(1-\rho^2)\mathrm{INR}_1}\right)+\frac{1}{2}\log\left(1+\beta_2(1-\rho^2)\mathrm{INR}_1\right), \tag{7.21d}$$

$$\begin{aligned} R_1+R_2 \leq & \frac{1}{2}\log\left(1+\frac{\beta_1(1-\rho^2)\mathrm{SNR}_1}{1+\beta_1(1-\rho^2)\mathrm{INR}_2}\right) \\ & +\frac{1}{2}\log\left(1+\beta_2\mathrm{SNR}_2+\beta_1\mathrm{INR}_2+2\rho\sqrt{\beta_2\mathrm{SNR}_2\beta_1\mathrm{INR}_2}\right), \end{aligned} \tag{7.21e}$$

$$\begin{aligned} R_1+R_2 \leq & \frac{1}{2}\log\left(1+\frac{\beta_2(1-\rho^2)\mathrm{SNR}_2}{1+\beta_2(1-\rho^2)\mathrm{INR}_1}\right) \\ & +\frac{1}{2}\log\left(1+\beta_1\mathrm{SNR}_1+\beta_2\mathrm{INR}_1+2\rho\sqrt{\beta_1\mathrm{SNR}_1\beta_2\mathrm{INR}_1}\right), \end{aligned} \tag{7.21f}$$

$$\begin{aligned} B \leq & \sigma_3^2\Big(1+\mathrm{SNR}_{31}+\mathrm{SNR}_{32}+2\sqrt{\mathrm{SNR}_{31}\mathrm{SNR}_{32}}(\rho\sqrt{\beta_1\beta_2} \\ & +\sqrt{(1-\beta_1)(1-\beta_2)})\Big), \end{aligned} \tag{7.21g}$$

for some $(\beta_1, \beta_2, \rho) \in [0,1]^3$.

The intuitions behind the proof of Theorem 13 are not different from those discussed in the case without feedback. Probably, the most important step on this proof is that codebooks are not assumed to be formed by codewords with zero mean. That is, the codeword considered in this proof might have a non-zero mean, as energy can also be carried in this way. The upper bounds on the information rates heavily rely on cut-set bounds [99], Fano's inequality [74] and genie aided models. The upper-bound on the energy transmission rate is an immediate consequence of Markov's inequality [100].

An Approximation to the Information-Energy Capacity Region

Using the inner region $\underline{\mathcal{E}}^{\mathrm{F}}$ and the outer region $\overline{\mathcal{E}}^{\mathrm{F}}$, described respectively by Theorem 12 and Theorem 13, the information-energy capacity region $\mathcal{E}^{\mathrm{F}}$ can be approx-

imated in the sense of Definition 3.

Theorem 14 (Approximation of $\mathcal{E}^{\mathrm{F}}$)**.** Let $\underline{\mathcal{E}}^{\mathrm{F}} \subset \mathbb{R}_+^3$ and $\overline{\mathcal{E}}^{\mathrm{F}} \subset \mathbb{R}_+^3$ be the sets of tuples (R_1, R_2, B) described by Theorem 12 and Theorem 13, respectively. Then, $\underline{\mathcal{E}}^{\mathrm{F}} \subset \mathcal{E}^{\mathrm{F}} \subset \overline{\mathcal{E}}^{\mathrm{F}}$, and for all $(R_1, R_2, B) \in \overline{\mathcal{E}}^{\mathrm{F}}$ it follows that $\left((R_1 - 1)^+, (R_2 - 1)^+, \left(B - \frac{B_{\max}}{2}\right)^+\right) \in \underline{\mathcal{E}}^{\mathrm{F}}$.

The proof of Theorem 14 is presented in [96]. Note that a constant gap approximation can be obtained by normalizing the energy transmission rate as suggested in the case without feedback.

7.3 Energy Transmission Enhancement with Feedback

Consider the following sets of energy rates: $\underline{\mathcal{B}} = \{b \in \mathbb{R}_+ : (R_1, R_2, b) \in \underline{\mathcal{E}}\}$, $\overline{\mathcal{B}} = \{b \in \mathbb{R}_+ : (R_1, R_2, b) \in \overline{\mathcal{E}}\}$, $\underline{\mathcal{B}}_{\mathrm{F}} = \{b \in \mathbb{R}_+ : (R_1, R_2, b) \in \underline{\mathcal{E}}_{\mathrm{F}}\}$, and $\overline{\mathcal{B}}_{\mathrm{F}} = \{b \in \mathbb{R}_+ : (R_1, R_2, b) \in \overline{\mathcal{E}}_{\mathrm{F}}\}$. The maximum improvement that can be achieved on the energy rate due to feedback can be shown to be at most a factor of two. The following proposition shows this by providing upper bounds on the ratios $\frac{\sup \underline{\mathcal{B}}_{\mathrm{F}}}{\sup \underline{\mathcal{B}}}$ and $\frac{\sup \overline{\mathcal{B}}_{\mathrm{F}}}{\sup \overline{\mathcal{B}}}$.

Proposition 5 (Rate improvement with Feedback)**.** *The energy rate achievable in the two-user G-IC with perfect channel-output feedback can be twice the energy rate achievable in the two-user G-IC without feedback. That is,*

$$1 < \frac{\sup \underline{\mathcal{B}}_{\mathrm{F}}}{\sup \underline{\mathcal{B}}} \leqslant 2. \tag{7.22}$$

Any improvement beyond a factor of two is not feasible. That is,

$$1 < \frac{\sup \overline{\mathcal{B}}_{\mathrm{F}}}{\sup \overline{\mathcal{B}}} \leqslant 2. \tag{7.23}$$

The proof of Proposition 5 is presented in [96]. The main conclusion from Proposition 5 is that channel-output feedback can at most double the energy rate in the G-IC. Note that a similar observation is made in the case of the GMAC in Chapter 6.

In the next section, some numerical examples are presented.

7.4 Examples

Consider the two-user G-ICs with and without channel-output feedback depicted in Figure 7.1(a) and Figure 7.1(b) with parameters $\mathrm{SNR}_1 = \mathrm{SNR}_2 = 20$ dB, $\mathrm{INR}_1 =$

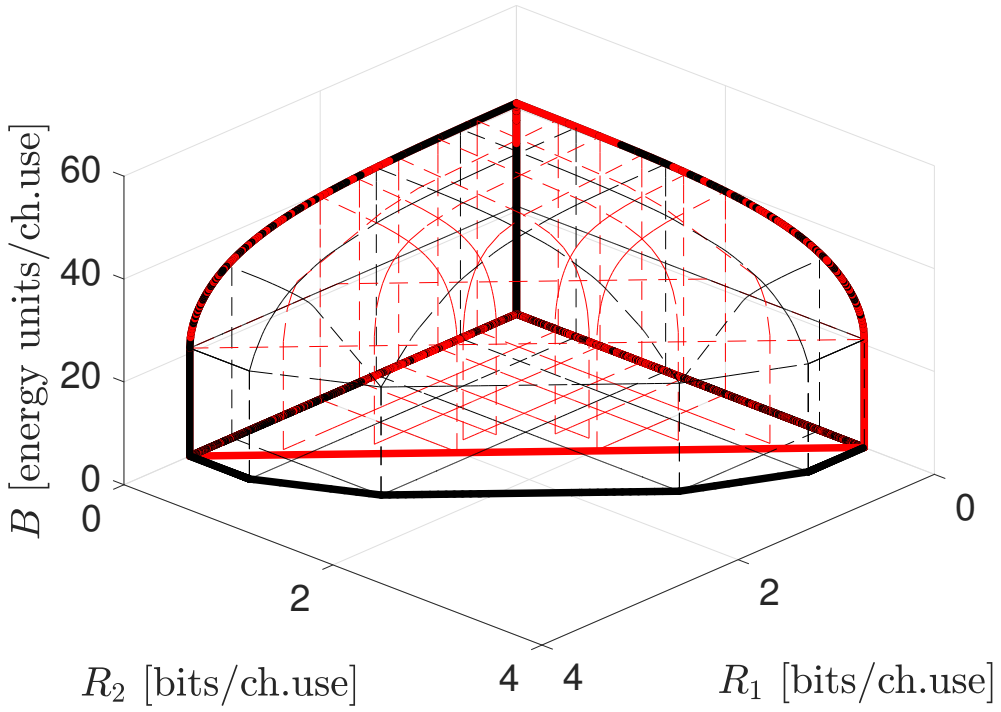

Figure 7.2: 3-D superposition of $\underline{\mathcal{E}}$ and $\overline{\mathcal{E}}$, with parameters $\mathrm{SNR}_1 = \mathrm{SNR}_2 = 20$ dB, $\mathrm{INR}_1 = \mathrm{INR}_2 = \mathrm{SNR}_{31} = \mathrm{SNR}_{32} = 10$ dB, and $\sigma_3^2 = 1$.

$\mathrm{INR}_2 = \mathrm{SNR}_{31} = \mathrm{SNR}_{32} = 10$ dB, and $\sigma_3^2 = 1$. The corresponding achievable region $\underline{\mathcal{E}}$ and converse region $\overline{\mathcal{E}}$ are shown in Figure 7.2. In the case with feedback, the corresponding achievable region $\underline{\mathcal{E}}^{\mathrm{F}}$ and converse region $\overline{\mathcal{E}}^{\mathrm{F}}$ are shown in Figure 7.3. Note the strict inclusions $\underline{\mathcal{E}} \subset \overline{\mathcal{E}}$ and $\underline{\mathcal{E}}^{\mathrm{F}} \subset \overline{\mathcal{E}}^{\mathrm{F}}$ (Definition 3). Note also that for all $B \leqslant 21$ energy units, the set of triplets $(R_1, R_2, B) \in \underline{\mathcal{E}}^{\mathrm{F}}$ and the set of triplets $(R_1, R_2, B) \in \overline{\mathcal{E}}^{\mathrm{F}}$ are prisms whose bases correspond to the inner and outer regions approximating the information capacity region. For all $B > 21$, the trade-off between information transmission rates and the energy transmission rate becomes evident as both regions $\underline{\mathcal{E}}^{\mathrm{F}}$ and $\overline{\mathcal{E}}^{\mathrm{F}}$ monotonically shrink when B increases (Remark 3). The same observation can be made for the case without feedback. Figure 7.4 shows the pairs (R_2, B) that are in the sets $\{(R_2, B) \in \mathbb{R}_+^2 : (r_1, R_2, B) \in \overline{\mathcal{E}}\}$ (solid line) and $\{(R_2, B) \in \mathbb{R}_+^2 : (r_1, R_2, B) \in \overline{\mathcal{E}}^{\mathrm{F}}\}$ (dashed line), with $r_1 = 0$ and $r_1 = 3$. Note that thanks to feedback, the information rate R_2 can be increased by one bit per channel use while keeping both the information rate R_1 and the energy rate B invariant.

Figure 7.5 shows the set of pairs (R_1, R_2) that are in the sets $\{(R_1, R_2) \in \mathbb{R}_+^2 : (R_1, R_2, b) \in \overline{\mathcal{E}}\}$ (solid line) and $\{(R_1, R_2) \in \mathbb{R}_+^2 : (R_1, R_2, b) \in \overline{\mathcal{E}}^{\mathrm{F}}\}$ (dashed line), with $b = 21$ and $b = 35$. Note that thanks to feedback, both the information rates R_1 and R_2 can be increased more than half a bit per channel use while keeping the energy rate B constant.

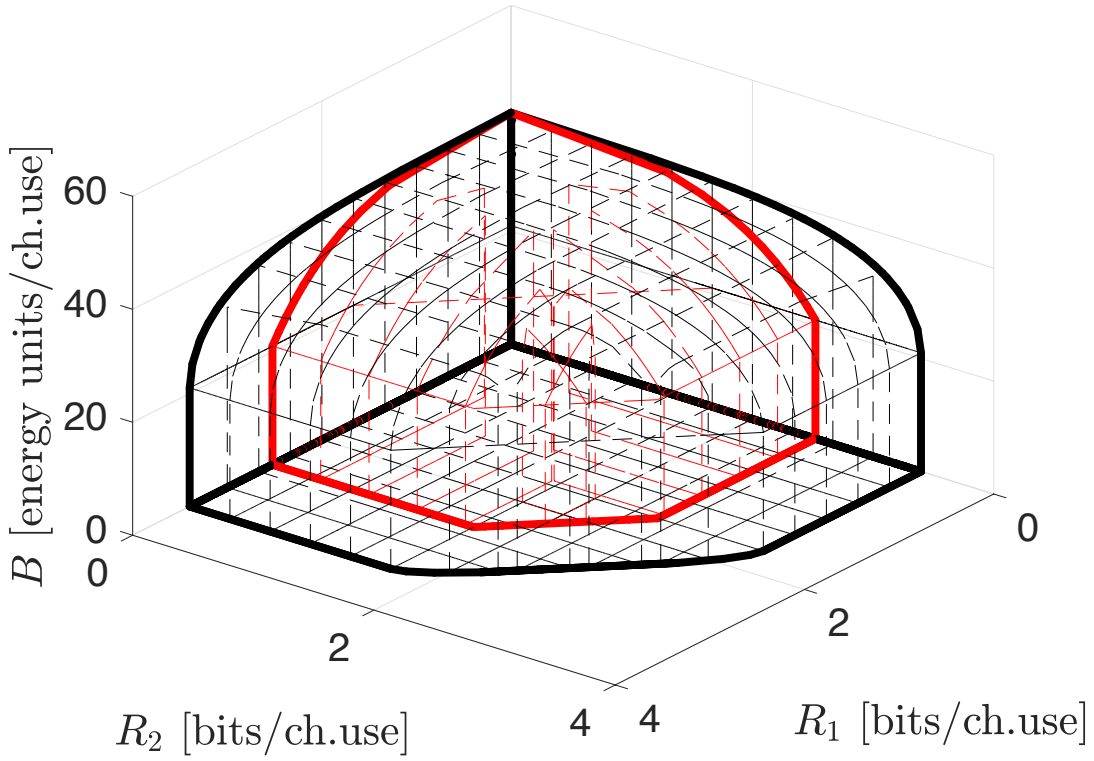

Figure 7.3: 3-D superposition of $\underline{\mathcal{E}}^{\mathrm{F}}$ and $\overline{\mathcal{E}}^{\mathrm{F}}$, with parameters $\mathrm{SNR}_1 = \mathrm{SNR}_2 = 20$ dB, $\mathrm{INR}_1 = \mathrm{INR}_2 = \mathrm{SNR}_{31} = \mathrm{SNR}_{32} = 10$ dB and $\sigma_3^2 = 1$.

Figure 7.6 shows the ratio $\frac{\sup \overline{\mathcal{B}}_{\mathrm{F}}}{\sup \overline{\mathcal{B}}}$ for different ratios of SNR at the EH, i.e., $\mathrm{SNR}_{31} = \mathrm{SNR}_{32} = \mathrm{SNR}$; $\frac{\mathrm{SNR}_{31}}{2} = \mathrm{SNR}_{32} = \mathrm{SNR}$; and $\frac{\mathrm{SNR}_{31}}{10} = \mathrm{SNR}_{32} = \mathrm{SNR}$, respectively. Note that the upper bound in Proposition 5 is tight in the case of the symmetric case.

7.5 Conclusions and Further Work

In this chapter, the information-energy capacity regions of the two-user Gaussian interference channel with and without perfect channel output feedback have been approximated by two regions, i.e., an achievable region and a converse region. When the energy transmission rate is normalized by the maximum energy rate, the approximation of these information-energy capacity regions is within a constant gap. In the proof of achievability, the key idea is the use of power-splitting between two signal components: an information-carrying component and a no-information component. Random coding arguments are used for the case of the information-carrying component, whereas a deterministic sequence known by all transmitters and receivers is used for the no-information component. The proof of the converse of the information rates follows along the same lines of the case in which only information is transmitted. The difference stems from lifting the constraints on the mean of the channel input signals. The proof of converse of the energy rate uses Markov's con-

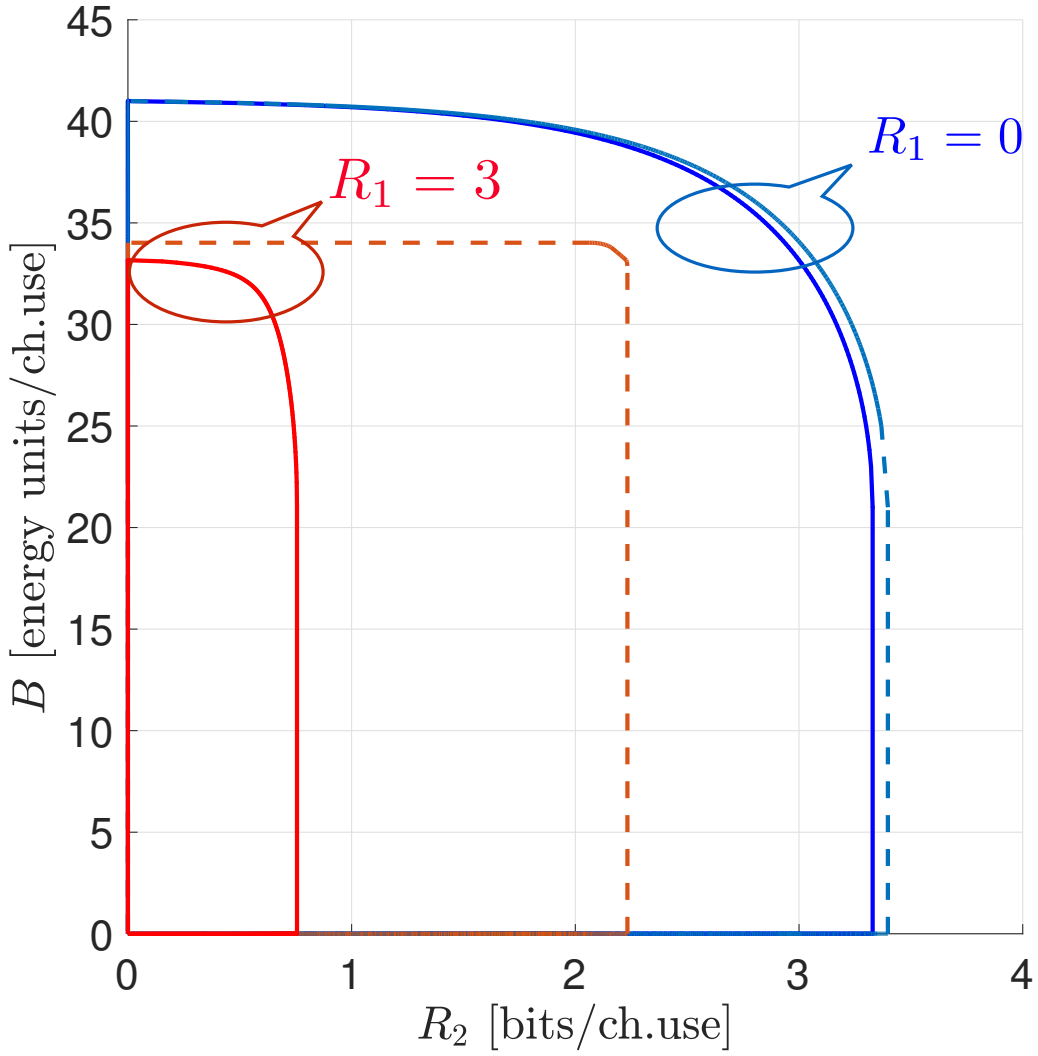

Figure 7.4: Convex hull of pairs (R_2, B) that are in the sets $\{(R_2, B) \in \mathbb{R}_+^2 : (r_1, R_2, B) \in \overline{\mathcal{E}}\}$ (solid line) and $\{(R_2, B) \in \mathbb{R}_+^2 : (r_1, R_2, B) \in \overline{\mathcal{E}}^{\mathrm{F}}\}$ (dashed line), with $r_1 \in \{0, 3\}$. Parameters $\mathrm{SNR}_1 = \mathrm{SNR}_2 = 20$ dB, $\mathrm{INR}_1 = \mathrm{INR}_2 = \mathrm{SNR}_{31} = \mathrm{SNR}_{32} = 10$ dB, and $\sigma_3^2 = 1$.

centration inequality.

The results presented in this chapter are a first step in the study of the fundamental limits of simultaneous information and energy transmission, nonetheless many questions are left open. On the one hand, there exits sufficient evidence that the use of multiple antennas at either the transmitters or the receivers enhances the energy rate [101]. However, very little is known from the perspectives of fundamental limits. On the other hand, an interesting question is about the degradation of the energy rates due to noisy feedback or rate-limited feedback. Similarly, another interesting question is about the benefits of other topologies of feedback, i.e., feedback from the receivers to both transmitters.

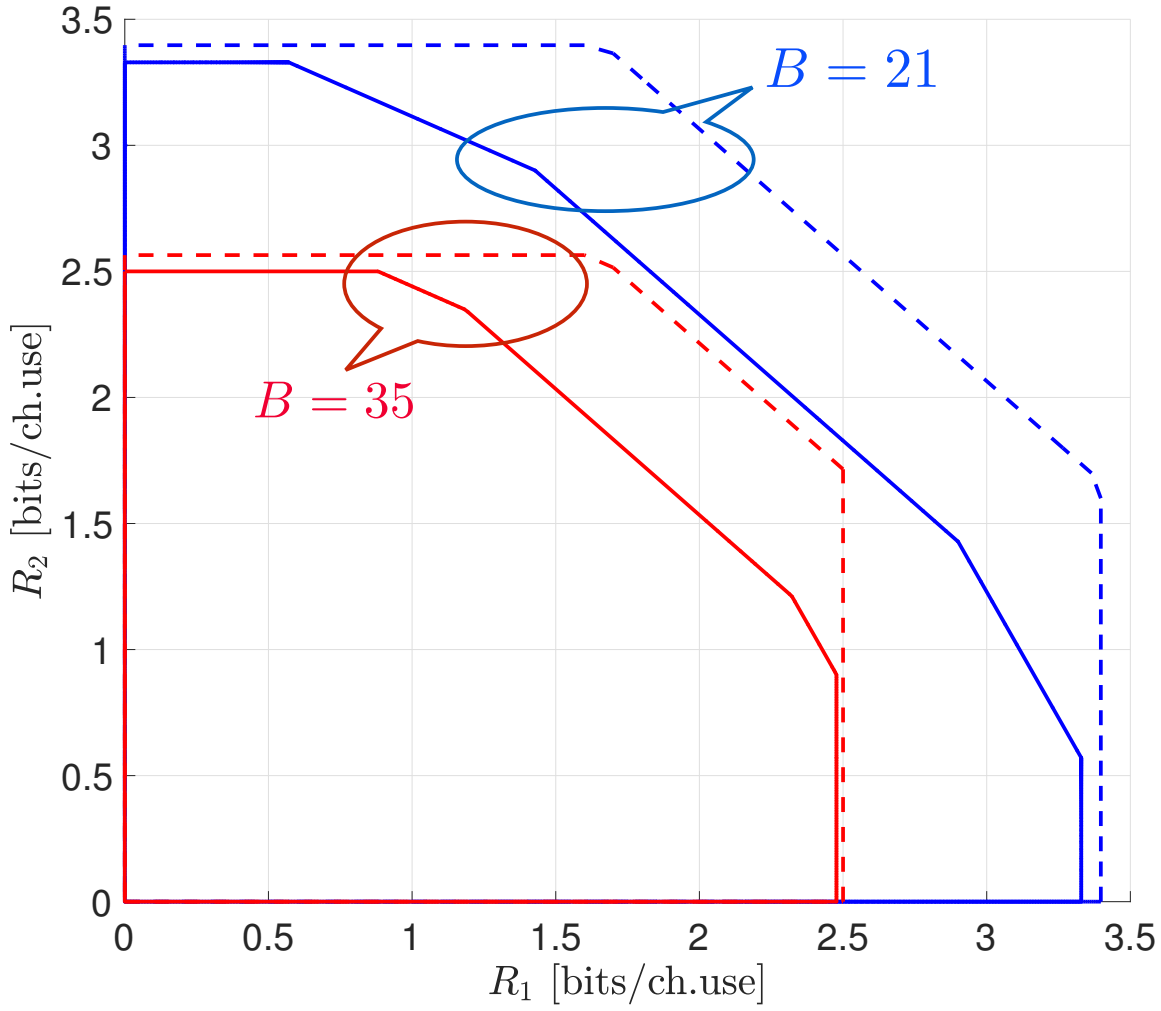

Figure 7.5: Convex hull of pairs (R_1, R_2) that are in the sets $\{(R_1, R_2) \in \mathbb{R}_+^2 : (R_1, R_2, b) \in \overline{\mathcal{E}}\}$ (solid line) and $\{(R_1, R_2) \in \mathbb{R}_+^2 : (R_1, R_2, b) \in \overline{\mathcal{E}}^{\mathrm{F}}\}$ (dashed line), with $b \in \{21, 35\}$. Parameters $\mathrm{SNR}_1 = \mathrm{SNR}_2 = 20$ dB, $\mathrm{INR}_1 = \mathrm{INR}_2 = \mathrm{SNR}_{31} = \mathrm{SNR}_{32} = 10$ dB, and $\sigma_3^2 = 1$.

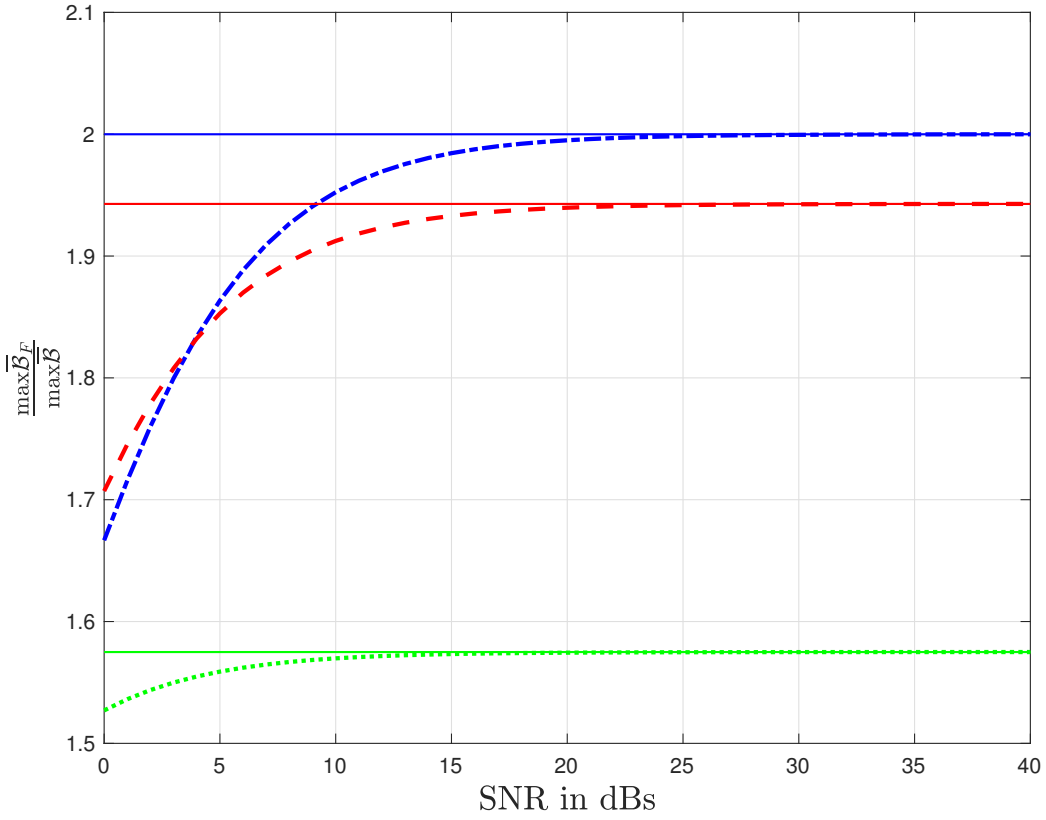

Figure 7.6: The ratio $\frac{\sup\overline{\mathcal{B}}_{\mathrm{F}}}{\sup\overline{\mathcal{B}}}$ for different ratios of SNR at the EH, i.e., $\mathrm{SNR}_{31} = \mathrm{SNR}_{32} = \mathrm{SNR}$; $\frac{\mathrm{SNR}_{31}}{2} = \mathrm{SNR}_{32} = \mathrm{SNR}$; and $\frac{\mathrm{SNR}_{31}}{10} = \mathrm{SNR}_{32} = \mathrm{SNR}$, respectively. Parameters $\mathrm{SNR}_1 = \mathrm{SNR}_2 = 20$ dB, $\mathrm{INR}_1 = \mathrm{INR}_2 = \mathrm{SNR}_{31} = \mathrm{SNR}_{32} = 10$ dB, and $\sigma_3^2 = 1$.

Part III

Data Injection Attacks in Power Systems

Chapter 8

Introduction

The pervasive deployment of sensing, monitoring, and data acquisition techniques in modern power systems enables the definition of functionalities and services that leverage accurate and real-time information about the system. This wealth of data supports network operators in the design of advanced control and management techniques that will inevitably change the operation of future power systems. An interesting side-effect of the data collection exercise that is starting to take place in power systems is that the unprecedented data analysis effort is shedding some light on the turbulent dynamics of power systems. While the underlying physical laws governing power systems are well understood, the large scale, distributed structure, and stochastic nature of the generation and consumption processes in the system results in a complex system. The large volumes of data about the state of the system are opening the door to modelling aspirations that were not feasible prior to the arrival of the smart grid paradigm.

The refinement of the models describing the power system operation will undoubtedly provide valuable insight to the network operator. However, that knowledge and the explanatory principles that it uncovers are also subject to be used in a malicious fashion. Access to statistics describing the state of the grid can inform malicious attackers by allowing them to pose the data-injection problem [102] within a probabilistic framework [23,103]. By describing the processes taking place in the grid as a stochastic process, the network operator can incorporate the statistical description of the state variables in the state estimation procedure and pose it within a Bayesian estimation setting. Similarly, the attacker can exploit the stochastic description of the state variables by incorporating it to the attack construction in the form of prior knowledge about the state variables. Interestingly whether the network operator or the attacker benefit more from adding a stochastic description to the state variables does not have a simple answer and depends greatly on the parameters describing the power system.

In the following chapters some of the basic attack constructions that exploit a stochastic description of the state variables are reviewed. The state estimation

problem is posed in a Bayesian setting and cast the bad data detection procedure as a Bayesian hypothesis testing problem. This revised detection framework provides the benchmark for the attack detection problem that limits the achievable attack disruption. Indeed, the trade-off between the impact of the attack, in terms of disruption to the state estimator, and the probability of attack detection is analytically characterized within this Bayesian attack setting. To conclude, this attack construction is later generalized by considering information-theoretic measures that place fundamental limits to a broad class of detection, estimation, and learning techniques.

8.1 Mathematical Model

8.1.1 Bayesian State Estimation

The state of the system is modelled by a vector of n random variables, denoted by $X^n = (X_1, X_2, \ldots, X_n)$, taking values in $\mathbb{R}^n$ with distribution P_{X^n}. The random variable X_i with $i = 1, 2, \ldots, n$, denotes the state variable i of the power system, and therefore, each entry represents a different physical magnitude of the system that the network operator wishes to monitor. The prior knowledge that is available to the network operator is described by the probability distribution P_{X^n}. The knowledge of the distribution is a consequence of the modelling based on historical data acquired by the network operator. Assuming a linearized system dynamics with m measurements corrupted by additive white Gaussian noise (AWGN), the measurements are modelled as the vector of random variables $Y^m = (Y_1, Y_2, \ldots, Y_n) \in \mathbb{R}^m$ with distribution P_{Y^m} given by

$$Y^m = \mathbf{H}X^n + Z^m, \tag{8.1}$$

where $\mathbf{H} \in \mathbb{R}^{m \times n}$ is the Jacobian of the linearized system dynamics around a given operating point and $Z^m \sim \mathcal{N}(0, \sigma^2 \mathbf{I})$ is thermal white noise with power spectral density σ^2. While the operating point of the system induces a dynamic on the Jacobian matrix $\mathbf{H}$, in the following we assume that the time-scale over which the operation point changes is small compared to the time-scale at which the state estimator operates to produce the estimates. For that reason, in the following we assume that the Jacobian matrix is fixed and the only sources of uncertainty in the observation process originate from the stochasticity of the state variables and the additive noise corrupting the measurements.

The aim of the state estimator is to obtain an estimate $\hat{X}^n$ of the state vector X^n from the system observations Y^m. In this chapter we adopt a linear estimation framework resulting in an estimate given by $\hat{X}^n = \mathbf{L}Y^m$, where $\mathbf{L} \in \mathbb{R}^{n \times m}$ is the linear estimation matrix determining the estimation procedure. In the case in which the operator knows the distribution P_{X^n} of the underlying random process governing the state of the network, the estimation is performed by selecting the estimate that minimizes a given error cost function. A common approach is to use the mean square

error (MSE) as the error cost function. In this case, the network operator uses an estimator $\mathbf{M}$ that is the unique solution to the following optimization problem:

$$\mathbf{M} = \arg \min_{\mathbf{L} \in \mathbb{R}^{n \times m}} \mathbb{E} \left[\frac{1}{n} \| X^n - \mathbf{L} Y^m \|_2^2 \right], \tag{8.2}$$

where the expectation is taken with respect to X^n and Z^m.

Under the assumption that the network state vector X^n follows an n-dimensional real Gaussian distribution with zero mean and covariance matrix $\mathbf{\Sigma}_{XX} \in \mathcal{S}_+^m$, i.e. $X^n \sim \mathcal{N}(\mathbf{0}, \mathbf{\Sigma}_{XX})$, the minimum MSE (MMSE) estimate is given by

$$\hat{X}^n \triangleq \mathbb{E}[X^n | Y^m] = \mathbf{M} Y^m \tag{8.3}$$

where,

$$\mathbf{M} = \mathbf{\Sigma}_{XX} \mathbf{H}^\mathsf{T} (\mathbf{H} \mathbf{\Sigma}_{XX} \mathbf{H}^\mathsf{T} + \sigma^2 \mathbf{I})^{-1}. \tag{8.4}$$

8.1.2 Deterministic Attack Model

The aim of the attacker is to corrupt the estimate by altering the measurements. Data-injection attacks alter the measurements available to the operator by adding an attack vector to the measurements. The resulting observation model with the additive attack vector is given by

$$Y_a^m = \mathbf{H} X^m + Z^m + \mathbf{a}, \tag{8.5}$$

where $\mathbf{a}^m \in \mathbb{R}^m$ is the attack vector and $Y_a^m \in \mathbb{R}^m$ is the vector containing the compromised measurements [102]. Note that in this formulation, the attack vector does not have a probabilistic structure, i.e. the attack vector is deterministic. The random attack construction is considered later in the chapter.

The intention of the attacker can respond to diverse motivations, and therefore, attack construction strategy changes depending on the aim of the attacker. In this chapter, we study attacks that aim to maximize the monitoring disruption, i.e. attacks that obstruct the state estimation procedure with the aim of deviating the estimate as much as possible from the true state. In that sense, the attack problem is bound to the cost function used by the state estimator to obtain the estimate, as the attacker aims to maximize it while the estimator aims to minimize it. In the MMSE setting described above, it follows that the the impact of the attack vector is obtained by noticing that the estimate when the attack vector is present is given by

$$\hat{X}_a^n = \mathbf{M}(\mathbf{H} X^n + Z^m) + \mathbf{M}\mathbf{a}. \tag{8.6}$$

The term $\mathbf{Ma}$ is referred to as the *Bayesian injection vector* introduced by the attack vector $\mathbf{a}$ and is denoted by

$$\mathbf{c} \triangleq \mathbf{Ma} = \mathbf{\Sigma}_{XX} \mathbf{H}^\mathsf{T} (\mathbf{H} \mathbf{\Sigma}_{XX} \mathbf{H}^\mathsf{T} + \sigma^2 \mathbf{I})^{-1} \mathbf{a}. \tag{8.7}$$

The *Bayesian injection vector* is a deterministic vector that corrupts the MMSE estimate of the operator resulting in

$$\hat{X}_a^n = \hat{X}^n + \mathbf{c}. \tag{8.8}$$

where $\hat{X}^n$ is given in (8.3).

As a part of the grid management, a network operator systematically attempts to identify measurements that are not deemed of sufficient quality for the state estimator. In practice, this operation can be cast as a hypothesis testing problem with hypotheses

$$\begin{aligned} \mathcal{H}_0: &\quad \text{There is no attack, and} \\ \mathcal{H}_1: &\quad \text{Measurements are compromised.} \end{aligned} \tag{8.9}$$

Assuming the operator knows the distribution of the state variables, P_{X^n}, and the observation model (8.5), then it can obtain the joint distribution of the measurements and the state variables for both normal operation conditions and the case when an attack is present, i.e. $P_{X^nY^m}$ and $P_{X^nY_a^m}$, respectively.

Under the assumption that the state variables follow a multivariate Gaussian distribution $X^n \sim \mathcal{N}(\mathbf{0}, \mathbf{\Sigma}_{XX})$ it follows that the vector of measurements Y^n follows an m-dimensional real Gaussian random distribution with covariance matrix

$$\mathbf{\Sigma}_{YY} = \mathbf{H}\mathbf{\Sigma}_{XX}\mathbf{H}^\mathsf{T} + \sigma^2\mathbf{I}, \tag{8.10}$$

and mean $\mathbf{a}$ when there is an attack; or zero mean when there is no attack. Within this setting, the hypothesis testing problem described before is adapted to the attack detection problem by comparing the following hypotheses:

$$\begin{aligned} \mathcal{H}_0: &\quad Y^m \sim \mathcal{N}(\mathbf{0}, \mathbf{\Sigma}_{YY}), \quad \text{versus} \\ \mathcal{H}_1: &\quad Y^m \sim \mathcal{N}(\mathbf{a}, \mathbf{\Sigma}_{YY}). \end{aligned} \tag{8.11}$$

A worst case scenario approach is assumed for the attackers, namely, the operator knows the attack vector, $\mathbf{a}$, used in the attack. However, the operator does not know a priori whether the grid is under attack or not, which accounts for the need of an attack detection strategy. That being the case, the optimal detection strategy for the operator is to perform a likelihood ratio test (LRT) $L(\mathbf{y}, \mathbf{a})$ with respect to the observations $\mathbf{y}$. Under the assumption that state variables follow a multivariate Gaussian distribution, the likelihood ratio can be calculated as

$$L(\mathbf{y}, \mathbf{a}) = \frac{f_{\mathcal{N}(\mathbf{0}, \mathbf{\Sigma}_{\mathbf{yy}})}(\mathbf{y})}{f_{\mathcal{N}(\mathbf{a}, \mathbf{\Sigma}_{\mathbf{yy}})}(\mathbf{y})} = \exp\left(\frac{1}{2}\mathbf{a}^\mathsf{T}\mathbf{\Sigma}_{YY}^{-1}\mathbf{a} - \mathbf{a}^\mathsf{T}\mathbf{\Sigma}_{YY}^{-1}\mathbf{y}\right), \tag{8.12}$$

where $f_{\mathcal{N}(\boldsymbol{\mu}, \mathbf{\Sigma})}$ is the probability density function of a multivariate Gaussian random vector with mean $\boldsymbol{\mu}$ and covariance matrix $\mathbf{\Sigma}$. Therefore, either hypothesis is accepted by evaluating the inequalities

$$L(\mathbf{y}, \mathbf{a}) \underset{\mathcal{H}_1}{\overset{\mathcal{H}_0}{\gtrless}} \tau, \tag{8.13}$$

where $\tau \in [0, \infty)$ is tuned to set the trade-off between the probability of detection and the probability of false alarm.

8.1.3 Random Attack Model

Consider an additive attack model as in (8.5) but with the distinction that the attack is a random process. The resulting vector of compromised measurements is given by

$$Y_A^m = \mathbf{H}X^m + Z^m + A^m, \tag{8.14}$$

where $A^m \in \mathbb{R}^m$ is the vector of random variables introduced by the attacker and $Y_A^m \in \mathbb{R}^m$ is the vector containing the compromised measurements. The attack vector of random variables is described by the distribution P_{A^m} which is the determined by the attacker. The attacker is assumed to be constrained from having access to the realizations of the state variables, and therefore, it holds that $P_{A^m X^n} = P_{A^m} P_{X^n}$ where $P_{A^m X^n}$ denotes the joint distribution of A^m and X^n.

Similarly to the deterministic attack case, a multivariate Gaussian framework is adopted for the state variables. That is $X^n \sim \mathcal{N}(\mathbf{0}, \mathbf{\Sigma}_{XX})$. Moreover, the attack vector distribution is assumed to be a zero-mean multivariate Gaussian distribution, i.e. $A^m \sim \mathcal{N}(\mathbf{0}, \mathbf{\Sigma}_{AA})$, where $\mathbf{\Sigma}_{AA} \in \mathcal{S}_+^m$ is the covariance matrix of the attack distribution. The rationale for choosing a Gaussian distribution for the attack vector follows from the fact that for the measurement model in (8.14) the additive attack distribution that minimizes the mutual information between the vector of state variables and the compromised measurements is Gaussian [104]. Later, it will become clear that minimizing this mutual information is central to the proposed information-theoretic attack construction and indeed one of the objectives of the attacker. Because of the Gaussianity of the attack distribution, the vector of compromised measurements is distributed as

$$Y_A^m \sim \mathcal{N}(\mathbf{0}, \mathbf{\Sigma}_{Y_A Y_A}), \tag{8.15}$$

where $\mathbf{\Sigma}_{Y_A Y_A} = \mathbf{H}\mathbf{\Sigma}_{XX}\mathbf{H}^\mathsf{T} + \sigma^2\mathbf{I} + \mathbf{\Sigma}_{AA}$ is the covariance matrix of the distribution of the compromised measurements. Note that while in the case of deterministic attacks the effect of the attack vector was captured by shifting the mean of the measurement vector, in the random attack case the attack changes the structure of the second order moments of the measurements. Interestingly, the Gaussian attack construction implies that knowledge of the second order moments of the state variables and the variance of the AWGN introduced by the measurement process suffices to construct the attack. This assumption significantly reduces the difficulty of the attack construction.

The operator of the power system makes use of the acquired measurements to detect the attack. The detection problem is cast as a hypothesis testing problem with hypotheses

$$\begin{aligned} &\mathcal{H}_0 : Y^m \sim \mathcal{N}(\mathbf{0}, \mathbf{\Sigma}_{YY}), \quad \text{versus} \\ &\mathcal{H}_1 : Y^m \sim \mathcal{N}(\mathbf{0}, \mathbf{\Sigma}_{Y_A Y_A}). \end{aligned} \tag{8.16}$$

The null hypothesis $\mathcal{H}_0$ describes the case in which the power system is not compromised, while the alternative hypothesis $\mathcal{H}_1$ describes the case in which the power system is under attack.

Two types of error are considered in hypothesis testing problems, Type I error is the probability of a "false negative" event; and Type II error is the probability of a "false alarm" event. The Neyman-Pearson lemma [105] states that for a fixed probability of Type I error, the likelihood ratio test (LRT) achieves the minimum Type II error when compared with any other test with an equal or smaller Type I error. Consequently, the LRT is chosen to decide between $\mathcal{H}_0$ and $\mathcal{H}_1$ based on the available measurements. The LRT between $\mathcal{H}_0$ and $\mathcal{H}_1$ takes following form:

$$L(\mathbf{y}) \triangleq \frac{f_{Y_A^m}(\mathbf{y})}{f_{Y^m}(\mathbf{y})} \underset{\mathcal{H}_0}{\overset{\mathcal{H}_1}{\gtrless}} \tau, \tag{8.17}$$

where $\mathbf{y} \in \mathbb{R}^m$ is a realization of the vector of random variables modelling the measurements, $f_{Y_A^m}$ and f_{Y^m} denote the probability density functions (p.d.f.'s) of Y_A^m and Y^m, respectively, and τ is the decision threshold set by the operator to meet the false alarm constraint.

Chapter 9

Design of Deterministic Attacks

9.1 Centralized Deterministic Attacks

This section describes the construction of data-injection attacks in the case in which there is a unique attacker with access to all the measurements on the power system. This scenario is referred to as *centralized attacks* in order to highlight that there exists a unique entity deciding the data-injection vector $\mathbf{a} \in \mathbb{R}^m$ in (8.5). The difference between the scenario in which there exists a unique attacker or several (competing or cooperating) attackers is subtle and it is treated in Section 9.2.

Let $\mathcal{M} = \{1, \ldots, m\}$ denote the set of all m sensors available to the network operator. A sensor is said to be compromised if the attacker is able to arbitrarily modify its output. Given a total energy budget $E > 0$ at the attacker, the set of all possible attacks that can be injected to the network can be explicitly described:

$$\mathcal{A} = \left\{ \mathbf{a} \in \mathbb{R}^m : \mathbf{a}^{\mathsf{T}} \mathbf{a} \leqslant E \right\}. \tag{9.1}$$

9.1.1 Attacks with Minimum Probability of Detection

The attacker chooses a vector $\mathbf{a} \in \mathcal{A}$ taking into account the trade-off between the probability of being detected and the distortion induced by the Bayesian injection vector given by (8.7). However, the choice of a particular data-injection vector is not trivial as the attacker does not have any information about the exact realizations of the vector of state variables $\mathbf{x}$ and the noise vector $\mathbf{z}$. A reasonable assumption on the knowledge of the attacker is to consider that it knows the structure of the power system and thus, it knows the matrix $\mathbf{H}$. It is also reasonable to assume that it knows the first and second moments of the state variables X^n and noise Z^m as this can be computed from historical data.

Under these knowledge assumptions, the probability that the network operator is unable to detect the attack vector $\mathbf{a}$ is

$$\mathsf{P}_{\mathsf{ND}}(\mathbf{a}) = \mathsf{E}\left[\mathbb{1}_{\{\mathsf{L}(\mathbf{y},\mathbf{a}) > \tau\}} \right], \tag{9.2}$$

where the expectation is taken over the joint probability distribution of state variables X^n and the AWGN noise vector Z^n, and $\mathbb{1}_{\{\cdot\}}$ denotes the indicator function. Note that under these assumptions, Y^m is a random variable with Gaussian distribution with mean $\mathbf{a}$ and covariance matrix $\mathbf{\Sigma}_{YY}$. Thus, the probability $\mathsf{P}_{\mathsf{ND}}(\mathbf{a})$ of a vector $\mathbf{a}$ being a successful attack, i.e., a non-detected attack is given by [106]

$$\mathsf{P}_{\mathsf{ND}}(\mathbf{a}) = \frac{1}{2}\mathsf{erfc}\left(\frac{\frac{1}{2}\mathbf{a}^{\mathsf{T}}\mathbf{\Sigma}_{\mathsf{YY}}^{-1}\mathbf{a} + \log\tau}{\sqrt{2\mathbf{a}^{\mathsf{T}}\mathbf{\Sigma}_{\mathsf{YY}}^{-1}\mathbf{a}}}\right). \tag{9.3}$$

Often, the knowledge of the threshold τ in (8.13) is not available to the attacker and thus, it cannot determine the exact probability of not being detected for a given attack vector $\mathbf{a}$. However, the knowledge of whether $\tau > 1$ or $\tau \leqslant 1$ induces different behaviors on the attacker. The following propositions follow immediately from (9.3) and the properties of the complementary error function.

Proposition 6 (Case $\tau \leqslant 1$)**.** *Let $\tau \leqslant 1$. Then, for all $\mathbf{a} \in \mathcal{A}$, $\mathsf{P}_{\mathsf{ND}}(\mathbf{a}) < \mathsf{P}_{\mathsf{ND}}((0,\ldots,0))$ and the probability $\mathsf{P}_{\mathsf{ND}}(\mathbf{a})$ is monotonically decreasing with $\mathbf{a}^{\mathsf{T}}\mathbf{\Sigma}_{YY}^{-1}\mathbf{a}$.*

Proposition 7 (Case $\tau > 1$)**.** *Let $\tau > 1$ and let also $\mathbf{\Sigma}_{YY} = \mathbf{U}_{YY}\mathbf{\Lambda}_{YY}\mathbf{U}_{YY}^{\mathsf{T}}$ be the singular value decomposition of $\mathbf{\Sigma}_{YY}$, with $\mathbf{U}_{YY}^{\mathsf{T}} = (\mathbf{u}_{YY,1},\ldots,\mathbf{u}_{YY,m})$ and $\mathbf{\Lambda}_{YY} = diag\,(\lambda_{YY,1},\ldots,\lambda_{YY,m})$ and $\lambda_{YY,1} \geqslant \lambda_{YY,2} \geqslant \ldots, \geqslant \lambda_{YY,m}$. Then, any vector of the form*

$$\mathbf{a} = \pm\sqrt{\lambda_{YY,k} 2\log\tau}\,\mathbf{u}_{YY,k}, \tag{9.4}$$

with $k \in \{1,\ldots,m\}$, is a data-injection attack that satisfies for all $\mathbf{a}' \in \mathbb{R}^m$, $\mathsf{P}_{\mathsf{ND}}(\mathbf{a}') \leqslant \mathsf{P}_{\mathsf{ND}}(\mathbf{a})$.

The relevance of Proposition 6 is that it states that when $\tau \leqslant 1$, any non-zero data-injection attack vector possesses a non zero probability of being detected. Indeed, the highest probability $\mathsf{P}_{\mathsf{ND}}(\mathbf{a})$ of not being detected is guaranteed by the null vector $\mathbf{a}$= (0, ..., 0), i.e., there is no attack. Alternatively, when $\tau > 1$ it follows from Proposition 7 that there always exists a non-zero vector that possesses maximum probability of not being detected. However, in both cases, it is clear that the corresponding data-injection vectors that induce the highest probability of not being detected are not necessarily the same that inflict the largest damage to the network, i.e., maximize the excess distortion.

From this point of view, the attacker faces the trade-off between maximizing the excess distortion and minimizing the probability of being detected. Thus, the attack construction can be formulated as an optimization problem in which the solution $\mathbf{a}$ is a data-injection vector that maximizes the probability $\mathsf{P}_{\mathsf{ND}}(\mathbf{a})$ of not being detected at the same time that it induces a distortion $\|\mathbf{c}\|_2^2 \geqslant \mathsf{D}_0$ into the estimate. In the case in which $\tau \leqslant 1$, it follows from Proposition 6 and (8.7) that this problem can be formulated as the following optimization problem:

$$\min_{\mathbf{a}\in\mathcal{A}} \mathbf{a}^{\mathsf{T}}\mathbf{\Sigma}_{YY}^{-1}\mathbf{a} \quad \text{s.t.} \quad \mathbf{a}^{\mathsf{T}}\mathbf{\Sigma}_{YY}^{-1}\mathbf{H}\mathbf{\Sigma}_{XX}^{2}\mathbf{H}^{\mathsf{T}}\mathbf{\Sigma}_{YY}^{-1}\mathbf{a} \geq \mathsf{D}_0. \tag{9.5}$$

The solution to the optimization problem in (9.5) is given by the following theorem.

Theorem 15. *Let* $\mathbf{G} = \boldsymbol{\Sigma}_{YY}^{-\frac{1}{2}}\mathbf{H}\boldsymbol{\Sigma}_{XX}^{2}\mathbf{H}^{\mathsf{T}}\boldsymbol{\Sigma}_{YY}^{-\frac{1}{2}}$ *have a singular value decomposition* $\mathbf{G} = \mathbf{U}_{\mathbf{G}}\boldsymbol{\Sigma}_{\mathbf{G}}\mathbf{U}_{\mathbf{G}}^{\mathsf{T}}$*, with* $\mathbf{U} = (\mathbf{u}_{\mathbf{G},i}, \ldots, \mathbf{u}_{\mathbf{G},m})$ *a unitary matrix and* $\boldsymbol{\Sigma}_{\mathbf{G}} = diag\big(\lambda_{\mathbf{G},1}, \ldots, \lambda_{\mathbf{G},m}\big)$ *a diagonal matrix with* $\lambda_{\mathbf{G},1} \geqslant \ldots \geqslant \lambda_{\mathbf{G},m}$*. Then, if* $\tau \leqslant 1$*, the attack vector* $\mathbf{a}$ *that maximizes the probability of not being detected* $\mathsf{P}_{\mathsf{ND}}(\mathbf{a})$ *while inducing an excess distortion not less than* D_0 *is*

$$\mathbf{a} \;=\; \pm\sqrt{\frac{\mathsf{D}_0}{\lambda_{\mathbf{G},1}}}\boldsymbol{\Sigma}_{YY}^{\frac{1}{2}}\mathbf{u}_{\mathbf{G},1}. \tag{9.6}$$

Moreover, $\mathsf{P}_{\mathsf{ND}}(\mathbf{a}) = \frac{1}{2}\mathrm{erfc}\left(\frac{\frac{\mathsf{D}_0}{2\lambda_{\mathbf{G},1}}+\log\tau}{\sqrt{\frac{2\mathsf{D}_0}{\lambda_{\mathbf{G},1}}}}\right)$.

Interestingly, the construction of the data-injection attack $\mathbf{a}$ in (9.6) does not require the exact knowledge of τ. That is, only knowing that $\tau \leqslant 1$ is enough to build the data-injection attack that has the highest probability of not being detected and induces a distortion of at least D_0.

In the case in which $\tau > 1$, it is also possible to find the data-injection attack vector that induces a distortion not less than D_0 and the maximum probability of not being detected. Such a vector is the solution to the following optimization problem.

$$\min_{\mathbf{a}\in\mathcal{A}} \frac{\frac{1}{2}\mathbf{a}^{\mathsf{T}}\boldsymbol{\Sigma}_{YY}^{-1}\mathbf{a} + \log\tau}{\sqrt{2\mathbf{a}^{\mathsf{T}}\boldsymbol{\Sigma}_{YY}^{-1}\mathbf{a}}} \;\text{ s.t. }\; \mathbf{a}^{\mathsf{T}}\boldsymbol{\Sigma}_{YY}^{-1}\mathbf{H}\boldsymbol{\Sigma}_{XX}^{2}\mathbf{H}^{\mathsf{T}}\boldsymbol{\Sigma}_{YY}^{-1}\mathbf{a} \geq \mathsf{D}_0. \tag{9.7}$$

The solution to the optimization problem in (9.7) is given by the following theorem.

Theorem 16. *Let* $\mathbf{G} = \boldsymbol{\Sigma}_{YY}^{-\frac{1}{2}}\mathbf{H}\boldsymbol{\Sigma}_{XX}^{2}\mathbf{H}^{\mathsf{T}}\boldsymbol{\Sigma}_{YY}^{-\frac{1}{2}}$ *have a singular value decomposition* $\mathbf{G} = \mathbf{U}_{\mathbf{G}}\boldsymbol{\Sigma}_{\mathbf{G}}\mathbf{U}_{\mathbf{G}}^{\mathsf{T}}$*, with* $\mathbf{U}_{\mathbf{G}} = (\mathbf{u}_{\mathbf{G},i}, \ldots, \mathbf{u}_{\mathbf{G},m})$ *a unitary matrix and* $\boldsymbol{\Sigma}_{\mathbf{G}} = diag\big(\lambda_{\mathbf{G},1}, \ldots, \lambda_{\mathbf{G},m}\big)$ *a diagonal matrix with* $\lambda_{\mathbf{G},1} \geqslant \ldots \geqslant \lambda_{\mathbf{G},m}$*. Then, when* $\tau > 1$*, the attack vector* $\mathbf{a}$ *that maximizes the probability of nondetection* $\mathsf{P}_{\mathsf{ND}}(\mathbf{a})$ *while producing an excess distortion not smaller than* D_0 *is*

$$\mathbf{a} = \begin{cases} \pm\sqrt{\frac{\mathsf{D}_0}{\lambda_{\mathbf{G},k^*}}}\boldsymbol{\Sigma}_{YY}^{\frac{1}{2}}\mathbf{u}_{\mathbf{G},k^*} & \text{if } \frac{\mathsf{D}_0}{2\log\tau\lambda_{\mathbf{G},\mathrm{rank}\,\mathbf{G}}} \geqslant 1, \\ \pm\sqrt{2\log\tau}\boldsymbol{\Sigma}_{YY}^{\frac{1}{2}}\mathbf{u}_{\mathbf{G},1} & \text{if } \frac{\mathsf{D}_0}{2\log\tau\lambda_{\mathbf{G},\mathrm{rank}\,\mathbf{G}}} < 1 \end{cases}$$

with

$$k^* = \arg \min_{k\in\{1,\ldots,\mathrm{rank}\mathbf{G}\}:\frac{\mathsf{D}_0}{\lambda_{\mathbf{G},k}}>2\log(\tau)} \frac{\mathsf{D}_0}{\lambda_{\mathbf{G},k}}. \tag{9.8}$$

9.1.2 Attacks with Maximum Distortion

In the previous subsection, the attacker constructs its data-injection vector $\mathbf{a}$ aiming to maximize the probability of non-detection $\mathsf{P}_{\mathsf{ND}}(\mathbf{a})$ while guaranteeing a minimum

distortion. However, this problem has a dual in which the objective is to maximize the distortion $\mathbf{a}^\mathsf{T}\boldsymbol{\Sigma}_{YY}^{-1}\mathbf{H}\boldsymbol{\Sigma}_{XX}^2\mathbf{H}^\mathsf{T}\boldsymbol{\Sigma}_{YY}^{-1}\mathbf{a}$ while guaranteeing that the probability of not being detected remains always larger than a given threshold $L_0' \in [0, \frac{1}{2}]$. This problem can be formulated as the following optimization problem:

$$\max_{\mathbf{a}\in\mathcal{A}} \mathbf{a}^\mathsf{T}\boldsymbol{\Sigma}_{YY}^{-1}\mathbf{H}\boldsymbol{\Sigma}_{XX}^2\mathbf{H}^\mathsf{T}\boldsymbol{\Sigma}_{YY}^{-1}\mathbf{a} \text{ s.t. } \frac{\frac{1}{2}\mathbf{a}^\mathsf{T}\boldsymbol{\Sigma}_{YY}^{-1}\mathbf{a} + \log\tau}{\sqrt{2\mathbf{a}^\mathsf{T}\boldsymbol{\Sigma}_{YY}^{-1}\mathbf{a}}} \leq L_0, \tag{9.9}$$

with $L_0 = \operatorname{erfc}^{-1}(2L_0') \in [0, \infty)$.

The solution to the optimization problem in (9.9) is given by the following theorem.

Theorem 17. *Let the matrix* $\mathbf{G} = \boldsymbol{\Sigma}_{YY}^{-\frac{1}{2}}\mathbf{H}\boldsymbol{\Sigma}_{XX}^2\mathbf{H}^\mathsf{T}\boldsymbol{\Sigma}_{YY}^{-\frac{1}{2}}$ *have a singular value decomposition* $\mathbf{U}_\mathbf{G}\boldsymbol{\Sigma}_\mathbf{G}\mathbf{U}_\mathbf{G}^\mathsf{T}$, *with* $\mathbf{U} = (\mathbf{u}_{\mathbf{G},i}, \ldots, \mathbf{u}_{\mathbf{G},m})$ *a unitary matrix and* $\boldsymbol{\Sigma}_\mathbf{G} = \mathit{diag}(\lambda_{\mathbf{G},1}, \ldots, \lambda_{\mathbf{G},m})$ *a diagonal matrix with* $\lambda_{\mathbf{G},1} \geqslant \ldots \geqslant \lambda_{\mathbf{G},m}$. *Then, the attack vector* $\mathbf{a}$ *that maximizes the excess distortion* $\mathbf{a}^\mathsf{T}\boldsymbol{\Sigma}_{YY}^{-\frac{1}{2}}\mathbf{G}\boldsymbol{\Sigma}_{YY}^{-\frac{1}{2}}\mathbf{a}$ *with a probability of not being detected that is not smaller than* $L_0 \in [0, \frac{1}{2}]$ *is*

$$\mathbf{a} = \pm\left(\sqrt{2}L_0 + \sqrt{2L_0^2 - 2\log\tau}\right)\boldsymbol{\Sigma}_{YY}^{\frac{1}{2}}\mathbf{u}_{\mathbf{G},1}, \tag{9.10}$$

when such a vector exists.

9.2 Decentralized Deterministic Attacks

Let $\mathcal{K} = \{1, \ldots, K\}$ be the set of attackers that can potentially perform a data injection attack on the network, e.g., a decentralized vector attack. Let also $\mathcal{C}_k \in \{1, 2, \ldots, m\}$ be the set of sensors that attacker $k \in \mathcal{K}$ can control. Assume that $\mathcal{C}_1, \ldots, \mathcal{C}_K$ are proper sets and form a partition of the set $\mathcal{M}$ of all sensors. The set $\mathcal{A}_k$ of data attack vectors $\mathbf{a}_k = (a_{k,1}, a_{k,2}, \ldots, a_{k,m})$ that can be injected into the network by attacker $k \in \mathcal{K}$ is of the form

$$\mathcal{A}_k = \{\mathbf{a}_k \in \mathbb{R}^m : \mathbf{a}_{k,j} = 0 \text{ for all } j \notin \mathcal{C}_k, \mathbf{a}_k^\mathsf{T}\mathbf{a}_k \leq E_k\}. \tag{9.11}$$

The constant $E_k < \infty$ represents the energy budget of attacker k. Let the set of all possible sums of the elements of $\mathcal{A}_i$ and $\mathcal{A}_j$ be denoted by $\mathcal{A}_i \oplus \mathcal{A}_j$. That is, for all $\mathbf{a} \in \mathcal{A}_i \oplus \mathcal{A}_j$, there exists a pair of vectors $(\mathbf{a}_i, \mathbf{a}_j) \in \mathcal{A}_i \times \mathcal{A}_j$ such that $\mathbf{a} = \mathbf{a}_i + \mathbf{a}_j$. Using this notation, let the set of all possible data-injection attacks be denoted by

$$\mathcal{A} = \mathcal{A}_1 \oplus \mathcal{A}_2 \oplus \ldots \oplus \mathcal{A}_K, \tag{9.12}$$

and the set of complementary data-injection attacks with respect to attacker k be denoted by

$$\mathcal{A}_{-k} = \mathcal{A}_1 \oplus \ldots \oplus \mathcal{A}_{k-1} \oplus \mathcal{A}_{k+1} \oplus \ldots \oplus \mathcal{A}_K. \tag{9.13}$$

Given the individual data injection vectors $\mathbf{a}_i \in \mathcal{A}_i$, with $i \in \{1, \ldots, K\}$, the global attack vector $\mathbf{a}$ is

$$\mathbf{a} = \sum_{i=1}^{K} \mathbf{a}_k \in \mathcal{A}. \tag{9.14}$$

The aim of attacker k is to corrupt the measurements obtained by the set of meters $\mathcal{C}_k$ by injecting an error vector $\mathbf{a}_k \in \mathcal{A}_k$ that maximizes the damage to the network, e.g., the excess distortion, while avoiding the detection of the global data-injection vector $\mathbf{a}$. Clearly, all attackers have the same interest but they control different sets of measurements, i.e., $\mathcal{C}_i \neq \mathcal{C}_k$, for a any pair $(i,k) \in \mathcal{K}^2$. For modeling this behavior, attackers use the utility function $\phi : \mathbb{R}^m \to \mathbb{R}$, to determine whether a data-injection vector $\mathbf{a}_k \in \mathcal{A}_k$ is more beneficial than another $\mathbf{a}'_k \in \mathcal{A}_k$ given the complementary attack vector

$$\mathbf{a}_{-k} = \sum_{i \in \{1,\ldots,K\} \setminus \{k\}} \mathbf{a}_i \in \mathcal{A}_{-k} \tag{9.15}$$

adopted by all the other attackers. The function ϕ is chosen considering the fact that an attack is said to be successful if it induces a non-zero distortion and it is not detected. Alternatively, if the attack is detected no damage is induced into the network as the operator discards the measurements and no estimation is performed. Hence, given a global attack $\mathbf{a}$, the distortion induced into the measurements is $\mathbb{1}_{\{L(Y_a^m, \mathbf{a}) > \tau\}} \mathbf{c}^\mathsf{T}\mathbf{c}$. However, attackers are not able to know the exact state of the network $\mathbf{x}$ and the realization of the noise $\mathbf{z}$ before launching the attack. Thus, it appears natural to exploit the knowledge of the first and second moments of both the state variables $\mathbf{x}$ and noise $\mathbf{z}$ and consider as a metric the expected distortion $\phi(\mathbf{a})$ that can be induced by the attack vector $\mathbf{a}$:

$$\phi(\mathbf{a}) = \mathsf{E}\left[\left(\mathbb{1}_{\{\mathsf{L}(\mathsf{Y}_\mathsf{a}^\mathsf{m}, \mathbf{a}) > \tau\}}\right) \mathbf{c}^\mathsf{T}\mathbf{c}\right], \tag{9.16}$$

$$= \mathsf{P}_{\mathsf{ND}}(\mathbf{a})\, \mathbf{a}^\mathsf{T} \boldsymbol{\Sigma}_{\mathsf{YY}}^{-1} \mathbf{H} \boldsymbol{\Sigma}_{\mathsf{XX}}^{2} \mathbf{H}^\mathsf{T} \boldsymbol{\Sigma}_{\mathsf{YY}}^{-1} \mathbf{a}, \tag{9.17}$$

where $\mathbf{c}$ is in (8.7) and the expectation is taken over the distribution of state variables X^n and the noise Z^m. Note that under this assumptions of global knowledge, this model considers the worst case scenario for the network operator. Indeed, the result presented in this section corresponds to the case in which the attackers inflict the most harm onto the state estimator.

9.2.1 Game Formulation

The benefit $\phi(\mathbf{a})$ obtained by attacker k does not only depend on its own data-injection vector $\mathbf{a}_k$, but also on the data-injection vectors $\mathbf{a}_{-k}$ of all the other attackers. This becomes clear from the construction of the global data-injection vector $\mathbf{a}$ in (9.14), the excess distortion $\mathbf{c}$ in (8.7) and the probability of not being detected $\mathsf{P}_{\mathsf{ND}}(\mathbf{a})$ in (9.3). Therefore, the interaction of all attackers in the network can be described by a game in normal form

$$\mathcal{G} = \left(\mathcal{K}, \{\mathcal{A}_k\}_{k \in \mathcal{K}}, \{u_k\}_{k \in \mathcal{K}}\right). \tag{9.18}$$

Each attacker is a player in the game $\mathcal{G}$ and it is identified by an index from the set $\mathcal{K}$. The actions player k might adopt are data-injection vectors $\mathbf{a}_k$ in the set $\mathcal{A}_k$ in (9.11). The underlying assumption in the following of this section is that, given a vector of data-injection attacks $\mathbf{a}_{-k}$, player k aims to adopt a data-injection vector $\mathbf{a}_k$ such that the expected excess distortion $\phi(\mathbf{a}_k + \mathbf{a}_{-k})$ is maximized. That is,

$$\mathbf{a}_k \in \mathrm{BR}_k\left(\mathbf{a}_{-k}\right), \tag{9.19}$$

where the correspondence $\mathrm{BR}_k : \mathcal{A}_{-k} \to 2^{\mathcal{A}_k}$ is the best response correspondence, i.e.,

$$\mathrm{BR}_k\left(\mathbf{a}_{-k}\right) = \arg\max_{\mathbf{a}_k \in \mathcal{A}_k} \phi\left(\mathbf{a}_k + \mathbf{a}_{-k}\right). \tag{9.20}$$

The notation $2^{\mathcal{A}_k}$ represents the set of all possible subsets of $\mathcal{A}_k$. Note that $\mathrm{BR}_k\left(\mathbf{a}_{-k}\right) \subseteq \mathcal{A}_k$ is the set of data-injection attack vectors that are optimal given that the other attackers have adopted the data-injection vector $\mathbf{a}_{-k}$. In this setting, each attacker tampers with a subset $\mathcal{C}_k$ of all sensors $\mathcal{C} = \{1, 2, \ldots, m\}$, as opposed to the centralized case in which there exists a single attacker that is able to tamper with all sensors in $\mathcal{C}$.

A game solution that is particularly relevant for this analysis is the NE [65].

Definition 10 (Nash Equilibrium)**.** *The data-injection vector* $\mathbf{a}$ *is an NE of the game* $\mathcal{G}$ *if and only if it is a solution of the fix point equation*

$$\mathbf{a} = \mathrm{BR}\left(\mathbf{a}\right), \tag{9.21}$$

with $\mathrm{BR} : \mathcal{A} \to 2^{\mathcal{A}}$ *being the global best-response correspondence, i.e.,*

$$\mathrm{BR}\left(\mathbf{a}\right) = \mathrm{BR}_1\left(\mathbf{a}_{-1}\right) \oplus \ldots \oplus \mathrm{BR}_K\left(\mathbf{a}_{-K}\right). \tag{9.22}$$

Essentially, at an NE, attackers obtain the maximum benefit given the data-injection vector adopted by all the other attackers. This implies that an NE is an operating point at which attackers achieve the highest expected distortion induced over the measurements. More importantly, any unilateral deviation from an equilibrium data-injection vector $\mathbf{a}$ does not lead to an improvement of the average excess distortion. Note that this formulation does not say anything about the exact distortion induced by an attack but the average distortion. This is mainly because the attack is chosen under the uncertainty of the state vector X^n and the noise term Z^m.

The following proposition highlights an important property of the game $\mathcal{G}$ in (9.18).

Proposition 8. *The game* $\mathcal{G}$ *in* (9.18) *is a potential game.*

In general, potential games [107] possess numerous properties that are inherited by the game $\mathcal{G}$ in (9.18). One of these properties is detailed by the following proposition.

Proposition 9. *The game* $\mathcal{G}$ *possesses at least one NE.*

9.2.2 Achievability of an NE

The attackers are said to play a sequential best response dynamic (BRD) if the attackers can sequentially decide their own data-injection vector $\mathbf{a}_k$ from their sets of best responses following a round-robin (increasing) order. Denote by $\mathbf{a}_k^{(t)} \in \mathcal{A}$ the choice of attacker k during round $t \in \mathbb{N}$ and assume that attackers are able to observe all the other attackers' data-injection vectors. Under these assumptions, the BRD can be defined as follows.

Definition 11 (Best Response Dynamics)**.** *The players of the game $\mathcal{G}$ are said to play best response dynamics if there exists a round-robin order of the elements of $\mathcal{K}$ in which at each round $t \in \mathbb{N}$, the following holds:*

$$\mathbf{a}_k^{(t)} \in \mathrm{BR}_k\left(\mathbf{a}_1^{(t)} + \ldots + \mathbf{a}_{k-1}^{(t)} + \mathbf{a}_{k+1}^{(t-1)} + \ldots + \mathbf{a}_K^{(t-1)}\right). \tag{9.23}$$

From the properties of potential games (Lemma 4.2 in [107]), the following proposition follows.

Lemma 1 (Achievability of NE attacks)**.** *Any BRD in the game $\mathcal{G}$ converges to a data-injection attack vector that is an NE.*

The relevance of Lemma 1 is that it establishes that if attackers can communicate in at least a round-robin fashion, they are always able to attack the network with a data-injection vector that maximizes the average excess distortion. Note that there might exists several NEs (local maxima of ϕ) and there is no guarantee that attackers will converge to the best NE, i.e., a global maximum of ϕ. It is important to note that under the assumption that there exists a unique maximum, which is not the case for the game $\mathcal{G}$ (see Theorem 18), all attackers are able to calculate such a global maximum and no communications is required among the attackers. Nonetheless, the game $\mathcal{G}$ always possesses at least two NEs, which enforces the use of a sequential BRD to converge to an NE.

9.2.3 Cardinality of the set of NEs

Let $\mathcal{A}_{\mathrm{NE}}$ be the set of all data-injection attacks that form NEs. The following theorem bounds the number of NEs in the game.

Theorem 18. *The cardinality of the set $\mathcal{A}_{\mathrm{NE}}$ of NE of the game $\mathcal{G}$ satisfies*

$$2 \leqslant |\mathcal{A}_{\mathrm{NE}}| \leqslant C \cdot \mathrm{rank}(\mathbf{H}) \tag{9.24}$$

where $C < \infty$ is a constant that depends on τ and $\mathbf{H}$ is in (8.14)*.*

9.3 Conclusions and Further Work

Deterministic attacks are specified by the power system and the statistical structure of the state variables. The attack problem is cast as a multiobjective optimization

problem in which the attacker aims to simultaneously minimize the MSE distortion induced by the injection vector and the probability of the attack being detected using a likelihood ratio test. Within this setting, the tradeoff between the achievable distortion and probability of detection is characterized by deriving optimal centralized attack constructions for a given distortion and probability of detection pair. This investigation is extended to decentralized scenarios in which several attackers construct their respective attack without coordination. In this setting, we have posed the interaction between the attackers in a game-theoretic setting. We show that the proposed utility function results in a setting that can be described as a potential game that allows us to claim the existence of an NE and the convergence of BRD to an NE.

Chapter 10

Design of Random Attacks

Modern sensing infrastructure is moving toward increasing the number of measurements that the operator acquires, e.g. phasor measurement units exhibit temporal resolutions in the order of miliseconds while supervisory control and data acquisition (SCADA) systems traditionally operate with a temporal resolution in the order of seconds. As a result, attack constructions that do not change within the same temporal scale at which measurements are reported do not exploit all the *degrees of freedom* that are available to the attacker. Indeed, an attacker can choose to change the attack vector with every measurement vector that is reported to the network operator. However, the deterministic attack construction changes when the Jacobian measurement matrix changes, i.e. with the operation point of the system. Thus, in the deterministic attack case, the attack construction changes at the same rate that the Jacobian measurement matrix changes and, therefore, the dynamics of the state variables define the update cadency of the attack vector.

This chapter studies the case in which the attacker constructs the attack vector as a random process that corrupts the measurements. By endowing the attack vector with a probabilistic structure, the attacker is provided with an attack construction strategy that generates attack vector realizations over time and that achieve a determined objective on average. In view of this, the task of the attacker in this case is to devise the optimal distribution for the attack vectors. In the following, the attack construction problem is posed within an information-theoretic framework and the attacks that simultaneously minimize the mutual information and the probability of detection are characterized.

10.1 Information-Theoretic Considerations

The aim of the attacker is twofold. First, it aims to disrupt the state estimation process by corrupting the measurements in such a way that the network operator acquires the least amount of knowledge about the state of the system. Second, the attacker aspires to remain stealthy and corrupt the measurements without being

detected by the network operator. In the following, information-theoretic measures are proposed to provide quantitative metrics for the objectives of the attacker.

The data-integrity of the measurements is measured in terms of the mutual information between the state variables and the measurements. The mutual information between two random variables is a measure of the amount of information that each random variable contains about the other random variable. By adding the attack vector to the measurements the attacker aims to reduce the mutual information which ultimately results in a loss of information about the state by the network operator. Specifically, the attacker aims to minimize $I(X^n; Y_A^m)$. In view of this, it seems reasonable to consider a Gaussian distribution for the attack vector as the minimum mutual information for the observation model in (8.5) is achieved by additive Gaussian noise.

The probability of attack detection is determined by the detection threshold τ set by the operator for the likelihood ratio test and the distribution induced by the attack on the vector of compromised measurements. An analytical expression of the probability of attack detection can be described in closed-form as a function of the distributions describing the measurements under both hypotheses. However, the expression is involved in general and it is not straightforward to incorporate it into an analytical formulation of the attack construction. For that reason, the asymptotic performance of the likelihood ratio test is considered to evaluate the detection performance of the operator. The Chernoff-Stein lemma [108] characterizes the asymptotic exponent of the probability of detection when the number of observations of measurement vectors grows to infinity. In this case, the Chernoff-Stein lemma states that for any likelihood ratio test and $\epsilon \in (0, 1/2)$, it holds that

$$\lim_{T\to\infty} \frac{1}{T} \log \beta_T^\epsilon = -D(P_{Y_A^m} || P_{Y^m}), \tag{10.1}$$

where $D(\cdot||\cdot)$ is the Kullback-Leibler (KL) divergence, β_T^ϵ is the minimum Type II error such that the Type I error α satisfies $\alpha < \epsilon$, and T is the number of m-dimensional measurement vectors that are available for the likelihood ratio test detection procedure. As a result, minimizing the asymptotic probability of false alarm given an upper bound on the probability of misdetection is equivalent to minimizing $D(P_{Y_A^m} || P_{Y^m})$, where $P_{Y_A^m}$ and P_{Y^m} denote the probability distributions of Y_A^m and Y^m, respectively.

The purpose of the attacker is to disrupt the normal state estimation procedure by minimizing the information that the operator acquires about the state variables, while guaranteeing that the probability of attack detection is sufficiently small, and therefore, remain stealthy.

When the two information-theoretic objectives are considered by the attacker, in [28], a stealthy attack construction is proposed by combining two objectives in one cost function, i.e.,

$$I(X^n; Y_A^m) + D(P_{Y_A^m} || P_{Y^m}) = D(P_{X^n Y_A^m} || P_{X^n} P_{Y^m}), \tag{10.2}$$

where $P_{X^n Y_A^m}$ is the joint distribution of X^n and Y_A^m. The resulting optimization problem to construct the attack is given by

$$\min_{A^m} D(P_{X^n Y_A^m} || P_{X^n} P_{Y^m}). \tag{10.3}$$

Therein, it is shown that (10.3) is a convex optimization problem and the covariance matrix of the optimal Gaussian attack is $\mathbf{\Sigma}_{AA} = \mathbf{H}\mathbf{\Sigma}_{XX}\mathbf{H}^{\mathsf{T}}$. However, numerical simulations on IEEE test system show that the attack construction proposed in the preceding text yields large values of probability of detection in practical settings.

To control the probability of attack detection of the attack, the preceding construction is generalized in [30] by introducing a parameter that weights the detection term in the cost function. The resulting optimization problem is given by

$$\min_{A^m} I(X^n; Y_A^m) + \lambda D(P_{Y_A^m} || P_{Y^m}), \tag{10.4}$$

where $\lambda \geq 1$ governs the weight given to each objective in the cost function. It is interesting to note that for the case in which $\lambda = 1$ the proposed cost function boils down to the effective secrecy proposed in [109] and the attack construction in (10.4) coincides with that in [28]. For $\lambda > 1$, the attacker adopts a conservative approach and prioritizes remaining undetected over minimizing the amount of information acquired by the operator. By increasing the value of λ the attacker decreases the probability of detection at the expense of increasing the amount of information acquired by the operator using the measurements.

10.2 Construction of Stealth Attacks

The attack construction in (10.4) is formulated in a general setting. The following propositions particularize the KL divergence and MI to our multivariate Gaussian setting.

Proposition 10. [108] *The KL divergence between m-dimensional multivariate Gaussian distributions $\mathcal{N}(\mathbf{0}, \mathbf{\Sigma}_{Y_A Y_A})$ and $\mathcal{N}(\mathbf{0}, \mathbf{\Sigma}_{YY})$ is given by*

$$D(P_{Y_A^m} || P_{Y^m}) = \frac{1}{2}\left(\log \frac{|\mathbf{\Sigma}_{YY}|}{|\mathbf{\Sigma}_{Y_A Y_A}|} - m + \operatorname{tr}\left(\mathbf{\Sigma}_{YY}^{-1}\mathbf{\Sigma}_{Y_A Y_A}\right)\right). \tag{10.5}$$

Proposition 11. [108] *The mutual information between the vectors of random variables $X^n \sim \mathcal{N}(\mathbf{0}, \mathbf{\Sigma}_{XX})$ and $Y_A^m \sim \mathcal{N}(\mathbf{0}, \mathbf{\Sigma}_{Y_A Y_A})$ is given by*

$$I(X^n; Y_A^m) = \frac{1}{2}\log \frac{|\mathbf{\Sigma}_{XX}||\mathbf{\Sigma}_{Y_A Y_A}|}{|\mathbf{\Sigma}|}, \tag{10.6}$$

where $\mathbf{\Sigma}$ is the covariance matrix of the joint distribution of (X^n, Y_A^m).

Substituting (10.5) and (10.6) in (10.4) leads to pose the Gaussian attack construction as the following optimization problem:

$$\min_{\mathbf{\Sigma}_{AA}\in\mathcal{S}_+^m} \; -(\lambda-1)\log|\mathbf{\Sigma}_{YY}+\mathbf{\Sigma}_{AA}| - \log|\mathbf{\Sigma}_{AA}+\sigma^2\mathbf{I}| + \lambda\mathrm{tr}(\mathbf{\Sigma}_{YY}^{-1}\mathbf{\Sigma}_{AA}). \tag{10.7}$$

The optimization domain $\mathcal{S}_+^m$ is a convex set. The following proposition characterizes the convexity of the cost function.

Proposition 12. *Let $\lambda \geq 1$. Then the cost function in the optimization problem in (10.7) is convex.*

The solution to (10.7) is characterized by the following theorem.

Theorem 19. *Let $\lambda \geq 1$. Then the solution to the optimization problem in (10.7) is*

$$\mathbf{\Sigma}_{AA}^{\star} = \frac{1}{\lambda}\mathbf{H}\mathbf{\Sigma}_{XX}\mathbf{H}^{\mathsf{T}}. \tag{10.8}$$

Corollary 4. *The mutual information between the vector of state variables and the vector of compromised measurements induced by the optimal attack construction is given by*

$$I(X^n;Y_A^m) = \frac{1}{2}\log\left|\mathbf{H}\mathbf{\Sigma}_{XX}\mathbf{H}^{\mathsf{T}}\left(\sigma^2\mathbf{I}+\frac{1}{\lambda}\mathbf{H}\mathbf{\Sigma}_{XX}\mathbf{H}^{\mathsf{T}}\right)^{-1}+\mathbf{I}\right|. \tag{10.9}$$

Theorem 19 shows that the generalized stealth attacks share the same structure of the stealth attacks in [28] up to a scaling factor determined by λ. The solution in Theorem 19 holds for the case in which $\lambda \geq 1$, and therefore, lacks full generality. However, the case in which $\lambda < 1$ yields unreasonably high probability of detection [28] which indicates that the proposed attack construction is indeed of practical interest in a wide range of state estimation settings.

The resulting attack construction is remarkably simple to implement provided that the information about the system is available to the attacker. Indeed, the attacker only requires access to the linearized Jacobian measurement matrix $\mathbf{H}$ and the second order statistics of the state variables, but the variance of the noise introduced by the sensors is not necessary. To obtain the Jacobian, a malicious attacker needs to know the topology of the grid, the admittances of the branches, and the operation point of the system. The second order statistics of the state variables on the other hand, can be estimated using historical data. In [28] it is shown that the attack construction with a sample covariance matrix of the state variables obtained with historical data is asymptotically optimal when the size of the training data grows to infinity.

It is interesting to note that the mutual information in (10.9) increases monotonically with λ and that it asymptotically converges to $I(X^n;Y^m)$, i.e. the case in which there is no attack. While the evaluation of the mutual information as shown in Corollary 4 is straightforward, the computation of the associated probability of

detection yields involved expressions that do not provide much insight. For that reason, the probability of detection of optimal attacks is treated in the following section.

10.3 Probability of Detection of Stealth Attacks

The asymptotic probability of detection of the generalized stealth attacks is governed by the KL divergence as described in (10.1). However in the non-asymptotic case, determining the probability of detection is difficult, and therefore, choosing a value of λ that provides the desired probability of detection is a challenging task. In this section we first provide a closed-form expression of the probability of detection by direct evaluation and show that the expression does not provide any practical insight over the choice of λ that achieves the desired detection performance. That being the case, we then provide an upper bound on the probability of detection, which, in turn, provides a lower bound on the value of λ that achieves the desired probability of detection.

10.3.1 Direct Evaluation of the Probability of Detection

Detection based on the LRT with threshold τ yields a probability of detection given by

$$\mathsf{P}_\mathsf{D} \triangleq \mathbb{E}\left[\mathbb{1}_{\left\{L(Y_A^m)\geq\tau\right\}}\right]. \tag{10.10}$$

The following proposition particularizes the above expression to the optimal attack construction described in Section 8.1.3.

Lemma 2. *The probability of detection of the LRT in (8.17) for the attack construction in (10.8) is given by*

$$\mathsf{P}_\mathsf{D}(\lambda) = \mathbb{P}\left[(U^p)^\mathsf{T}\boldsymbol{\Delta}U^p \geq \lambda\left(2\log\tau + \log\left|\mathbf{I}+\lambda^{-1}\boldsymbol{\Delta}\right|\right)\right], \tag{10.11}$$

where $p = rank(\mathbf{H}\boldsymbol{\Sigma}_{XX}\mathbf{H}^\mathsf{T})$, $U^p \in \mathbb{R}^p$ is a vector of random variables with distribution $\mathcal{N}(\mathbf{0},\mathbf{I})$, and $\boldsymbol{\Delta} \in \mathbb{R}^{p\times p}$ is a diagonal matrix with entries given by $(\boldsymbol{\Delta})_{i,i} = \lambda_i(\mathbf{H}\boldsymbol{\Sigma}_{XX}\mathbf{H}^\mathsf{T})\lambda_i(\boldsymbol{\Sigma}_{YY}^{-1})$, where $\lambda_i(\mathbf{A})$ with $i = 1,\ldots,p$ denotes the i-th eigenvalue of matrix $\mathbf{A}$ in descending order.

Notice that the left-hand term $(U^p)^\mathsf{T}\boldsymbol{\Delta}U^p$ in (10.11) is a weighted sum of independent χ^2 distributed random variables with one degree of freedom where the weights are determined by the diagonal entries of $\boldsymbol{\Delta}$ which depend on the second order statistics of the state variables, the Jacobian measurement matrix, and the variance of the noise; i.e. the attacker has no control over this term. The right-hand side contains in addition λ and τ, and therefore, the probability of attack detection is described as a function of the parameter λ. However, characterizing the distribution of the resulting random variable is not practical since there is no closed-form expression for the distribution of a positively weighted sum of independent χ^2 random variables

with one degree of freedom [110]. Usually, some moment matching approximation approaches such as the Lindsay-Pilla-Basak method [111] are utilized to solve this problem but the resulting expressions are complex and the relation of the probability of detection with λ is difficult to describe analytically following this course of action. In the following an upper bound on the probability of attack detection is derived. The upper bound is then used to provide a simple lower bound on the value λ that achieves the desired probability of detection.

10.3.2 Upper Bound on the Probability of Detection

The following theorem provides a sufficient condition for λ to achieve a desired probability of attack detection.

Theorem 20. *Let $\tau > 1$ be the decision threshold of the LRT. For any $t > 0$ and $\lambda \geq \max(\lambda^\star(t), 1)$ then the probability of attack detection satisfies*

$$\mathsf{P}_\mathsf{D}(\lambda) \leq e^{-t}, \tag{10.12}$$

where $\lambda^*(t)$ is the only positive solution of λ satisfying

$$2\lambda \log \tau - \frac{1}{2\lambda}\mathrm{tr}(\mathbf{\Delta}^2) - 2\sqrt{\mathrm{tr}(\mathbf{\Delta}^2)t} - 2||\mathbf{\Delta}||_\infty t = 0. \tag{10.13}$$

and $||\cdot||_\infty$ is the infinity norm.

It is interesting to note that for large values of λ the probability of detection decreases exponentially fast with λ. We will later show in the numerical results that the regime in which the exponentially fast decrease kicks in does not align with the saturation of the mutual information loss induced by the attack.

10.4 Examples

We evaluate the performance of stealth attacks in practical state estimation settings. In particular, the IEEE 14-Bus, 30-Bus and 118-Bus test systems are considered in the simulation. In state estimation with linearized dynamics, the Jacobian measurement matrix is determined by the operation point. We assume a DC state estimation scenario [112, 113], and thus, we set the resistances of the branches to 0 and the bus voltage magnitude to 1.0 per unit. Note that in this setting it is sufficient to specify the network topology, the branch reactances, real power flow, and the power injection values to fully characterize the system. Specifically, we use the IEEE test system framework provided by MATPOWER [114]. We choose the bus voltage angle to be the state variables, and use the power injection and the power flows in both directions as the measurements.

As stated in Section 10.3.1, there is no closed-form expression for the distribution of a positively weighted sum of independent χ^2 random variables, which is required to calculate the probability of detection of the generalized stealth attacks

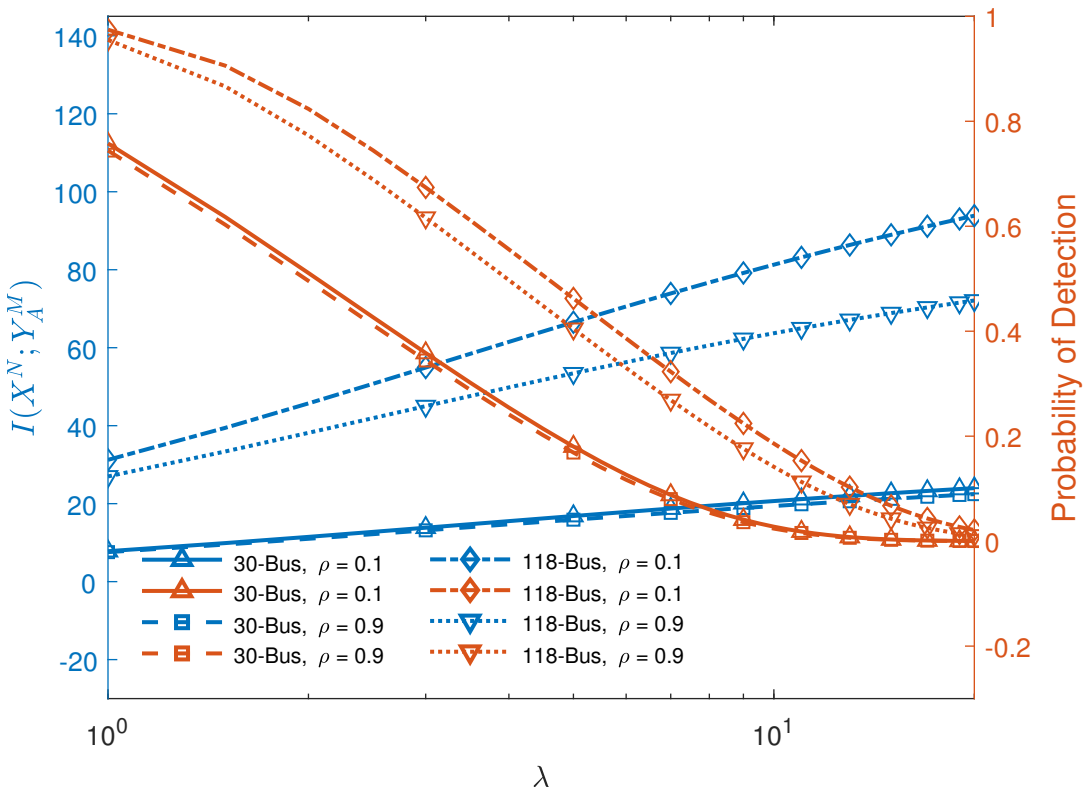

Figure 10.1: Performance of the generalized stealth attack in terms of mutual information and probability of detection for different values of λ and system size when $\rho = 0.1$, $\rho = 0.9$, SNR $= 10$ dB and $\tau = 2$.

as shown in Lemma 2. For that reason, the Lindsay–Pilla–Basak method and the MOMENTCHI2 package [115] are used to numerically evaluate the probability of attack detection.

The covariance matrix of the state variables is modelled as a Toeplitz matrix with exponential decay parameter ρ, where the exponential decay parameter ρ determines the correlation strength between different entries of the state variable vector. The performance of the generalized stealth attack is a function of weight given to the detection term in the attack construction cost function, i.e. λ, the correlation strength between state variables, i.e. ρ, and the Signal-to-Noise Ratio (SNR) of the power system which is defined as

$$\text{SNR} \triangleq 10 \log_{10} \left(\frac{\text{tr}(\mathbf{H}\boldsymbol{\Sigma}_{XX}\mathbf{H}^{\mathsf{T}})}{m\sigma^2} \right). \tag{10.14}$$

Figure 10.1 and Figure 10.2 depict the performance of the optimal attack construction for different values of λ and ρ with SNR $= 10$ dB and SNR $= 20$ dB, respectively, when $\tau = 2$. As expected, larger values of the parameter λ yield smaller values of the probability of attack detection while increasing the mutual information between the state variables vector and the compromised measurement vector. Observe that the probability of detection decreases approximately linearly for moderate values of

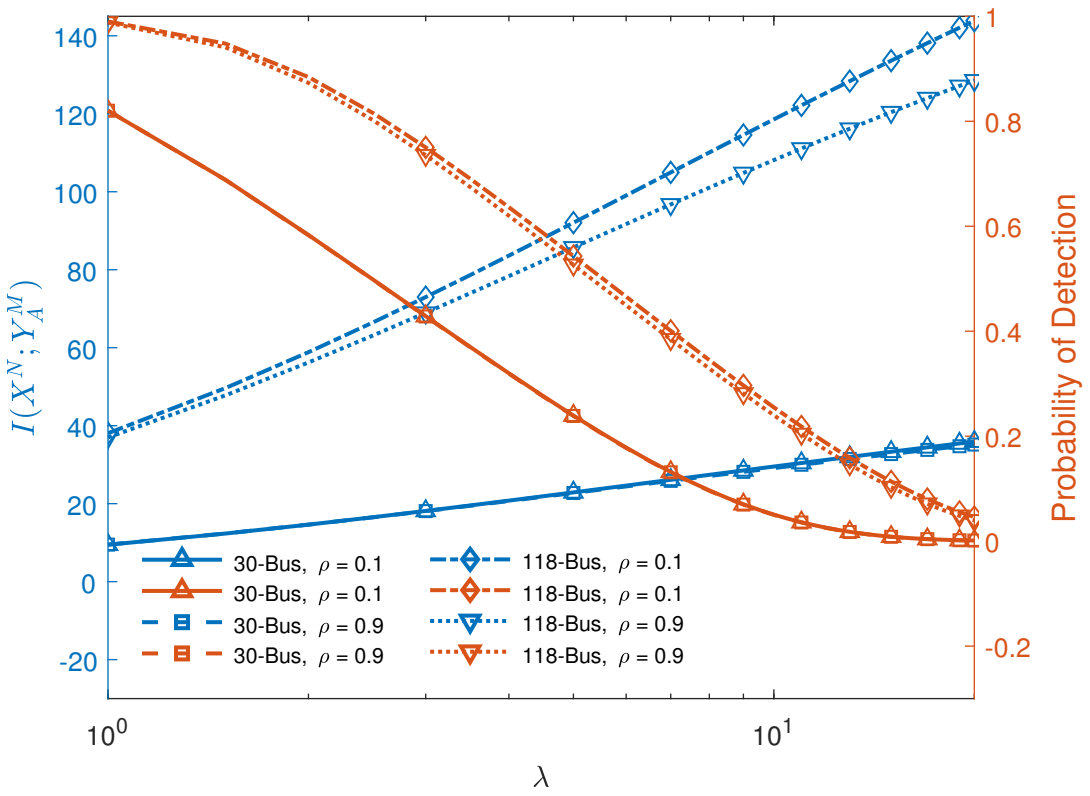

Figure 10.2: Performance of the generalized stealth attack in terms of mutual information and probability of detection for different values of λ and system size when $\rho = 0.1$, $\rho = 0.9$, SNR $= 20$ dB and $\tau = 2$.

λ. On the other hand, Theorem 20 states that for large values of λ the probability of detection decreases exponentially fast to zero. However, for the range of values of λ in which the decrease of probability of detection is approximately linear, there is no significant reduction on the rate of growth of mutual information. In view of this, the attacker needs to choose the value of λ carefully as the convergence of the mutual information to the asymptote $I(X^n; Y^m)$ is slower than that of the probability of detection to zero.

The comparison between the 30-Bus and 118-Bus systems shows that for the smaller size system the probability of detection decreases faster to zero while the rate of growth of mutual information is smaller than that on the larger system. This suggests that the choice of λ is particularly critical in large size systems as smaller size systems exhibit a more robust attack performance for different values of λ. The effect of the correlation between the state variables is significantly more noticeable for the 118-bus system. While there is a performance gain for the 30-bus system in terms of both mutual information and probability of detection due to the high correlation between the state variables, the improvement is more noteworthy for the 118-bus case. Remarkably, the difference in terms of mutual information between the case in which $\rho = 0.1$ and $\rho = 0.9$ increases as λ increases which indicates that the cost in terms of mutual information of reducing the probability of detection is

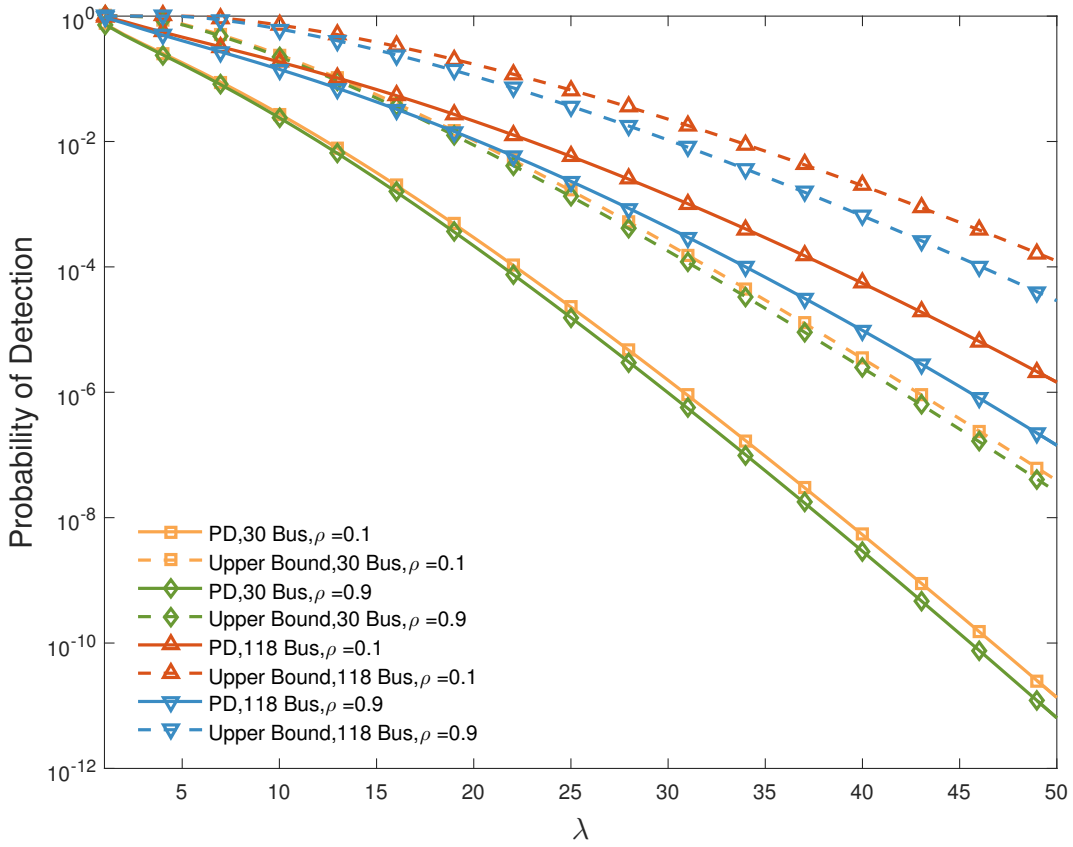

Figure 10.3: Upper bound on probability of detection given in Theorem 20 for different values of λ when $\rho = 0.1$ or 0.9, SNR $= 10$ dB, and $\tau = 2$.

large in the small values of correlation.

The performance of the upper bound given by Theorem 20 on the probability of detection for different values of λ and ρ when $\tau = 2$ and SNR $= 10$ dB is shown in Figure 10.3. Similarly, Figure 10.4 depicts the upper bound with the same parameters but with SNR $= 20$ dB. As shown by Theorem 20 the bound decreases exponentially fast for large values of λ. Still, there is a significant gap to the probability of attack detection evaluated numerically. This is partially due to the fact that our bound is based on the concentration inequality in [116] which introduces a gap of more than an order of magnitude. Interestingly, the gap decreases when the value of ρ increases although the change is not significant. More importantly, the bound is tighter for lower values of SNR for both 30-bus and 118-bus systems.

10.5 Conclusions and Further Work

The random attack produces different attack vectors for each set of measurements that are reported to the state estimator. The attack vectors are generated by sampling a defined attack vector distribution that yields attack vector realizations to be added to the measurements. The attack aims to disrupt the state estimation

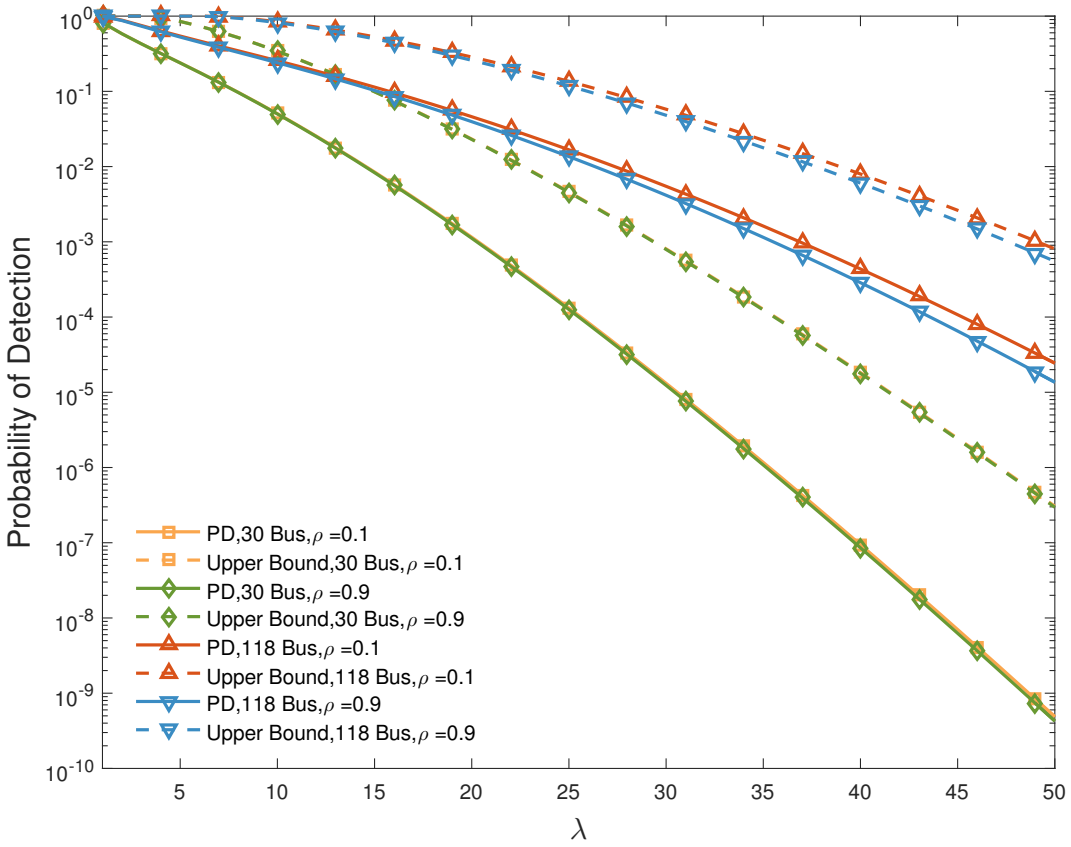

Figure 10.4: Upper bound on probability of detection given in Theorem 20 for different values of λ when $\rho = 0.1$ or 0.9, SNR $= 20$ dB, and $\tau = 2$.

process by minimizing the mutual information between the state variables and the altered measurements while minimizing the probability of detection. The rationale for posing the attack construction in information-theoretic terms stems from the fundamental character that information measures grant to the attack vector. By minimizing the mutual information, the attacker limits the performance of a wide range of estimation, detection, and learning options for the operator.

Appendices

Appendix A

Curriculum Vitae

A.1 Scholarship

A.1.1 Current Positions

Chargé de Recherche (Research Scientist)
INRIA - Centre de Recherche de Sophia Antipolis Méditerranée
Sophia Antipolis, France

Visiting Research Collaborator
Department of Electrical Engineering
Princeton University
Princeton, NJ, USA.

A.1.2 Education

- Ph.D., in Electronics and Communications, July 2011
  École Nationale Supérieure des Télécommunications, Paris, France.
  Manuscript: *Game Theoretic Approaches to Spectrum Sharing in Decentralized Self-Configuring Networks.*
  Advisors: Prof. Pierre Duhamel and Prof. Samson Lasaulce.
- M.Sc., in Mobile Communication Systems, December 2007
  École Nationale Supérieure des Télécommunications, Paris, France.
  Manuscript: *Decentralized Power Allocation in IDMA Networks.*
  Advisors: Prof. Laura Cottatellucci and Prof. Mérouane Debbah.
- B.Sc., in Electronics and Telecommunications Engineering, September 2005
  Universidad del Cauca, Popayán, Colombia.

A.1.3 Sabbatical Leaves

Princeton University Sept. 2017 - Sept. 2018
Princeton, NJ, USA.

A.1.4 Research Appointments

Start	End	Institutions	Positions and status
Dec. 2013	Present	INRIA	CR Classe Normale - Jan. 2020 - present: EPI NEO - Aug. 2017 - Jan. 2020: EPI MARACAS - Dec. 2013 - Aug. 2017: EPI SOCRATES `www-sop.inria.fr/members/Samir.Perlaza/`
Dec. 2013	Present	Princeton University	Department of Electrical Engineering - Sep. 2018 - Present: Visiting Research Collaborator - Sep. 2017 - Sep. 2018: Sabbatical Year. - Dec. 2013 - Sep. 2017: Visiting Research Collaborator `www.princeton.edu/~perlaza/`
Jan. 2012	Nov. 2013	Princeton University	Post-doc
Apr. 2011	Dec. 2011	CentraleSupelec	Post-doc

A.1.5 Industrial Experience

Orange Labs - France Telecom R&D,
Issy les Moulineaux, France. January 2008 to January 2011
Research Engineer

A.2 Student Advising

A.2.1 Postdoctoral Students

- **Sadaf Ul-Zuhra** - Academic Period: 2021 - 2023.
  Jointly advised with Eitan Altman (INRIA).
  Alma Mater: Indian Institute of Technology Bombay, Bombay, India.
- **Selma Belhadj-Amor** - Academic Period: 2014 - 2016.
  Jointly advised with Jean-Marie Gorce (INSA de Lyon).
  Alma Mater: Télécom ParisTech, Paris, France.
  Current Position: Data Analyst at BBM, Singapore.

A.2.2 Phd Students

- **Xiuzhen Ye** Academic Period: 2019 - 2022
  University of Sheffield, Department of Automatic Control and Systems Engineering, Sheffield, UK.
  Phd Student jointly advised with Iñaki Esnaola (Assistant Professor, University of Sheffield, UK) and Rob Harrison (Professor, University of Sheffield, UK).
  Thesis Topic: Data Injection Attacks in Power Systems

- **Dadja Toussaint** Academic Period: 2018 - 2021
  Université de Lyon, France
  Phd Student jointly advised with Jean-Marie Gorce (HDR, INSA- Lyon, France) and Philippe Mari (HDR, INSA-Rennes, France).
  Thesis Topic: Information Transmission with Latency and Reliability Constraints.

- **David Kibloff** Academic Period: 2015 - 2019
  Ecole doctoral EEA de Lyon.
  Phd student jointly advised with Guillaume Villemaud (HDR, INSA- Lyon, France).
  Thesis Title: Information-Theoretic Contributions to Covert Communications
  Current Position: Postdoctoral Fellow at Telecom ParisTech.

- **Nizar Khalfet** Academic Period: 2015 - 2019
  Ecole doctoral EEA de Lyon.
  Phd Student jointly advised with Jean-Marie Gorce (HDR, INSA- Lyon, France).
  Thesis Title: Simultaneous Information and Energy Transmission
  Current Position: Postdoctoral Fellow at University of Cyprus

- **Victor Quintero** Academic Period: 2014 - 2017
  Ecole doctoral EEA de Lyon. **INSA-Lyon Best Thesis Award**
  Phd student jointly advised with Jean-Marie Gorce (HDR, INSA- Lyon, France).
  Thesis Title: Noisy Channel-Output Feedback in the Interference Channel
  Current Position: Assistant Professor at Universidad del Cauca, Colombia.

A.2.3 Visiting Students

Students hosted within the INRIA team MARACAS.

- **Matei Catalin Moldoveanu**
  Master Student at University of Sheffield (Research Intern, 2019).

- **Michalis Eliodorous**
  PhD Student at University of Cyprus (Research Intern, 2019).

- **Nuria Vinyes**
  Undergraduate Student at Universidad Politécnica de Cataluña (Research Intern, 2019).

- **Charlotte Hoefler-Hoerle**
  Undergraduate Student at INSA de Lyon (programme “parcours recherche” de l’INSA de Lyon)

A.2.4 Master Students

- **INSA de Lyon, Département des Télécommunications**. I have participated in advising the following students during their final year projects at INSA–Lyon: Samia Bouchareb (2015) and Naslaty Ali Kari (2016), Lélio Chetot (2016), Matias Dwek (2016), and Mamy Niang (2016), Charlotte Hoefler-Hoerle (2019), Adam Ben-Ltaifa (2019), Carl Hatoum (2019).
- **ENS de Lyon, Département d'Informatique**. I have advised Tran Xuan Thang during his M2-level project (2019).

A.3 Awards and Acknowledgments

- **Prime d'encadrement Doctoral et de Recherche (PEDR)**, granted by INRIA in 2021.
- **Exploratory Action at INRIA** for characterizing the interplay between data acquisition and information processing in decentralized decision making by bringing together tools from information theory and game theory. Sophia Antipolis, France, February, 2021.
- **Fellowship of The Finnish Society of Sciences and Letters** for visiting the School of Energy Systems at Lappeenranta University of Technology, Finland. April, 2019.
- **2018 "Make our Planet Great Again" Fellowship**. The "Make Our Planet Great Again" Initiative was launched by the President of France Emmanuel Macron in June 2017 to reinforce the international engagements of the 2015 Paris Agreement on Climate Change. Project **"Energy-self-sufficient Mission Critical Communication Systems"** to be jointly carried out with **Rensselaer Polytechnic Institute, NY, USA.**
- **2017 INSA de Lyon Thesis Award**. Awarded to Victor Quintero for the thesis "Noisy Channel-Output Feedback in the Interference Channel". Domain of Information and Digital Societies. November 2018
- **Marie Sklodowska-Curie Fellow (2015-2017)**. H2020 Marie Sklodowska-Curie Actions - Individual Fellowship. EU Grant 659316. June 2015.
- **IEEE Senior Member**. Elevation to Senior Member of the IEEE Society. June 2015.
- **Prime d'encadrement Doctoral et de Recherche (PEDR)**, granted by INRIA in 2014.
- **Best Student Paper Award in the IEEE Intl. Conf. on Cognitive Radio Oriented Wireless Networks and Communications (CROWNCOM))** for the paper "On the Benefits of Bandwidth Limiting in Decentralized Vector Multiple Access Channels" by **Perlaza, S. M.**, Debbah, M.,

Lasaulce, S. and Bogucka, H. Hannover, Germany, June, 2009.

- **Recommendation from the IEEE MMTC Review Board Chair (2011)** to the paper "Satisfaction Equilibrium: A General Framework for QoS Provisioning in Self-Configuring Networks", by **Perlaza, S. M.** and Tembine, H. and Lasaulce, S. and Debbah, M. in the IEEE Global Communications Conference (GLOBECOM), Miami, USA, December, 2010.
- **IEEE Communications Letters Editorial Board: Certificate of Appreciation as Exemplary Reviewer (2010)**. November 2010.
- **Alβan Fellow (2006 - 2007)**. Recipient of one of the Alβan Fellowships: The European Union Programme of High Level Scholarship for Latin America. Grant E06M101130CO.
- **Baccalaureate "Honoris Causa"** granted by Colegio Nacional de Bachillerato - Instituto Tecnico on behalf of the National Minister of Education of Colombia. Santander de Quilichao, Colombia, December 2000.
- **City Council Agreement No. 028 of 1999** to create the award **Ciudad de los Samanes - Samir Alberto Medina Perlaza** in Santander de Quilichao, Colombia. This award is given to the top-ranked students in the national exams to access higher education in a ceremony held every year at the City Hall.

A.4 Scientific Dissemination

A.4.1 Tutorials

- **"Emerging Topics in 5G Networks: Simultaneous Wireless Information and Energy Transfer"**, Tutorial at the **IEEE Global Communications Conference** (GLOBECOM), Singapore, Singapore, December 2017. Joint work with Marco Maso (Huawei, France), Marco di Renzo (CNRS, France) and Bruno Clerckx (Imperial College London, UK).
- **"Emerging Topics in 5G Networks: Simultaneous Wireless Information and Energy Transfer"**, Tutorial at the **European Signal Processing Conference** (EUSIPCO), Kos Island, Greece, August 2017. Joint work with Marco Maso (Huawei, France), Marco di Renzo (CNRS, France) and Bruno Clerckx (Imperial College London, UK).
- **"Emerging Topics in 5G Networks: Simultaneous Wireless Information and Energy Transfer"**, Tutorial at the **IEEE International Conference on Communications** (ICC), Paris, France, May, 2017. Joint work with Marco Maso (Huawei, France) and Marco di Renzo (CNRS, France).
- **"Simultaneous Energy and Information Transmission"**, Tutorial at the **European Wireless Conference** (EW), Oulu, Finland, May, 2016. Joint

work with Ioannis Krikidis (University of Cyprus, Cyprus) and Selma Belhadj Amor (INRIA, France).

- **"Simultaneous Energy and Information Transmission"**, Tutorial at the 23rd **International Conference on Telecommunications** (ICT), Thessaloniki, Greece, May, 2016. Joint work with Selma Belhadj Amor (INRIA, France).
- **"Simultaneous Energy and Information Transmission"**, Tutorial at the 11th **International Conference on Cognitive Radio Oriented Wireless Networks** (CROWNCOM), Grenoble, France, May, 2016. Joint work with Selma Belhadj Amor (INRIA, France).
- **"Output Feedback in Wireless Communications"**, Tutorial at the **IEEE International Conference on Communications** (ICC), London, UK, June, 2015. Joint work with H. Vincent Poor (Princeton University, NJ) and Ravi Tandon (Virginia Tech, VA).

A.4.2 Keynotes

- **"Recent Advances in Simultaneous Information and Energy Transmission"**. Keynote at the 16th International Symposium on Wireless Communications Systems (ISWCS) - Workshop on Energy Harvesting Communication Networks. Oulu, Finland, August 27, 2019. **(Workshop Canceled)**
- **"Key Technologies in the IoT: Simultaneous Wireless Information and Energy Transmission"**. Keynote at the First Winter School on Information Theory and Signal Processing for Internet of Things, Villeurbanne, France, November 20, 2018.
- **"On the Benefits of Feedback in Wireless Communications"**, Keynote at the 12th International Conference on Wireless Communications, Networking and Mobile Computing (WICOM), Guilin, Popular Republic of China, August 2017.
- **"Games Arising in Decentralized Wireless Networks"**, Keynote at the Colombian Congress of Computer Sciences, Pereira, Colombia, September, 2014.

A.4.3 Interviews and Press Features

- Interview to Samir M. Perlaza "A view of the Internet of Things" in IEEE Communications Society – Cognitive Networks Technical Committee Newsletter, vol. 5, No. 1, May 2019.
- Review article by Walid Saad, "QoS Provisioning in Self-Configuring Networks: Beyond Nash Equilibrium", Vol. 2, No. 1, February 2011. on the

paper "Satisfaction Equilibrium: A General Framework for QoS Provisioning in Self-Configuring Networks", by **Perlaza, S. M.** and Tembine, H. and Lasaulce, S. and Debbah, M. in Proc. of the IEEE Global Communications Conference (GLOBECOM), Miami, USA, December, 2010.

A.4.4 Invited Talks

- "Cyber-Physical Systems seen through the lenses of an information theorist". Invited talk at INRIA, Centre de Recherche Sophia Antipolis Méditerranée, Comité des Equipes Projets, Sophia Antipolis, France, April 28, 2020.
- "Cyber-Physical Systems seen through the lenses of an information theorist". Invited talk at INRIA, Centre de Recherche Sophia Antipolis Méditerranée, Equipe-Projet NEO, Sophia Antipolis, France, April 22, 2020.
- "Transforming Broadcast Codes to perform Covert Communications". Invited talk at Department of Automatic Control and Systems Engineering, University of Sheffield, UK, November 26, 2019.
- "Transforming Broadcast Codes to perform Covert Communications". Invited talk at Centre d'Enseignement et de Recherche en Informatique (CERI), Université d'Avignon, France, November 14, 2019.
- "Simultaneous Information and Energy Transmission in Decentralized Networks". Invited talk at INRIA, Centre de Recherche Sophia Antipolis Méditerranée, Sophia Antipolis, France, September 24, 2019.
- "Simultaneous Information and Energy Transmission Systems". Invited talk at EURECOM, Sophia Antipolis, France, September 26 2019.
- "On Ultra-Reliable and Low Latency Simultaneous Information and Energy Transmission Systems". Invited talk at Lappeenranta University of Technology, Finland. School of Energy Systems. Lappeenranta, April 08 2019.
- "Information-Theoretic Security in the Smart Grid". Invited talk at Lappeenranta University of Technology, Finland. School of Energy Systems. Lappeenranta, April 07, 2019.
- "On Ultra-Reliable and Low Latency Simultaneous Information and Energy Transmission Systems". Invited talk at Université Notre-Dame-de-Louaizé, March 22, 2019, Zouk Mosbeh, Lebanon.
- "Simultaneous Wireless Information and Energy Transmission". Invited talk at Université de Lille. Institut d'électronique de microélectronique et de nanotechnologie (IEMN), October 4, 2018, Lille, France.
- "On the Strong Converses in the Multiple Access Channel", Invited talk at Electrical Engineering Department - Information Theory Reading Group at Princeton University. September 15, 2017, Princeton N.J. USA.

- "Simultaneous Wireless Information and Energy Transmission". Invited talk at École Nationale Supérieure de l'Électronique et de ses Applications (ENSEA). Équipe Traitement de l'Information et Systèmes (ETIS), May 18, 2017, Cergy-Pontoise, France.
- "On the Benefits of Feedback in Wireless Communications". Invited talk at the Department of Telecommunications, CentraleSupélec, Gif-sur-Yvette, France, December 2, 2016.
- "On the Benefits of Feedback in Wireless Communications". Invited talk at the Department of Electrical Engineering and Computer Science, Technical University of Berlin, Berlin, Germany, November 18, 2016.
- "Simultaneous Wireless Information and Energy Transmission". Invited talk at the University of Sheffield. Department of Automatic Control and Systems Engineering, April 6, 2016, Sheffield, UK.
- "On the Impact of Network-State Knowledge on the Feasibility of Secrecy". Invited talk at the London Probability Seminar, advances in information theory, Imperial College London, Juin 10, 2015, London, UK.
- "On the Impact of Network-State Knowledge on the Feasibility of Secrecy". Invited talk at the MESCAL Seminar, Inria, Rhône-Alpes Research Centre, Mai 21, 2015, Montbonnot, France.
- "Feedback in Distributed Wireless Communications". Invited talk at École Nationale Supérieure de l'Électronique et de ses Applications (ENSEA). Equipes Traitement de l'Information et Systèmes (ETIS), Juin 12, 2014, Cergy-Pontoise, France.
- "On the Impact of Network-State Knowledge on the Feasibility of Secrecy". Invited talk at GDR-ISIS Sécurité au niveau de la couche physique dans les réseaux sans-fil, Telecom ParisTech, May 22, 2014, Paris, France.
- "Feedback in Distributed Wireless Communications". Invited talk at University of Sheffield. Department of Automatic Control and Systems Engineering, April 27, 2014, Sheffield, UK.
- "Feedback in Distributed Wireless Communications". Invited talk at Inria Grenoble-Rhône-Alpes Research Centre, February 18, 2014, Montbonnot, France.
- "Games arising in Decentralized Multiuser Channels". Invited talk at Université Paris-Sud, Laboratoire de Recherche en Informatique (LRI), Jul. 16, 2013, Orsay, France.
- "Games arising in Decentralized Multiuser Channels". Invited talk at the Division of Communication Systems, Linköping University, March 22, 2013, Linköping, Sweden.

- "Perfect Output Feedback in the Decentralized Interference Channel". Invited talk at the "Centre d'Innovation en Télécommunications et Integration de Services - Citi-Lab", INRIA, March 11, 2013, Lyon, France.
- "Game Theory and Decentralized Interference Channels". Invited e-talk at the Wireless Networking, Signal Processing and Security Lab at University of Houston, February 1, 2013, Houston, TX.
- "Machine Learning: The bridge connecting Information, Game and Learning Theory". Invited talk at Telecom ParisTech, Department of Image and Signal Processing Group of Statistics and Applications, September 12, 2012, Paris, France.
- "How to achieve Stable Operating Points in Femtocell Networks?". Invited Speaker at the 5th International Workshop on Femtocells (and HetNets). February, 13 - 14 2012. King's College London, London, UK
- "Learning in Games Arising from Wireless Communication Systems". Invited Talk at Bell-Labs. December 13th, 2011, Paris, France.
- "Game Theory in Wireless Communications (some applications)". Invited Talk at Universidad ICESI, August 18th, 2011, Cali - Colombia.
- "Satisfaction Equilibrium: Definition, Learning Dynamics and Applications". Workshop on Algorithmic Game Theory: Dynamics and Convergence in Distributed Systems. Université de Grenoble, Laboratoire LIG. June 20th, 2011. Grenoble, France.
- "QoS Provisioning in Cognitive Small Cell Networks: Beyond Nash Equilibrium". Bell Labs - Supelec, Annual Meeting. Supelec, Alcatel Lucent Chair in Flexible Radio. May 26th, 2011. Gif sur Yvette, France.
- "Learning Equilibria with Partial Information in Cognitive Radio Networks". GDR-ISIS Seminar, "10 ans de Radio Intelligente : Bilan et perspectives". Telecom ParisTech. May 9, 2011. Paris, France.
- "Strategic Learning for Interference Mitigation in Femto Cell Networks". Centre for Wireless Communications (CWC) at University of Oulu. August 27, 2010. Oulu, Finland.
- "Dynamic Spectrum Access in Self-Configuring Networks". France Telecom R&D - Orange Labs, December 10, 2009. Issy les Moulineaux, France.
- "On the Base Station Selection and Base Station Sharing in Self-Configuring Networks". Signal Processing Division and Telecom Dept. at Supélec. September 18, 2009. Gif-sur-Yvette, France.
- "Game Theory for Dynamic Spectrum Access". France Telecom R&D - Orange Labs, April 26, 2009, Issy les Moulineaux, France.

- "Distributed Resource Allocation in IDMA Networks". Signal Processing Division and Telecom Dept. at Supélec, Mars 20, 2008. Gif-sur-Yvette, France.
- "A Game-Theoretic Framework for Power Allocation in Self-Organizing IDMA Networks". ENST Bretagne. December 7, 2007. Brest , France.
- "Decentralized Power Allocation in IDMA Systems". Department of Mobile Communications - Institut Eurecom. December 13, 2007. Sophia Antipolis, France

A.5 International Projects

- Principal (French) Investigator of EU funded H2020-MSCA-RISE-2019 project: "Testing and Evaluating Sophisticated information and communication Technologies for enaBling scalablE smart griD Deployment (TESTBED2)". Grant Agreement no. 872172.

  TESTBED2 is an interdisciplinary project that combines three academic disciplines - Electronic & Electrical Engineering, Computing Sciences and Macroeconomics, to address the developing of new techniques to improve the scalability of smart grid services, particularly considering the joint evolution of decarbonised power, heat and transport systems. Overall, the main objective of this project is to coordinate the action of 12 Universities and 5 enterprises (3 SMEs and 2 large enterprises) with complementary expertise to develop and test various promising strategies for ensuring the scalability of smart grid services, thereby facilitating successful deployment and full roll-out of smart grid technologies.

- Principal (French) Investigator of EU funded H2020-ERA-NET-MED-2015 project: "COMMunication systems with renewable Energy micro-griD (COMMED)". EU Project locally handled by ANR under Grant Agreement ANR-15-NMED-0009-03.

  The main objective of this project is to study the fundamental interplay between communication and power networks in the context of smart micro-grids and renewable energy sources. On the one hand, we study advanced signal processing techniques and communication methods that optimize the operation of smart micro-grid systems. On the other hand, we focus on mobile communication networks with base stations based on renewable energy sources and we investigate communication and networking techniques that take into account both data traffic and energy profiles to support high quality-of-service (QoS). The objectives of each technical work have been assigned in such a way as to ensure that the project's target is realised during the project's time period. The theoretical results derived will be tested using the telecommunication network of MTN in Cyprus but also the state-of-the-art equipment of the CITI/INRIA research lab in France. The outcome of this project will

provide a theoretical framework and a practical demonstration for the optimal cooperation between communication networks and power networks in the context of smart micro-grids and renewable energy sources which is in line with the objectives of the call's theme "Renewable Energy". The consortium has the expertise and the infrastructure to implement the objectives set and bring the project to a successful end.

- Principal Investigator of H2020 Marie Sklodowska-Curie Fellowship under EU Grant agreement 659316

  The project CYBERNETS focuses on the study of Cybernetic Communication Networks (CCN). CCNs are wireless networks that are context-aware, possess learning capabilities and artificial intelligence to guarantee reliability, efficiency and resilience to changes, failures or attacks via autonomous, self-configuring and self-healing individual and network behavior. Typical examples of CCNs are beyond-5G cellular systems and critical communication systems, e.g., law enforcement, disaster relief, body- area, medical instruments, space, and indoor/outdoor commercial applications. A practical implementation of a CCN requires extending classical communication systems to embrace the dynamics of fully decentralized systems whose components might exhibit either cooperative, non-cooperative or even malicious behaviors to improve individual and/or global performance. In this context, CYBERNETS aims to develop a relevant understanding of the interactions between information theory, game theory and signal processing to tackle two particular problems from both theoretical and practical perspectives: (I) use of feedback and (II) behavior adaptation in fully decentralized CCNs. In the former, the main objectives are: (i) to determine the fundamental limits of data transmission rates in CCNs with feedback; and (ii) to develop and test in real-systems, transmit-receive configurations to provide a proof-of-concept of feedback in CCNs. For the achievement of these practical objectives, CYBERNETS relies on the world-class testbed infrastructure of INRIA at the CITI Lab for fully closing the gap between theoretical analysis and real-system implementation. In the latter, the main objectives are: (i) to identify and explore alternatives for allowing transmitter-receiver pairs to learn equilibrium strategies in CCNs with and without feedback; (ii) to study the impact of network-state knowledge on scenarios derived from the malicious behavior of network components.

A.6 Community Service

A.6.1 Editorships

- Editor of the **IEEE Transactions on Communications** since 2018.
- Editor of the **IET Smart Grid** from 2018 to 2021.
- Associate Editor of the **Frontiers in Communications and Networks**,

since 2020 - present

- Guest Editor of the **IEEE Internet of Things Journal**, Special Issue on "Artificial Intelligence Powered Edge Computing for Internet of Things". Publication date: October 2020.

A.6.2 Committee Memberships

- Member of the On-Line Committee of the IEEE Information Theory Society. Sep. 2019 - Aug. 2022.
- Publication Chair of the International Symposium on Information Theory (ISIT), July, 2019, Paris, France.

A.6.3 Reviewing Activity

- **International Journals:** IEEE Journal on Selected Areas in Communications, IEEE Journal on Selected Topics in Signal Processing, IEEE Trans. on Wireless Communications, IEEE Trans. on Communications, IEEE Trans on Vehicular Technologies, IEEE Communications Letters, IEEE Trans. on Mobile Computing, IEEE Trans. on Information Theory, EURASIP Journal on Advances in Signal Processing, EURASIP Journal on Wireless Communications and Networking.
- **International Conferences:** Regural reviewer for ISIT, ITW, Eusipco, VTC, Rawnet, WiOpt, GameComm, Globecom, Colcom, PIMRC, Crowncom, WCMC, W-GREEN, ICT, IWCMC, ICC, Infocom, among others.

A.6.4 Conference Chairs

- Chair of the **"Special Session on Security and Privacy for Future Wireless Communication Systems",** at the 25th International ITG Workshop on Smart Antennas (WSA 2021) November 10-12, 2021, Sophia Antipolis, France.
- Chair of the **"Workshop on Resource Allocation, Cooperation and Competition in Wireless Networks (RAWNET)",** June 19, 2020, Volvos, Greece.
- Chair of the special session on **"Data Analytics for Power Systems"** hosted at the 2019 IEEE Data Science Workshop, June 2-5, 2019, Minneapolis, MN, USA.
- Chair of the **Workshop on Information and Decision Making**. A satellite event of the IEEE International Symposium on Information Theory (ISIT), Institut Henri Poincaré, Paris, France, July 10, 2019.

- Chair of the **International Workshop on Mathematical Tools for the IoT (MOTION)**. A full day workshop at the IEEE Wireless Communications and Networking Conference (WCNC), Marrakech, Morocco, April 15, 2019.
- Chair of the **Special Session on Energy Harvesting and Wireless Powered Communications**. A special session based on invited papers at the IEEE International Workshop on Signal Processing Advances in Wireless Communications (SPAWC), Cannes, France, July 5, 2019.
- Chair of the **Special Session on Estimation in Cyber-Physical Energy Systems**. A special session based on invited papers at the Eight IEEE Sensor Array and Multichannel Signal Processing (SAM2014). June, 2014, Coruña, Spain.

A.6.5 Evaluation Committees and Thesis Juries

- **Miguel Arrieta**, Phd thesis "Universal Privacy Guarantees for Smart Meters" at the Department of Automatic Control and Systems Engineering, University of Sheffield, November 29 2019, Sheffield, UK.
- **Committé du Prix Paul CASEAU** for the 2017 edition of the thesis award.
- **Alexander López-Parrado**, Phd thesis "Wideband Spectrum Sensing Algorithms Based on Sparse Fourier Transform: Design, Analysis and Implementation", Doctoral School of Electrical and Electronics Engineering, Universidad del Valle, February 15 2017, Cali, Colombia.
- **Chao He**, Phd thesis "Radiodiffusion avec CSIT retardée: Analyse de SNR fini et voie de retour hétérogène" at the École Doctorale de Sciences et Technologies de l'Information et de la Communication, CentraleSupélec, December 2 2016, Paris, France.

A.6.6 Technical Program Committees

- **IEEE International Workshop on Wirelessly Powered Systems and Networks (WPSN 2021)**
  14 – 16 July, 2021, Virtual Event
  Member of the Technical Program Committee
- **IEEE International Symposium on Personal, Indoor and Mobile Radio Communications (PIMRC)**
  13 – 16 September, 2021, Helsinki, Finland.
  Member of the Technical Program Committee, Track 4: Mobile and Wireless Networks
- **IEEE International Conference on Communications (ICC)**.
  14 – 18 June, 2021, Montreal, Canada.

Member of the Technical Program Committee of the Wireless Communications Symposium.

- **IEEE Wireless Communications and Networking Conference (WCNC)**.
  29 March – 1 April 2021, Nanjing, China
  Member of the Technical Program Committee (all tracks)
- **International Conference on Performance Evaluation Methodologies and Tools (ValueTools)**.
  October 29-31, 2021, Guangzhou, People's Republic of China
  Member of the Technical Program Committee.
- **International Conference on Computing, Networking and Communications (ICNC 2020)**.
  17-20 February, 2020, Big Island, Hawaii, USA.
  Member of the Technical Program Committee.
- **IEEE International Conference on Communications (ICC)**.
  7-11 June, 2020, Dublin, Ireland.
  Member of the Technical Program Committee of the Wireless Communications Symposium.
- **IEEE International Symposium on Personal, Indoor and Mobile Radio Communications (PIMRC 2020)**
  31 August – 3 September, 2020, London, UK.
  Member of the Technical Program Committee, Track 3: Mobile and Wireless Networks.
- **IEEE International Symposium on Personal, Indoor and Mobile Radio Communications (PIMRC 2019)**.
  8-11 September 2019, Istanbul, Turkey
  Member of the Technical Program Committee, Track 1: Fundamentals and PHY, and Track 3: Mobile and Wireless Networks.
- **IEEE Global Communications Conference (Globecom)**.
  9-13 December 2018, Abu Dhabi, UAE
  Member of the Technical Program Committee of Workshop on Green and Sustainable 5G Wireless Networks.
- **IEEE International Symposium on Personal, Indoor and Mobile Radio Communications (PIMRC 2018)**.
  9-12 September 2018, Bologna, Italy
  Member of the Technical Program Committee, Track 3: Mobile and Wireless Networks.
- **IEEE International Symposium on Personal, Indoor and Mobile Radio Communications (PIMRC 2017)**.
  08-13 October 2017, Montreal, QC, Canada.
  Member of the Technical Program Committee, Track 3: Mobile and Wireless

Networks.

- **IEEE Wireless Communications and Networking Conference (WCNC)**.
  19-22 March 2017, San Francisco, CA.
  Member of the Technical Program Committee, PHY and Fundamentals Track.
- **3rd Workshop on Physical-layer Methods for Wireless Security**.
  Workshop taking place at IEEE CNS 2016 in Philadelphia, PA, USA, Oct 17-19, 2016.
  Member of the Technical Program Committee.
- **Workshop on Wireless Energy Harvesting Communication Network**.
  Workshop taking place at IEEE Global Communications Conference (GLOBECOM) in Washington, DC USA, Dec. 8, 2016.
  Member of the Technical Program Committee.
- **IEEE WCNC'2016 Workshop on Green and Sustainable 5G Wireless Networks (GRASNET)**.
  April 3, 2016, Doha, Qatar
  Member of the Technical Program Committee.
- **6th International Conference on Game Theory for Networks (GameNets)**.
  May 10-12, 2016, Kelowna, BC, Canada.
  Member of the Technical Program Committee.
- **IEEE ICC 2015 Workshop on Next Generation Backhaul/Fronthaul Networks (BackNets)**.
  June 8, 2015, London, UK
  Member of the Technical Program Committee.
- **IEEE ICC 2015 Workshop on Wireless Physical Layer Security (WPLS)** June 8, 2015, London, UK
  Member of the Technical Program Committee.
- **IEEE ICC 2015 Workshop on Small Cell and 5G Networks (SmallNets)**.
  June 8, 2015, London, UK
  Member of the Technical Program Committee.
- **IEEE PIMRC Workshop on Cooperative and Heterogeneous Cellular Networks (WDN-CN)**.
  September 2, 2014, Washington, DC, USA
  Member of the Technical Program Committee.
- **IEEE ICC 2014 Workshop on Small Cell and 5G Networks (SmallNets)**.
  June 10, 2014, Sydney, Australia
  Member of the Technical Program Committee.
- **IEEE INFOCOM Workshop on Communications and Control for**

Smart Energy Systems.
April 27 - May 2, 2014, Toronto, CA
Member of the Technical Program Committee.

- **The 2nd IEEE Global Conference on Signal and Information Processing**.
  Track: Game Theory for Signal Processing and Communications
  December 3-5, 2014, Atlanta, GA, USA
  Member of the Technical Program Committee.

- **Conference on Decision and Game Theory for Security (GameSec)**.
  November 6-7, 2014, Los Angeles, CA, USA
  Member of the Technical Program Committee.

- **5th International Wireless Summit 2013 (Wireless Vitae, WPMC, WWSMC)**.
  June 24-27, 2013, Atlantic City, NJ, USA.
  Member of the Technical Program Committee.

- **International workshop on Self-Organization in heterogeneous NETworks (ISONET)**.
  Workshop in conjunction with IEEE ICC 2013.
  June 9-13, 2013, Budapest, Hungary.
  Member of the Technical Program Committee.

- **The Second IEEE INFOCOM Workshop on Green Networking and Smart Grids**.
  Workshop in conduction with IEEE INFOCOM 2013.
  19 April, 2013. Turin, Italy.
  Member of the Technical Program Committee.

- **IEEE Symposium on Computers and Informatics**.
  7-9 April, 2013. Langkawi, Malaysia.
  Member of the Technical Program Committee.

- **International Conference on Computing, Networking and Communications (ICNC)**.
  28-31 January, 2013. San Diego, CA, USA.
  Member of the Technical Program Committee.

- **IEEE 4th Int. Workshop on Heterogeneous and Small Cell Networks (HetSNets)** .
  Workshop in conjunction with IEEE Globecom 2012.
  December 3-7, 2012, Anaheim, California.
  Member of the Technical Program Committee.

- **International WDN Workshop on Cooperative and Heterogeneous Cellular Networks**.
  Workshop in conjunction with IEEE PIMRC 2012.

9 -12 September, 2012. Sydney, Australia.
Member of the Technical Program Committee.

- **Second Workshop on Cooperative Heterogeneous Networks (coHetNet2012)**.
  30 July - 2 August, 2012. Munich, Germany
  Member of the Technical Program Committee.

- **Fourth International Workshop on Indoor and Outdoor Femto Cells (IOFC2012)**.
  14 May 2012, Paderborn, Germany
  Member of the Technical Program Committee.

- **IEEE ICC 2012 Workshop on Small Cell Wireless Networks (SmallNets)**.
  10-15 June 2012, Ottawa, Canada.
  Member of the Technical Program Committee.

- **IEEE 74th Vehicular Technology Conference: VTC2011-Fall**.
  5-8 September 2011, San Francisco, United States
  Member of the Technical Program Committee (Wireless Networks Track).

- **3rd International Workshop on Security and Communication Networks (IWSCN 2011)**.
  May 18–20, 2011 Gjovik, Norway
  Member of the Technical Program Committee.

- **International Wireless Communications and Mobile Computing Conference (IWCMC 2011)**.
  July 5-8, 2011. Istanbul, Turkey
  Member of the Technical Program Committee (Mobile Computing Symposium).

Appendix B

Teaching

B.1 Academic Year 2020-2021

B.1.1 Selected Topics in Information Theory

"INFO5147 – Selected Topics in Information Theory" is a 30-hour Master 2 course taught at École Normale Supérieure de Lyon (ENS de Lyon), Computer Science Department, during Fall 2020 - 2021. This course was taught together with Malcolm Egan (INRIA) and Jean-Marie Gorce (INSA de Lyon). My participation in this course is 16 hours (Lectures 1- 8).

Course Description

This course is divided into two parts: Theoretical Foundations and Applications.

The objective of the first part is to level the ground to study information theory outside the classical framework of communications theory. The motivation for studying information theory outside its most prominent application domain is to widen and strengthen its connections with other disciplines and mathematical theories, in particular, real analysis, measure theory, probability theory, optimization, game theory, and statistics. This choice provides a more general look to information theory and might inspire new applications in different fields. Certainly, by adopting this choice, information theory can be truly appreciated as a developing mathematical theory whose impact on pure and applied sciences is yet to be discovered.

The second part focuses on the applications of information theory in statistics, in particular, stochastic approximations and expectation maximization algorithms; and communications theory, more specifically, storage and data transmission. These problems are studied from a modern perspective in which asymptotic assumptions are avoided. That is, these problems are formulated taking into account that data storage takes place with finite storage capacity; and data transmission takes place within a finite period. This rises the consideration of distorsion and decoding-error probabilities that are certainly bounded away from zero. Within this context, the

fundamental limits of data storage and data transmission are studied in scenarios that are close to real-system implementations. Open problems in multi-user information theory in the finite blocklength regime are briefly presented. The end of this part is dedicated to a brief introduction to compressive sensing and its applications in networking.

Content

- Part I: Theoretical Foundations
  - Lecture 1: Elements of Measure Theory by S. Perlaza – Sep. 08, 2020. 10h15 - 12h15
    - Review of algebra of sets
    - Review of Darboux-Riemann integration
    - The problem of measure
    - Jordan and Lebesgue measures
  - Lecture 2: Elements of Measure Theory by S. Perlaza – Sep. 10, 2020. 15h45 - 17h45
    - Lebesgue measurable functions
    - Lebesgue integral
    - Measures, measurable spaces
  - Lecture 3: Elements of Measure Theory by S. Perlaza – Sep. 15, 2020. 10h15 - 12h15
    - A general theory of Lebesgue integration
    - Monotone convergence theorem
    - Dominated convergence theorem
  - Lecture 4: Measure Theoretic Probability by S. Perlaza – Sep. 17, 2020. 15h45 - 17h45
    - The Radon-Nikodym derivative
    - Distance between measures
    - Probability spaces and random variables
    - Expectation, conditional expectation, and independence
  - Lecture 5: Information Measures by S. Perlaza – Sep. 22, 2020. 10h15 - 12h15
    - Information and measures of information
    - Information, joint information, and conditional information

    - Entropy, joint entropy, and conditional entropy
  - Lecture 6: Information Measures by S. Perlaza – Sep. 24, 2020. 15h45 - 17h45
    - Relative information and Relative entropy
    - Mutual information
    - Bounds on information measures
  - Lecture 7: Hypothesis Testing – by S. Perlaza Sep. 29, 2020. 10h15 - 12h15
    - The problem of statistical hypothesis testing
    - Bayesian method
    - Minmax method
  - Lecture 8: Hypothesis Testing – by S. Perlaza Oct. 1, 2020. 15h45 - 17h45
    - Neyman-Pearson method
    - Method of Types
    - Sanov's theorem
    - Chernoff-Stein lemma
- Part II - A: Applications to Maximum Likelihood Estimation and Model Selection
  - Lecture 9: Expectation-Maximization Algorithms by M. Egan – Oct. 6, 2020. 10h15 - 12h15
  - Lecture 10: Information Theoretic Criteria for Model Selection by M. Egan – Oct. 8, 2020. 15h45 - 17h45
- Part II - B: Applications to Communication Theory
  - Lecture 11: Information and Estimation by J.-M. Gorce – Oct. 13, 2020. 10h15 - 12h15
  - Lecture 12: Lossless and Lossy Compression by J.-M. Gorce – Oct. 15, 2020. 15h45 - 17h45
  - Lecture 13: Channel Coding by J.-M. Gorce – Oct. 20, 2020. 10h15 - 12h15
  - Lecture 14: Multi-User Networks by J.-M. Gorce – Oct. 22, 2020. 15h45 - 17h45
- Final Exams

- Lecture 15: Student Contest (Final Exams) – Nov. 10, 2020. 10h15 - 12h15
- Lecture 16: Student Context (Final Exams) – Nov. 12, 2020. 15h45 - 17h45

Evaluation

- Weekly homeworks (40 %)
- In-class work (10 %) – In the form of oral questions
- Final Exam (50 %) – In the form of 30-minute presentation (possibly on the blackboard)

B.2 Academic Year 2019 -2020

B.2.1 Advanced Topics in Information Theory

"INFO5147 – Advanced Topics in Information Theory" is a 30-hour Master 2 course taught at École Normale Supérieure de Lyon (ENS de Lyon), Computer Science Department, during Fall 2019 - 2020. This course was taught together with Jean-Marie Gorce (INSA de Lyon). My participation in this course is 16 hours (Lectures 1- 7).

Course Description

The course "Advanced Topics in Information Theory" at the Computer Science Department at ENS de Lyon opened for the fall semester 2019. This course was taught by Samir M. Perlaza and Jean-Marie Gorce. It explores connections between information theory and other fields in physics and mathematics to tackle some selected topics including Concentration Inequalities, Detection and Estimation, Hypothesis Testing, Decision-Making Processes, Data Compression, Data Transmission, and Data Analytics.

Content

- Lecture 1 by S. Perlaza (Sep. 13, 2019): Elements of Measure Theory
- Lecture 2 by S. Perlaza (Sep. 20, 2019): Measure Theoretic Probability
- Lecture 3 by S. Perlaza (Sep. 27, 2019): Information Measures
- Lecture 4 by S. Perlaza (Oct. 4, 2019): Concentration Inequalities
- Lecture 5 by S. Perlaza (Oct. 11, 2019): Hypothesis Testing — Part I
- Lecture 6 by S. Perlaza (Oct. 18, 2019): Hypothesis Testing — Part II
- Lecture 7 by S. Perlaza (Oct. 25, 2019): Hypothesis Testing — Part III

- Lecture 8 by J. M. Gorce (Nov. 8, 2019): Data Transmission (1): Point-to-Point Channels
- Lecture 9 by J. M. Gorce (Nov. 22, 2019): Data Transmission (2): Point-to-Point Channels
- Lecture 10 by J. M. Gorce (Nov. 29, 2019): Data Storage (1): Lossless Compression
- Lecture 11 by J. M. Gorce (Dec. 6, 2019): Data Storage (2): Lossy Compression
- Lecture 12 by J. M. Gorce (Dec. 13, 2019): Data Transmission in Networks: MAC and BC
- Lecture 13 by J. M. Gorce (Dec. 20, 2019): Data Transmission in Networks: Interference Channels and Interference Management
- Lecture 14 by J. M. Gorce (Jan. 10, 2020): Large Scale Networks: Stochastic-Geometry based Approaches
- Final Exam (Jan. 17, 2020)

Evaluation

- Weekly homeworks (40 %)
- In-class work (10 %) – In the form of oral questions
- Final Exam (50 %) – In the form of 30-minute presentation

B.3 Academic Year 2017 -2018

B.3.1 Network Information Theory

"INFO5147 – Network Information Theory" was a 28-hour Master 2 course taught at École Normale Supérieure de Lyon (ENS de Lyon), Computer Science Department, during Fall 2016 - 2017. This course was taught together with Jean-Marie Gorce (INSA de Lyon). My participation in this course is 16 hours.

Course Description

This course builds upon the course on fundamentals of information theory. Using these foundations, which are reviewed in the first two lectures, this course explores the fundamental limits of data transmission in several canonical multi-user channels: (i) Multiple Access Channels; (ii) Broadcast Channels; (iii) Interference Channels and (iv) Relay Channels. In all these scenarios, the notion of achievable, converse and capacity region are thoroughly studied. The analysis focuses mainly in the blocklength asymptotic regime. Thus, most of these results are studied using classical methods based on typicality. Two lectures are devoted to the study of tools that

allow the analysis of these canonical channels from a non-asymptotic block-length point of view. In the last part of the course, more advanced topics such as channel output feedback, highly dense networks and simultaneous information and energy transmission are studied.

Content

- Lecture 1 by S. Perlaza (September 09, 2016): A Review on Information Measures
- Lecture 2 by S. Perlaza (September 16, 2016): Weak and Strong Typicality
- Lecture 3 by J.M. Gorce (October 07, 2016): Point-to-Point Channels
- Lecture 4 by S. Perlaza (October 14, 2016): Multiple Access Channels - Part I
- Lecture 5 by S. Perlaza (October 21, 2016): Multiple Access Channels - Part II
- Lecture 6 by J.M. Gorce (November 04, 2016): Broadcast Channels
- Lecture 7 by J.M. Gorce (November 22, 2016): Relay Channels - Part I
- Lecture 8 by J.M. Gorce (November 25, 2016): Relay Channels - Part II
- Lecture 9 by S. Perlaza (December 13, 2016): Interference Channels
- Lecture 10 by S. Perlaza (December 16, 2016): Feedback
- Lecture 11 by J.M. Gorce (January 04, 2017): Non-Asymptotic Block length Regime
- Lecture 12 by S. Perlaza (January 06, 2017): Energy and Information Transmission
- Final Exam (January 11, 2018)

Evaluation

- Weekly homeworks (40 %)
- In-class work (10 %) – In the form of oral questions
- Final Exam (50 %) – In the form of 30-minute presentation

Appendix C

Scientific Production

C.1 Patents

(P1) Perlaza, S. M. and Salingue, G. ,"Procédé de sélection de canal par un émetteur, procédé et dispositif d'émission de données et programme d'ordinateur associés", France, Sept., 2010. No. 10 03894, France Telecom - Orange Labs.

(P2) Perlaza, S. M. and Lasaulce, S. and Salingue, G.,"Strategic communications in Wireless Self-Configuring Networks", France, Dec. 2010, No. 11 54719, France Telecom - Orange Labs.

C.2 Books

(B1) Ali Tajer, and **Samir M. Perlaza**, and H. Vincent Poor, (Editors) "Advanced Data Analytics for Power Systems". Cambridge University Press, Cambridge, UK, 2021.

C.3 Book Chapters

(BC-4) Perlaza, S. M. and Iñaki Esnaola and Sun Ke, "Data Injection Attacks", in Ali Tajer, Samir M. Perlaza and H. Vincent Poor (Eds.), "Advanced Data Analytics for Power Systems", Cambridge Univ. Press, 2020.

(BC-3) Perlaza, S. M. and Lasaulce, S. "Game-Theoretic Solution Concepts and Learning Algorithms", in Tansu Alpcan, Holger Boche, Michael Honig, H. Vincent Poor (Eds.), "Mechanisms and Games for Dynamic Spectrum Allocation", Cambridge Univ. Press, 2014.

(BC-2) Bennis, M. and **Perlaza, S. M.** and Debbah, M. "Game Theory and Femtocell Communications: Making Network Deployment Feasible" in Saeed, R. A. and Chaudhari, B. S. (Editors), "Femtocell Communications: Business Opportunities and Deployment Challenges". IGI Global, USA, 2011.

(BC-1) **Perlaza, S. M.** and Lasaulce, S. and Debbah, M. and Chaufray, J-M., "Game Theory for Dynamic Spectrum Access", in Y. Zhang, J. Zheng, and H.-H. Chen (Eds.), Cognitive Radio Networks: Architectures, Protocols and Standards, Auerbach Publications, 2010.

C.4 Journal Papers

(J-23) Eitan Altman, Izza Mounir, Fatim-Zahra Najid, and **Samir M. Perlaza**, "On the true number of COVID-19 infections: Effect of Sensitivity, Specificity and Number of Tests in Prevalence Estimation", International Journal of Environmental Research and Public Health, 2020.

(J-22) Dadja Anade, Jean-Marie Gorce, Philippe Mary, and **Samir M. Perlaza**, "An upper bound on the error induced by saddlepoint approximations - Applications to information theory", Entropy, vol. 22, no. 6, pp. 1–39, Jun., 2020.

(J-21) Sun Ke, Iñaki Esnaola, **Samir M. Perlaza**, and H. Vincent Poor, "Stealth Attacks on the Smart Grid". IEEE Transactions on Smart Grid, vol. 11, no. 2, pp. 1276-1285, Mar., 2020.

(J-20) Nizar Khalfet and **Samir M. Perlaza**, "Simultaneous Information and Energy Transmission in the Two-User Gaussian Interference Channel". IEEE Journal on Selected Areas in Communications, Special Issue on Wireless Transmission of Information and Power, vol. 37, no. 1, pp. 156-170, Jan. 2019.

(J-19) Cristian Genes and Iñaki Esnaola and **Samir M. Perlaza** and Luis F. Ochoa and Daniel Coca, "Robust Recovery of Missing Data in Electricity Distribution Systems". IEEE Transactions on Smart Grid, vol. 10, no. 4, pp. 4057-4067, Jul., 2019.

(J-18) Victor Quintero and **Samir M. Perlaza** and Iñaki Esnaola and Jean-Marie Gorce. "Approximate Capacity Region of the Two-User Gaussian Interference Channel with Noisy Channel-Output Feedback" IEEE Transactions on Information Theory, vol. 64 no. 7, pp. 5326-5358, Jul., 2018.

(J-17) Victor Quintero and **Samir M. Perlaza** and Iñaki Esnaola and Jean-Marie Gorce. "When Does Output Feedback Enlarge the Capacity of the Interference Channel?" IEEE Transactions on Communications, vol. 66 no. 2, pp. 615-628, Feb., 2018.

(J-16) Goonewardena, M. and **Perlaza, S. M.** and Yadav, A. and Ajib, W. "Generalized Satisfaction Equilibrium for Service-Level Provisioning in Wireless Networks". IEEE Transactions on Communications, vol. 65 no. 6, pp. 2427 – 2437, Jun. 2017.

(J-15) Belhadj Amor, S. and **Perlaza, S. M.** and Krikidis, I. and Poor, H. V., "Feedback Enhances Simultaneous Information and Energy Transmission in

Multiple Access Channels". IEEE Transactions on Information Theory, vol. 63, no. 8, pp. 5244–5265, Aug 2017.

(J-14) Yang, C. and Li, J. and Semasinghe, P. and Hossain, E. and **Perlaza, S. M.** and Han, Zhu. "Distributed Interference and Energy-Aware Power Control for Ultra-Dense D2D Networks: A Mean Field Game", IEEE Transactions on Wireless Communications, vol. 16 no. 2, pp. 268-279, Feb. 2017.

(J-13) Esnaola, I. and **Perlaza, S. M.**, Poor, H. V., and Kosut, Oliver. "Maximum Distortion Attacks in Electricity Grids", IEEE Transactions on Smart Grid, vol. 7, no. 4, pp. 2007-2015, Jul. 2016.

(J-12) **Perlaza, S. M.** and Tandon, R. and Poor, H. V. and Han, Z. "Perfect Output Feedback in the 2-User Decentralized Interference Channel". IEEE Transactions on Information Theory, vol. 61 no. 10 pp. 5441- 5462, Oct. 2015.

(J-11) Ding, Z. and **Perlaza, S. M.** and Esnaola, I. and Poor, H. V. "Power Allocation Strategies in Energy Harvesting Wireless Cooperative Networks". IEEE Transactions on Wireless Communications, vol. 13 no. 2 pp. 846-860, Feb. 2014.

(J-10) Rose, L. and **Perlaza, S. M.** and Debbah, M. and C. Le Martret, "Self-Organization in Decentralized Networks: A Trial and Error Learning Approach", IEEE Transactions in Wireless Communications, vol. 13 no. 1 pp. 268-279, Jan. 2014.

(J-9) Chorti, A. and **Perlaza, S. M.** and Poor, H.V. and Han, Z. "On the Resilience of Wireless Multiuser Networks to Passive and Active Eavesdroppers". IEEE Journal on Selected Areas in Communications, vol. 31, no. 9, pp. 1850–1863, Sep. 2013.

(J-8) Bennis, M. and **Perlaza, S. M.** and Blasco, P. and Han Z. and Poor, H.V., "Self-Organization in Small Cell Networks: A Reinforcement Learning Approach". IEEE Transactions on Wireless Communications, vol. 12 no. 7, pp. 3202–3212, Jul. 2013.

(J-7) **Perlaza, S. M.** and Lasaulce, S. and Debbah, M., "Equilibria of Channel Selection Games in Parallel Multiple Access Channels". Eurasip Journal on Wireless Communications and Networks, vol. 2013, no. 15, pp. 1–23, Jan. 2013.

(J-6) Couillet, R., and **Perlaza, S. M.**, and Tembine, H. and Debbah, M., "Electrical Vehicles in the Smart Grid: A Mean Field Game Analysis", IEEE Journal on Selected Areas in Communications, vol. 30, no. 7, pp. 1086–1096, Jul. 2012.

(J-5) **Perlaza, S. M.** and Tembine, H. and Lasaulce, S. and Debbah, M., "Quality-Of-Service Provisioning in Decentralized Networks: A Satisfaction Equilibrium

Approach". IEEE Journal in Selected Topics in Signal Processing. Special Issue in Game Theory for Signal Processing. vol. 6, n. 2, pp. 104–116, Apr. 2012.

(J-4) **Perlaza, S. M.** and Florez, V. Q. and Tembine, H. and Lasaulce, S., "On the Convergence of Fictitious Play in Channel Selection Games", IEEE Latin America Transactions, vol. 9, no. 4, pp. 470–476, Sep. 2011. **(Invited Paper)**

(J-3) Rose, L. and **Perlaza, S. M.**, and Lasaulce, S. and Debbah, M., "Learning Equilibria with Partial Information in Wireless Networks", IEEE Communications Magazine, Special Issue in Game Theory for Wireless Communications, vol. 49, n. 8, pp. 136–142, Aug. 2011.

(J-2) **Perlaza, S. M.** and Fawaz, N. and Lasaulce, S. and Debbah, M., "From Spectrum Pooling to Space Pooling: Opportunistic Interference Alignment in MIMO Cognitive Networks". IEEE Trans. in Signal Processing, vol.58, no.7, pp. 3728–3741, Jul. 2010.

(J-1) **Perlaza, S. M.** and Villalobos, G.A. and Vera, P. V., "Sistemas de Telecomunicaciones por Satélite Frente a la Convergencia". Colombian Magazine in Telecommunications (RCT), CINTEL, vol.13, no. 38, pp. 74–76, 2005.

C.5 International Conferences

(C-58) Dadja Anade, Jean-Marie Gorce, Philippe Mary, and **Samir M. Perlaza**, "Saddlepoint Approximations of Cumulative Distribution Functions of Sums of Random Vectors", in Proc. IEEE Intl. Symposium on Information Theory (ISIT), Melbourne, Australia, Jul., 2021.

(C-59) Xiuzhen Ye, Iñaki Esnaola, **Samir M. Perlaza**, and Robert F. Harrison, "Information Theoretic Data Injection Attacks with Sparsity Constraints", submitted to the IEEE International Conference on Communications, Control, and Computing Technologies for Smart Grids, Virtual Conference, Nov., 2020

(C-58) Dadja Anade, Jean-Marie Gorce, Philippe Mary, and **Samir M. Perlaza**, "On the saddlepoint approximation of the dependence testing bound in memoryless channels", in Proc. of the IEEE International Conference on Communications (ICC), Dublin, Ireland, Jun., 2020.

(C-57) David Kibloff, **Samir M. Perlaza**, Ligong Wang. "Embedding Covert Information in a Given Broadcast Code" in Proc. IEEE Intl. Symposium on Information Theory (ISIT), Paris, France, Jul., 2019.

(C-56) Nizar Khalfet and **Samir M. Perlaza**. "On the Maximum Energy Transmission Rate in Ultra-Reliable and Low Latency SIET" in Proc. of the Third International Balkan Conference on Communications and Networking (BalkansCom), Skopje, North Macedonia, Jun., 2019.

(**Invited paper**)

(C-55) Cristian Genes, Iñaki Esnaola, **Samir M. Perlaza** and Daniel Coca. "Recovery of Missing Data in Correlated Smart Grid Datasets" in Proc. IEEE Data Science Workshop (DSW), Minneapolis, MN, USA, Jun., 2019
(**Invited paper**)

(C-54) Nizar Khalfet and **Samir M. Perlaza**. "On Ultra-Reliable and Low Latency Simultaneous Information and Energy Transmission Systems" in Proc. of the 19th IEEE International Workshop on Signal Processing Advances in Wireless Communication, Cannes, France, Jun., 2019.
(**Invited paper**)

(C-53) Alex Dytso, Malcolm Egan, **Samir M. Perlaza**, Jean-Marie Gorce, H. Vincent Poor and Shlomo (Shitz) Shamai, "Optimal Inputs for Some Classes of Degraded Wiretap Channels" in Proc. IEEE Information Theory Workshop (ITW), Guangzhou, China, Nov., 2018.

(C-52) Victor Quintero, **Samir M. Perlaza**, Jean-Marie Gorce, and H. Vincent Poor, "Approximate Nash Region of the Gaussian Interference Channel with Noisy Output Feedback" in Proc. IEEE Information Theory Workshop (ITW), Guangzhou, China, Nov., 2018.

(C-51) Malcolm Egan and **Samir M. Perlaza**,. "Capacity Approximation of Continuous Channels by Discrete Inputs" in Proc. 52th Annual Conference on Information Sciences and Systems (CISS), Princeton, NJ, USA, Mar., 2018.
(**Invited paper**)

(C-50) **Samir M. Perlaza**, Ali Tajer, and H. Vincent Poor. "Simultaneous Energy and Information Transmission: A Finite Block-Length Analysis" in Proc. of the 19th IEEE International Workshop on Signal Processing Advances in Wireless Communication, Kalamata, Greece, Jun., 2018.
(**Invited paper**)

(C-49) Nizar Khalfet and **Samir M. Perlaza**. "Simultaneous Information and Energy Transmission in Gaussian Interference Channels" in Proc. of the 2018 International Zurich Seminar on Information and Communication, Zurich, Switzerland, Feb., 2018.

(C-48) Nizar Khalfet and **Samir M. Perlaza**. "Simultaneous Information and Energy Transmission in Gaussian Interference Channels with Feedback" in Proc. 55th Annual Allerton Conference on Communication, Control, and Computing, Monticello, IL, US, Oct., 2017.

(C-47) Victor Quintero, **Samir M. Perlaza**, and Jean-Marie Gorce. "Region d'Équilibre de Nash du Canal Linéaire Déterministe à Interférences avec Rétroalimentation Dégradée" in Proc. of the Colloque GRETSI, Juan-les-Pins, France, Sep., 2017.

(C-46) Ke Sun, Iñaki Esnaola, **Samir M. Perlaza**, and H. Vincent Poor. "Information Theoretic Attacks in the Smart Grid" in Proc. IEEE International Conference on Smart Grid Communications, Dresden, Germany, Oct., 2017.

(C-45) Malcolm Egan, **Samir M. Perlaza**, Vyacheslav Kungurtsev. "Capacity Sensitivity in Additive Non-Gaussian Noise Channels" in Proc. IEEE Intl. Symposium on Information Theory (ISIT), Aachen, Germany, Jun., 2017.

(C-44) Victor Quintero, **Samir M. Perlaza**, Jean-Marie Gorce, and H. Vincent Poor. "Nash Region of the Linear Deterministic Interference Channel with Noisy Output Feedback" in Proc. IEEE Intl. Symposium on Information Theory (ISIT), Aachen, Germany, Jun., 2017.

(C-43) Victor Quintero, **Samir M. Perlaza**, and Jean-Marie Gorce. "On the Efficiency of Nash Equilibria in the Interference Channel with Noisy Feedback" in Proc. European Wireless Conference. Workshop COCOA – COmpetitive and COoperative Approaches for 5G networks, Dresden, Germany, May, 2017.

(C-42) David Kibloff, **Samir M. Perlaza**, Guillaume Villemaud and Leonardo S. Cardoso. "On the Duality Between State-Dependent Channels and Wiretap Channels", in Proc. IEEE Global Conference on Signal and Information Processing (GlobalSIP), Washington, DC, USA, Dec. 2016.
(**Invited paper**)

(C-41) Selma Belhadj Amor and **Samir M. Perlaza**. "Decentralized K-user Gaussian multiple access channels", in Proc. International conference on NETwork Games, Control and OPtimization (NETGCOOP 2016), Avignon, France, Nov. 2016.
(**Invited paper**)

(C-40) Victor Quintero, **Samir M. Perlaza**, Iñaki Esnaola and Jean-Marie Gorce. "Approximate Capacity of the Gaussian Interference Channel with Noisy Channel Output Feedback", in Proc. IEEE Information Theory Workshop (ITW), Cambridge, UK, Sep., 2016.

(C-39) Selma Belhadj Amor, **Samir M. Perlaza**, I. Krikidis and H. Vincent Poor, "Feedback Enhances Simultaneous Information and Energy Transmission in Multiple Access Channels" in Proc. IEEE Intl. Symposium on Information Theory (ISIT), Barcelona, Spain, Jul., 2016.

(C-38) Cristian Genes, Iñaki Esnaola, **Samir M. Perlaza**, Luis F. Ochoa, and Daniel Coca. "Recovering Missing Data via Matrix Completion in Electricity Distribution Systems" in Proc. 17th IEEE International workshop on Signal Processing advances in Wireless Communications (SPAWC), Edinburgh, UK, Jul., 2016.
(**Invited paper**)

(C-37) Iñaki Esnaola, **Samir M. Perlaza**, H Vincent Poor and Oliver Kosut. "Decentralized MMSE Attacks in Electricity Grids" in Proc. IEEE Workshop

on Statistical Signal Processing (SSP), Palma de Mallorca, Spain, Jun 2016.
(**Invited paper**)

(C-36) Selma Belhadj Amor and **Samir M. Perlaza**, "Fundamental Limits of Simultaneous Energy and Information Transmission" in Proc. 23rd International Conference on Telecommunications (ICT), Thessaloniki, Greece, May 2016.
(**Invited paper**)

(C-35) Mathew Goonewardena, **Samir M. Perlaza**, Animesh Yadav, Wessam Ajib, "Generalized Satisfaction Equilibrium: A Model for Service-Level Provisioning in Networks", In Proc. European Wireless Conference (EW 2016), Oulu, Finland, May 2016.
(**Invited paper**)

(C-34) Victor Quintero, Samir M. Perlaza, Iñaki Esnaola, and Jean-Marie Gorce, "When Does Channel-Output Feedback Increase the Capacity Region of the Two-User Linear Deterministic Interference Channel?" in Proc. 11th EIA International Conference on Cognitive Radio Oriented Wireless Networks (CROWNCOM), Grenoble, France, May, 2016.

(C-33) Selma Belhadj Amor and Selma Belhadj Amor and Samir M. Perlaza "Decentralized Simultaneous Energy and Information Transmission in Multiple Access Channels" in Proc. 50th Annual Conference on Information Sciences and Systems (CISS), Princeton, NJ, USA, Mar., 2016.

(C-32) Selma Belhadj Amor, **Samir M. Perlaza**, Ioannis Krikidis. "Gaussian Multi-Access Channel with Minimum Received Energy Constraint", in Proc. 5th International Conference on Communications and Networking (ComNet), Hammamet, Tunisia, Nov., 2015.
(**Invited paper**)

(C-31) Victor Quintero, **Samir M. Perlaza** and J.-M. Gorce. "Noisy Channel-Output Feedback Capacity of the Linear Deterministic Interference Channel", in Proc. of the IEEE Information Theory Workshop (ITW), Jeju Island, Korea, October, 2015.

(C-30) Iñaki Esnaola, **Samir M. Perlaza** and H. Vincent Poor. "Equilibria in Data Injection Attacks", in Proc. of the IEEE Global Conference on Signal and Information Processing (GlobalSIP), Atlanta, GA, USA, Decembre, 2014.

(C-29) **Samir M. Perlaza**, Ravi Tandon, and H. Vincent Poor. "Symmetric Decentralized Interference Channels with Noisy Feedback", in Proc. of the IEEE Intl. Symposium on Information Theory (ISIT), Honolulu, HI, USA, July, 2014.

(C-28) **Samir M. Perlaza**, Ravi Tandon, and H. Vincent Poor. "Decentralized Interference Channels with Noisy Feedback Possess Pareto Optimal Nash Equilibria", in Proc. of the 6th International Symposium on Communications,

Control, and Signal Processing (ISCCSP), Athens, Greece, May 2014. (**Invited paper**)

(C-27) Zhiguo Ding, **Samir M. Perlaza**, Iñaki Esnaola, and H. Vincent Poor. "Simultaneous Information and Power Transfer in Wireless Cooperative Networks". in Proc. of the 8th International Conference on Communications and Networking in China, Guilin, People's Republic of China, Aug. 2013. (**Invited paper**)

(C-26) Perlaza, S. M. and Chorti, A. and Poor, H. V. and Han, Z. "On the Tradeoffs Between Network State Knowledge and Secrecy", in Proc. of the IEEE Global Wireless Summit (GWS), Atlantic City, NJ, Jun. 2013.

(C-25) Forouzandehmehr, N. and **Perlaza, S. M.** and Han, Z. and Poor, H. V. "A Satisfaction Game for Heating, Ventilation and Air Conditioning Control of Smart Buildings", in Proc. of the IEEE Global Communications Conference (GLOBECOM), Atlanta, GA, Dec. 2013.

(C-24) Perlaza, S. M. and Chorti, A. and Poor, H. V. and Han, Z. "On the Impact of Network-State Knowledge on the Feasibility of Secrecy", in Proc. of the IEEE Intl. Symposium on Information Theory (ISIT), Istanbul, Turkey, Jul. 2013.

(C-23) Rose, L. and **Perlaza, S. M.** and Debbah, M. andLe Martret, C. , "Achieving Pareto Optimal Equilibria in Energy Efficient Clustered Ad Hoc Networks", in Proc. of the IEEE Intl. Conference on Communications (ICC), Budapest, Hungary, Jun. 2013.

(C-22) Perlaza, S. M. and Tandon, R. and Poor, H. V. and Han, Z. "The Nash Equilibrium Region of the Linear Deterministic Interference Channel with Feedback", in Proc. of the Allerton Conference on Communication, Control, and Computing (Allerton-2012), Monticello, IL, Oct. 2012.

(C-21) Chorti, A. and **Perlaza, S. M.** and Han, Z. and Poor, H. V. "Physical Layer Security in Wireless Networks with Passive and Active Eavesdroppers", in Proc. of the IEEE Global Communications Conference (GLOBECOM), Anaheim, CA, Dec. 2012.

(C-20) Perlaza, S. M. and Han, Z. and Poor, H. V., "Learning Epsilon Satisfaction Equilibrium via Trial and Error in Decentralized Wireless Networks", in Proc. of the 46th Annual Asilomar Conference on Signals, Systems, and Computers (ASILOMAR), Pacific Grove, CA, Nov. 2012.

(C-19) Perlaza, S. M. and Han, Z. and Poor, H. V. and and Niyato, D. "On the Decentralized Management of Scrambling Codes in Small Cell Networks", in Proc. of the 13th IEEE International Conference on Communication Systems (ICCS), Singapore, Singapore, Nov. 2012.

(C-18) Merriaux, F. and **Perlaza, S. M.** and Lasaulce, S. and Han, Z. and Poor,

H. V., "Achievability of Efficient Satisfaction Equilibrium in Self-Configuring Networks", in Proc. of the 3rd International Conference on Game Theory for Networks (GAMECOMM), Vancouver, Canada, May 2012.

(C-17) Rose, L. and **Perlaza, S. M.** and Debbah, M. and C. Le Martret, "Distributed Power Allocation with SINR Constraints Using Trial and Error Learning", in Proc. of the IEEE Wireless Communications and Networking Conference (WCNC), Paris, France, Apr. 2012.

(C-16) Bennis, M. and **Perlaza, S. M.** and Debbah M., "Learning Coarse Correlated Equilibrium in Two-Tier Wireless Networks", in Proc. of the IEEE Intl. Conference on Communications (ICC), Ottawa, Canada, Jun. 2012.

(C-15) Couillet, R. and **Perlaza, S. M.** and Tembine, H. and Debbah, M., "A Mean Field Game Analysis of Electric Vehicles in the Smart Grid", in Proc. of the 1st IEEE INFOCOM Workshop on Green Networking and Smart Grids, Orlando, FL, Mar. 2012

(C-14) Perlaza, S. M. and Debbah, M., "Modeling Noisy Feedback in Decentralized Self-Configuring Networks", in Proc. of the 45th Annual Asilomar Conference on Signals, Systems, and Computers (ASILOMAR), Pacific Grove, CA, Nov. 2011

(C-13) Rose, L. and **Perlaza, S. M.** and Debbah, M., "On the Nash equilibria in Decentralized Parallel Interference Channels", in Proc. of the IEEE ICC Workshop on Game Theory and Resource Allocation for 4G, Kioto, Japan, Jun. 2011.

(C-12) Bennis, M. and **Perlaza, S. M.**, "Decentralized Cross-Tier Interference Mitigation in Cognitive Femtocell Networks", in Proc. of the IEEE International Conference on Communications (ICC), Kioto, Japan, Jun. 2011.

(C-11) Perlaza, S. M. and Lasaulce, S. and Tembine, H. and Debbah, M., "Learning to Use the Spectrum in Self-Configuring Heterogeneous Networks: A Logit Equilibrium Approach", in Proc. of the 4th International ICST Workshop on Game Theory in Communication Networks (GAMECOMM), Paris, France, May 2011.

(C-10) Perlaza, S. M. and Tembine, H. and Lasaulce, S. and Debbah, M., "Satisfaction Equilibrium: A General Framework for QoS Provisioning in Self-Configuring Networks", in the IEEE Global Communications Conference (GLOBECOM), Miami, FL, Dec. 2010. (**Candidate for Best Conference Paper Award of the IEEE MMTC Review Board Chair**)

(C-9) Perlaza, S. M. and Tembine, H. and Lasaulce, S. and Florez, V. Q., "On the Fictitious Play and Channel Selection Problems", submitted to IEEE Latin-American Conference on Communications (LATINCOM), Bogotá, Colombia, Sep. 2010.

(C-8) Perlaza, S. M. and Tembine, H. and Lasaulce, S., "How can Ignorant but Patient Cognitive Terminals Learn Their Strategy and Utility?" in the IEEE Intl. Workshop on Signal Processing Advances for Wireless Communications (SPAWC), Marrakesh, Morroco, Jun. 2010.

(C-7) Perlaza, S. M., and Belmega, E. V. and Lasaulce, S. and Debbah, M., "On the base station selection and base station sharing in self-configuring networks", in Fourth International Conference on Performance Evaluation Methodologies and Tools, Pisa, Italy, Oct. 2009.
(**Invited paper**).

(C-6) Perlaza, S. M. and Fawaz, N. and Lasaulce, S. and Debbah, M., "Alignement d'interférence opportuniste avec des terminaux multi-antennes", in the Gretsi Conference, Dijon, France, Sep. 2009.

(C-5) Le Treust, M and **Perlaza, S. M.** and Lasaulce, S., "Contrôle de puissance distribué efficace énergétiquement et jeux répétés", in the Gretsi Conference, Dijon, France, Sep. 2009.

(C-4) Perlaza, S. M., and Debbah, M. and Lasaulce, S. and Bogucka, H. "On the benefits of bandwidth limiting in vector multiple access channels", in EURASIP/IEEE Intl. Conf. on Cognitive Radio Oriented Wireless Networks and Communications(CROWNCOM), Hannover, Germany, Jun. 2009.
(**Best Student Paper Award**)

(C-3) Perlaza, S. M., and Debbah, M. and Lasaulce, S. and Chaufray, J-M., "Opportunistic interference alignment in MIMO interference channels", in IEEE Intl. Symposium on Personal, Indoor and Mobile Radio Communications (PIMRC), Cannes, France, Sep. 2008.
(**Invited paper**).

(C-2) Perlaza, S. M., and Cottatellucci, L. and Debbah, M., "A Game Theoretic Framework for Decentralized Power Allocation in IDMA Systems", in IEEE Intl. Symposium on Personal, Indoor and Mobile Radio Communications (PIMRC), Cannes, France, Sep. 2008.

(C-1) Perlaza, S. M. and Hoyos E. A. and Vera, P., "Reconfigurable Satellite Payload Model based on Software Radio Technologies", in IEEE Intl. Conf. of the Andean Region (ANDESCOM), Quito, Ecuador, Sep. 2006.

C.6 INRIA Technical Reports

(TR-12) Dadja Anade, Jean-Marie Gorce, Philippe Mary, and **Samir M. Perlaza**, "Saddlepoint Approximations of Cumulative Distribution Functions of Sums of Random Vectors", Research Report, INRIA, No. RR-9388, Lyon, France, Apr., 2021.

(TR-11) Eitan Altman, Izza Mounir, Fatim-Zahra Najid, and **Samir M. Perlaza**,

"On the true number of COVID-19 infections: Effect of Sensitivity, Specificity and Number of Tests in Prevalence Estimation", Research Report, INRIA, No. RR-9344, Sophia Antipolis, France, May, 2020.

(TR-10) Dadja Anade, Jean-Marie Gorce, Philippe Mary, and **Samir M. Perlaza**, "An upper bound on the error induced by saddlepoint approximations - Applications to information theory", Research Report, INRIA, No. RR-9329, Lyon, France, Apr., 2020.

(TR-09) Nizar Khalfet, and **Samir M. Perlaza**, and Ali Tajer, and H. Vincent Poor, "On Ultra-Reliable and Low Latency Simultaneous Information and Energy Transmission Systems" Technical Report, INRIA, No. RR-9261, Lyon, France, May., 2019.

(TR-08) Nizar Khalfet, and **Samir M. Perlaza**, and Ali Tajer, and H. Vincent Poor, "On Ultra-Reliable and Low Latency Simultaneous Information and Energy Transmission Systems", Technical Report, INRIA, No. RR-9261, Lyon, France, May., 2019.

(TR-07) David Kibloff and **Samir M. Perlaza** and Ligong Wang, "Broadcast Codes Can be Enhanced to Perform Covert Communications" Research Report, INRIA, No. RR-9249, Lyon, France, Jan., 2019.

(TR-06) Nizar Khalfet and **Samir M. Perlaza**, "Simultaneous Information and Energy Transmission in the Interference Channel", Technical Report, INRIA, No. RR-9102, Lyon, France, Nov., 2017.

(TR-05) Malcolm Egan, **Samir M. Perlaza**, Vyacheslav Kungurtsev, "Capacity Sensitivity in Continuos Channels" Technical Report, INRIA, No. RR-9012, Lyon, France, Jan., 2017.

(TR-04) Victor Quintero, and **Samir M. Perlaza**, and Jean-Marie Gorce, and H. Vincent Poor, "Decentralized Interference Channels with Noisy Output Feedback", Technical Report, INRIA, No. RR-9011, Lyon, France, Jan., 2017.

(TR-03) Selma Belhadj Amor and **Samir M. Perlaza**, "Decentralized K-user Gaussian Multiple Access Channels" Technical Report, INRIA, No. RR-8949, Lyon, France, Aug., 2016.

(TR-02) Mathew Goonewardena, and **Samir M. Perlaza**, and Animesh Yadav, and Wessam Ajib. "Generalized Satisfaction Equilibrium: A Model for Service-Level Provisioning in Networks" Technical Report, INRIA, No. RR-8883, Lyon, France, Jan., 2016.

(TR-01) Selma Belhadj Amor, and **Samir M. Perlaza**, and H. Vincent Poor, "Decentralized Simultaneous Energy and Information Transmission in Multiple Access Channels", Technical Report, INRIA, No. RR-8847, Lyon, France, Apr., 2015.

C.7 Other Publications

- Zubin Bharucha, Emilio Calvanese, Jiming Chen, Xiaoli Chu, Afef Feki, Antonio De Domenico, Ana Galindo-Serrano, Weisi Guo, Raymond Kwan, Jimin Liu, David López-Pérez, Massod Maqbool, Ying Peng, **Samir M. Perlaza**, Guillaume de la Roche, Serkan Uygungelen, Alvaro Valcarce and Jie Zhang. **Small Cell Deployments: Recent Advances and Research Challenges**. Summary of the outcomes of the 5th International Workshop on Femtocells held at King's College London, UK, on the 13th and 14th of February, 2012.

- Corvino, V. and Moretti, M. and **Perlaza, S. M.** and Debbah, M. and Lasaulce, S. and Jouini, W. and Palicot, J. and Moy, C. and Serrador, A. and Bogucka, H. and Sroka, P. and Rodrigues, E. B. and López-Benitez, M. and Umbert, A. and Casadevall, F. and Pèrez-Romero, J. "**Definition and evaluation of Joint Radio Resource Management and Advanced Spectrum Management Algorithms**", NEWCOM++ Network of Excellence in Wireless Communications, Deliverable DR9.2, January 12, 2010.

- **Perlaza, S. M.** and Rose L. and Debbah, M. and Le Martret, C., "**Dynamic Spectrum Allocation in Military Ad Hoc Networks**". in D3.1.2: Intermediate report N.2 for task T3.1 Cognitive Manager. CORASMA Project (Contract B-781-IAP4-GC) COgnitive RAdio for dynamic Spectrum MAnagement

- Belmega, E. V. and Debbah, M. and Lasaulce, S. and **Perlaza, S. M.**, "Energy-efficient cost-effective decentralized self-configuring networks", Forum DIGITEO 2010, poster, École Polytechnique. October 2010. Palaiseau, France.

- Belmega, E. V. and He, G. and Le Treust, M. and **Perlaza, S. M.**, Tembine, H. and Debbah, M. and Lasaulce, S., "Game theoretic tools for flexible networks", Journée des doctorants, poster, Supélec, Mars 2010. Gif-sur-Yvette, France.

Bibliography

[1] S. M. Perlaza, R. Tandon, H. V. Poor, and Z. Han, "The Nash equilibrium region of the linear deterministic interference channel with feedback," in *Proc. 50th Annual Allerton Conference on Communications, Control, and Computing*, Monticello, IL, Oct. 2012.

[2] ——, "Perfect output feedback in the two-user decentralized interference channel," *IEEE Trans. Inf. Theory*, vol. 61, no. 10, pp. 5441–5462, Oct. 2015.

[3] S. M. Perlaza, R. Tandon, and H. V. Poor, "Decentralized interference channels with noisy feedback possess Pareto optimal Nash equilibria," in *Proc. of the 6th International Symposium on Communications, Control, and Signal Processing (ISCCSP 2014)*, Athens, Greece, May. 2014.

[4] ——, "Symmetric decentralized interference channels with noisy feedback," in *Proc. IEEE Intl. Symposium on Information Theory (ISIT)*, Honolulu, HI, USA, Jun. 2014.

[5] V. Quintero, S. M. Perlaza, and J.-M. Gorce, "Noisy channel-output feedback capacity of the linear deterministic interference channel," in *IEEE Information Theory Workshop*, Jeju Island, Korea, Oct. 2015.

[6] V. Quintero, S. M. Perlaza, I. Esnaola, and J.-M. Gorce, "Approximate capacity of the Gaussian interference channel with noisy channel-output feedback," in *Proc. IEEE Information Theory Workshop (ITW)*, Sep. 2016.

[7] V. Quintero, S. M. Perlaza, J.-M. Gorce, and H. V. Poor, "Nash region of the linear deterministic interference channel with noisy output feedback," in *Proc. IEEE International Symposium on Information Theory (ISIT)*, Aachen, Germany, Jun. 2017.

[8] V. Quintero, S. M. Perlaza, I. Esnaola, and J.-M. Gorce, "When does output feedback enlarge the capacity of the interference channel?" *IEEE Trans. Commun.*, vol. 66, no. 2, pp. 615–628, Feb. 2018.

[9] ——, "When does channel-output feedback increase the capacity region of the two-user linear deterministic interference channel?" in *Proc. 11th EIA International Conference on Cognitive Radio Oriented Wireless Networks (CROWNCOM)*, Grenoble, France, May 2016.

[10] V. Quintero, S. M. Perlaza, J.-M. Gorce, and H. V. Poor, "Decentralized interference channels with noisy output feedback," INRIA, Lyon, France, Tech. Rep. 9011, Jan. 2017.

[11] V. Quintero, S. M. Perlaza, I. Esnaola, and J.-M. Gorce, "Approximate capacity region of the two-user Gaussian interference channel with noisy channel-output feedback," *IEEE Trans. Inf. Theory*, vol. 64, no. 7, pp. 5326 – 5358, Jul. 2018.

[12] S. Belhadj Amor, S. M. Perlaza, and I. Krikidis, "Simultaneous energy and information transmission in Gaussian multiple access channels," in *Proc. 5th International Conference on Communications and Networking (ComNet)*, Hammamet, Tunisia, Nov. 2015.

[13] S. Belhadj Amor and S. M. Perlaza, "Decentralized simultaneous energy and information transmission in multiple access channels," in *Proc. 2016 Annual Conference on Information Science and Systems (CISS)*, Princeton, NJ, USA, Mar. 2016.

[14] ——, "Decentralized k-user Gaussian multiple access channels," in *Proc. International conference on NETwork Games, COntrol and OPtimization (Netgcoop 2016)*, Avignon, France, Nov. 2016.

[15] S. B. Amor, S. M. Perlaza, I. Krikidis, and H. V. Poor, "Feedback enhances simultaneous energy and information transmission in multiple access channels," in *Proc. of IEEE International Symposium on Information Theory (ISIT)*, Barcelona, Spain, Jul. 2016, pp. 1974–1978.

[16] S. M. Belhadj Amor and S. M. Perlaza, "Fundamental limits of simultaneous energy and information transmission," in *Proc.* 23*rd International Symposium on Telecommunications*, Thessaloniki, Greece, May 2016.

[17] S. Belhadj Amor, S. M. Perlaza, I. Krikidis, and H. V. Poor, "Feedback enhances simultaneous wireless information and energy transmission in multiple access channels," *IEEE Trans. Inf. Theory*, vol. 63, no. 8, pp. 5244–5265, Aug. 2017.

[18] N. Khalfet and S. M. Perlaza, "Simultaneous information and energy transmission in Gaussian interference channels with feedback," in *Proc. 55th Annual Allerton Conference on Communications, Control, and Computing*, Allerton, USA., Oct. 2017.

[19] ——, "Simultaneous information and energy transmission in Gaussian interference channels," in *Proc. International Zurich Seminar on Information and Communication*, Zurich, Switzerland, Feb. 2018.

[20] S. M. Perlaza, A. Tajer, and H. V. Poor, "Simultaneous energy and information transmission: A finite block-length analysis," in *Proc. of the 19th IEEE*

International Workshop on Signal Processing Advances in Wireless Communications (SPAWC), Kalamata, Greece, Jun. 2018.

[21] S. M. Perlaza and N. Khalfet, "On the maximum energy transmission rate in ultra-reliable and low latency SIET," in *Proc. of the Third International Balkan Conference on Communications and Networking*, Skopje, North Macedonia, Jun. 2019.

[22] N. Khalfet, S. M. Perlaza, A. Tajer, and H. V. Poor, "On ultra-reliable and low latency simultaneous information and energy transmission systems," in *Proc. of the 19th IEEE International Workshop on Signal Processing Advances in Wireless Communications (SPAWC)*, Cannes, France, Jul. 2019.

[23] I. Esnaola, S. M. Perlaza, H. V. Poor, and O. Kosut, "Maximum distortion attacks in electricity grids," *IEEE Trans. Smart Grid*, vol. 7, no. 4, pp. 2007–2015, Jul. 2016.

[24] I. Esnaola, S. M. Perlaza, and H. V. Poor, "Equilibria in data injection attacks," in *Proc. IEEE Global Conference on Signal and Information Processing*, Atlanta, GA, USA, Dec. 2014, pp. 779–783.

[25] I. Esnaola, S. M. Perlaza, H. V. Poor, and O. Kosut, "Decentralized maximum distortion mmse attacks in electricity grids," *INRIA, Lyon, Tech. Rep. 466*, Sep. 2015.

[26] I. Esnaola, S. Perlaza, H. V. Poor, and O. Kosut, "Decentralized maximum distortion MMSE attacks in electricity grids," in *Proc. IEEE Workshop on Statistical Signal Processing (SSP)*, Palma de Mallorca, Spain, Jun. 2016.

[27] C. Genes, I. Esnaola, S. M. Perlaza, L. F. Ochoa, and D. Coca, "Recovering missing data via matrix completion in electricity distribution systems," in *Proc. IEEE Workshop on Signal Process. Advances in Wireless Commun.*, Edinburgh, UK, Jul. 2016, pp. 1–6.

[28] K. Sun, I. Esnaola, S. Perlaza, and H. Poor, "Information-theoretic attacks in the smart grid," in *Proc. IEEE Int. Conf. on Smart Grid Comm.*, Dresden, Germany, Oct. 2017, pp. 455–460.

[29] C. Genes, I. Esnaola, S. M. Perlaza, L. F. Ochoa, and D. Coca, "Robust recovery of missing data in electricity distribution systems," *IEEE Transactions on Smart Grid*, vol. 10, no. 4, pp. 4057–4067, Jul. 2019.

[30] K. Sun, I. Esnaola, S. Perlaza, and H. Poor, "Stealth attacks on the smart grid," *IEEE Trans. Smart Grid*, vol. 11, no. 2, pp. 1276–1285, Mar. 2020.

[31] C. Genes, I. Esnaola, and D. Coca, "Recovery of missing data in correlated smart grid datasets," in *Proc. IEEE Data Science Workshop*, Minneapolis, United States, Jun. 2019.

[32] X. Ye, I. Esnaola, S. M. Perlaza, and R. F. Harrison, "Information theoretic data injection attacks with sparsity constraints," in *Proc. of the IEEE International Conference on Communications, Control, and Computing Technologies for Smart Grids (Smartgridcomm)*, virtual conference, Nov. 2020.

[33] A. Carleial, "A case where interference does not reduce capacity," *IEEE Trans. Inf. Theory*, vol. 21, no. 5, pp. 569–570, Sep. 1975.

[34] T. S. Han and K. Kobayashi, "A new achievable rate region for the interference channel," *IEEE Trans. Inf. Theory*, vol. 27, no. 1, pp. 49–60, 1981.

[35] H. Sato, "The capacity of the Gaussian interference channel under strong interference," *IEEE Trans. Inf. Theory*, vol. 27, no. 6, pp. 786–788, Nov. 1981.

[36] H.-F. Chong, M. Motani, H. K. Garg, and H. El Gamal, "On the Han-Kobayashi region for the interference channel," *IEEE Trans. Inf. Theory*, vol. 54, no. 7, pp. 3188–3195, Jul. 2008.

[37] A. Carleial, "Interference channels," *IEEE Trans. Inf. Theory*, vol. 24, no. 1, pp. 60–70, Sep. 1978.

[38] T. M. Cover and C. S. K. Leung, "An achievable rate region for the multiple-access channel with feedback," *IEEE Transactions on Information Theory*, vol. 27, no. 3, pp. 292–298, May 1981.

[39] R. H. Etkin, D. N. C. Tse, and W. Hua, "Gaussian interference channel capacity to within one bit," *IEEE Trans. Inf. Theory*, vol. 54, no. 12, pp. 5534–5562, Dec. 2008.

[40] S. Li, Y. Huang, T. Liu, and H. Pfizer, "On the limits of treating interference as noise for two-user symmetric Gaussian interference channel," in *Proc. IEEE International Symposium on Information Theory (ISIT)*, Hong Kong, Hong Kong, Jun. 2015.

[41] C. Geng, N. Naderializadeh, A. Avestimehr, and S. Jafar, "On the optimality of treating interference as noise," *IEEE Transactions Information Theory*, vol. 61, no. 4, pp. 1753–1767, Apr. 2015.

[42] A. Dytso, D. Tuninetti, and N. Devroye, "On discrete alphabets for the two-user Gaussian interference channel with one receiver lacking knowledge of the interfering codebook," *IEEE Transactions Information Theory*, vol. 61, no. 3, pp. 257–1276, Mar. 2015.

[43] ——, "Interference as noise: Friend or foe?" *IEEE Transactions Information Theory*, vol. 66, no. 6, pp. 3561–3596, Jun. 2016.

[44] C. Suh and D. N. C. Tse, "Feedback capacity of the Gaussian interference channel to within 2 bits," *IEEE Trans. Inf. Theory*, vol. 57, no. 5, pp. 2667–2685, May. 2011.

[45] S. A. Jafar, "Interference alignment: A new look at signal dimensions in a communication network," *Foundations and Trends in Communications and Information Theory*, vol. 7, no. 1, pp. 1–134, 2010.

[46] A. Sahai, V. Aggarwal, M. Yüksel, and A. Sabharwal, "On channel output feedback in deterministic interference channels," in *Proc. IEEE Information Theory Workshop*, Taormina, Italy, Oct. 2009.

[47] A. Sahai, V. Aggarwal, M. Yuksel, and A. Sabharwal, "Capacity of all nine models of channel output feedback for the two-user interference channel," *IEEE Trans. Inf. Theory*, vol. 59, no. 11, pp. 6957–6979, 2013.

[48] F. M. J. Willems, "Information theoretical results for multiple access channels," Ph.D. dissertation, Katholieke Universiteit, Department of Electrical Engineering, Leuven, Belgium, Oct. 1982.

[49] F. M. J. Willems and E. C. Van Der Meulen, "The discrete memoryless multiple-access channel with cribbing encoders," *IEEE Trans. Inf. Theory*, vol. IT-31, no. 3, pp. 313–327, May. 1985.

[50] D. Tuninetti, "On interference channel with generalized feedback (IFC-GF)," in *Proc. of International Symposium on Information Theory (ISIT)*, Nice, France, Jun. 2007, pp. 2661–2665.

[51] S. Yang and D. Tuninetti, "Interference channel with generalized feedback (a.k.a. with source cooperation): Part I: Achievable region," *IEEE Trans. Inf. Theory*, vol. 5, no. 57, pp. 2686–2710, May. 2011.

[52] A. Vahid, C. Suh, and A. S. Avestimehr, "Interference channels with rate-limited feedback," *IEEE Trans. Inf. Theory*, vol. 58, no. 5, pp. 2788–2812, May. 2012.

[53] M. Ashraphijuo, V. Aggarwal, and X. Wang, "On the symmetric k-user linear deterministic interference channels with limited feedback," in *Proc. 52nd Annual Allerton Conference on Communication, Control, and Computing (Allerton).*, Oct. 2014.

[54] ——, "On the symmetric k-user interference channels with limited feedback," *IEEE Trans. Inf. Theory*, vol. 62, no. 12, pp. 6969–6985, Oct. 2016.

[55] R. Zamir, *Lattice Coding for Signals and Networks.* University Printing House, Cambridge CB2 8BS, UK: Cambridge University Press, 2014.

[56] C. Karakus, I.-H. Wang, and S. Diggavi, "Gaussian interference channel with intermittent feedback," *IEEE Trans. Inf. Theory*, vol. 61, no. 9, pp. 4663–4699, Sep. 2015.

[57] M. Gastpar and G. Kramer, "On noisy feedback for interference channels," in *Asilomar Conference on Signals, Systems and Computers*, Oct-Nov. 2006.

[58] S.-Q. Le, R. Tandon, M. Motani, and H. V. Poor, "Approximate capacity region for the symmetric Gaussian interference channel with noisy feedback," *IEEE Trans. Inf. Theory*, vol. 61, no. 7, pp. 3737–3762, Jul. 2015.

[59] ——, "The capacity region of the symmetric linear deterministic interference channel with partial feedback," in *Proc. 50th Annual Allerton Conference on Communication, Control, and Computing (Allerton)*, Oct. 2012.

[60] A. P. Hekstra and F. M. J. Willems, "Dependence balance bounds for single-output two-way channels," *IEEE Trans. Inf. Theory*, vol. 35, no. 1, pp. 44–53, Jan. 1989.

[61] V. M. Pabhakaran and P. Viswanath, "Interference channel with source cooperation," *IEEE Trans. Inf. Theory*, vol. 57, no. 1, pp. 156–186, Jan. 2011.

[62] G. Kramer, "Feedback strategies for white Gaussian interference networks," *IEEE Trans. Inf. Theory*, vol. 48, no. 6, pp. 1423–1438, Jun. 2002.

[63] D. Tuninetti, "An outer bound region for interference channels with generalized feedback," in *IEEE Information Theory and Applications Workshop (ITA)*, Feb. 2010, pp. 1–5.

[64] ——, "An outer bound for the memoryless two-user interference channel with general cooperation," in *IEEE Information Theory Workshop (ITW)*, Sep. 2012, pp. 217–221.

[65] J. F. Nash, "Equilibrium points in n-person games," *Proc. National Academy of Sciences of the United States of America*, vol. 36, no. 1, pp. 48–49, Jan. 1950.

[66] N. Nisan, T. Roughgarden, Éva Tardos, and V. V. Vazirani, *Algorithmic game theory*. Cambridge, UK: Cambridge University Press, 2007.

[67] R. J. Aumann, "Subjectivity and correlation in randomized strategies," *Journal of Mathematical Economics*, vol. 1, no. 1, pp. 67–96, Mar. 1974.

[68] S. M. Perlaza, H. Tembine, S. Lasaulce, and M. Debbah, "Quality-Of-Service provisioning in decentralized networks: A satisfaction equilibrium approach," *IEEE Journal of Selected Topics in Signal Processing*, vol. 6, no. 2, pp. 104–116, Apr. 2012.

[69] R. A. Berry and D. N. C. Tse, "Shannon meets Nash on the interference channel," *IEEE Trans. Inf. Theory*, vol. 57, no. 5, pp. 2821–2836, May 2011.

[70] S. T. Chung, S. J. Kim, J. Lee, and J. M. Cioffi, "A game-theoretic approach to power allocation in frequency-selective Gaussian interference channels," in *Proc. IEEE International Symposium on Information Theory (ISIT)*, Yokohama, Japan, Jul. 2003, p. 316.

[71] L. Rose, S. M. Perlaza, and M. Debbah, "On the Nash equilibria in decentralized parallel interference channels," in *Proc. IEEE Intl. Conference on Communications (ICC)*, Kyoto, Japan, Jun. 2011.

[72] W. Yu and J. M. Cioffi, "Competitive equilibrium in the Gaussian interference channel," in *Proc. IEEE International Symposium on Information Theory (ISIT)*, Sorrento, Italy, Jun. 2000, p. 431.

[73] S. Avestimehr, S. Diggavi, and D. N. C. Tse, "Wireless network information flow: A deterministic approach," *IEEE Trans. Inf. Theory*, vol. 57, no. 4, pp. 1872–1905, Apr. 2011.

[74] R. Fano, *Transmission of information - a statistical theory of communication.* MIT Press, Mar. 1961.

[75] H.-F. Chong, M. Motani, and H. K. Garg, "A comparison of two achievable rate regions for the interference channel," in *ITA Workshop*, Feb. 2006.

[76] R. D. Yates, D. Tse, and Z. Li, "Secret communication on interference channels," in *Proc. of the IEEE International Symposium on Information Theory (ISIT)*, Toronto, Canada, Jul. 2008.

[77] R. Berry and D. N. C. Tse, "Information theoretic games on interference channels," in *Proc. of the IEEE International Symposium on Information Theory (ISIT)*, Toronto,Canada, Jul. 2008.

[78] N. Tesla, *Apparatus for transmitting electrical energy.* New York, NY: United States Patent Office, Dec. 1914, vol. US1119732 A.

[79] P. Grover and A. Sahai, "Shannon meets Tesla: Wireless information and power transfer," in *Proc. IEEE International Symposium on Information Theory*, Austin, TX, USA, Jun. 2010, pp. 2363–2367.

[80] M. Varasteh, B. Rassouli, and B. Clerckx, "Wireless information and power transfer over an AWGN channel: Nonlinearity and asymmetric Gaussian signaling," in *Proc. IEEE Information Theory Workshop*, Kaohsiung, Taiwan, Nov. 2017.

[81] L. R. Varshney, "Transporting information and energy simultaneously," in *Proc. IEEE International Symposium on Information Theory*, Toronto, ON, Canada, Jul. 2008, pp. 1612–1616.

[82] S. M. Perlaza, A. Tajer, and H. V. Poor, "Simultaneous energy and information transmission: A finite block-length analysis," in *Proc. 19th IEEE International Workshop on Signal Processing Advances in Wireless Communication*, Kalamata, Greece, Jun. 2018.

[83] K. G. Shenoy and V. Sharma, "Finite blocklength achievable rates for energy harvesting AWGN channels with infinite buffer," in *Proc. IEEE International Symposium on Information Theory (ISIT)*, Barcelona, Spain, Jul. 2016.

[84] L. R. Varshney, "On energy/information cross-layer architectures," in *Proc. IEEE International Symposium on Information Theory*, Cambridge, MA, USA, Jul. 2012, pp. 1356–1360.

[85] K. Tutuncuoglu and A. Yener, "Energy harvesting networks with energy cooperation: Procrastinating policies," *IEEE Transactions on Communications*, vol. 63, no. 11, pp. 4525–4538, Nov. 2015.

[86] B. Varan and A. Yener, "Matching games for wireless networks with energy cooperation," in *Proc. IEEE Wireless Communications and Networking Conference (WCNC)*, Doha, Qatar, Apr. 2016.

[87] J. Hu, K. Yang, G. Wen, and L. Hanzo, "Integrated data and energy communication network: A comprehensive survey," *IEEE Communications Surveys & Tutorials*, vol. 20, no. 4, pp. 3169–3219, 2018.

[88] B. Gurakan, B. Sisman, O. Kaya, and S. Ulukus, "Energy and data cooperation in energy harvesting multiple access channel," in *Proc. of the International Symposium on Modeling and Optimization in Mobile, Ad Hoc, and Wireless Networks (WiOpt)*, Tempe, Arizona, USA, May 2016.

[89] B. Gurakan, "Energy cooperation in energy harvesting communications systems," Ph.D. dissertation, Graduate School of the University of Maryland, Department of Electrical and Computer Engineering, College Park, Maryland, USA, 2016.

[90] B. Clerckx, R. Zhang, R. Schober, D. W. K. Ng, D. I. Kim, and H. V. Poor, "Fundamentals of wireless information and power transfer: From RF energy harvester models to signal and system designs," *IEEE Journal on Selected Areas in Communications*, vol. 37, no. 1, pp. 4–33, Jan. 2019.

[91] A. M. Fouladgar; and O. Simeone, "On the transfer of information and energy in multi-user systems," *IEEE Communications Letters*, vol. 16, no. 11, pp. 1733–1736, Nov. 2012.

[92] L. H. Ozarow, "The capacity of the white Gaussian multiple access channel with feedback," *IEEE Transactions on Information Theory*, vol. 30, no. 4, pp. 623–629, Jul. 1984.

[93] T. M. Cover, "Some advances in broadcast channels," in *Advances in Communication Systems, Vol. 4, Theory and Applications*, A. Viterbi, Ed. New York: Academic Press, 1975, ch. 4.

[94] A. D. Wyner, "Recent results in the Shannon theory," *IEEE Transactions on Information Theory*, vol. 20, no. 1, pp. 2–10, 1974.

[95] M. Varasteh, B. Rassouli, and B. Clerckx, "On capacity-achieving distributions over complex AWGN channels under nonlinear power constraints and their applications to SWIPT," *CoRR*, vol. abs/1712.01226, 2017. [Online]. Available: http://arxiv.org/abs/1712.01226

[96] N. Khalfet and S. M. Perlaza, "Simultaneous information and energy transmission in the interference channel," INRIA Grenoble - Rhône-Alpes, Grenoble, France, Tech. Rep. 9102, Oct. 2017.

[97] R. H. Etkin, D. N. C. Tse, and H. Wang, "Gaussian interference channel capacity to within one bit," *IEEE Trans. Inf. Theory*, vol. 54, no. 12, pp. 5534–5562, Dec. 2008.

[98] P. Bergmans, "Random coding theorems for broadcast channels with degraded components," *IEEE Trans. Inf. Theory*, vol. 19, no. 2, pp. 197–207, Mar. 1973.

[99] C. E. Shannon, "The zero-error capacity of a noisy channel," *IRE Transactions on Information Theory*, vol. 2, no. 3, pp. 8–19, Sep. 1956.

[100] W. Feller, *An Introduction to Probability Theory and Its Application*, 2nd ed. New York, NY: John Wiley and Sons, 1971, vol. 2.

[101] R. Zhang and C. K. Ho, "MIMO broadcasting for simultaneous wireless information and power transfer," *IEEE Transactions on Wireless Communications*, vol. 12, no. 5, pp. 1989–2001, May. 2013.

[102] Y. Liu, P. Ning, and M. K. Reiter, "False data injection attacks against state estimation in electric power grids," in *Proc. ACM Conf. on Computer and Communications Security*, Chicago, IL, USA, Nov. 2009, pp. 21–32.

[103] O. Kosut, L. Jia, R. J. Thomas, and L. Tong, "Malicious data attacks on the smart grid," *IEEE Trans. Smart Grid*, vol. 2, no. 4, pp. 645–658, Dec. 2011.

[104] I. Shomorony and A. S. Avestimehr, "Worst-case additive noise in wireless networks," *IEEE Trans. Inf. Theory*, vol. 59, no. 6, pp. 3833–3847, Jun. 2013.

[105] J. Neyman and E. S. Pearson, "On the problem of the most efficient tests of statistical hypotheses," in *Breakthroughs in Statistics*, ser. Springer Series in Statistics. Springer New York, 1992, pp. 73–108.

[106] H. V. Poor, *An Introduction to Signal Detection and Estimation*. 2nd ed. New York: Springer-Verlag, 1994.

[107] D. Monderer and L. S. Shapley, "Potential games," *Games and Economic Behavior*, vol. 14, no. 1, pp. 124–143, May 1996.

[108] T. M. Cover and J. A. Thomas, *Elements of Information Theory*. John Wiley & Sons, Nov. 2012.

[109] J. Hou and G. Kramer, "Effective secrecy: Reliability, confusion and stealth," in *Proc. IEEE Int. Symp. on Information Theory*, Honolulu, HI, USA, Jun. 2014, pp. 601–605.

[110] D. A. Bodenham and N. M. Adams, "A comparison of efficient approximations for a weighted sum of chi-squared random variables," *Stat Comput*, vol. 26, no. 4, pp. 917–928, Jul. 2016.

[111] B. G. Lindsay, R. S. Pilla, and P. Basak, "Moment-based approximations of distributions using mixtures: Theory and applications," *Ann. Inst. Stat. Math.*, vol. 52, no. 2, pp. 215–230, Jun. 2000.

[112] A. Abur and A. G. Expósito, *Power System State Estimation: Theory and Implementation*. CRC Press, Mar. 2004.

[113] J. J. Grainger and W. D. Stevenson, *Power System Analysis*. McGraw-Hill, 1994.

[114] R. D. Zimmerman, C. E. Murillo-Sánchez, and R. J. Thomas, "MATPOWER: Steady-state operations, planning, and analysis tools for power systems research and education," *IEEE Trans. Power Syst.*, vol. 26, no. 1, pp. 12–19, Feb. 2011.

[115] D. Bodenham. *Momentchi2: Moment-Matching Methods for Weighted Sums of Chi-Squared Random Variables*. (2016) [Online]. Available: https://cran.r-project.org/web/packages/momentchi2/index.html.

[116] B. Laurent and P. Massart, "Adaptive estimation of a quadratic functional by model selection," *Ann. Statist.*, vol. 28, no. 5, pp. 1302–1338, 2000.